# Investigating the role of CREB3L2 in terminal B-cell differentiation and B-cell neoplasia

Muna Mohamed Salim Al-Maskari

Submitted in accordance with the requirement for the degree of Doctor of Philosophy (PhD)

University of Leeds

Leeds Institute of Cancer Pathology

Section of Experimental Haematology

August.2016

The candidate confirms that the work submitted is my own and that appropriate credit has been given where reference has been made to the work of others.

**Acknowledgements**

I would like to express my gratitude to all who helped me throughout my PhD. My sincere gratitude to my supervisors Dr Reuben Tooze and Dr Gina Doody for being patient with me and providing me with useful guidance and constant supervision. Great thanks to my parents and friends for their encouragement, help and moral support. Moreover, I am very grateful to all the post doctors in our section (experimental haematology) for their kind help, advice and support. Finally, I would like to thank my husband who was always around, providing me with help, love and encouragement.

## I. Abstract:

CREB3L2 (cAMP Response Element Binding protein 3 Like 2) is a bZIP domain containing transcription factor. It is one of several endoplasmic reticulum (ER)-stress transducers that lead to an unfolded protein response (UPR). CREB3L2 is activated by regulated proteolysis via Site-1/Site-2 (S1P/S2P) proteases, due the accumulation of misfolded proteins in the ER. Such regulation is shared with other transcription factors (TFs) such as ATF6 and SREBP. During B-cell differentiation, the UPR is important for plasma cell adaptation to high levels of antibody secretion. However, to date only one UPR regulator has been implicated in plasma cell differentiation, XBP1. The high expression of *CREB3L2* in plasma cells suggests that it may also contribute to secretory adaptation and offers the opportunity for therapeutic targeting. Therefore, the aim of this project is to test the involvement of the transcription factor CREB3L2 in plasma cell differentiation through investigating its expression, regulation and function in human B-cell differentiation and B-cell tumours.

Evaluation in myeloma and ABC-DLBL cell lines revealed a direct relationship between CREB3L2 activation and UPR induction. In primary cells, CREB3L2 is expressed at the earliest stages of plasma cell differentiation and then becomes strongly induced and activated as the cells transition to the plasma cell state. To investigate the potential role of CREB3L2, S1P and S2P inhibitors were employed to block it's processing. Inhibition of S1P/S2P during plasma cell differentiation led to a profound reduction in plasmablast number linked to a decrease in proliferation and an increase in autophagy. While few cells survive following treatment with the inhibitors, phenotypically the cells appear normal. In contrast, immunoglobulin secretion is severely reduced. Moreover, inhibition of S1P is associated with a unique gene expression profile involving gene signatures related to IRF4 and mTOR function as well as metabolic pathways.

To further investigate the contribution of CREB3L2 to the events observed with S1P/S2P inhibitors, siRNA-mediated knockdown and ChIP-seq experiments were performed in primary differentiating B-cells. Although the changes in gene expression after knockdown did not reach statistical significance, genes showing variation have known roles in ER stress responses, autophagy and plasma cell development. Moreover, ChIP-seq of CREB3L2 demonstrated direct binding to several of the differentially expressed genes. The ChIP-seq experiment also included an evaluation of ATF6 and XBP1 binding in the same cells. The results revealed a high degree of overlap for binding, including to loci previously identified in the gene expression analyses.

In conclusion, the results show that S1P/S2P control CREB3L2 processing in differentiating B-cells and suggest that CREB3L2 is involved in the early commitment to plasma cell fate, prior to the requirement for XBP1. CREB3L2 is likely to function in combination with other RIP-activated TFs by regulating genes involved in metabolism, necessary for effective transition to high secretory activity. Thus, S1P/S2P-regulated pathways play a pivotal role in the B-cell to plasma cell transition and represent a previously unrecognised component of the regulatory network that turns these cells into efficient antibody “factories.”

## II. Table of content

## III. List of figures

## IV. List of tables:

## V. Abbreviations

| | |
|---|---|
| ATF4 | Activation transcription factor 5 |
| ATF5 | Activation transcription factor 5 |
| ATF6 | Activation transcription factor 6 |
| BBF2H7 | Box B Factor 2 Human homology in chromosome 7 |
| BCL6 | B-cell lymphoma 6 |
| BLIMP1 | B-lymphocytes induced maturation protein 1 |
| bZIP | basic leucine zipper |
| CREB3L2 | cAMP Responsive Element Binding Protein 3 Like 2 |
| eIF2α | eukaryotic initiation factor 2 on α subunit |
| ER | Endoplasmic Resticulum |
| ERAD | ER-associated degradation |
| GC | Germinal Centre |
| GST | Glutathione S-Transferase |
| IRE1 | Inositol-requiring enzyme-1 |
| IRF4 | Interferon regulatory factor 4 |
| LGFMS | Low-grade fibromyxide sarcoma |
| MHC | Major-Histocompatibility Complex |
| PAX5 | Paired box protein 5 |
| PERK | PKR-like endoplasmic reticulum kinase |
| RIP | Regulated intramembrane proteolysis |
| S1P | Site 1 protease |
| S2P | Site 2 protease |
| SCAP | SREBP cleavage activating protein |
| SHM | Somatic Hypermutation |
| SREBP | Sterol regulatory element binding protein |
| TF | Transcription Factor |
| UPR | Unfolded Protein Response |
| XBP1 | X-box binding protein 1 |
| XBP1s | XBP1 spliced |
| XBP1u | XBP1 unspliced |

# 1. Introduction

In vertebrates, the immune system has developed a defensive network divided into two groups: innate immunity and adaptive immunity. Innate immunity is a nonspecific type that is present from birth and includes the membrane barriers of the organism, their associated secretions and keratinisation, as well as factors in the blood and tissues such as complement, granulocytes and macrophages. In contrast the adaptive immune system has the capacity to mount a response, which is specific to the invading organism, and can establish memory of a previous encounter. The major cells of the adaptive immune response are T- and B-lymphocytes. They share unique features; specifically they have unique antigen receptors that recognise a wide range of ligands (antigens). The diversity of these antigen receptors is generated via somatic gene rearrangement in the V (D) J segments of the heavy and light chains of the immunoglobulins or T-cell receptor genes that provide their unique specificity for antigen. Moreover, for T-cells their recognition of antigen is dependent on antigen presentation via the major-histocompatibility complex (MHC). This provides one of the major differences between B- and T-lymphocytes; B-lymphocytes recognize their antigens as whole intact three-dimensional structures whereas T-cells recognize their antigens as processed peptide fragments presented via MHC molecules. Other features also distinguish B-cell and T-cell receptors. Firstly, B-cells express immunoglobulins either as membrane bound receptors or as secreted forms sharing the same specificity following plasma cell differentiation. As secreted antibody the immunoglobulin of the B-cell receptor contributes to immunological memory and the cross-talk between innate and adaptive immunity. Secondly the nature of the functional effect of immunoglobulin can be altered during an immune response via the process of heavy-chain class-switching. Finally the affinity of the B-cell receptor can be improved during an immune response, such that its affinity for antigen is greater on secondary encounter. In contrast T-lymphocytes express T-cell receptors (TCR) only as a membrane bound form, do not undergo functional

class-switching and show no evidence of maturation for improved affinity within an individual T-cell clone. Thus B-lymphocytes have several unique developmental stages. The plasma cell stage, which represents the terminal effector stage of the B-cell lineage, accompanies the transition of the membrane bound B-cell receptor to the secreted immunoglobulin molecule (3).

Conversion to a “professional secretory cell” status is a hallmark of plasma cell differentiation. The increase in protein production results in an increased burden on the endoplasmic reticulum (ER), the site of protein manufacture, modification by glycosylation, disulphide bond formation and structural folding. An evolutionarily conserved collection of signalling pathways termed the unfolded protein response (UPR) allows the ER to maintain function in the face of an imbalance. It is known that the UPR is critical in plasma cells for adaptation to functional secretory activity and may affect plasma cell longevity (4). However to date only one UPR regulator has been principally implicated in plasma cell differentiation, XBP-1. The key attributes that XBP-1 governs are the expansion of the secretory apparatus and the production of high levels of immunoglobulin (5, 6). Despite this, the initial stages of plasma cell differentiation are not affected by loss of XBP-1. These data suggest that other factors may be playing a role in preparing the cell for secretion in what can be termed an “anticipatory” UPR. In recent years, a novel family of ER stress transducers have been described that share significant homology with the classical UPR-activated transcription factor ATF6. This CREB3 family of transcription factors have been implicated in regulating development, metabolism, secretion, survival and transformation in other cell lineages, with evidence for cell-type specific effects (7). One family member, CREB3L2, is specifically up regulated during plasma cell differentiation (4, 8). The range of biological processes that have been attributed to CREB3-family regulation would fit well with the requirements needed during plasma cell differentiation. The role of non-classical UPR-related factors, in particular the CREB family, of which CREB3L2 is strongly expressed in plasma cells, has not been studied

in the B-cell lineage and may provide an important contribution and the opportunity for therapeutic targeting. Therefore, in this project I aim to test the involvement of CREB3L2 in the process of plasma cell differentiation.

## 1.1 B-cell differentiation

B-lymphocytes arise from haematopoietic stem cells in the bone marrow in response to many different stimuli such as cytokines. The B-cell receptor is the principle distinguishing feature of the lineage and is composed of a unique heavy and light chain combination in each B-cell, with each immunoglobulin molecule representing a combination of 2 heavy chain and two light chain proteins. Two loci, kappa and lambda can generate light chains, while one heavy chain locus is present. During B-cell differentiation the heavy chain locus rearranges first, and after productive rearrangement of one allele, the other allele is silenced ensuring that only one heavy chain rearrangement is expressed (3).

The first distinguishable B-cell is the pro-B cell with only heavy chain $D_H$, $J_H$ gene segments rearranged and without immunoglobulin production. The second stage in the B-cell lineage is the pre-B cell that is characterized by heavy chain VDJ unit formation accompanied by surrogate light chain. After positive selection the, pre-B cells differentiate to immature B-cells, which are characterized by the productive rearrangement of one allele of either kappa or lambda loci, and expression of monomeric IgM at the B-cell surface as an antigen specific receptor (Figure 1.1). The monomeric IgM results from μ of the heavy chain paring with the light chains. The specificity of the immunoglobulin is provided by the combined rearranged heavy and light chain variable regions. Immature B-cells differentiate in to mature B-cells expressing $IgM^+$ $IgD^+$ at their surfaces in peripheral lymphoid organs. Several functional subsets such as follicular and marginal zone B-cells arise (3).

There are 2 major types of B-cell activation, T-cell dependent and T-cell independent (Figure 1.1). In T-cell dependent B-cell activation, both an antigen specific B-cell and T-cell have to interact. During the interaction the B-cell has to endocytose antigen via its B-cell receptor (BCR) and present this antigen as processed peptide, via MHC class II to the T-cell. The T-cell must also have been previously activated by a professional antigen presenting cells (APC) such as a dendritic cell via their MHC class II (9, 10). On the other hand, some types of B-cells can be activated independently from T-cells by toll-like receptor activation or highly repetitive antigen receptor ligands to drive T-independent differentiation (11).

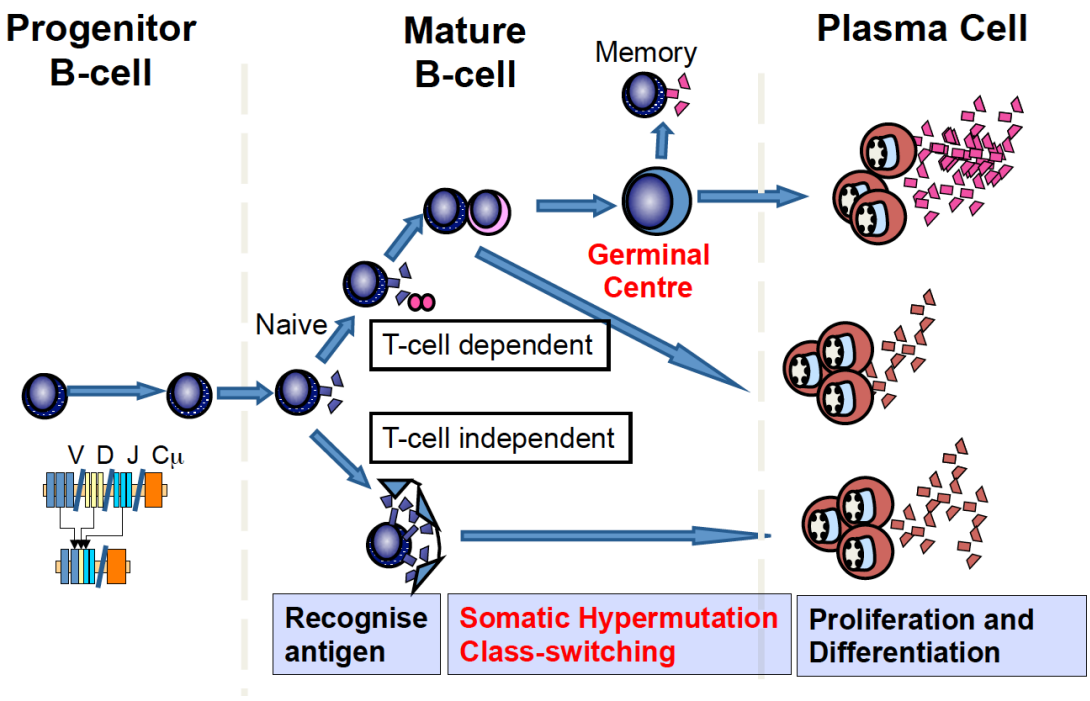


**Figure-1.1: B-cell development**. B-cells undergo Ig gene rearrangement in the bone marrow leading to the expression of a functional surface BCR. Selected B-cells migrate to the periphery and upon encounter with antigen can differentiate into short-lived plasma cells or form a germinal centre (GC). B-cells in the GC undergo class switching and somatic hypermutation, leading to improved antibody affinity and functional adaptation. B-cells exiting the GC may become memory B-cells or differentiate into antibody secreting cells that migrate to bone marrow niches for long-term survival (adapted from Dr. Reuben Tooze).

Upon encountering an antigen, to which they are specific, naïve B-cells migrate to the margin of the B-cell follicle and T-zone in the secondary lymphoid organs (lymph node, spleen and Peyer's patches of the intestine). Here, B-cells depend on encounter with an appropriately activated and antigen specific CD4+ T follicular helper ($T_{FH}$) cells in order to engage in the "cognate interaction" necessary for further activation and differentiation. This cognate interaction occurs principally via MHC class II and CD40, as a co-stimulatory molecule on B-cells and its ligand CD154 on $T_{FH}$. In addition there is local cytokine secretion (Il-2, Il-4, Il-5 and IL-21) by the $T_{FH}$. The activated B-cells either turn into plasmablast and migrate to the medulla of the lymph node (most of the plasma cells formed at that stage are short-lived) or return to the B-cell follicle where they proliferate extensively forming a secondary follicle. A few days of B-cell proliferation results in the formation of a germinal centre (GC) (Figure 1.1). The GC is composed of three zones; dark zone, light zone and surrounded by a mantle zone where the residual naïve B-cells of the primary follicle are located. The dark zone is composed mainly of centroblast; proliferating B-cells whereas, the light zone is composed of centrocytes; smaller cells with lower rate of division. In the dark zone, centroblasts undergo somatic hypermutation (SHM); a high rate of mutation selectively targeting the variable region of the rearranged immunoblobulin gene segments. The SHM process is essentially random and is coupled to affinity maturation in order to select B-cells with improved affinity for antigen. The process of affinity maturation occurs in the light zone and is derived from competition of B-cells for a limited supply of antigen presented on follicular dendritic cells. This results in the emergence of B-cells with higher affinity and loss by apoptosis of B-cells with lower affinity. Such B-cells may re-enter the dark zone to engage in another round of mutation and selection for even higher affinity or develop in to memory B-cells that may also have undergone immunoglobulin class switch recombination or into plasma cells that migrate to the bone marrow, and become long lived (3, 4, 7, 12-15) (Figure 1.1).

At present the factors controlling these decisions in the GC are still being defined. However, it is suggested that the affinity of BCR plays an important role (16). In addition, IRF4 plays role in controlling the decision in such that the strength of BCR signalling influences IRF4 expression. High BCR signalling avidity induces higher levels of IRF4 hence, inhibiting GC reaction and induces plasma cell differentiation (17).

### 1.1.1 Transcription factors involved in B-cell differentiation

B-cell differentiation is regulated by the sequential action of multiple TFs that are called master regulators (12, 13, 18). They can be divided into several groups; the first group includes those factors necessary for maintaining the core B-cell program such as PAX5 (Paired box protein 5, also known as B-cell lineage-specific activator protein; BSAP). The second group regulates specific stages of mature B-cell differentiation in particular the germinal centre response, such as BCL6 (B-cell lymphoma 6). The third group controls the final step of B-cell to plasma cell differentiation and includes IRF4 (Interferon regulatory factor 4), BLIMP1 (B-lymphocytes induced maturation protein 1) and XBP1 (X-box binding protein 1) (12, 13) (Figure-1.2).

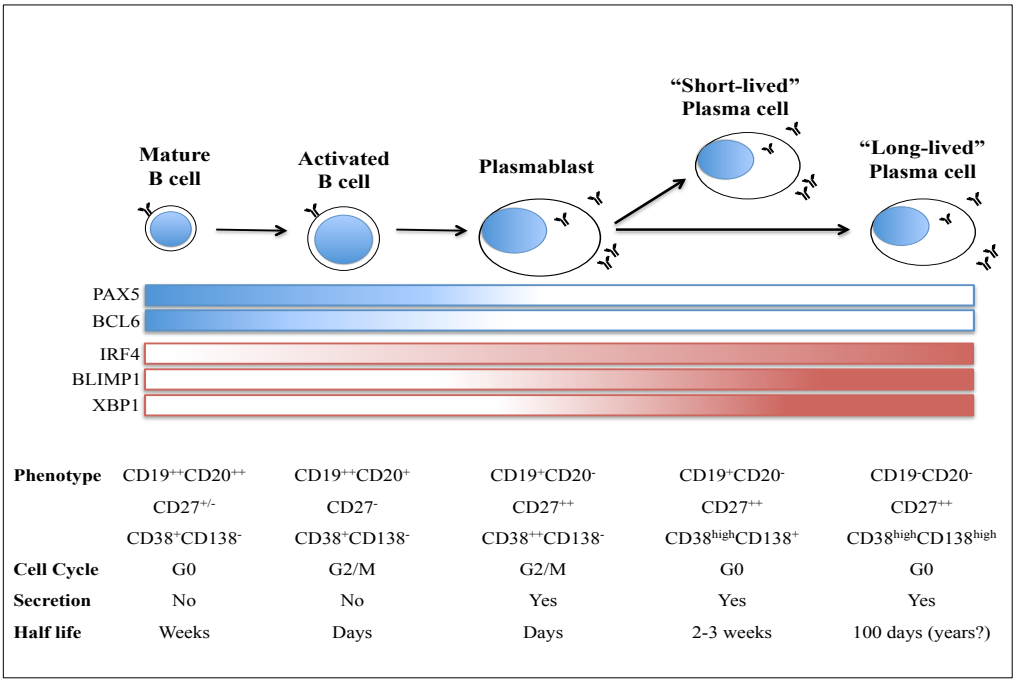


| | | | | | |
|---|---|---|---|---|---|
| **Phenotype** | $CD19^{++}CD20^{++}$ $CD27^{+/-}$ $CD38^{+}CD138^{-}$ | $CD19^{++}CD20^{+}$ $CD27^{-}$ $CD38^{+}CD138^{-}$ | $CD19^{+}CD20^{-}$ $CD27^{++}$ $CD38^{++}CD138^{-}$ | $CD19^{+}CD20^{-}$ $CD27^{++}$ $CD38^{high}CD138^{+}$ | $CD19^{-}CD20^{-}$ $CD27^{++}$ $CD38^{high}CD138^{high}$ |
| **Cell Cycle** | G0 | G2/M | G2/M | G0 | G0 |
| **Secretion** | No | No | Yes | Yes | Yes |
| **Half life** | Weeks | Days | Days | 2-3 weeks | 100 days (years?) |

**Figure-1.2: The figure depicts the various stages of differentiation from B-cell to mature PC, including the associated transcriptional factor expression profile (PAX5, BCL6 in blue boxes and IRF4, BLIMP1, XBP-1 in red boxes, characteristic surface phenotype, cycle status, immunoglobulin secretory activity and half life (adapted from Dr. Gina Doody).**

#### 1.1.1.1 Factors that maintain the B-cell program

The establishment of the B-cell fate as discussed in part 1.1 reflects the sequential action of TFs that together determine B-cell specification, and repress alternate cell fate decisions. In cooperation with other factors such as PU.1, EBF1 and E2A, PAX5 is required for maintaining the B-cell program in mature B-cells. Moreover, it is required for B-cell activation through regulation of its target genes such as *CD79a* (Igα), *CD19* and *BLNK* (B-cell linker) that are important for BCR signalling (16, 19-21). An additional role is the repression of *XBP1* that is crucial for plasma cell differentiation (13). Thus PAX5 maintains B-cell identity and inhibits plasma cell formation.

Somatic hypermutation and affinity maturation is a critical feature of the B-cell lineage, and formation of GCs is tightly controlled. BCL6 is the central transcriptional regulator of the GC (12, 13). It is present at high level in GC B-cells, and BCL6 deletion prevents GC formation (13, 22). BCL6 acts in several ways including suppression of *BCL2* to promote a pro-apoptotic environment facilitating affinity maturation (16) and represses the exit of B-cells from the GC. This is achieved by repressing *IRF4* and *BLIMP1*, the two transcription factors essential for PC differentiation, hence preventing the progression to plasma cell formation (23, 24). Strong BCR signalling is proposed as the mechanism that removes BCL6 repression of *BLIMP1* and *IRF4* leading to plasma cell progression (23).

#### 1.1.1.2 Factors that maintain the plasma cell program

IRF4 is one of the TFs known to be essential for establishing the plasma cell program. It is a dose dependent TF: expressed at low level in B-cell lineage but higher level upon differentiation (12, 25). It is expressed in activated B-cells before BLIMP1 suggesting it as the initiator of plasma cell formation. In GC B-cells it can supress *BCL6* hence activating BLIMP1. It also directly up-regulates *BLIMP1*, for example following IL-21 stimulation IRF4 binds in

conjunction with phospho-STAT3 to a regulatory region of *BLIMP1* thus, promoting plasma cell formation (26-28).

BLIMP1 (also known as PRDM1) is one of the crucial TFs for plasma cell formation and immunoglobulin (Ig) secretion (12, 13). It is encoded by the *PRDM1* gene (12). It is expressed in all ASCs in mice and human but absent in the early stages of B-cell lineage. In BLIMP1 knockout mice mature plasma cells fail to form indicating its requirement in the terminal differentiation of plasma cells. However in conditional knockout mice, a population of cells expressing IRF4 forms which have weak secretory activity, indicating that BLIMP1 is required for the establishment rather than the initiation of the plasma cell program (12). It regulates plasma cell differentiation through repressing *BCL6* and *PAX5* genes, as well as other aspects of the B-cell program and triggering plasma-cell differentiation by activating XBP1 (12, 13, 19, 24, 25). BLIMP1 is also implicated in driving the exit from cell cycle that accompanies terminal plasma cell differentiation.

The final central regulator of plasma cell differentiation is XBP1. This is a bZIP containing transcription factor, which is an evolutionarily conserved component of the unfolded protein response (UPR) of the endoplasmic reticulum. It is an essential transcription factor that couples B-cell differentiation to expansion of the secretory pathway (12, 29-31). This will be discussed further below.

### 1.2 The Unfolded Protein Response (UPR)

Cells are exposed to many different sources of exogenous or endogenous stress that can impact on the secretory apparatus. The exogenous sources include viruses, hypoxia, radiation, free radicals, toxins, microbial pathogens and nutrient deprivation. On the other hand, the endogenous sources of endoplasmic reticulum stress (ER-stress) principally result from the accumulation of unfolded/misfolded proteins during protein synthesis or due to

a dramatic change in the secretory load placed on a cell (32). The proper folding of the newly synthesized proteins and post-translational modifications are essential for proteins to gain their three-dimensional structure and hence, proper protein function. Therefore, all organisms have developed mechanisms to ensure proper protein folding (33, 34).

The endoplasmic reticulum (ER) is responsible for protein synthesis, folding and posttranslational modifications. There are several conditions known to interfere and affect protein synthesis and folding such as calcium depletion, oxidative stress, hypoglycaemia and hypoxia that lead to the formation of misfolded/unfolded protein. These accumulate in the ER and result in ER stress. ER stress if not resolved will cause cellular damage. However, the ER responds to such stress by activating a series of pathways together known as the UPR (34-36). This evolutionarily conserved response was firstly described in yeast cells, which has only one UPR signalling pathway (IRE1; inositol-requiring enzyme-1 coupled to HAC1p the ortholog of XBP1). Higher eukaryotes have evolved two additional UPR-components PKR-like endoplasmic reticulum kinase (PERK), and activating transcription factor 6 (ATF6) (35). Together these comprise the three principal ER-stress transducers (32, 37).

The UPR is an adaptive response, and the accumulation of misfolded proteins in the ER activates the UPR to attenuate translation hence decreasing the ER load. Additionally, activation of the UPR leads to the induction of genes encoding ER-chaperones that are required for proper protein folding. Furthermore, the activation of the UPR is crucial for enhancing the degradation of accumulated misfolded proteins in the ER via ER-associated degradation (ERAD) (33, 35).

### 1.2.1 UPR signalling pathways

In the absence of ER-stress, IRE1, PERK and ATF6 proteins remain inactive bound to the immunoglobulin heavy chain binding protein (BIP; also known as GRP78 and HSPAS). The accumulation of misfolded proteins causes ER-stress leading to the binding of BIP to the misfolded proteins and its consequent dissociation from IRE1, PERK and ATF6 (32, 33, 37-39). However, release from BIP, at least from IRE1 and PERK, is not sufficient to trigger the UPR signalling cascade. Structural studies of yeast Ire1 identified a groove in the luminal domain, similar to that found in MHC molecules, that facilitates direct binding with unfolded proteins (40) Additional functional studies provided evidence that Ire1 is directly activated by increased level of unfolded proteins and the function of BiP is to stabilize inactive monomeric Ire1 in the steady state (41, 42). By inference, the structural similarity of the PERK ER luminal domain suggests it is also likely to be activated by directly binding to unfolded proteins (43).

#### 1.2.1.1 IRE1

IRE1 is a type-1 transmembrane protein of about 110 kDa. In mammals, two homologs of yeast Ire1 have been identified; IRE1α and IRE1β. The former is highly expressed in pancreas and placenta whereas the latter is mainly expressed in intestinal epithelial cells. Although they have comparable cleavage, specificity suggesting that they recognise the same substrate, they differ in their tissue expression (32, 33, 38).

IRE1 has endoribonuclease and kinase activities. Misfolded proteins in the ER bind directly to IRE1 through a groove in its luminal domain and trigger BIP dissociation, stimulating IRE1 auto-phosphorylation and homo-dimerization which in turn activates its endoribonuclease activity to splice a 26 nucleotide sequence from *XBP1* mRNA (the only known substrate for IRE1) (Figure-1.3) (32, 33, 38). This results in a translational frame-shift, which produces a larger

form of XBP1 (spliced XBP1; XBP1s) of 376 amino acids that translocates into the nucleus and activates its target genes. In contrast, unspliced XBP1 (XBP1u) encodes a short-lived protein, which is composed of 261 amino acids.

#### 1.2.1.2 PERK

PERK is a type-1 transmembrane protein that in resting cells is bound to BIP in a similar manner to IRE1. However, upon the accumulation of misfolded proteins, the PERK kinase is activated and undergoes auto-phosphorylation following BIP dissociation. Moreover, due to the structure similarities in the luminal domain between IRE1 and PERK, it has been found that the unfolded proteins can bind directly to it through a groove in its luminal domain and also influence it activation (43) (Figure-1.3). This leads to the phosphorylation of eIF2α (eukaryotic initiation factor 2 on α subunit), which results in translation attenuation, hence decreasing the load that is made on the ER.

On the other hand, activating transcription factor 4 (ATF4) escapes suppression by PERK resulting in its preferential translation and activation of some UPR target genes such as growth-arrest DNA damage gene 34 (GADD34).

#### 1.2.1.3 ATF6

This type 2 transmembrane protein has two mammalian homologs: ATF6α (90kDa) and ATF6β (110kDa). ATF6 has both a nuclear and Golgi localisation signal but is retained in the ER by interaction with BIP. Upon accumulation of unfolded proteins in the ER, BiP dissociates from ATF6α allowing its Golgi localisation. In the Golgi ATF6 is then cleaved via S1P (site 1 protease) and S2P (site 2 protease). S1P cleaves the luminal domain of ATF6 while S2P cleaves the N-terminus of ATF6. The final cleavage releases the 50-kDa cytosolic fragment of ATF6α, which then translocates into the nucleus and activates its target genes such as *BiP* and *XBP1* (Figure-1.3) (32, 33, 38).

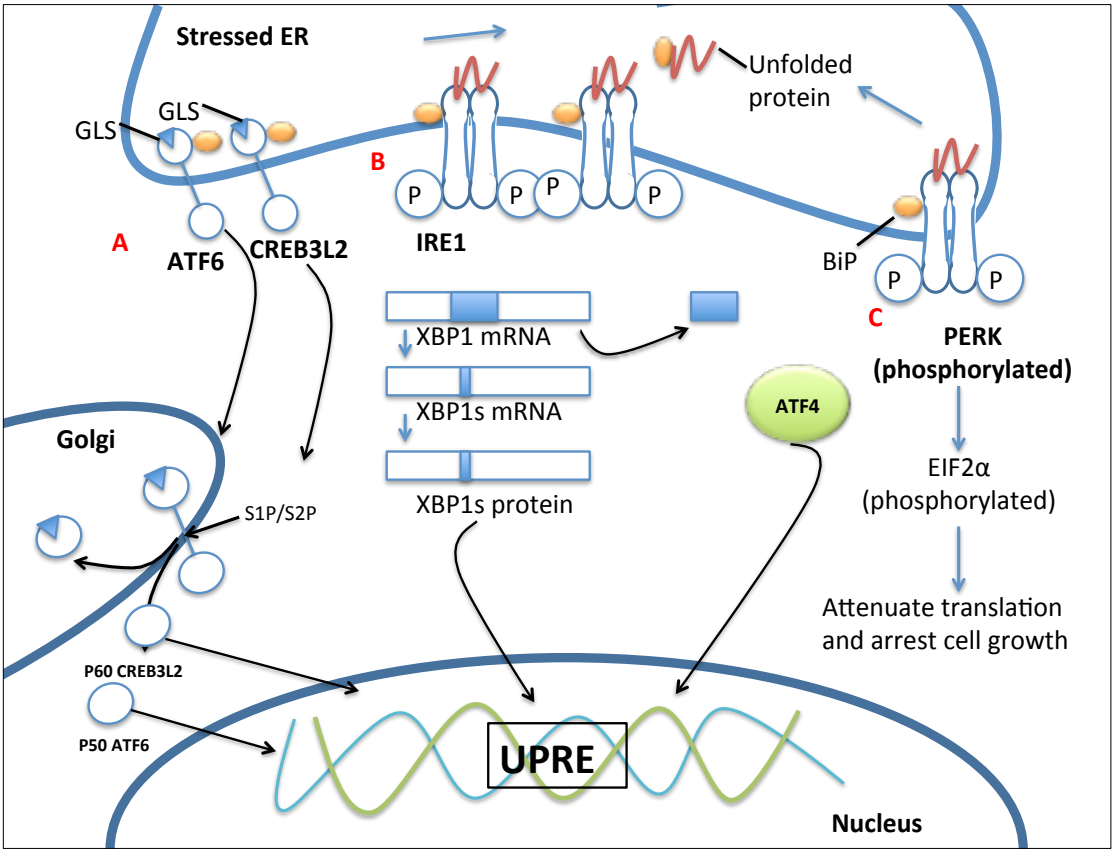


**Figure-1.3: The three axes of the mammalian UPR.** Misfolded proteins in the ER directly bind to IRE1 and PERK as well as causing BiP to dissociate from the attached proteins (ATF6, IRE1 and PERK) that stimulate A, B and C pathways; **A.** ATF6 migrates to the Golgi and is cleaved via S1P/S2P. The cleaved p50 ATF6 translocates in to the nucleus and activates its target genes. CREB3L2 has a similar regulatory pathway as ATF6, producing p60 that migrates to the nucleus to activate its target genes **B**. IRE1 phosphorylates and causes splicing of *XBP1* mRNA. The spliced form of XBP1 translocates in to the nucleus and activates its target genes. **C**. PERK phosphorylates and causes the phosphorylation of EIF2α leading to attenuate translation and arrest cell growth hence decreasing the load on ER. However, ATF4 escapes that repression and translocates to the nucleus and activates its target genes (5).

### 1.3 Role of the UPR in B-cell differentiation

Plasma cells are terminally differentiated antibody secretory cells arising from B-cells. The unique feature of plasma cells is the ability to secrete immunoglobulins, which increase throughout the differentiation. To accommodate the huge amount of the secreted immunoglobulins, plasma cells have increased the ratio of the cytoplasm to nucleus to accommodate the enlarged ER (16, 44). Such large amounts of the secreted immunoglobulins may increase the load on ER and cause ER-stress. However, plasma cells have adapted a physiological response to ER-stress called the UPR. The UPR is required for the proper function and survival of secretory cells such as plasma cells, pancreatic β cells, chondrocytes and skeletal muscle cells, acting by increasing the expression of ER chaperones and folding enzymes while at the same time decreasing protein synthesis or even commencing cell cycle arrest to reduce the load on ER (30, 45). In the case of plasma cells, the stimulation of an UPR induces the expression of heat shock protein BiP/GRP78, which is required for proper folding of the immunoglobulins (16, 46, 47). In addition, UPR activation in plasma cells triggers IRE1 release from BiP hence, XBP1 splicing to form XBP1s that is known to be one of the most crucial modulators in plasma cell differentiation(16, 48).

Early reports indicated that the UPR is required for B-cell differentiation in response to LPS (lipopolysaccharide) (44, 49) however, the precise link was not known until 2001 when Reimold et al. (31),found that XBP1 is expressed in myeloma cell lines, splenic B-cells and in plasma cells in vitro in response to LPS stimulation. The important role of XBP1 in terminal B-cell differentiation was subsequently confirmed by the demonstration that ectopically expressed XBP1s can restore antibody secretion in *Xbp*1$^{-/-}$ B-cells (29). Additionally, using a CH12 B-cell line model, p50ATF-6α and XBP1s were induced as B-cells differentiated to antibody secretory cells in response to LPS (50). However, in the same model CHOP was not induced. These results suggested that certain components of the UPR such as IRE1 and ATF6 are

important in B-cell differentiation, but that PERK might be dispensable (30, 50). The lack of PERK involvement was corroborated in a study demonstrating that PERK was not activated during B-cell differentiation in response to LPS and that B-cells deficient in PERK develop normally and secrete immunoglobulins (51). Furthermore, the role of ATF6 in plasma cell differentiation is also questionable. Splenic B-cells from *Atf6*$\alpha^{-/-}$ mice produced normal levels of immunoglobulin when stimulated with LPS in vitro and the mice mounted normal antibody responses in vivo when challenged with either T-D or T-I antigens (52).

The activation of IRE1 and PERK during the UPR shows similar kinetics in most cell types studied (53) ,prompting the question of how the pathways are differentially controlled during B-cell differentiation. Possible explanations are the presence of a negative regulator of PERK, such as p58 IPK or that a higher threshold is required for PERK activation compared to IRE1 (51).
Interestingly, the UPR also intersects with TLR signalling pathways in cells of the immune system, providing scope for modifying the UPR in the context of different types of infections (54).

**1.4 UPR in B-cells: The overload model**

XBP1 is an important transcription factor for B-cell development (31, 39, 55, 56). The Glimcher lab was the first to describe the role of XBP1 in plasma cell differentiation starting from the observations that the level of XBP1 was high in the absence of PAX5 in pre-pro-B cells thus PAX5 was identified as having a negative regulatory effect on XBP1 in the early stages on B-cell development (55). This was followed in the work of Reimold et al 2001 on the role of XBP1 on plasma cell formation using chimeric mice reconstituted with XBP1 deficient bone marrow (31). These experiments showed that XBP1 deficiency resulted in profound reduction in plasma cell number and immunoglobulin secretion, suggesting that XBP1 plays a crucial role in the differentiation of B-cells to plasma cells (31). This was followed by a further study confirming the

role of XBP1 in plasma cell differentiation and linking it with UPR by Iwakoshi et al 2003. This work found that XBP1s was required to restore Ig production in *Xbp1*$^{-/-}$ B-cells. Moreover, XBP1 was required to handle the huge amount of Ig secreted through activation of the UPR and IRE1 dependent splicing of *XBP1* (57).

These combined findings led to a secretory overload model of UPR activation during plasma cell differentiation. Two cytokines IL-4 and IL-6 that promote plasma cell differentiation were linked to *XBP1* expression (57). An auto-regulatory loop was proposed between XBP1 and IL-6 that links UPR with plasma cell differentiation (29, 57). This model starts with B-cell activation by anti-CD40, BCR and IL-4 driving the B-cell to proliferate, differentiate and secrete immunoglobulins. The increase in expression and switch to secretory form of immunoglobulins leads to accumulation of unfolded protein in the ER, inducing a UPR through IRE1 splicing of *XBP1*. This produces an adaptive response to reduce the load on ER in the activated B-cells through expansion of the ER to accommodate the secreted immunoglobulins. Once XBP1s is formed, it induces the production of IL-6, which in turn induces plasma cell proliferation and Ig secretion (Figure-1.4) establishing a loop (29).

Additional work from the Staudt lab established a relationship between BLIMP1 and XBP1 by gene expression profiling in BLIMP-1 deficient and XBP1 deficient mice (58). The profiles revealed that BLIMP1 acts upstream of XBP1 in a de-repression model. PAX5 represses *XBP1* in activated B-cells, but BLIMP1 represses *PAX5* hence removing the repressive action of PAX5 on *XBP1*. Thus BLIMP1 dependent repression of *PAX5* allows expression of XBP1 and a productive UPR required for Ig secretion. This suggests a dependence of XBP1 on BLIMP1 expression. This relationship was confirmed in by the finding that BLIMP1 was induced in the *Xbp1*$^{-/-}$ cells whereas; XBP1 was not induced in the *Blimp1*$^{-/-}$ cells indicating that XBP1 is downstream of BLIMP1 (58).

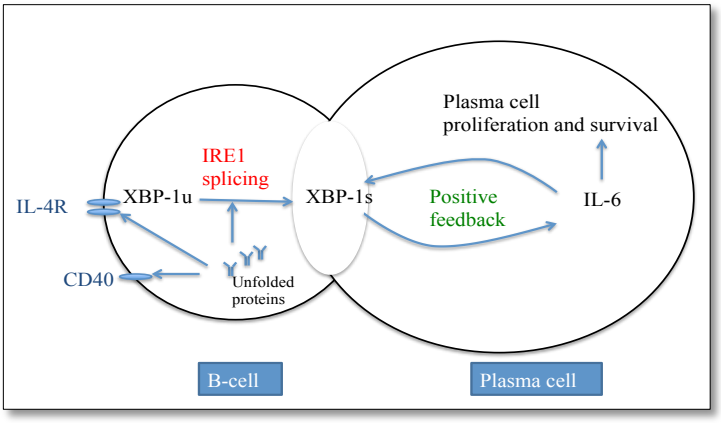


**Figure-1.4: Auto-regulatory loop between XBP1 and IL-6.** This model provides a link between plasma cell differentiation and the UPR, starting with the initial stages of differentiation leading to an increase in the secretory capacity and load on ER. The accumulation of large amounts of immunoglobulin in the ER induces a UPR and activates IRE1 splicing of XBP1. Once XBP1s is formed, it induces the production of IL-6, which in turn induces plasma cell proliferation and Ig secretion establishing a loop (8).

## 1.5 The UPR in B-cells: Conflicting results, the high-secretory model

More recently the central role of the UPR in plasma cell differentiation has been challenged. There were several conflicting results related to XBP1. The first results emerged from the Ploegh lab, which found that XBP1 was essential for IgM translation but was not required for other glycoprotein production or degradation in B-cells induced to differentiate upon LPS stimulation (56). In subsequent work from the same lab, it was found that activation of XBP1 occurred normally in B-cells lacking any secreted IgM indicating that XBP1 activation was a differentiation-dependent event not due to the accumulation of secreted Igs, and thus in conflict with the predictions of the overload model (39).

Furthermore using a B-cell conditional knockout mouse, the Glimcher lab found that XBP1 was not required for the early stages of plasma cell differentiation including phenotypic maturation but was required for high-level

immunoglobulin secretion (5). These data have been additionally corroborated in the work of Taubenheim et al., 2012 who showed that XBP1 deficiency did not affect plasma cell number using $Xbp^{fl/fl}Cd19^{cre/+}$(fl/fl) mice (6). They also found that XBP1 does not function as a key regulator in establishing plasma cell differentiation.

However in both studies, absence of XBP1 affected plasma cell capacity to establish a normal secretory apparatus and secrete high immunoglobulins levels confirming that XBP1 does have a principal role in controlling the primary function of plasma cells (6).

Currently, it is not known whether XBP1 acts alone during plasma cell differentiation or whether there are other factors that may cooperate and compensate when it is deficient. The evidence so far is that PERK and ATF6α are not important in the physiological B-cell UPR (51) (52). However, it remains unclear whether ATF6β can substitute for the loss of ATF6α. In yeast, Ire1 is the only UPR sensor, while plants additionally have two ATF6-like proteins that are processed by S1P/S2P cleavage (59). In plants the activation of S1P/S2P can be triggered by a number of additional stress stimuli, including heat shock and changes in salt concentration. Interestingly, in higher eukaryotes the S1P/S2P pathway of regulation is shared with a number of other transcriptional regulators such as SREBP and the CREB3 family.

**1.6 S1P/S2P**

The ATF6 pathway of the UPR is controlled by the induced translocation of ATF6 to the Golgi and its regulated intramembrane proteolysis (RIP) via S1P/S2P cleavage at this site. This pathway is shared by ATF6 with SREBP and the CREB3 family (60-65). SREBP (Sterol regulatory element binding protein) (64, 65) is a master regulator of lipid homeostasis (65). In an inactive state, it remains bound to SCAP (SREBP cleavage activating protein) on the

ER membrane (65). However, low sterol levels or high carbohydrates levels trigger the SREBP-SCAP complex to leave the ER and enter the Golgi apparatus to be cleaved by S1P and S2P (64-66). The cleaved SREBP translocates into the nucleus and activates its target genes via Sterol Response Elements (SRE) (64). Thus SREBP shares a very similar pattern of regulation to ATF6. While the role of SREBP in plasma cell differentiation remains to be determined, the target of this project is CREB3L2, which belongs to the CREB3 family of ER-resident transcription factors also activated by RIP (2).

### 1.7 CREB3 subfamily

The CREB3 (cAMP Responsive Element Binding protein 3) subfamily is composed of several transcription factors that contain a bZIP (basic leucine zipper) domain. More than 55 bZIP containing transcription factors have been reported in human. However, due to their sequence similarities in the coiled-coil region, they have been further divided into 16 families and among these is the family composed of OASIS/CREB3L1, BBF2H7/CREB3L2, CREB-H/CREB3L3 and AIbZIP/CREB3L4 (Figure-1.5) (2, 67).

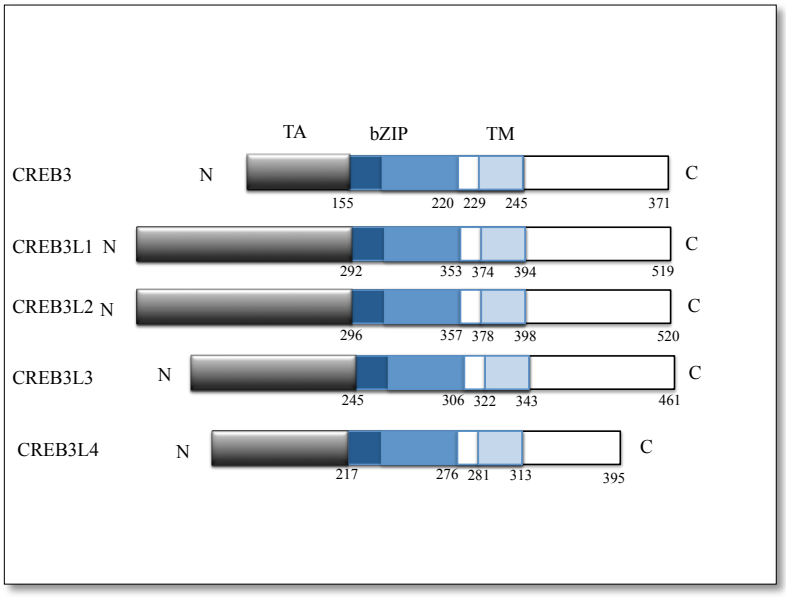


**Figure-1.5: Diagrammatic structure of CREB3 subfamily members**. TA, Transcriptional Activation. bZIP, basic Leucine Zipper domain. TM, Trans membrane domain. N, N-terminus. C, C-terminus (2).

The family of proteins to which CREB3L2 belongs, includes 4 additional members. All of these proteins are controlled by RIP in that they get cleaved at their N-terminus in the Golgi, and their N-termini translocate into the nucleus to activate their target genes and resolve ER stress (2, 67, 68). They differ in their tissue distribution; CREB3L1 is highly expressed in osteoblasts, CREB3L3 in the liver and CREB3L4 in prostate cancer cells (2, 67).

CREB3L1 and CREB3L2 are bZIP transcription factors, forming a chimeric oncoprotein with FUS in low-grade fibromyxoid sarcoma (LGFMS). 95% of LGFMS cases are due to FUS-CREB3L2 7; 16 (q32-34; p11) whereas, only 5% of the cases are due to FUS-CREB3L1 11; 16(p11; p11). CREB3L3 is highly expressed in normal hepatocytes. In addition, it acts as growth suppressor where it is under expressed in hepatocellular tumours suggesting its role in tumorgensis (2). Moreover, it is activated by the UPR through cleavage via S1P/S2P (69). CREB3L4 is induced by androgen and is highly expressed in prostate cancer cells (2). In addition, it is required for the development of germ cells and UPR during spermiogensis (69).

**1.8 CREB3L2/BBF2H7**

The principal focus of this study is CREB3L2, also known as BBF2H7 (Box B Factor 2 Human homology in chromosome 7). It was first identified in the chimeric gene (*Fus/CREB3L2*) in two cases of LGFMS (70-72). Subsequent studies demonstrated that the *FUS/CREB3L2* chimeric gene is specific for the diagnosis of LGFMS (71, 73, 74).

The *CREB3L2* locus spans more than 120 kbp of genomic DNA (12 exons) at chromosome 7q33 (71, 75). It is homologous to CREB3L1, CREB3L3, CREB3L4 and drosophila Bbf-2 in its bZIP domain with the highest similarity to CREB3L1, indicating they may have comparable functions. However CREB3L2 and CREB3L1 have different expression patterns. CREB3L2 is

highly expressed in chondrocytes and placenta but weakly in prostate and colon whereas, CREB3L1 is highly expressed in prostate and pancreas with moderate expression in colon (71).

In work leading up to this project the Tooze and Doody lab have developed an in vitro model of human plasma cell differentiation (4). In a detailed characterisation of gene expression spanning multiple stages of the differentiation, this work identified *CREB3L2* as amongst the genes mostly strongly induced in plasma cells, and distinct from other CREB3 family members (76). The observation that *CREB3L2* is highly expressed in normal plasma cells compared to B-cells has also been confirmed in other studies (8, 77). Furthermore, in the gene expression profiling experiments *CREB3L2* has a similar dynamics to other TFs critical in PC differentiation including *PRDM1* and *IRF4* (figure-1.6 A-B).

Thus *CREB3L2* displays a pattern of regulation concordant with plasma cell differentiation and expansion of the secretory apparatus suggesting a potential role for this CREB3 family member in the differentiation process (4).

**A**

CREB3L2 belongs to a "PB/PC" cluster

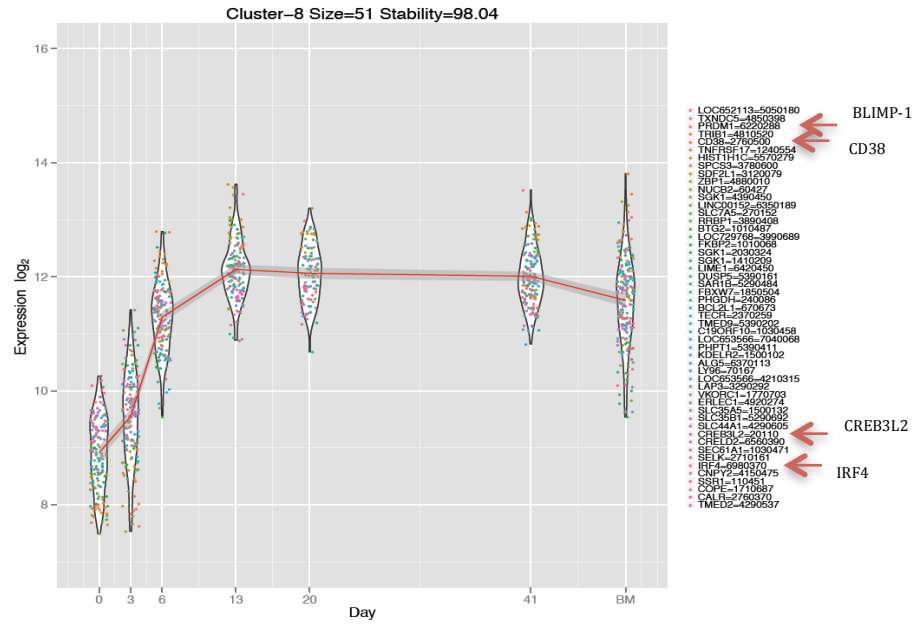


Mario Cocco, Mathew Care

**B**

CREB3L2 expression in PC differentiation

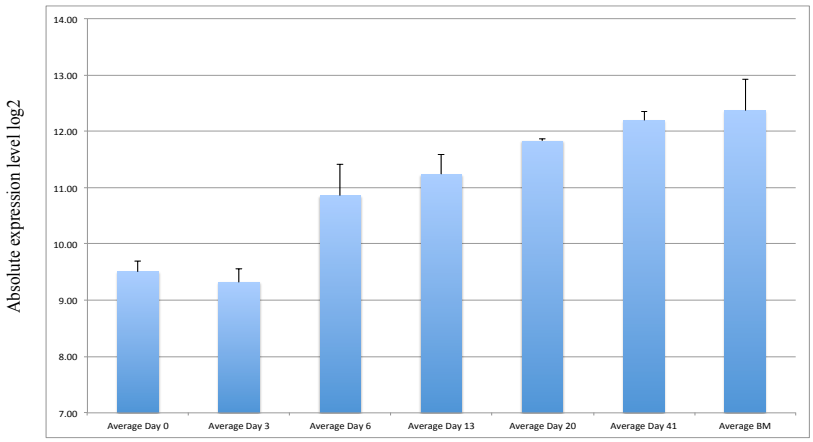


Mario Cocco, Matt Care

5

**Figure-1.6: *CREB3L2* expression in plasma cell differentiation. A**. The kinetic expression pattern of 50 genes forming a PB/PC cluster obtained from timed sampling of in vitro differentiated human B-cells or ex vivo purified plasma cells. **B.** Average *CREB3L2* expression from 3 donors during PC differentiation as determined by microarray (adapted from Mario Cocco and Matt Care).

Both the regulatory inputs driving *CREB3L2* expression and the direct targets of this TF are not fully defined. In developing cartilage, *Creb3l2* is upregulated by the master transcription factor Sox9, which controls chondrocyte differentiation and also regulates expression of cartilage matrix proteins (78). During chondrogenesis, the increased production of cartilage matrix proteins triggers a UPR, resulting in the enhanced processing and stability of CREB3L2. In this setting, CREB3L2 can transcriptionally activate *Sec23a,* which encodes for the Sec23A protein (coat protein complex 2; COPII) required for protein transportation from ER to Golgi (2, 79, 80). The loss of Sec23A in Creb3l2 deficient animals led to an accumulation of ECM proteins in the ER and enhanced ER-stress. *Creb3l2* knockout mice develop severe chondrodysplasia, consistent with a vital role in chondrogensis, and fail to fully develop the chest cavity leading to early death (2, 79).

ATF5 was identified as another target of CREB3L2 in mouse in a genome-wide RNAi screen (81). This study revealed CREB3L2 downstream of RAS-mitogen-activated protein kinase can activate ATF5, which in turn induced MCL1 (anti-apoptotic factor) expression, hence increasing the survival of glioma cells (81). This was followed up in the work of Izumi et al. who confirmed a role for CREB3L2 in controlling ATF5-MCL1 in chondrocytes (82). The findings in this report led to the conclusion that CREB3L2-ATF5-MCL1 may represent a general pathway, which suppresses apoptosis induced by ER-stress (82). Importantly MCL1 is known to be one of the critical determinants of long-lived plasma cells in the bone marrow (83).

### 1.9 cyclic AMP and UPR response elements

A striking feature of the transcription factors involved in the UPR is the usage of related DNA-elements to control partially overlapping sets of target genes. The transcriptional response depends on binding of the individual TF to a specific sequence in promoter or distal gene regulatory element and the subsequent interaction with transcriptional machinery. Understanding how

DNA-occupancy by these factors relates to each other is essential to explain their distinct roles in the UPR and in differentiation (35).

A bZIP domain is shared between the CREB3 subfamily, ATF4, ATF6 and XBP1. These factors nonetheless differ in their DNA-binding specificity. The consensus sequences for the distinct regulatory element recognised by these factors are known as: Cyclic AMP response element (CRE- TGACGTCA), UPR response element (UPRE- TGACGTG (G/A) or the variant CGACGTGG), ER stress response element (ERSE- CCAAT (N9) CCACG), and ER stress response element-II (ERSE-II- ATTGG (N1) CCACG). The CRE represents the canonical element for the CREB/ATF family of bZIP proteins, and the UPRE a motif controlled preferentially by XBP1 as a homodimer, and these are most closely related (84). However both ERSEs and UPREs are enriched amongst sites bound by XBP1 in vivo (85).

ERSEs are bound by either XBP1 or ATF6 at the CCACG component while the general transcription factor NF-Y binds at the CCAAT element. Explaining some functional redundancy between the ATF6 and XBP1 arms of the UPR. While a specific consensus selected by CREB3L2 is not established the known motif data suggest that CREB3L2 is likely to act via canonical CRE sites and thus control a distinct set of regulatory elements, which may partially overlap, with those of XBP1 (35, 85).

In conclusion, the UPR is a critical element for plasma cells to adapt to high secretory activity during terminal B-cell differentiation. However, to date XBP1 is the only known regulator of the UPR that is implicated in plasma cell differentiation. On the other hand, high expression of *CREB3L2* in plasma cells suggests possible involvement of this factor and its regulated cleavage may provide a potential therapeutic target.

### 1.10 Aims

The aim of this project will be to investigate the expression, regulation and function of CREB3L2 in human B-cell differentiation and B-cell tumours.

Specifically:

1. To establish the patterns of CREB3L2 expression during B-cell differentiation and in human B-cell lines.
2. To determine the regulation of CREB3L2 in response to B-cell activation and the unfolded protein response in normal human B-cells and B-cell malignancies.
3. To determine impact of site-1/2 protease inhibition on CREB3L2 and related responses during plasma cell differentiation and in B-cell malignancies.

# 2. Material and Methods

## 2.1 Recombinant DNA techniques

### 2.1.1 Cloning

#### Bacterial strains

The following bacterial strains of E. coli were used:

DH5α: F-Δ*lac*Z ΔM15 Δ(lacZYA-*arg*F) U169 *rec*A1 *end*A1 *hsd*R17($r_K$-$m_K$+) *sup*E44 *thi*-1 *gyr*A96 *rel*A1

BL21 Gold: F- *ompT hsdS* ($r_B$-$m_B$-) *dcm+* Tet *gal endA* Hte

Bacteria were grown in Luria Broth (LB) (1% (w/v) bactopeptone, 0.5% (w/v) NaCl, 0.5% (w/v) yeast extract, pH 7.5) in the presence of the appropriate antibiotic at 37$^{o}$C, or in some instances at 30$^{o}$C, with continual agitation. Transformed stocks of bacteria were additionally maintained on LB agar plates (LB containing 1.5% (w/v) bactoagar).

#### 2.1.1.A pIRES2-EGFP vectors

Human *CREB3L2* (encoding amino acids 1-378 with amino terminal HA-tag) in pUC57 (Genescript), human *ZBTB32* (encoding amino acids 1-502 with amino terminal HA-tag) in pUC57 (Genescript) and pIRES2-EGFP vector (Clontech) were digested using EcoRI (New England Biolabs) and BglII (New England Biolabs) with EcoRI buffer (New England Biolabs). The vector was treated with calf intestinal phosphatase (CIP) (New England Biolabs) to remove the 5' phosphate group required by ligases in order to prevent vector re-ligation. The digested constructs were visualised using 0.8% agarose gel electrophoresis and ethidium bromide (EtBr) staining. Fragments of the correct size were excised from agarose gels, purified using a QIAquick® Gel Extraction Kit (QIAGEN), ligated at room temperature using T4 DNA ligase (Invitrogen) and transformed into DH5α competent cells by incubating at 42$^{o}$C for 2 minutes. DNA from the transformed cells was extracted using a

QIAprep®Spin Miniprep kit (QIAGEN) and checked for the presence of appropriate insert by digestion with *EcoRI* and *BglII*. After that, larger amounts of the constructs were prepared using PureLink™ HiPure Plasmid Filter Midiprep kit (Invitrogen). The constructs' concentration was obtained using a NanoDrop spectrophotometer to determine the $OD_{260}$ (Labtech).

### 2.1.1.B pGEX6P-1 vectors

Human *CREB3L2* (encoding amino acids 1-378) in pUC57 (Genescript), human *ZBTB32* (amino acids 1-117) in pUC57 (Genescript) and pGEX6P-1 vector were digested by BamHI (New England Biolabs) and SalI (New England Biolabs) with BamHI buffer (New England Biolabs). The vector was CIP treated and resulting fragments were visualised using 0.8% agarose gel electrophoresis and EtBr staining.

Then the required fragments were purified using a QIAquick® Gel Extraction Kit (QIAGEN), ligated at room temperature using T4 DNA ligase (Invitrogen) and transformed into competent DH5α or BL-21 Gold cells. DNA from the transformed cells was prepared using a QIAprep®Spin Miniprep kit (QIAGEN) and checked by digestion with BamHI and SalI. After that, larger amounts of the constructs were obtained using a PureLink™ HiPure Plasmid Filter Midiprep kit (Invitrogen). The constructs' concentration was obtained using a NanoDrop spectrophotometer (Labtech).

### 2.1.2 Agarose gel electrophoresis

0.8 % (w/v) of agarose was dissolved in 1X TBE buffer (89mM Tris-base, 80mM boric acid, 2mM EDTA) with the addition of 2 drops of ethidum bromide (0.625mg/ml, Fisher Scientific). DNA mixed with buffer containing 40% sucrose, 30% (v/v) glycerol, 0.25% (w/v) xylene cyanol FF and 0.25% Bromophenol blue was loaded into the gel and run at 90 volts. A molecular weight ladder (1Kb+; Invitrogen) was used to assess the DNA product size and visualised using the Geldoc XR system (Bio-Rad).

## 2.2 Cell culture

### 2.2.1 Cell lines

The human cervical epithelial cell line Hela was used for transfections and evaluation of vectors generated in the course of this study. Human multiple myeloma cell lines (U266 and H929) were obtained from the American Type Culture Collection (ATCC). Human B-cell lines OCI-LY3 and OCI-LY10 representative of activated B-cell type diffuse large B-cell lympoma were a gift of Dr Eric Davis. Cells were routinely cultured in RPMI-1640 medium (Sigma) containing 10% heat-inactivated fetal calf serum (HIFCS, Invitrogen) and L-glutamine.

**Population and ethics**

Whole blood obtained from healthy volunteer donors was collected in EDTA tubes after informed consent. Approval for this study was provided by U.K. National Research Ethics Service via the Leeds East Research Ethics Committee (approval reference: 07/Q1206/47).

### 2.2.2 In vitro generation of human plasma cells

**Buffers:**

- MACS buffer no preservative, 10 % BSA
- 20 units/ml hIL-2: STOCK, 10,000 units/ml
- 50 ng/ml hIL-21: STOCK, 100 μg/ml
- 10 μg/ml F(ab)2: STOCK, 1.2 mg/ml
- 20 μl/ml Amino acids: STOCK, 50X
- 5μl/ml Lipid mix: STOCK, 200X
- 11 μl/ml Tx Hybridoma
- 10 ng/ml hIL-6: STOCK, 100,000 ng/ml
- 100 units/ml INF-γ: STOCK, $1X10^7$ units/ml

**Irradiated CD40L-expressing murine L cells**

Murine L cells stably transfected with human CD40L were seeded in Iscove's Modified Dulbecco's Medium (IMDM) with 10% HIFCS in to one T175 flask and placed in a humidified incubator maintained at 37$^{o}$C and 5% $CO_2$. Two days later, the cells were trypsinised and split into four T175 (1:6). After two days, the cells were trypsinised and passed through a cell strainer into 2X 50 ml falcon tubes to avoid clumps. Then the cells were counted using trypan blue and re-suspended with IMDM/10%HIFCS so that each falcon tube should not contain more than $10^8$ cells. After that, the cells were irradiated in ice 2 times, 25 Gray for 45 minutes with gentle mixing in between. Next, 100 μl of the cells were used to check CD40L expression by flow cytometry using CD154 antibody. Then, 1X$10^6$ of irradiated murine L cells expressing human CD40L were prepared in 1.5 ml freezing vials and stored at -80$^{o}$C.

Seeding of irradiated CD40L-expressing murine L cells: 24 h prior to processing the blood samples, 1 vial of irradiated CD40L cells (according to the number of the donors) was thawed and washed with 10 ml of IMDM complete media. Then, the cells were re-suspended with 12 ml of fresh complete IMDM media and plated into a 24-well plate (0.5 ml/well; 6.25 X $10^4$/well). The plate was placed in the 37$^{o}$C humidified incubator with 5% $CO_2$.

**Day-0**

50 ml of human peripheral blood was collected in EDTA (EK3) tubes and diluted 1:2 with room temperature phosphate buffered saline (PBS). Then, 17 ml of lymphoprep reagent was added to a 50 ml falcon tube and 34 ml of the diluted blood was slowly added on top of the lymphoprep. The tubes were centrifuged 2400rpm/ 1114 x *g* for 20 minutes at 18$^{o}$C using an acceleration value of 5 and no brake in an Eppendorf 5810R centrifuge. After centrifugation, the buffy coat was isolated and transferred to a 50 ml tube and

washed three times; twice with cold PBS and once with MACS buffer (1x PBS, 0.5% FCS, 2mM EDTA) and centrifuged at 1500 rpm for 10 minutes. Next, the total peripheral blood mononuclear cells (PBMCs) were counted using trypan blue. B-cells were isolated by magnetic labelling using a memory B-cell isolation kit (composed of biotin antibody cocktail against CD2, CD14, CD16, CD36, CD43, CD235a (GlycoprotienA) and microbeads; Miltenyi Biotech). Then, the cells were separated using an LD Column in a magnetic field in MACS buffer. The cells were counted and re-suspended in IMDM media to give 2.5 X $10^5$/ml/well. 0.5 ml of IMDM media with 2X cytokines and anti-B cell receptor (IL-2 ($n^2$ X 20/10000, Roche), IL-21 ($n^2$ X 50/100000, PeproTech) and $F(ab)_2$ ($n^2$ X 10/1200, Jackson ImmunoResearch) and 0.5 ml of cells in IMDM were added to each well with CD40L cells and placed in the 37$^o$C humidified incubator with 5% $CO_2$.

**Day-3**

The cells were collected from the wells and counted using trypan blue. The cells were re-suspended with IMDM media/10%FCS with 1X supplements (IL-2 (n X 20/10000), IL-21 (n X 50/100000, PeproTech), amino acids (n X 1/50, Sigma), TX-HYB (n X 11µl/ml, Gentaur) and lipids (n X 1/200, Sigma) and re-seeded at density of 1X$10^5$/well in to a 24-well plate.

**Day-6**

The cells were collected from the wells and counted using trypan blue. The cells were re-seeded into a 12-transwell plate using conditioned media obtained from cultured M210B4 cells and specific supplements (IL-6 ($n^2$ X 10/100000, Sigma), IL-21 ($n^2$ X 50/100000, PrproTech), amino acids ($n^2$ X 1/50, Sigma), TX-HYB ($n^2$ X 11µl/ml, Gentaur), INF-α ($n^2$ X 100/10000000, Sigma) and lipids ($n^2$ X 1/200, Sigma) at cell density of 5 X $10^5$/well.

After day-6: The cells can be re-seeded at day-10 or 13 or 20 using the same conditions as day-6.

**Induction of the unfolded protein response**

The endogenous expression (full-length and cleaved forms) of CREB3L2 was studied in the U266 myeloma cell line using reagents know to generate ER-stress: thapsigargin and DTT. Live cells were counted using a Hemacytometer and trypan blue dye. $1X10^6$ cells were spun at 1500 rpm for 5 min and re-suspended with 11 ml of fresh RPMI-1640 media and distributed in to seven $25cm^2$ flasks (1.5 ml each). After that, 1 µM thapsigargin and 1mM DTT were prepared in RPMI-1640 media. 1.5ml of each ER-stressor or media alone was added to the corresponding flask and incubated at $37^oC$ for the indicated time (t=0 or unstressed, 2h, 4h or 6h). At each time point, the cells were washed once with PBS and re-suspended with 50 µl 2X sample loading buffer containing the reducing agent 2-mercaptoethanol, boiled for 15 minutes and loaded on to a 10% SDS-PAGE gel and subsequently evaluated by Western blotting.

### 2.2.3 Plasmid transfection

The CREB3L2-pIRES2EGFP construct was checked by transfecting it into Hela cells. Prior to transfection, the cells were split into 6-well plates and grown until they reached 80% confluence. The construct was then introduced into the cells using the Gene Juice transfection reagent (Novagen) according to the manufacturer's instructions. Briefly, for each well a ratio of 1 µg of purified plasmid DNA was mixed with 3 µl of Gene Juice reagent prior incubation with the cells. GFP expression was checked by fluorescence microscopy 24-48 hours post transfection.

### 2.2.4 siRNA-mediated knockdown

CREB3L2 was knocked-down using Amaxa nucleofection technology. 2 X $10^6$ myeloma cells were used per nucleofection and resuspended in solution V containing either 400 or 600 pmoles of siRNA. Transfection was accomplished using the D.023 program on the Amaxa nucleofector. Cells were then added to 4 ml complete RPMI-1640 media and incubated for 24 hours and 48 hours (table-6). The siRNAs used were CREB3L2 siRNA 1 (s34890), CREB3L2 siRNA 2 (s34891), and scramble/negative control (catalogue number 4390843) purchased from ThermoFisher.

Human B-cells were isolated from normal donors and cultured using the in vitro generation of mature plasma cells protocol up to day-3. CREB3L2 was knocked down in the day-3 B-cells using a human memory B cell kit from Lonza . 2 X $10^6$ human B-cells were used per nucleofection with 400 pmoles of siRNA. Cells were transfected using the U.015 program on the Amaxa machine and then added to 4 ml IMDM media with supplements (Il-2, Il-21, amino acids, lipid mix and TX-HYB) into a 6-well plate and incubated for 24 hours and 48 hours (table-6). A second attempt was performed using 600pmoles of CREB3L2 siRNA 1 and or 2.

## 2.3 Techniques for protein analysis

## Glutathione S transferase (GST)-fusion proteins expression and purification

### 2.3.1 Small scale GST-fusion protein production

Small scale GST-CREB3L2 fusion protein production was attempted first to check CREB3L2 expression from several bacterial strains (DH5α and BL21-Gold). Transformed bacteria was used to inoculate 3 ml of Luria Broth containing 100 µg/ml ampicillin (LB-Amp) (Starter culture) and grown at 37$^{o}$C for 24 hours. Then, 750 µl of bacterial culture was diluted in to 10 ml LB-Amp and grown until it reached an $OD_{600}$ of 0.6-0.8. Then the culture was induced with 10 µl 0f 100 mM Isopropyl β-D-1- thiogalactopyranoside (IPTG) for 2 hours and spun at 15000g, 4$^{o}$C to sediment the bacteria. After that, the pellet was re-suspended with cold PBS and sonicated (10 seconds, 4 bursts at 5 microns) to release the protein from the cells. Then the sample was centrifuged at 15,000g, 4$^{o}$C to separate the soluble from the non-soluble proteins. After that, 50 µl of pre-washed 50% Glutathione Sepharose$^{TM}$ 4B (GE Healthcare) was added to the soluble protein and incubated overnight on a rotating wheel at 4$^{o}$C. Then, 15 µl of the sample was mixed with 15 µl of 2X sample loading buffer (10mg bromophenol blue, 15ml 20% SDS, 10ml glycerol, 12.5ml upper tris and 12.5ml $dH_2O$) containing the reducing agent 2-mercaptoethanol, boiled for 5 min and loaded on to a 10% SDS-polyacrylamide gel (Table-1). The gel was stained with Coomassie Blue protein stain for 30 minutes and de-stained with 45% methanol/45% acetic acid. Finally, the gel picture was captured using Geldoc XR (Biorad).

### 2.3.2 Large scale GST-fusion protein production

To generate large-scale protein production, 10 ml of LB-Amp was inoculated with transformed bacteria (Starter culture) and grown at 37$^{o}$C for 24 hours. Then, 10 ml of bacterial culture was diluted into 1000 ml LB-Amp and grown at 37$^{o}$C until it reached an $OD_{600}$ of 0.6-0.8. Then the bacteria were induced

with 1ml of 100mM IPTG for 2 hours and spun at 4$^{o}$C to harvest the bacteria.

After that, the pellet was re-suspended with cold PBS and sonicated (20 seconds, 7 bursts at 5-10 microns). To enhance protein solubility, 200 µl of Triton® X-100 (Sigma) was added to the protein and incubated for 1 hour at 4$^{o}$C on a rotating wheel. Then the sample was centrifuged and the supernatant was transferred into a tube containing 1 ml of pre-washed 50% Glutathione Sepharose$^{TM}$ 4B (GE Healthcare) and incubated for 1 hour on a rotating wheel at 4$^{o}$C. Then, the protein was purified by column chromatography and eluted with GST elution buffer (10 mM reduced glutathione, 50 mM Tris pH 8.0). Then, 15 µl of the sample and 15 µl of 2X reducing sample buffer was boiled and loaded on to a 10% SDS-polyacrylamide gel (Table-2.1). The gel was stained with Coomassie Blue protein stain for 30 minutes and then de-stained. Finally, the gel picture was captured using Geldoc XR. The GST-CREB3L2 fusion protein was concentrated using a centricon filter (Milipore Amicon Bioseparations).

**Table-2.1:** The composition of 10% Polyacrylamide gel

| | **Tris Buffer** | **$dH_20$** | **Poly-acrylamide 30% (w/v) Acrylamide Bis: 0.8% (w/v)** | **10% APS (1g/10ml)** | **Temed (FW 116.2)** |
|---|---|---|---|---|---|
| Resolving gel | Lower (1.25ml) 1.5M Tris pH8.8 0.4% SDS | 2.05ml | 1.7ml | 30µl | 5µl |
| Stacking gel | Upper (1.25ml) 0.5M Tris pH6.8 0.4% SDS | 3.25ml | 0.5ml | 30µl | 5µl |

### 2.3.3 Western blot evaluation

Cells were lysed by RIPA buffer (50 mM Tris pH 7.4, 150 mM NaCl, 1 mM EDTA, 1% NP40, 0.5% sodium deoxycholate, 0.1% SDS with the addition of protease inhibitors), loaded on to 10% or 12% SDS-polyacrylamide gel (Table-2.1) and transferred to nitrocellulose membrane (0.45 micron; Thermo Scientific) using transfer buffer (25 mM Tris, 192 mM Glycine and 20% Methanol) with 100 volts for 1 hour. The quality of transfer was assessed by Ponceau stain (0.2% ponceau/3% trichloroacetic acid). Then, the membrane was blocked using blocking buffer (1% non-fat milk/PBS/0.01%Tween® 20) for 1 hour at room temperature. Primary antibodies were diluted in buffer containing 2%BSA/PBS/0.01% Tween® 20 using the recommended dilutions (Table-2.2) and incubated with the membrane on a rocking platform for 1 hour at room temperature. After that, the membrane was washed 3 times (20 minutes each) with the wash buffer (1% PBS/0.01% Tween® 20). The secondary antibody was diluted in the blocking buffer and applied to the membrane for 30 minutes at room temperature on a rocking platform. Then, the membrane was washed 3 times with the wash buffer and treated with Supersignal® West Pico Chemiluminescent substrate (Thermo Scientific) for 5 minutes. The membrane was exposed to film (Amersham Hyperfilm$^{TM}$ECL; GE Healthcare) and developed using X-ray developer (SRX-101A)**.**

**Table-2.2:** Antibodies used in Western blotting

| **Antigen** | **Company** | **Target** | **Recommended dilution** | **Secondary antibody** |
|---|---|---|---|---|
| CREB3L2 | Abcam | HA-tag | 1:10,000 | Goat anti-rabbit 1:20,000 |
| CREB3L2 | Aviva | N-terminus | 1:1000 | |
| CREB3L2 | Novus Biological | N-terminus | 1:500 | |
| CREB3L2 | ProteinTech | N-terminus | 1:500 | |
| CREB3L2 | abcam | C-terminus | 1:1000 | |
| XBP1s | Biolegend | N-terminus | 1:500 | |
| ATF6 NBP1-40256-0.1mg | Novus Biological | N-terminus | 1:500 | Goat anti-mouse 1:20,000 |
| SREBP1 (2A4) ab3259 | abcam | N-terminus | 1:1000 | |
| SREBP1 ab135133 | abcam | N-terminus | 1:1000 | Goat anti-rabbit 1:20,000 |
| Actin A1978 | Sigma life science | N-terminus | 1:100,000 | Goat anti-mouse 1:20,000 |
| Atg3 | Signalling | Atg3 | 1:1000 | Goat anti-rabbit 1:2000 |
| Atg5 | | Atg5 | | |
| Atg7 | | Atg7 | | |
| Atg12 | | Atg12 | | |
| LC3 | | LC3 | | |

### 2.3.4 Immuno-precipitation technique (IP)

5 X $10^6$ cells were lysed by RIPA buffer and 2 μg of each antibody was added to 200 μl of the lysate and incubated for 1 hour on a rotating wheel at 4$^o$C. This was followed by the addition of 30 μl of Protein A Agarose (Thermo Scientific) and incubated for 1 hour on a rocking platform at 4$^o$C to allow the binding of Protein A Agarose with protein-antibody complex. Then the samples were centrifuged for 1 minute, 3000rpm/855 x *g* at 4$^o$C followed by washing steps (4 times with RIPA buffer). Then, 25 μl of 2X gel loading buffer with 2-merceptoethanol was added, mixture boiled for 5 minutes and loaded on to a 10% SDS-PAGE gel. The gel was transferred to nitrocellulose membrane, blocked in 1% milk/PBS-T and probed with appropriate antibody (Table-2.2).

## 2.4 Enzyme Linked ImmunoSpot (ELISpot) Assay for detection of secreted IgM and IgG

### Preparation of ELISpot plates

The coating mAb MT91/145 (IgG) and coating anti-IgM antibody were diluted to 15 μg/ml and 10 μg/ml, respectively, in sterile PBS, pH 7.4. Then, the PVDF membranes in the plates were pre-wet using 50 μl of 70% sterile ethanol for maximum of 2 minutes and washed 5 times using 200 μl/well with sterile water. After that, 100 μl/well of the diluted antibodies were added and incubated 6-8 hours at room temperature or overnight at 4$^o$C.

### Incubation of cells in the plates

The plates were washed 5 times with 200 μl/well of sterile PBS and then blocked with 200 μl/well of IMDM/10%FCS for 30 minutes at room temperature. After that, the isolated human B cells (Day-6) were re-

suspended in IMDM/cytokines without TX-HYB mix and added to the wells. The plates were placed in a 37°C humidified incubator with 5% $CO_2$ for 16-24 hours.

**Detection of spots**

The detection mAbs MT78/145 biotin and anti-IgM biotin antibody were diluted to 1 μg/ml in sterile PBS/0.5%BSA. Then, the samples were removed from the plates and washed 5 times with 200 μl/well of sterile PBS. Next, 100 μl/well of the diluted antibodies were added to the corresponding plate and incubated for 2 hours in dark at room temperature. After incubation, the plates were washed 5 times with 200 μl/well of sterile PBS. Afterward, 100 μl/well of 1:1000 streptavidin-HRP antibody in sterile PBS/0.5%BSA was added to each plate and incubated for 1 hour in dark at room temperature. After incubation, the plates were washed 5 times with 200 μl/well of sterile PBS.

In order to detect the spots, 100 μl/well of filtered 3,3',5,5'-Tetramethylbenzidine (TMB) substrate solution was added to each plate and incubated until the spots developed and then washed thoroughly with deionized water and left to dry. Once dried, the plates were stored at dark until analysed.

**2.5 Human IgG and IgM ELISA quantification**

**Buffers:**

- ELISA Coating buffer: 0.05 M Carbonate-Biocarbonate, pH 9.6
- ELISA Wash solution: 50 mM Tris, 0.14 M NaCl, 0.05% Tween 20, pH 8.0
- ELISA Blocking buffer: 50 mM Tris, 0.14 M NaCl, 1% BSA, pH 8.0
- Sample/Conjugate Diluent: 50 mM Tris, 0.14 M NaCl, 1% BSA, 0.05% Tween 20, pH 8.0
- Enzyme substrate TMP
- ELISA Stop solution: 0.18 M $H_2SO_4$

**Human IgM**

ELISAs were performed as per the manufacturer's instructions for the human IgM quatification kit (E80-100, Bethyl Laboratories, Inc). 96-well plates were coated with 100 μl of 1:100 affinity purified antibody in coating buffer for 1 hr at room temperature. After incubation, the plates were washed five times with ELISA washing buffer. Then, 200 μl of the ELISA blocking buffer was added to prevent the non-specific binding and incubated for 1 hr at room temperature or overnight at 4$^{o}$C. After that, the plates were washed five times using ELISA washing buffer. The standards (1-8) were diluted using the sample/conjugate Diluent according to the following Table-2.3.

**Table-2.3:** Dilution/concentration of IgM ELISA standards.

| Standard | ng/ml | RS10-110-4 (0.44 mg/ml IgM) | Sample Diluent |
|---|---|---|---|
| 1 | 1000 | 10 μl | 4.4 ml |
| 2 | 500 | 500 μl from std 1 | 500 μl |
| 3 | 250 | 500 μl from std 2 | 500 μl |
| 4 | 125 | 500 μl from std 3 | 500 μl |
| 5 | 62.5 | 500 μl from std 4 | 500 μl |
| 6 | 31.25 | 500 μl from std 5 | 500 μl |
| 7 | 15.6 | 500 μl from std 6 | 500 μl |
| 8 | 0 | Blank | 500 μl |

In addition, the samples were diluted according to the predicted concentration in order to fit within the standards' range.

Next, 100 μl of the standards/samples were added to the appropriate wells and incubated for 1 hour at room temperature. After that, the plate was washed the same as described before. Then, 100 μl of 1:75,000 HRP detection antibody (A80-100P) in the sample conjugate diluent was prepared

and added to each well and incubated for I hour at room temperature. After incubation, the plate was washed as described above and 100 μl of TMB substrate was added to each well and incubated in the dark for 15 minutes at room temperature until the enzymatic reaction develops to the blue colour according to the IgM concentration. After that, the reaction was stopped using 100 μl of stop solution (0.18 M $H_2SO_4$) and the concentrations were quantified using a plate reader and a standard curve.

**Human IgG**

ELISA quantification for human IgG was performed using a kit from Bethyl Laboratories, Inc. (Cat. No. E80-104**)**, in an analogous manner to the IgM assay. The IgG assay utilised the appropriate standards (intial-8) diluted using the sample/conjugate Diluent according to the following table-2.4 and were detected with the paired anti-IgG secondary.

**Table-2.4:** Dilution/concentration of IgG ELISA standards.

| Standard | ng/ml | RS10-110-4 (4.4 mg/ml IgG) | Sample Diluent |
|---|---|---|---|
| Initial | 1000 | 5 μl | 22 ml |
| 1 | 500 | 500 μl from initial | 500 μl |
| 2 | 250 | 500 μl from std 1 | 500 μl |
| 3 | 125 | 500 μl from std 2 | 500 μl |
| 4 | 62.5 | 500 μl from std 3 | 500 μl |
| 5 | 31.25 | 500 μl from std 4 | 500 μl |
| 6 | 15.6 | 500 μl from std 5 | 500 μl |
| 7 | 7.8 | 500 μl from std 6 | 500 μl |
| 8 | 0 | Blank | 500 μl |

## 2.6 Cell phenotype evaluation by flow cytometry

Approximately $2x10^5$ cells per sample were stained with the indicated antibodies. Cells were centrifuged at 1500 rpm for 5 minutes before being washed with FACs buffer (PBS, 0.5%BSA, 0.05% azide). Non-specific staining was blocked using 25 μl of the blocking buffer (932 μl FACS buffer/10% BSA, 16.6 μl human IgG (Sigma), 50 μl NMS) and incubated for 15 minutes at 4°C. Then, the cells were stained using ISO/4-colour antibodies (Table-2.5) or anti-CD154 for 20 minutes at 4°C. After that, the cells were suspended in cold FACs buffer and the phenotype was evaluated on an LSRIII flow cytometer (BD Biosciences) using DIVA software (BD Biosciences).

**Table-2.5:** List of the BD antibodies used for cell phenotype studies by flow cytometry.

| ISO | Antibody Cocktail |
|---|---|
| PE | CD19 PE |
| V450 | CD20 V450 |
| PEcy7 | CD38 PECy7 |
| APC | CD138 APC |
| | CD154 PE |
| | CD27 FITC |

## 2.7 Carboxyfluorescein Succinimidyl Ester (CFSE) cell proliferation assay

1.5 X $10^6$ human B cells were isolated from the total PBMC as described above. The cells were spun down at 1500rpm/435 x g (Eppendorf centrifuge 5810R, 17.3cm radius) for 5 minutes and the resulting pellet was re-suspended with 1 ml PBS/5%FCS. After that, 110 μl of PBS/5%FCS and 1.1 μl of 5 mM CFSE dye were added gently and quickly to the cells in the dark

and incubated for 5 minutes at room temperature. After incubation, the cells were washed twice with PBS/5%FCS and re-suspended with IMDM media and incubated on top of CD40L-expressing L cells (Day-0). The cells were treated with the inhibitors and their corresponding vehicle on Day-3 and analysed on Day-6 using flow cytometry.

## 2.8 Techniques for analysis of gene expression and regulation

### RNA extraction

Cells were lysed by 800 µl of Trizol®. Then, 160 µl of chloroform was added to the mixture, mixed by inversion and centrifuged at 12,000g for 15 minutes at 4$^{o}$C to allow the separation between the aqueous and organic phases. RNA (top aqueous layer) was transferred into a new tube. Then, 10 µg of RNase free glycogen was added. RNA was precipitated using 0.4 ml of isopropyl alcohol, incubated for 10 minutes at room temperature and spun at 12,000g for 10 minutes at 4$^{o}$C. The precipitate was washed with 1 ml of 75% ethanol and air-dried. RNA was dissolved in 45 µl of $dH_2O$ and incubated for 10 minutes at 55$^{o}$C followed by treatment with DNase1 (DNA-free Kit, Ambion) for 1 hour at 37$^{o}$C. Then, 5 µl of inactivating agent was added to the sample and incubated for 2 minutes at room temperature.

### cDNA synthesis

5 µl of RNA (DNaseI treated) was mixed with Mix 1 (Table-2.6) and incubated at 65$^{o}$C for 5 minutes to denature the double-stranded RNA and to prevent re-annealing. Then, 10 µl of Mix 2 was added and incubated at 42$^{o}$C for 50 minutes to synthesise cDNA. Then, the sample was incubated at 70$^{o}$C for 15 minutes to terminate the synthesis followed by chilling on ice for 5 minutes. After that, 0.5 µl of RNase H (2U/µl) was added to remove RNA template leaving behind only cDNA. A control without reverse transcriptase was generated at the same time.

**Table-2.6:** Reaction mixtures required for cDNA synthesis

| **Mix 1** | **Mix 2** |
|---|---|
| 1µl Oligo dT | 4µl 5X Buffer |
| 1µl dNTPs | 2µl DTT |
| 3µl $dH_2O$ | 2µl $MgCl_2$ |
| | 1µl RNase Out |
| | 0.25µl RT |
| | 0.75µl $dH_2O$ |

**Real-time PCR (q-PCR)**

Real-time PCR was used to amplify the two transcripts of *CREB3L2* using specific primers that were designed by Primer3 software version 4.0 (Table-2.7). A 10 µl reaction was used in such that 5 µl of Fast Start Universal Sybr Green (Roche), 2.6 µl dH2O, and 0.4 µl primer (100 nM) mixture was added to 2 µl of the cDNA sample and the reaction was performed using a Stratagene Mx3005P machine. In a separate reaction, the gene *PPP6C* was used as a control due to its known stable expression as determined in previous gene expression analysis (4). Table-2.8 shows the thermal set up used for the q-PCR.

**Table-2.7:** The sequence of primers used in real-time PCR.

| **Primer** | **Sequence** |
|---|---|
| PPP6C | For 5'-AGGCTAAATGGCCTGATCGTA-3'<br>Rev 5'-TCTCCAGGCATTAGCATTTCC-3' |
| Transcript 1 (both) | For 5'-CCTCATGTACCACACGCACT-3'<br>Rev5'-GGTTCCACCTCCATTGACAC-3' |
| Transcript 1 (Isoform 1) | For 5'-CCCCTGTCAAAATCAGAGGA-3'<br>Rev 5'-TTTTTCTCCAGGCTGTCCAT-3' |
| Transcript 2 (Isoform 2) | For 5'-TGACGATGAGGTGGAAAGTG-3'<br>Rev5'-CAGAGTGACAGACGGAACGA-3' |

**Table-2.8:** Thermal set up for q-PCR used.

<table>
<tr><td rowspan="4"></td><td>10:00<br>95$^{o}$C</td><td>00:15<br>95$^{o}$C</td><td></td><td>1:00<br>95$^{o}$C</td><td rowspan="3"></td><td>00:30<br>95$^{o}$C</td></tr>
<tr><td rowspan="3"></td><td rowspan="3"></td><td>1:00<br>60$^{o}$C</td><td rowspan="3"></td><td rowspan="3"></td></tr>
<tr><td rowspan="2"></td><td rowspan="2">00:30<br>55$^{o}$C</td></tr>
<tr><td>2:00<br>50$^{o}$C</td><td></td></tr>
<tr><td>1 cycle</td><td>1 cycle</td><td colspan="2">40 cycles</td><td colspan="3">1 cycle</td></tr>
</table>

## 2.9 ChIP (Chromatin Immunoprecipitation) Assay

**Buffers:**

- 1 M HEPES, pH 8.0
- 0.5 M EDTA, pH 8.0
- 0.5 M EGTA, pH 8.0
- 10X Cross linking buffer: 500 mM HEPES, 1M NaCl, 10 mM EDTA, 5 mM EGTA
- 1X Cross-linking buffer: 0.5 ml 10X Cross linking buffer, 3.3 ml 16 % Formaldehyde, 1.2 ml $dH_2O$
- 2M Glycine: 1.5 g Glycine in 10 ml PBS
- ChIP Buffer A: 10 mM HEPES, 10 mM EDTA, 0.5 mM EGTA, 0.25 % Triton X-100
- ChIP Buffer B: 10 mM HEPES, 200 mM NaCl, 1 mM EDTA, 0.5 mM EGTA, 0.01 % Triton X-100

- 25 ml of dH2O was added first to stop precipitation and (DMSO, H2O soluble) protease inhibitors (Leupeptin, Antipain, Aprotinin, AEBSF, Pepstatin A and Chymostatin) were added immediately before use
- 20 % SDS (BioRad)
- ChIP IP buffer: 25 mM Tris HCl pH 8.0, 2 mM EDTA, 150 mM NaCl, 1 % Triton X-100, 0.25 % SDS
- Protease inhibitors were added immediately before use
- ChIP IP without SDS: 25 mM Tris HCl pH 8.0, 2 mM EDTA, 150 mM NaCl, 1 % Triton X-100
- Glycerol Storage buffer: ChIP IP buffer without SDS, 20 % Glycerol
- RIPA buffer: 10 mM Tris HCl pH 8.0, 1 mM EDTA, 0.5 mM EGTA, 140 mM NaCl, 1 % Triton X-100, 0.1 % NaDOC, 0.1 % SDS
- LiCl buffer: 10 mM Tris HCl pH 8.0, 1 mM EDTA, 0.17 M LiCl, 0.5 % NP40, 0.5 % NaDOC
- Sodium Biocarbonate 0.5 M: 0.21g $NaHCO_3$ in 5 ml dH2O (Made up fresh just before use)
- Elution buffer: 0.1 M $NaHCO_3$, 1 % SDS
- 1M TE buffer pH 8.0
- 1M Tris-HCl pH 6.5
- 3 M Sodium acetate pH 5.2

**Chromatin preparation from suspension cells**

2 X $10^7$ myeloma cells were harvested and suspended in 20 ml of RPMI-1640 media. The cells were cross-linked using 2 ml of freshly prepared 1X cross-linking buffer containing formaldehyde and incubated on a rotor at room temperature for 30 minutes. After the cross-linking, the formaldehyde was quenched using 7.34 ml of 2 M glycine in PBS for 5 minutes on a rotor at room temperature. The cells were pelleted (1500rpm/435g, 5 minutes) then, washed twice with 25 ml ice cold PBS (1500rpm/435g, 5 minutes at $4^oC$). After that, the cells were lysed using 2 ml ChIP buffer A followed by 2 ml ChIP buffer B with an incubation period of 10 minutes and centrifugation (16,100 x

g, 5 minutes at 4°C) after the addition of each buffer. After that, 600 μl of ChIP IP buffer was added to the pellet and split in to 2 X 1.5 ml eppendorfs and sonicated using Bioruptor (Diagenode IP) water bath sonicator for 15 minutes. After sonication, the tubes were centrifuged to remove the debris. 200 μl of the glycerol storage buffer was added to the supernatant (chromatin) and stored at -80°C.

**Immunoprecipitation of protein-chromatin complexes**

300 μl of beads (Immobilised Protein A-Thermo Scientific) were blocked using 60 μl of BSA (10 mg/ml) for 2 hours at 4°C. At that time, the chromatin sample was thawed on ice and 200 μl of ChIP IP buffer without SDS was added to increase the volume size to 1 ml. After that, 60 μl of blocked beads was added to the chromatin sample to pre-clear the chromatin and incubated for 2 hours at 4°C on a rotor. Then, the beads were discarded and the supernatant was divided in to 5 tubes; 2 tubes for specific antibody (200 μl each), 2 tubes for the IgG control (200 μl each), and 1 tube for the INPUT (100 μl).

**For CREB3L2**: 5 μl (2μg) of CREB3L2 antibody (NBP1-88697, Novus Biologicals) was added to each tube and incubated on a rotor overnight at 4°C.

**For IgG**: 1 μl (2μg) of IgG antibody was added to each tube and incubated on a rotor overnight at 4°C.

**For the INPUT**: 10 μl of RNase A (1mg/ml) was added and incubated for 30 minutes at 37°C. Then, 5 μl of 20% SDS and 5 μl of proteinase K (10 mg/ml) were added to the INPUT to digest the protein and inactivate the nucleases that might degrade the DNA during the purification step and incubated for 2.5 hours at 37°C. After the incubation, the cross-linking of the chromatin INPUT sample was reversed by the incubation at 65°C overnight.

ChIP samples: After incubating chromatin samples (CREB3L2/IgG) with the appropriate antibodies, 50 μl of pre-prepared beads were added to each sample and incubated 5 hours on rotor at 4°C. After that, the ChIP samples were centrifuged and the supernatant was discarded. The chromatin/beads were washed 4X with RIPA buffer, 2X with LiCl buffer and 2X TE buffer.
Then, 500 μl Elution buffer, 33 μl NaCl and 4 μl Proteinase K were added and incubated at 65°C overnight.

**DNA purification**

ChIP sample:

ChIP samples were cooled down and spun. Then, 10 μl of 0.5 M EDTA and 20 μl of 1M Tris-HCl pH.6.5 were added to the ChIP samples and incubated at 45°C for 1 hour to neutralize the reversion of the cross-linking. After the incubation, ChIP samples were cooled down. Then, 500 μl of 3:1 phenol:chloroform was added to each tube and centrifuged at 16,100 x g for 15 minutes at room temperature. After that, 500 μl of chloroform was added to the supernatant and centrifuged at 16,100 x g for 15 minutes at room temperature. Next, 4 μl of glycogen (Roche, 5 mg/ml), 50 μl of 3 M sodium acetate (pH 5.2) and 900 μl of ice-cold absolute ethanol were added to each tube and incubated at -20°C for 30 minutes. Then, the tubes were centrifuged at 16,100 x g for 15 minutes at 4°C. After that, the pellets were washed with 1 ml 75% ice-cold ethanol. The pellets were air dried for 5 minutes and then, re-suspended with 80 μl of 0.1 TE (pH 8.0) at 55°C for 10 minutes and stored at 4°C for short-term storage and at -20°C for long-term storage.

INPUT:

The INPUT sample was cooled down and spun. Then, 150 μl of 3:1 phenol:chloroform was added to each tube and centrifuged at 16,100 x g for 5 minutes at room temperature. After that, 150 μl of chloroform was added to

the supernatant and centrifuged at 16,100g x g for 5 minutes at room temperature. Next, 4 μl of glycogen (5 mg/ml) and 250 μl of ice-cold absolute ethanol were added to each tube and incubated at -20$^{o}$C for 30 minutes. Then, the tubes were centrifuged at 16,100 x g for 15 minutes at 4$^{o}$C. After that, the pellets were washed with 250 μl of 75% ice-cold ethanol. The pellets were air dried for 5 minutes and then, re-suspended with 80 μl of 0.1X TE buffer (pH 8.0) at 55$^{o}$C for 10 minutes and stored at 4$^{o}$C for short-term storage and at -20$^{o}$C for long-term storage.

## 2.10 Gene expression profiling

RNA samples were collected from human B-cells that were isolated using a memory B-cell isolation kit (Miltenyi Biotec) and treated with PF-429242/d$H_2O$ and or Nelfinavir/ethanol.

The RNA samples were extracted as described above re-suspended in 45 μl d$H_2O$, 40 μl was stored at -80$^{o}$C and the rest at -20$^{o}$C for RNA testing. RNA samples were quantified using Qubit® 2.0 Fluorometer (cat No Q32866) and the quality of RNA samples were checked using the Agilent RNA 6000 Nano kit (2100 analyser). After that, RNA samples were amplified using Illumina® Totalprep$^{TM-96}$ RNA Amplification Kit (Figure-2.1).

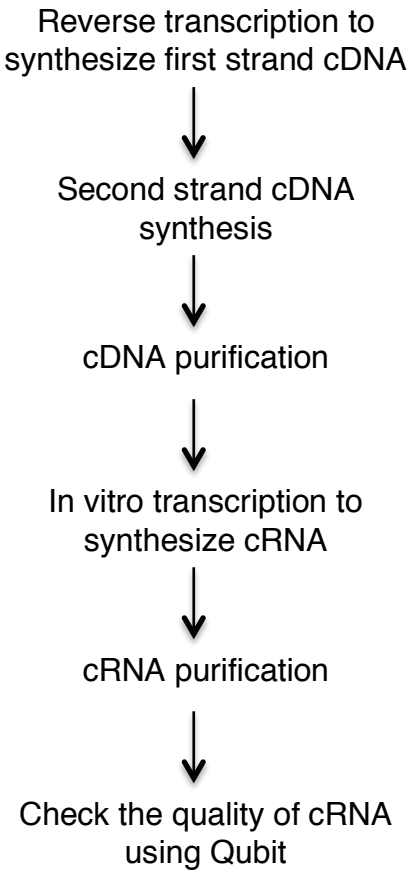


**Figure-2.1:** RNA amplification steps using Illumina® Totalprep$^{TM-96}$ RNA Amplification Kit.

**RNA amplification using Illumina® Totalprep$^{TM-96}$ RNA Amplification Kit:**
As shown in Figure-2.1, RNA was first reverse transcribed to synthesize the first cDNA strand using a thermal cycler (Table-2.9) and reverse transcription master mix (Table-2.10).

**Tabl-2.9:** Reverse transcription thermal cycler program

| Temperature | Time | Cycles |
|---|---|---|
| 42$^{o}$C | 2 hours | 1 |
| 4$^{o}$C | Hold | - |

**Table-2.10:** Reverse transcription master mix

| Amount | Component |
|---|---|
| 2 μl | 10X First Strand Buffer |
| 4 μl | dNTP Mix |
| 1 μl | T7 Oligo(dT) Primer |
| 1 μl | RNase Inhibitor |
| 1 μl | ArrayScript$^{TM}$ Reverse Transcription |

Then, the second strand of the cDNA was synthesised using the appropriate thermal cycler program (Table-2.11) and second strand master mix (Table-2.12).

**Table-2.11:** The synthesis of cDNA second strand thermal cycler

| Temperature | Time | Cycles |
|---|---|---|
| 16$^{o}$C | 2 hours | 1 |
| 4$^{o}$C | Hold | - |

**Table-2.12:** Second strand master mix

| Amount | Component |
|---|---|
| 63 μl | Nuclease-free water |
| 10 μl | 10X Second Strand Buffer |
| 4 μl | dNTP Mix |

| | |
|---|---|
| 2 μl | DNA Polymerase |
| 1 μl | RNase H |

After that, the synthesised cDNA was purified using cDNAPure beads. Next, the purified cDNA was in vitro transcriped (IVT) to synthesise the cRNA using the appropriate thermal cycler program (Table-2.13) and IVT master mix (Table-2.14).

**Table-2.13:** IVT thermal cycler program

| Temperature | Time | Cycles |
|---|---|---|
| 37$^{o}$C | 4-14 hours | 1 |
| 4$^{o}$C | Hold | - |

**Table-2.14:** IVT master mix

| Amount | Component |
|---|---|
| 2.5 μl | Biotin-NTP mix |
| 2.5 μl | T7 10X Reaction Buffer |
| 2.5 μl | T7 Enzyme Mix |

After the incubation, cRNA samples were purified using the cRNA binding beads and eluted with 40 μl cRNA elution buffer at 55$^{o}$C. Then, the cRNA samples were quantified using the Qubit kit and stored at -20$^{o}$C (short time storage) or -80$^{o}$C for long time storage until hybridised.

cRNA samples were hybridized using whole-Genome expression direct hybridisation assay.

**Whole-Genome Gene Expression Direct Hybridisation Assay**

750ng/15μl of cRNA samples were dispensed on to the BeadChip and inserted into the Hyb Chamber, which then incubated in the Illumina Hybridization Oven for 14-20 hours at 58°C. Meanwhile, the High-Temp wash buffer (lot No 10005610) was prepared and placed in to a Hybex Waterbath insert with base temperature of 55°C and left overnight. After the incubation, the BeadChip was removed from the oven and the wash buffers (100% EtOH, High-Temp wash buffer (prepared 24 hours before) and E1BC wash buffer) were prepared. The BeadChip was washed using High-Temp buffer, then E1BC, followed by 100% EtOH and High-Temp wash buffer. After that, the BeadChip was blocked using E1 blocking buffer and then stained using Cy3-Streptavidin. After that, the BeadChip was dried and stored in a dark environment until ready to be scanned. The BeadChip was scanned with Illumina BeadScanner and the initial data were processed using Illumina GenomeStudio Gene Expression Module (Gene Expression Omnibus: GSE41208). HUGO Gene Nomenclature was used to annotate the final report. The threshold was 3. Any probe was less than 3 were removed from the analysis. R Limma was used to generate the linear model and the differentially expressed genes were assessed using Limma empirical Bayes module (bioinformatic analysis performed by Dr Matthew Care).

## 2.11 Chromatin Immunoprecipitation Sequencing (ChIP-Seq)

ChIP assay was performed as described in Section 2.9. The additional antibodies used included anti-ATF6 (NBP140256, Novus Biologicals) and anti-XBP1s (619502, Biolegend). The libraries were prepared for input chromatin according to the manufacturer's instructions using Illumina ChIP-seq Sample Prep kit (Illumina®). However, the libraries for ChIP samples were prepared using MicroPlex Library Preparation TM kit (Diagenode). In addition, AMPure XP beads (Beckman Coulter) were used for size selection and the samples were run on an Illumina Hiseq 2500. Dr Mario Cocco performed library

preparation and purification. Peak calling was performed by Dr Matthew Care as previously described (86).

## 3. Generating reagents required for the evaluation of CREB3L2

The aim of this project is to study the role of CREB3L2 in B-cell differentiation and the UPR. Therefore, the first step was to generate CREB3L2 constructs in mammalian and bacterial expression vectors to be used for the study. In parallel, similar constructs were also made for the transcription factor ZBTB32. *ZBTB32* was identified as one of the most characteristic genes associated with ABC-DLBCL (87) and may potentially contribute to the regulation of the transition from plasmablast to plasma cell in the same operational window as CREB3L2; however, no further work was completed on this factor beyond the generation of the vectors described below. The mammalian expression constructs have the potential to be used as positive controls for validation of antibodies and to allow overexpression of the proteins for functional assessment. The GST-fusion proteins may be used as immunogens for the development of new antibodies or alternatively could be employed for biochemical assays to determine DNA or protein interaction partners.

### 3.1 Generation of CREB3L2-pGEX6P-1 and CREB3L2-pIRES2EGFP constructs

#### 3.1.1 Cloning

*CREB3L2* and *ZBTB32* were cloned into two vectors: pIRES2-EGFP for mammalian expression and pGEX6P-1 for bacterial expression. The pIRES2-EGFP vector contains a CMV promoter to drive expression of *CREB3L2* or *ZBTB32* at high levels in mammalian cell lines. As the name implies, there is also an IRES-EGFP expression cassette located downstream of *CREB3L2* which allows a convenient means of monitoring transfection. The pGEX6P-1 vector is used to generate N-terminal GST-fusion proteins that can be expressed in large quantities in bacterial hosts and purified using the GST-tag.

### 3.1.1A CREB3L2-pIRES2EGFP and ZBTB32-pIRES2EGFP constructs

The amino terminal portions (containing the DNA-binding domain) of human *CREB3L2* (amino acids 1-378) and *ZBTB32* (amino acids 1-502) were cloned into the pIRES2-EGFP vector (as described in the Materials and Methods, Figure-6A). Two positive clones from each construct (CREB3L2-pIRES2EGFP and ZBTB32 pIRES2EGFP) were selected and verified by re-streaking them on to kanamycin-LB plates and processing a further four clones for evaluation by restriction digest (Figure 3.1 B and C).

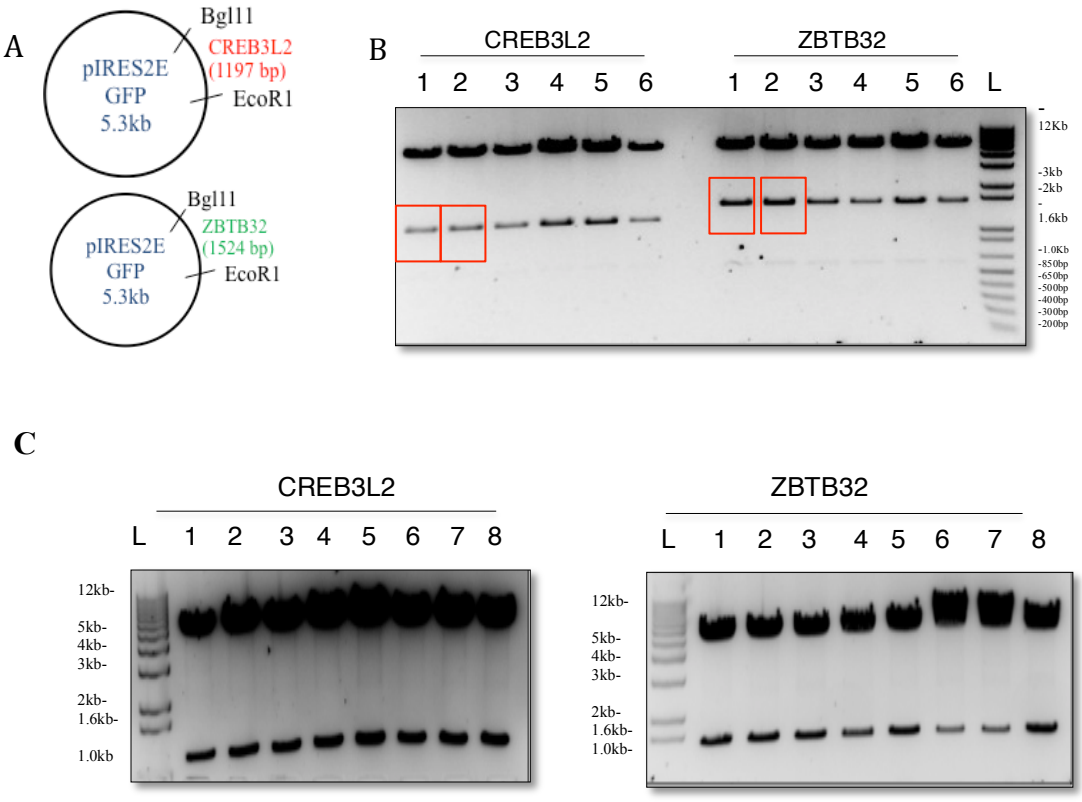


**Figure 3.1: Cloning of *CREB3L2* and *ZBTB32* into pIRES2-EGFP vector (A-C). A**. Diagrammatic representation of CREB3L2 and ZBTB32 constructs with the restriction enzymes used for cloning and verification indicated. **B.** CREB3L2-pIRES2EGFP and ZBTB32-pIRES2EGFP miniprep digestion. The expected insert sizes were 1197 bp and 1524 bp, respectively. Red boxes indicate inserts of correct molecular weight. These clones were subsequently validated in part C. **C.** Validation of CREB3L2-pIRES2EGFP and ZBTB32-pIRES2EGFP clones by additional round of colony selection and miniprep digestion. Numbering at the top indicates the designated clone number. L, molecular weight ladder.

### 3.1.1B CREB3L2-pGEX6P-1 and ZBTB32-pGEX6P-1 constructs

Three unsuccessful attempts were made to clone the amino termini of *CREB3L2* and *ZBTB32* into pGEX6P-1 vector using BamHI and SalI with NEB2 (10 mM Tris-HCl pH7.9, 10 mM $MgCl_2$, 50 mM NaCl, 1 mM DTT) and NEB3 (50 mM Tris-HCl pH7.9, 10 mM $MgCl_2$, 100 mM NaCl, 1 mM DTT) buffers. In each instance, the diagnostic restriction digests failed to generate fragments of the expected molecular weights for vectors with inserts (Figure 3.2).

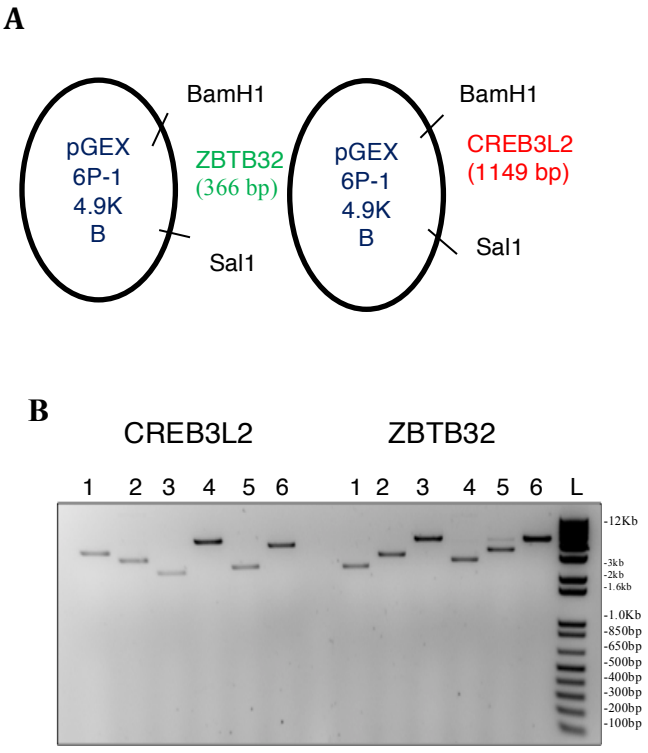


**Figure 3.2: A**. Diagrammatic representation of *CREB3L2* and *ZBTB32* insertion in to pGEX6P-1. **B.** Digests of CREB3L2- and ZBTB32-pGEX6P-1 with BamHI and SalI. Numbering at the top indicates the designated clone number. L, molecular weight ladder.

To solve the problem, the parental vector pGEX6P-1 was re-digested with two different combinations of enzymes; one digested with BamHI and SalI and the second with BamHI and XhoI (since XhoI and Sal1 have compatible cohesive ends). In addition, *CREB3L2* and *ZBTB32* inserts were re-digested using the same restriction enzymes but with changing the buffer to the unique BamHI buffer (150mM NaCl, 10mM Tris, pH 7.9, 10mM $MgCl_2$, 1mM DTT).
*CREB3L2* and *ZBTB32* were successfully liberated from the pUC57 vector (Figure 3.3), extracted, ligated in to pGEX6P-1, transformed into *DH5α* competent cells and grown on ampicillin-LB plates.

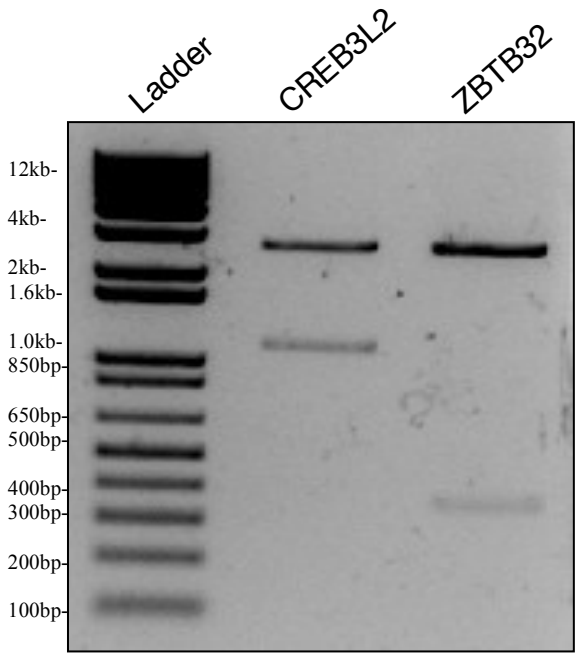


**Figure 3.3: CREB3L2 and ZBTB32 digestion.** 0.8% agarose gel electrophoresis of pUC57-CREB3L2 and pUC57-ZBTB32 digestion with BamHI and SalI giving the expected insert sizes of 1149bp and 366bp, respectively.

To determine the outcome of CREB3L2-pGEX6P-1 transformation, eight clones were selected, DNA purified and digested by BamHI and SalI with BamHI buffer. Among the eight, only one clone (CREB3L2-pGEX6P-1 13) had the right molecular weight (Figure 3.4 A). This was therefore re-streaked on to ampicillin-LB plates and four clones were selected for validation (Figure 3.4 B).

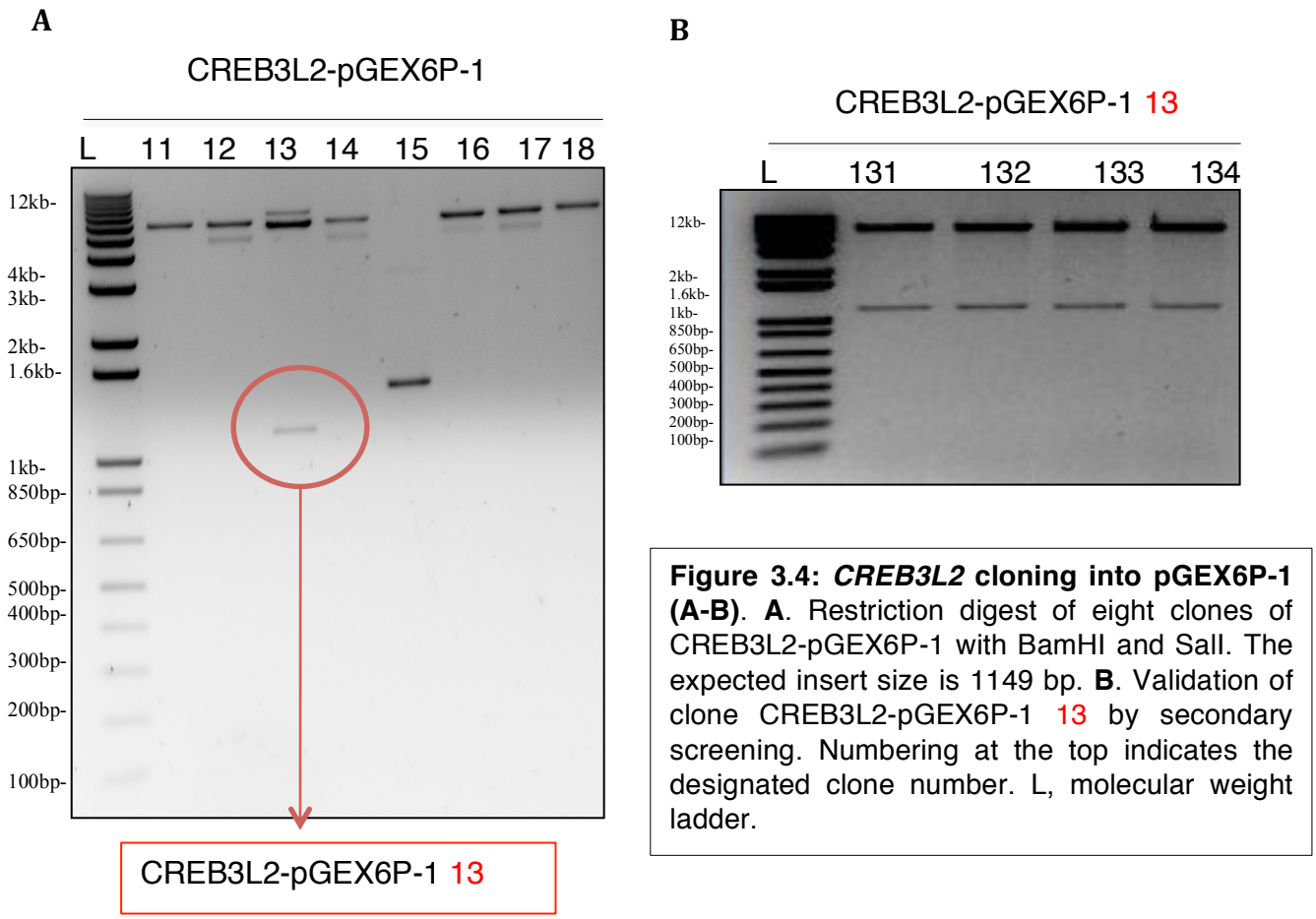


**Figure 3.4: *CREB3L2* cloning into pGEX6P-1 (A-B)**. **A**. Restriction digest of eight clones of CREB3L2-pGEX6P-1 with BamHI and SalI. The expected insert size is 1149 bp. **B**. Validation of clone CREB3L2-pGEX6P-1 13 by secondary screening. Numbering at the top indicates the designated clone number. L, molecular weight ladder.

On the other hand, none of the eight clones that were chosen from ZBTB32-pGEX6P-1 transformation worked (Figure 3.5A). Therefore, different sets of restriction enzymes were chosen to digest the purified ZBTB32-pGEX6P-1 and CREB3L2-pGEX6P-1 (Figure 3.5B). By changing the restriction enzymes used to evaluate the presence of *ZBTB32*, all the eight clones that were purified were shown to have the expected size of insert. Two positive clones (ZBTB32-pGEX6P-1 21 and ZBTB32-pGEX6P-1 23) were selected and validated by re-streaking them on to ampicillin-LB plates (Figure 3.5C). Additionally, six clones of CREB3L2 had the right molecular weight, which then were validated by re-streaking one positive clone (CREB3L2-pGEX6P-1 23) on to ampicillin-LB plates, purified and digested using the same enzymes (Figure 3.5D).

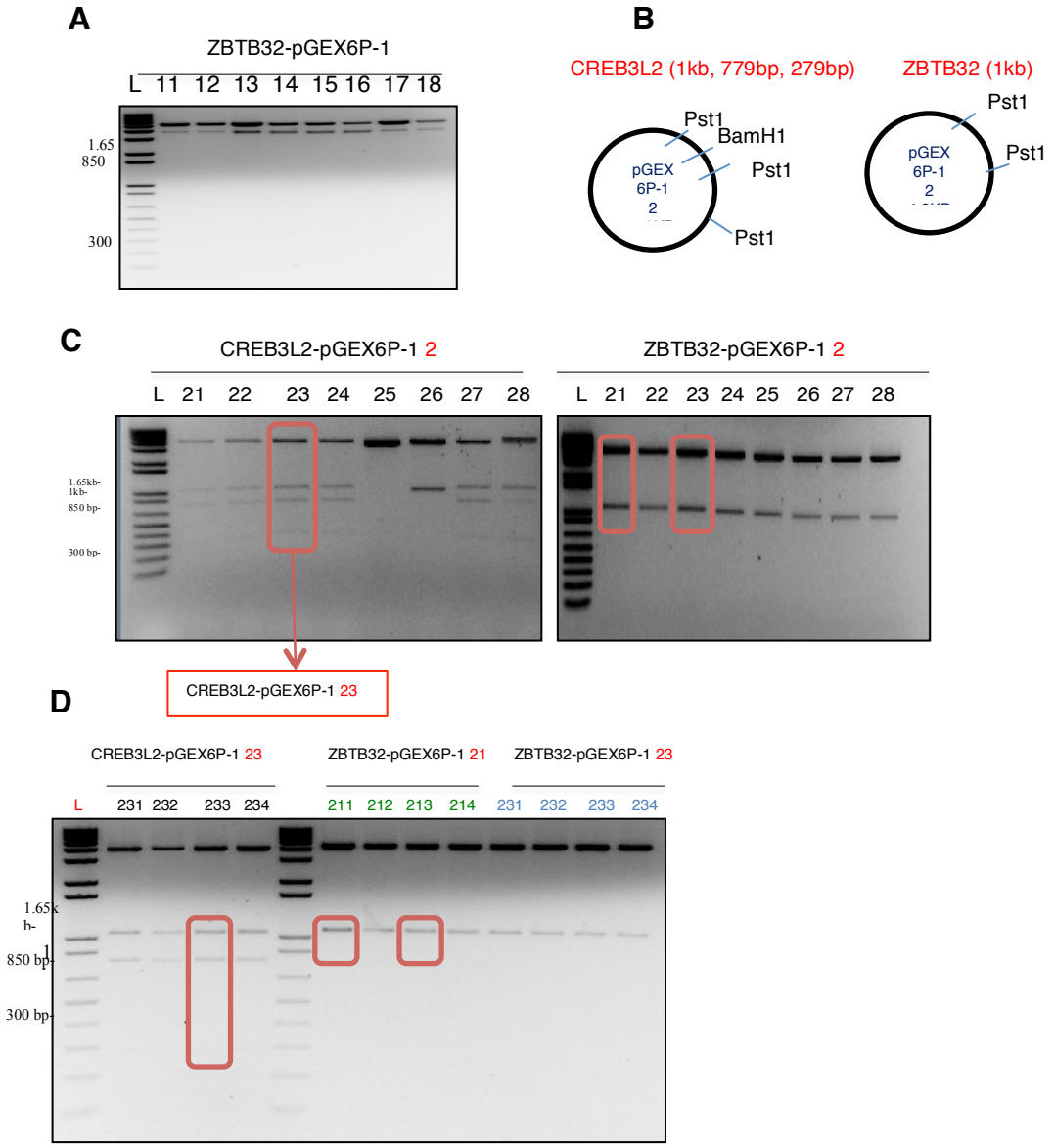


**Figure 3.5: Optimising the generation of ZBTB32-pGEX6P-1 and CREB3L2-pGEX6P-1 constructs (A-D). A.** Restriction digest of eight clones of ZBTB32-pGEX6P-1 with BamHI and SalI. **B.** Diagrammatic representation of CREB3L2- and ZBTB32-pGEX6P-1 digestion using BamHI and PstI for CREB3L2 and PstI only for ZBTB32. **C.** Restriction digest of eight clones of CREB3L2-pGEX6P-1 with BamHI, PstI and ZBTB32-pGEX6P-1 with PstI. The expected insert sizes were 1kb, 779bp, and 279bp for CREB3L2-pGEX6P-1 and 1kb for ZBTB32-pGEX6P-1. Three positive clones (CREB3L2-pGEX6P-1 23, ZBTB32-pGEX6P-1 21 and ZBTB32-pGEX6P-1 23) were validated by re-streaking them on to Ampicillin-LB plates. **D.** Validation of the selected clones by secondary screening. Numbering at the top indicates the designated clone number. L, molecular weight ladder.

Based on successful evaluation by restriction digest, the following constructs were prepared for future tests:

CREB3L2-pIRES2EGFP (clone 14)

CREB3L2-pIRES2EGFP (clone 21)

CREB3L2-pGEX6P-1 (clone 132)

CREB3L2-pGEX6P-1 (clone 233)

ZBTB32-pIRES2EGFP (clone12)

ZBTB32-pIRES2EGFP (clone13)

ZBTB32-pGEX6P-1 (clone 211)

ZBTB32-pGEX6P-1 (clone 213)

### 3.2 Generation of GST-CREB3L2 fusion proteins

*CREB3L2* was cloned into the pGEX6P-1 vector harbouring an N-terminal GST-tag. GST-CREB3L2 proteins (CREB3L2-pGEX6P-1 (132) and CREB3L2-pGEX6P-1 (233)) were induced in transformed *DH5α* and subsequently purified using affinity column chromatography. The generation and purification of small scale GST-CREB3L2 fusion protein revealed a protein with molecular weight of around the predicted size of 81 KDa (Figure 3.6A). A large scale GST-fusion protein production was performed to purify larger amount of GST-CREB3L2, however, a protein of the expected molecular weight was not obtained (Figure 3.6B).

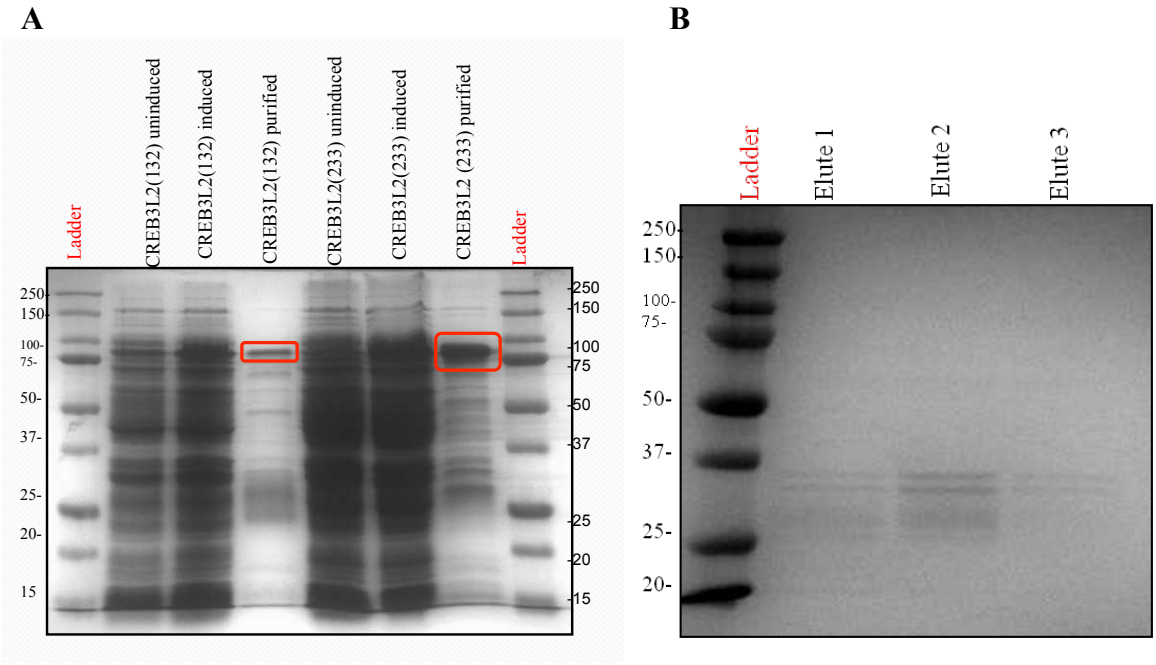


**Figure 3.6: Generation of GST-CREB3L2**. **A.** Small scale production from two separate clones with the following samples: whole cell lysate from un-induced bacteria, whole cell lysate from induced bacteria, affinity purified fusion protein. **B.** Large scale protein production from clone CREB3L2 233. Samples are 3 consecutive eluates from the affinity column. Proteins were detected by Coomassie staining of 10% SDS-PAGE gels.

In order to check whether the lack of protein detection could be due to solubility and elution issues, the bacterial pellets and the Sepharose-bound material were run on a 10% SDS-PAGE gel. However, GST-CREB3L2 was not found in the pellets or the beads (Figure-12A). The next step was to test the induction as the experiment in Figure 3.7A was carried out using a newly prepared batch of IPTG.

Three different preparations of IPTG were examined using a small-scale ZBTB32-pGEX6P-1 purification (because this protein worked well with both the small and large scales): the batch used in Figure 11B and 12A, the previous batch used in the small-scale trial, and a freshly prepared solution. The test revealed that all three sets of IPTG worked (Figure 3.7B 1, 2) with the least induction efficiency using the old IPTG (Figure 3.7B 3). Therefore, large scale GST-CREB3L2 expression was repeated using the new IPTG but it still did not work, with only degradation products detected (Figure 3.7C).

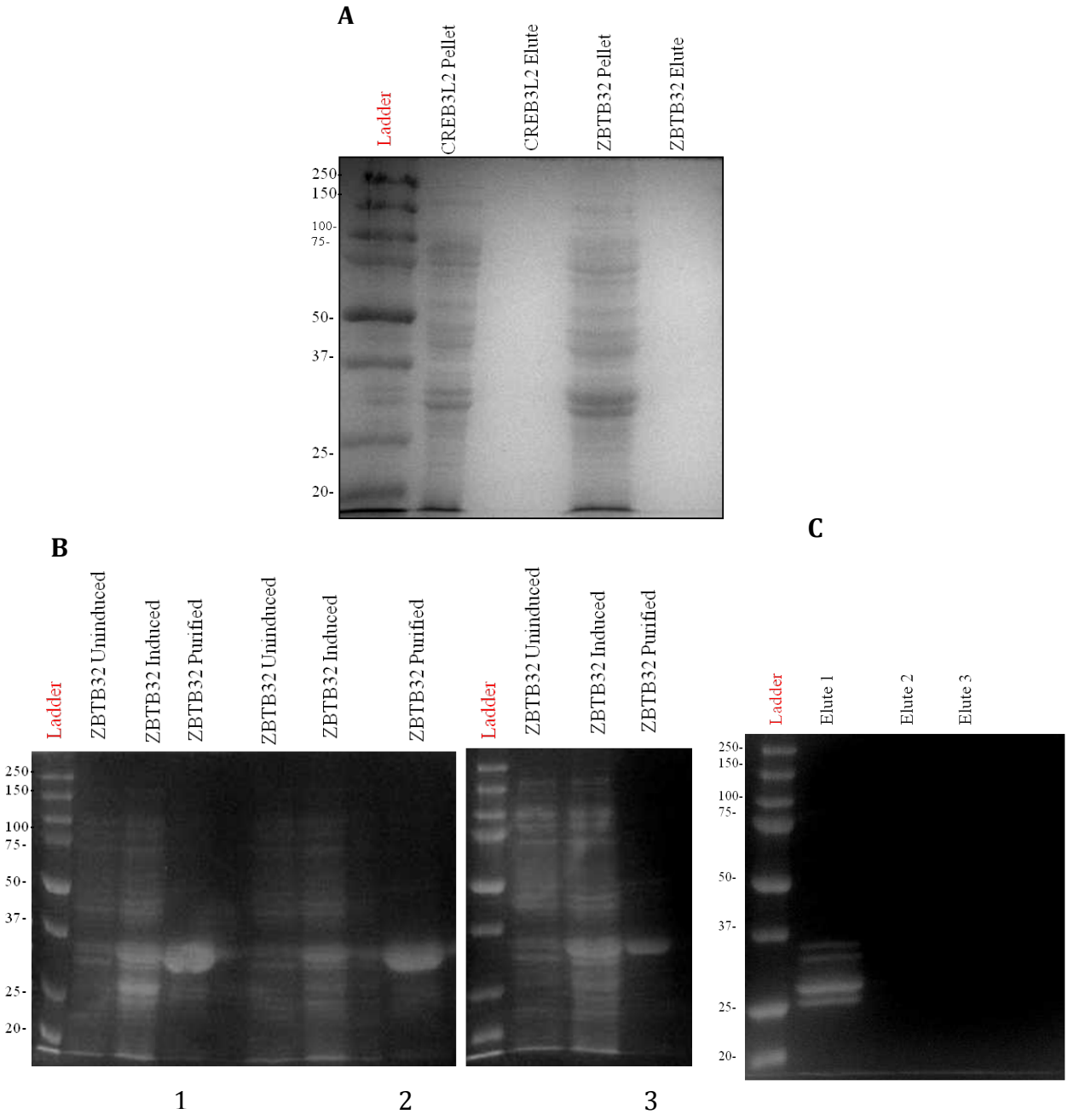


**Figure 3.7: Optimisation of GST-CREB3L2 large-scale expression. A.** Checking the bacterial pellets and Sepharose-bound material from CREB3L2 and ZBTB32. **B.** Examination of three different preparations of IPTG (1, 2, and 3) using a small-scale ZBTB32-pGEX6P-1 purification. **C**. Large scale protein production from clone CREB3L2 233 using IPTG number 2 in Figure-7B. Samples are 3 consecutive eluates from the affinity column. Proteins were detected by Coomassie staining of 10% SDS-PAGE gels.

To minimise the degradation products, CREB3L2-pGEX6P-1 was transformed into the BL21-Gold strain of bacteria, because it is protease deficient, and the large-scale purification was repeated. However, full-length purified protein was still not obtained (Figure 3.8A). Then, the solubility and elution functions were examined as described previously. This analysis revealed bands with the correct molecular weight for GST-CREB3L2 in the bacterial pellets suggesting a sonication problem (Figure 3.8B). To solve the sonication issue, ten individual small-scale GST-fusion proteins were generated and purified using column chromatography. Nevertheless, purified protein was not recovered (Figure 3.8C).

Surprisingly, when the beads and pellet were examined, a band was noticed in the beads that was loaded in 10% SDS-PAGE raising another problem which is elution (Figure 3.8D). Therefore, another 10 small-scale preps were generated and purified using a new reduced Glutathione elution buffer, (Figure 3.8E) but without success.

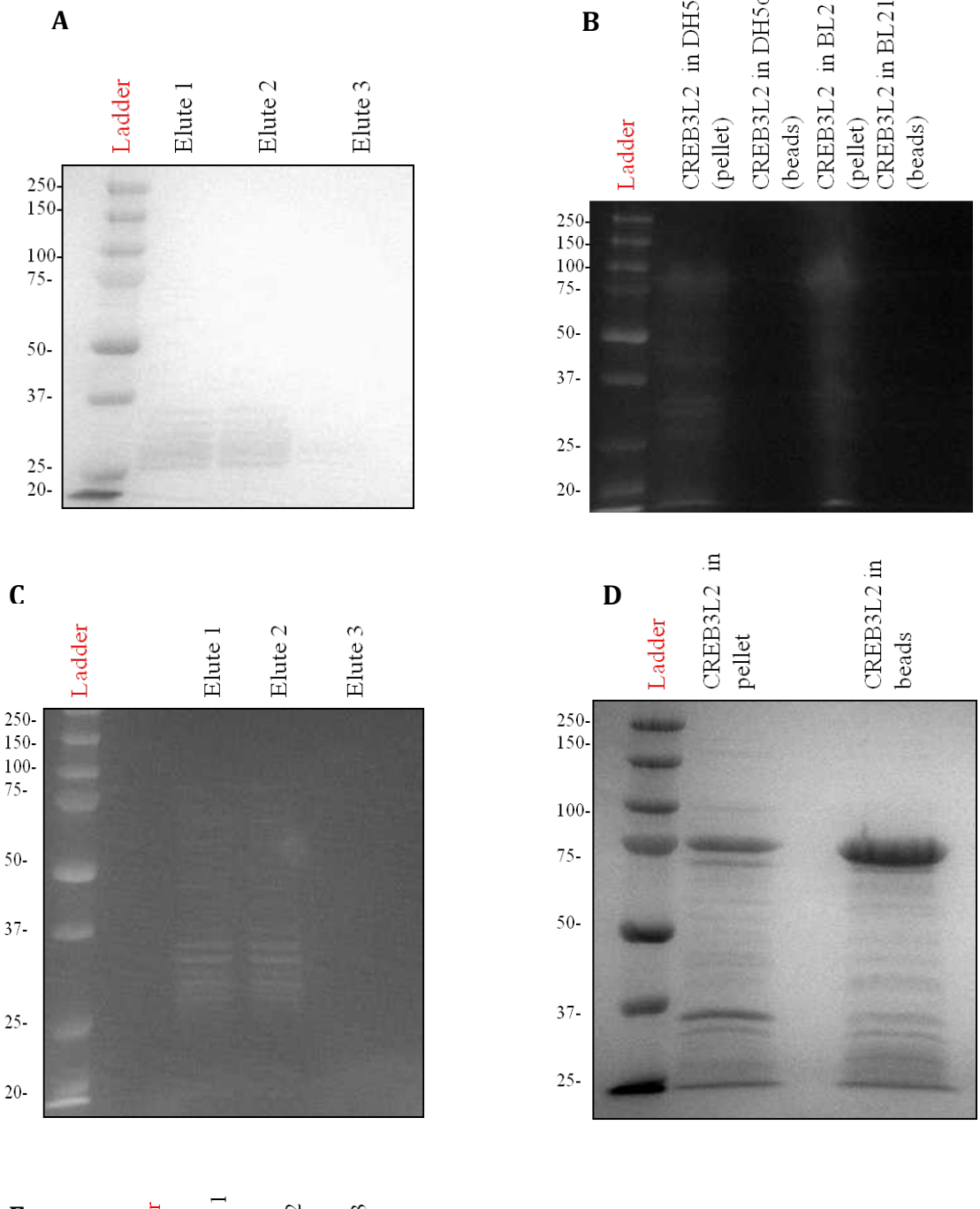


**Figure 3.8: Optimisation of the large-scale GST-CREB3L2 expression (A-E). A**. A large-scale preparation of GST-CREB3L2 transformed into BL21-Gold strain of bacteria. Samples are 3 consecutive elutes from the affinity column. **B**. Assessment of protein in cell pellets and affinity beads. **C**. The generation of 10 individual small-scale GST-fusion proteins and the purification using column chromatography. **D**. Examination of protein retention in cell pellet or on beads for the GST-fusion proteins purified in Figure-8C. **E.** Another 10 small scale GST-fusion proteins preparations using a new reduced Glutathione elution buffer. Samples are 3 consecutive eluates from the affinity column. All proteins were detected by Coomassie staining of 10% SDS-PAGE gels.

A previous publication suggested using a higher concentration of reduced Glutathione with the addition of sodium chloride (NaCl) for eluting GST-fusion proteins (88). Thus, a small scale experiment was conducted to check the suitability of the new elution buffer in eluting GST-CREB3L2; three small scale preps of GST-fusion proteins were examined such that one was boiled, the second eluted using the previously used elution buffer and the third was eluted using the new higher stringency buffer (20mM reduced glutathione, 100mM Tris, 120mM NaCl). The experiment revealed better elution in the third condition with the new buffer (Figure 3.9A, B). Thus, the subsequent GST-CREB3L2 fusion protein generations were 10 small-scale preps using the new elution buffer to avoid elution and sonication challenges.

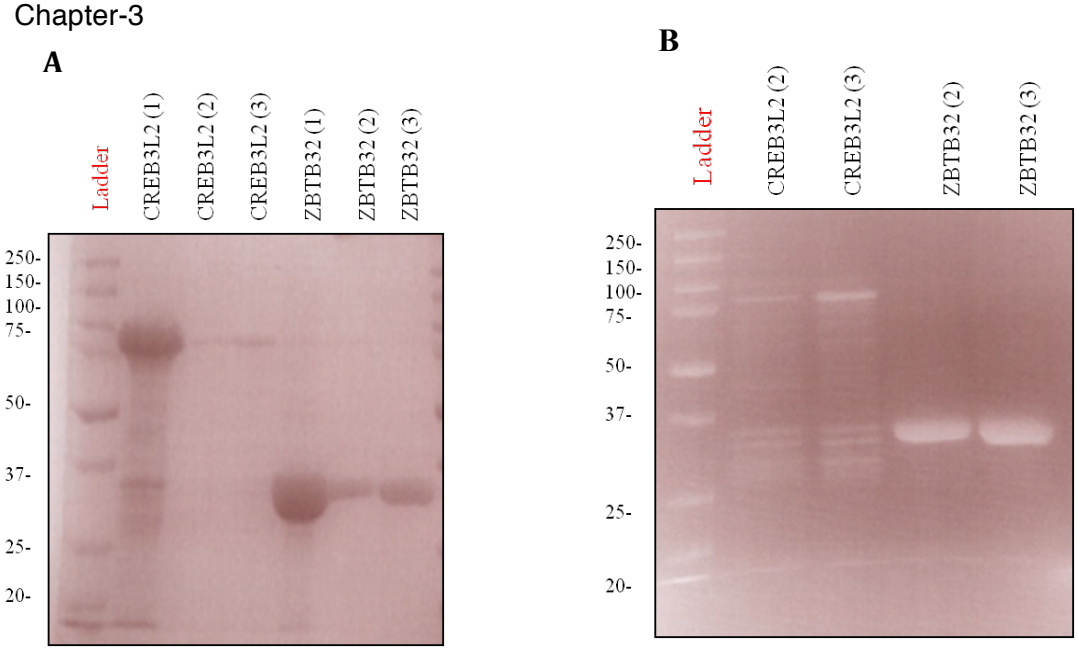


**Figure 3.9: Optimisation of large scale GST-CREB3L2 fusion protein expression using a new elution buffer**. **A**. Examination of three small scale preps of GST-fusion proteins such that one prep was boiled (1), the second (2) was eluted using the previously used elution buffer and the third (3) was eluted using the new higher stringency buffer (20mM reduced glutathione, 100mM Tris, 120mM NaCl). **B.** Validation of the new elution buffer with a repeat experiment.

Since the generation of large scale GST-CREB3L2 fusion protein was not successful, multiple small scales (40 in total) were performed with the use of new elution buffer (Figure 3.10) in an attempt to generate sufficient protein for use as an immunogen for antibody generation.

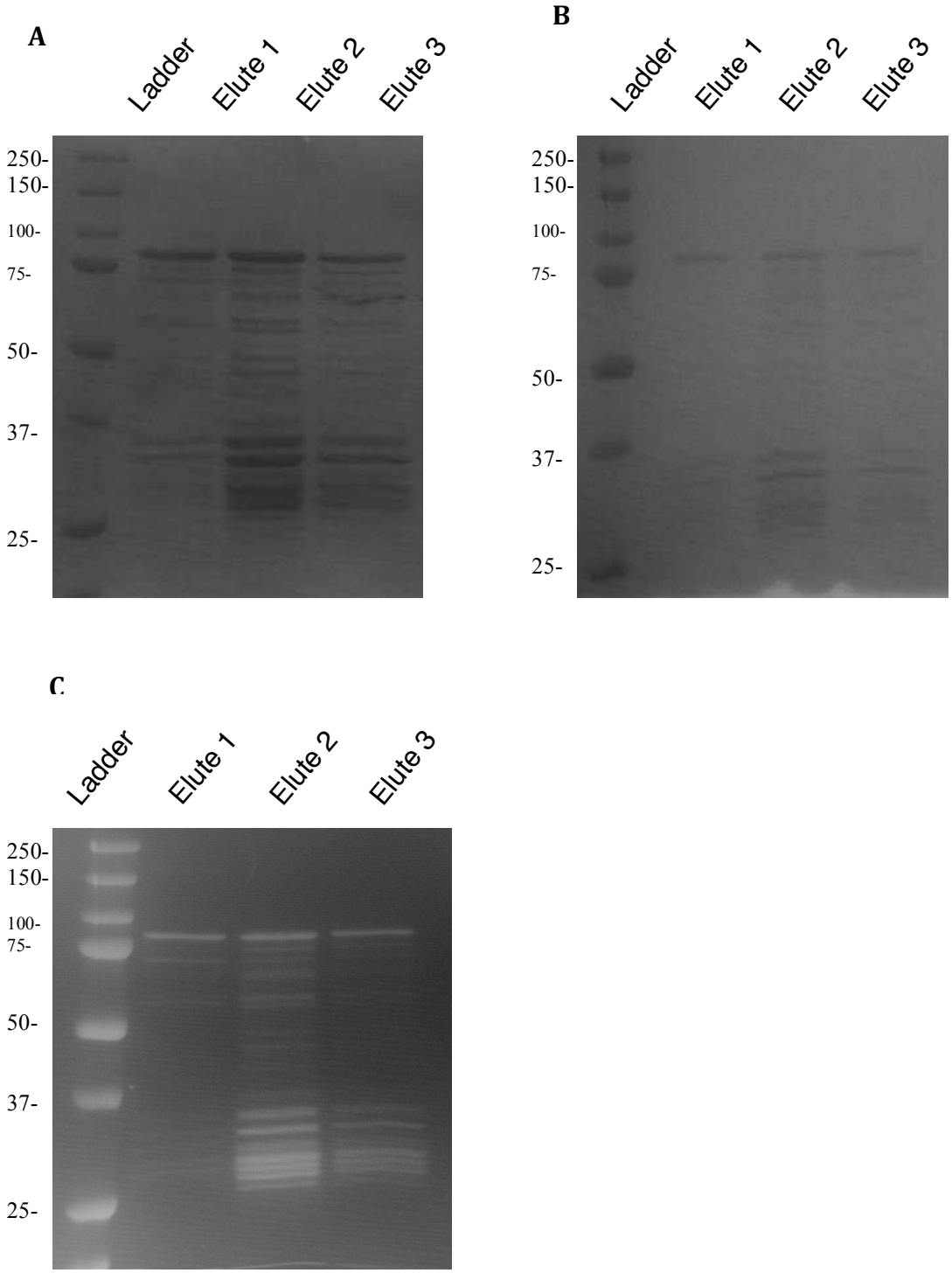


**Figure 3.10: Multiple small-scale preps of GST-CREB3L2 fusion protein**. **A**. The generation of 10 individual small-scale GST-fusion proteins and purification using column chromatography. **B.** Another 10 individual small-scale GST-fusion proteins generated and purified using column chromatography. **C**. The generation of 20 individual small-scale GST-fusion proteins and purification using column chromatography. Samples are 3 consecutive eluates from the affinity column. Proteins were detected by Coomassie staining of 10% SDS-PAGE gels.

### 3.2.1 Preparation of GST-CREB3L2 fusion protein for immunization

The goal of the fusion protein production was to generate in the order of 250-1000 µg for a rabbit immunisation protocol. In order to evaluate the GST-CREB3L2 protein concentration, elutes were combined and run on 10% SDS-PAGE (neat, 1:5, and 1:10) to estimate its concentration as compared with a BSA standard series (2mg/ml, 1mg/ml, 0.5mg/ml and 0.25mg/ml) (Figure 3.11). By comparing it with the BSA concentrations, the concentration was less than 0.25 mg/ml for the total protein content. However, ideally 0.5mg/ml is required for immunisation, therefore, the protein preparation required concentration.

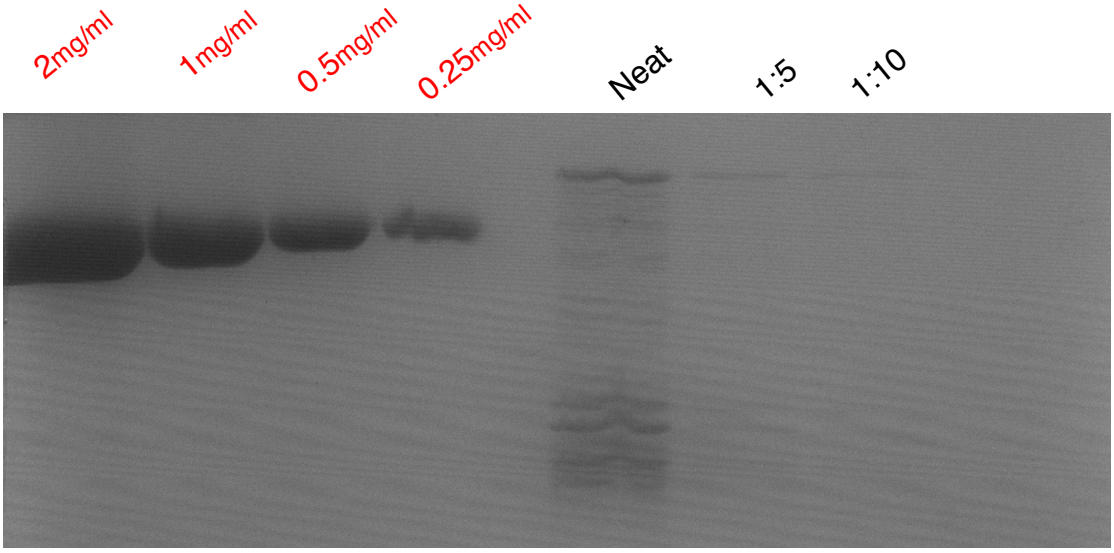


**Figure 3.11: Estimation of GST-CREB3L2 fusion protein concentration**. GST-CREB3L2 fusion protein eluates were combined and run on 10% SDS-PAGE (neat, 1:5, and 1:10). BSA standard series (2mg/ml, 1mg/ml, 0.5mg/ml and 0.25mg/ml) were run as well to estimate the GST-CREB3L2 fusion protein concentration. Proteins were detected by Coomassie staining of 10% SDS-PAGE gels.

### 3.2.2 Concentration of GST-CREB3L2 fusion protein

GST-CREB3L2 fusion protein was concentrated using a Centricon filter (Millipore, Amicon). The procedure was carried out according to the manufacturer's recommendation. The collected protein was run on 10% SDS-PAGE along with the BSA standard series (1mg/ml, 0.5mg/ml, 0.25mg/ml and 0.125mg/ml) to estimate its concentration after the procedure (Figure 3.12). The analysis revealed an approximate concentration of 0.25 mg/ml, which is half the required concentration. Therefore, it was anticipated that 20-40 more small-scale preps would be required to achieve the desired concentration for the five injections given during the rabbit immunisation protocol.

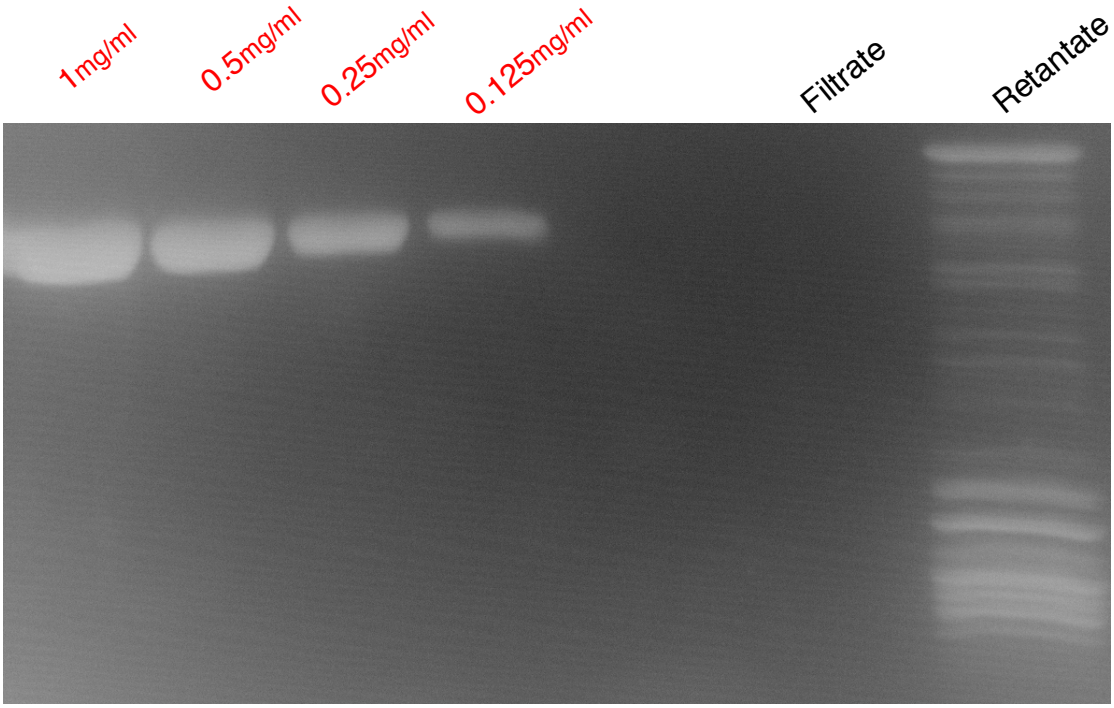


**Figure 3.12: Concentrating GST-CREB3L2 fusion protein by Centricon filtration.** GST-CREB3L2 fusion protein was concentrated using Centricon filter revealing the fusion protein in the retentate with no protein detected in the filtrate. The fusion protein concentration was estimated by comparing it with the BSA standard series (1mg/ml, 0.5mg/ml, 0.25mg/ml and 0.125mg/ml). Proteins were detected by Coomassie staining of 10% SDS-PAGE gels.

## 3.3 Validation of CREB3L2 antibodies by Western Blotting and Immunoprecipitation techniques

### 3.3.1 Western blot analysis

Previous publications investigating the role of CREB3L2 had employed an antisera generated by the authors against a fusion protein encoding amino acids 1-292 of the murine protein (89), but commercially available antibodies had not be used in the literature. The available CREB3L2 antibodies (Aviva αCREB3L2, Proteintech αCREB3L2 and Novus αCREB3L2) were validated by Western blot analysis through their recognition of CREB3L2-containing lysate prepared from HeLa cell transfections. Antibody to the HA tag acted as a positive control. The analysis revealed a specific binding of CREB3L2 antibodies (Proteintech αCREB3L2 and Novus αCREB3L2) with the CREB3L2 protein (approximately 68 kDa) (Figure 3.13). However, CREB3L2 antibody from Aviva showed only non-specific binding.

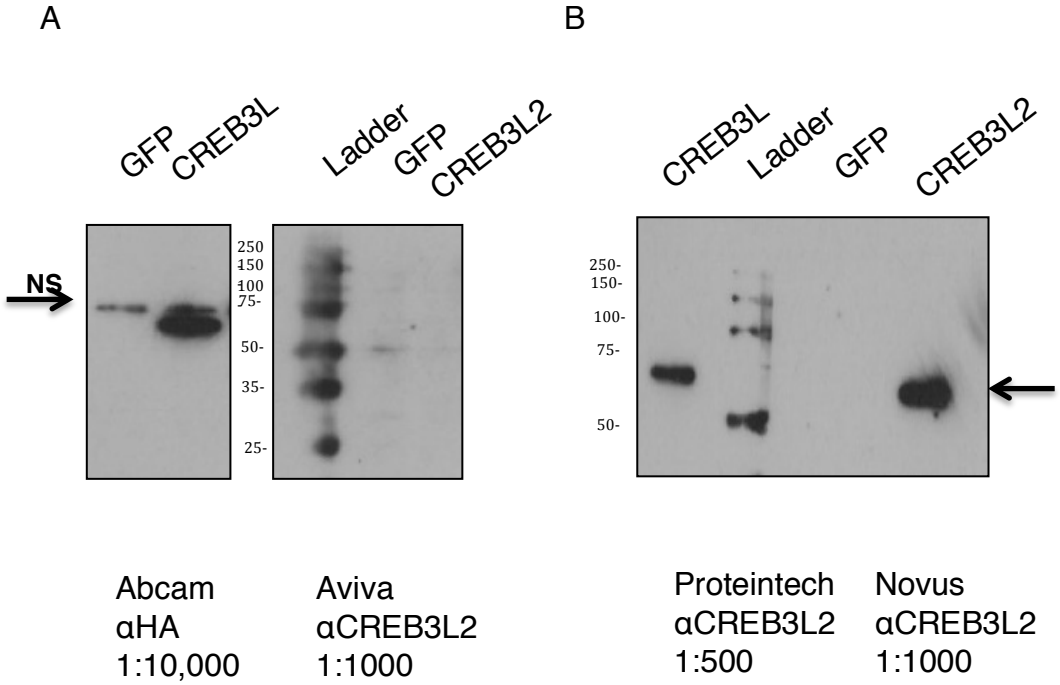


**Figure 3.13: Validation of CREB3L2 antibodies by Western blot analysis (A-B).** Three available CREB3L2 antibodies from Aviva, Proteintech and Novus were validated by Western blot analysis. The positive control used was antibody to the HA tag. The numbers shown at the bottom of the figure were the antibodies' recommended dilution from the corresponding company. NS, non-specific band. Arrow indicates CREB3L2.

### 3.3.2 Immuno-precipitation technique (IP)

The CREB3L2 antibodies that were analysed by Western blot were further evaluated for their ability to IP. Using HA-CREB3L2 transfected Hela cells revealed that all three available CREB3L2 antibodies could precipitate CREB3L2 protein, with the least efficiency from the Aviva CREB3L2 antibody (Figure 3.14). Therefore, the two antibodies that effectively recognised CREB3L2 (from Novus and Proteintech) were used in subsequent studies.

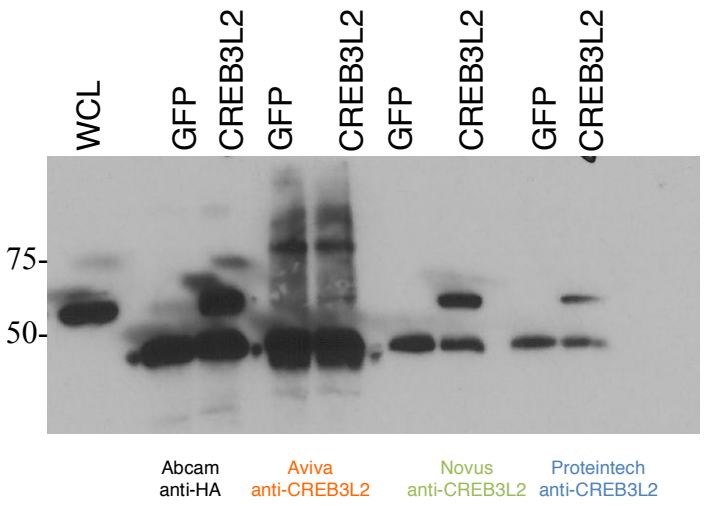


**Figure 3.14: Validation of CREB3L2 antibodies by immuno-precipitation technique.** The CREB3L2 antibodies that were examined by Western blot analysis were validated by IP. The test was controlled by GFP (vector only) as a negative control and antibody to HA as a positive control. WCL (whole cell lysate) was used to check the HA-CREB3L2 protein from a Hela cell transfection.

### 3.4 Discussion

The aims of this project are to investigate the expression, regulation and function of CREB3L2 in human B-cell differentiation and B-cell tumours. This chapter describes the reagents required for CREB3L2 studies in the project were successfully generated. The initial goal was to produce appropriate mammalian and bacterial expression constructs for CREB3L2 (CREB3L2-pIRES2EGFP and CREB3L2-pGEX6P-1). In both instances, two rounds of selection and restriction digest tests verified the correct cloning. Subsequently, the production of protein from the mammalian expression construct was confirmed by transient transfection into HeLa cells. The ability to express the active cleaved portion of CREB3L2 with an HA tag was a useful tool in evaluating the commercially available CREB3L2 antibodies by Western blot analysis and immuno-precipitation techniques. Moreover, the constructs will be useful in studying CREB3L2 target genes using binding assays such as EMSA and ChIP and functional studies such as promoter reporter assays.

The next step was the generation of GST-CREB3L2 fusion proteins (small and large scales) that could be used to make CREB3L2 antibody. The small-scale GST-CREB3L2 fusion protein generation was successful however, the large-scale presented difficulties. The lack of detectable protein in the large-scale prep necessitated a number of trouble-shooting steps. First solubility and elution efficiency were checked in the bacterial pellets and the Sepharose-bound material. Then, IPTG induction capability was examined using another protein, ZBTB32, due to its successful GST-fusion protein generation in both small and large scales. However, neither the solubility nor the elution tests provided a positive result; therefore the large-scale was repeated using newly prepared IPTG since there appeared to be a failure to induce protein (Figure-7B; 2). The induction problem was resolved, yet only degradation products were detected and no full length CREB3L2 fusion

protein was purified. To overcome this issue, the CREB3L2-pGEX6P-1 construct was transformed into protease-deficient competent bacteria (BL21-Gold) and the large scale was repeated using the same IPTG used previously. Even with these new adaptations, the procedure did not result in the required fusion protein. However, this time the fusion protein was found in the bacterial pellet suggesting a sonication problem. Thus, to solve that issue, ten small-scale GST-fusion protein preps were prepared and purified using column chromatography. Again, there was no detectable full-length protein, suggesting that the failure was not due to sonication challenges only.

Surprisingly, the examination of the Sepharose bound material revealed the presence of a large amount of protein (Figure-8D), raising another issue, which is elution. Interestingly, it has been published that the use of reduced Glutathione in high concentration (20mM) with NaCl (120mM) improves the elusion efficiency (88).Thus, a small experiment was conducted to compare the elution efficiency (Figure-9 A-B) revealing a better elution using higher concentration of reduced Glutathione and salt in the elution buffer, confirming the published data. Thus, from the optimisation steps described above, GST-CREB3L2 fusion proteins can be generated in multiple small-scales (10-20) using a higher stringency elution buffer (10mM Reduced Glutathione, 120mM NaCl, 100mM Tris pH 8.0) to avoid sonication and elution challenges, respectively.

Forty small-scale preps of GST-CREB3L2 were generated (Figure-10) and eluates were combined to estimate GST-CREB3L2 concentration. In this case, other protein quantification assays, such as the Lowry assay, cannot be used because glutathione can interfere with the results. Furthermore, the protein preps contain a range of breakdown products and it is useful to determine the proportion of full-length fusion protein. Therefore, eluates were combined and the concentration was estimated by comparing it with a standard series of BSA dilutions on 10 % SDS-PAGE. The estimated amount was less than 0.25mg/ml (Figure-11) so the fusion protein was concentrated

using a Centricon filter that separates the fusion proteins in the retantate and other proteins, which are less than 10kDa in the filtrate. However, the obtained fusion protein was only 0.25mg/ml (Figure-12), which is less than the optimal required concentration (0.5mg/ml). Thus, another 20-40 small-scales generation will be needed to generate sufficient amounts of protein. Although, the commercially available antibodies appear to work in the assays tested, it would be useful to proceed with the plan to generate an in-house antibody that would provide a plentiful source of a single batch of reagent. The fact that many degradation products are present in the fusion protein prep is not a problem for subsequent use as an immunogen, since many epitopes are short amino acid sequences derived from larger proteins. In contrast, if the fusion protein were to be used for binding assays such as EMSA, an intact protein would be required.

In summary, the reagents required for additional CREB3L2 studies have been generated; the CREB3L2 construct for expression in mammalian cells has been cloned and tested, the commercially available CREB3L2 antibodies validated and the GST-CREB3L2 fusion proteins were generated.

# 4. Tracking *CREB3L2* expression and cleavage

## 4.1 Tracking *CREB3L2* expression in different cell lines by real-time PCR

Full-length CREB3L2 is encoded by 12 exons and generates a protein that is retained in the ER until cleavage by UPR-activated proteases. The amino terminal portion that constitutes the active transcription factor is made up of a transactivation region, a basic DNA-binding domain and a leucine zipper (67). In addition to the main isoform, Panagopoulos et al. identified an alternative *CREB3L2* transcript arising from an intronic polyadenylation site. The shorter form of *CREB3L2* produces a protein that is limited to the transactivation domain with the potential for regulatory activity when tested with a GAL4 DNA-binding domain fusion assay (75). Quantitative real-time PCR was used to check expression of the two *CREB3L2* isoforms (Figure 4.1) in six different cell lines derived from B-lineage tumours and representative of different stages of B cell differentiation (Myeloma lines U266 and H929; ABC-DLBCL lines OCI-LY3 and OCI-LY10; Hodgkin's lymphoma lines L428 and L1236). *PPP6C* was used as a control due to its stable expression during in vitro B-cell differentiation to the plasma cell stage (4). The CT values for each primer pair were first normalised to the values for the control (*PPP6C*) and then normalised using the H929 cell line. The analysis revealed that both *CREB3L2* transcripts are expressed in the six cell lines used; with the lowest *CREB3L2* expression detected in the OCI-LY3 cell line (Figure 4.2). The two isoforms were expressed to a similar extent in the majority of cell lines, with a single exception for OCI-LY10, which had reduced amounts of isoform 2.

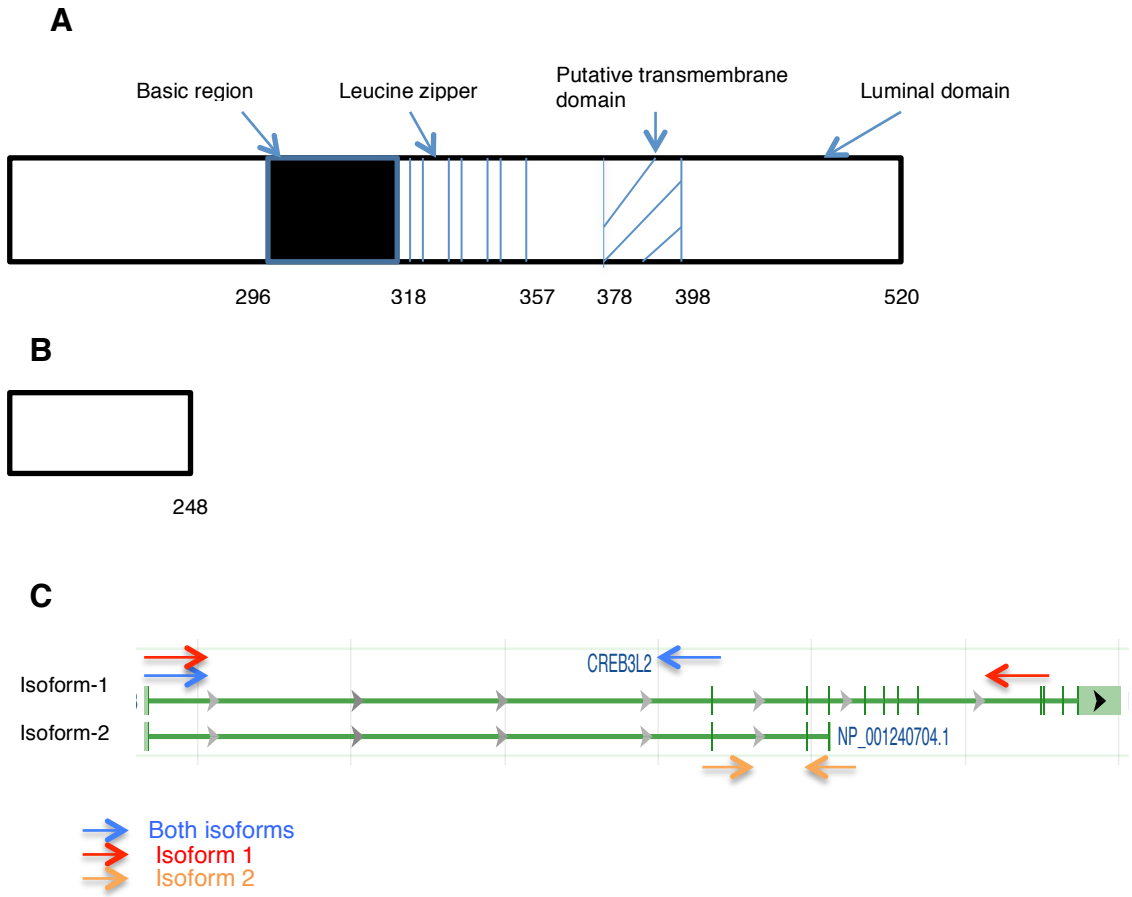


**Figure 4.1: Assessment of *CREB3L2* isoforms. A.** Diagrammatic representation of *CREB3L2* isoform-1 structure. **B**. Diagrammatic representation of *CREB3L2* isoform-2 structure. **C.** The sets of primer pairs used to amplify the two isoforms of *CREB3L2* are indicated on the diagram depicting the intron/exon structure of *CREB3L2* isoforms modified from the NCBI entry. Arrows are not drawn to scale, but indicate the exon in which the primer is located.

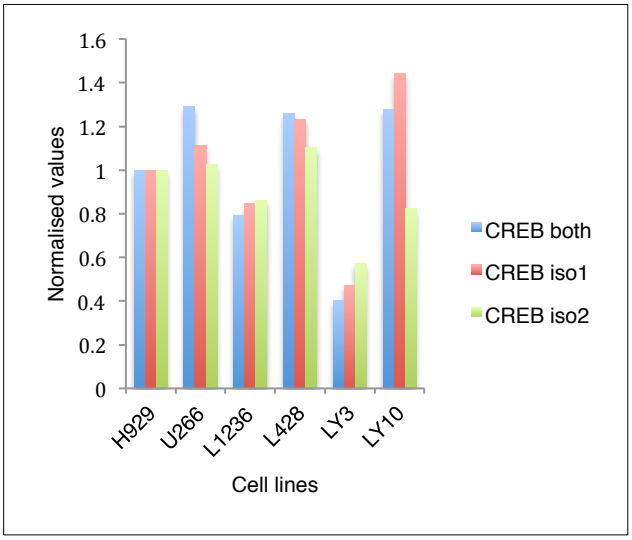


**Figure 4.2: *CREB3L2* expression in different cell lines.** The expression of the two transcripts of *CREB3L2* was checked in six different cell lines: U266, H929, OCI-LY3, OCI-LY10, L428 and L1236 using three primer pairs. CT values for each primer pair were first normalised to the values for the control (*PPP6C*) and then normalised using H929 cell line.

## 4.2 Tracking CREB3L2 expression and cleavage in myeloma cell lines and ABC-DLBCL cell lines

The ER is dedicated to the synthesis and export of proteins and lipids. One of the main functions that occur during this process is the proper folding of proteins with the assistance of multiple chaperones. Any disruption of its function leads to the accumulation of mis-folded proteins in the ER, hence ER-stress, which can lead to apoptotic cell death. However, eukaryotes have developed a mechanism to deal with the accumulation of misfolded or over-abundant proteins termed the UPR, which composed of three arms: PERK, IRE1 and ATF6. In 2014, Saito et al. described an additional novel ER-stress transducer in chondrocytes called CREB3L2 (90).

The mRNA expression pattern of *CREB3L2* in differentiating B-cells suggests that it is likely to form part of the UPR in this lineage. To determine the extent of CREB3L2 processing that occurs in B-cells, first the endogenous expression of CREB3L2 protein was examined in myeloma cell lines (U266 and H929) and in ABC-DLBCL cell lines (OCI-Ly3 and OCI-Ly10) using two ER-stressors that are known to trigger the UPR: 1μM Thapsigargin (TG) and 1mM DTT at the indicated times (2hr and 4hr) (Figure 4.3 and Figure 4.4 respectively). In addition, β-ACTIN was used as a loading control to confirm that an equal amount of protein was used in each lane. It has been shown by Kondo S et al, (2007) that CREB3L2 full length (FL) and cleaved form (CF) are predicted to be approximately 80 kDa and 60 kDa, respectively, using Western blotting (67). Lysate from Hela cells transfected with the CREB3L2 amino-terminus encoding construct served as a positive control to indicate the mobility of the cleaved form.

The results show that upon ER-stress by TG or DTT, the two forms of CREB3L2 (FL and CF), are expressed and increase over time with a relative ratio of approximately 2:1 of FL: CF in U266, OCI-Ly3 and OCI-Ly10 cells (Figure-4.3 and Figure-4.4). A slightly different pattern was observed in H929

cells such that the increase in the relative ratio was approximately 1:1 in FL: CF (Figure-4.3).

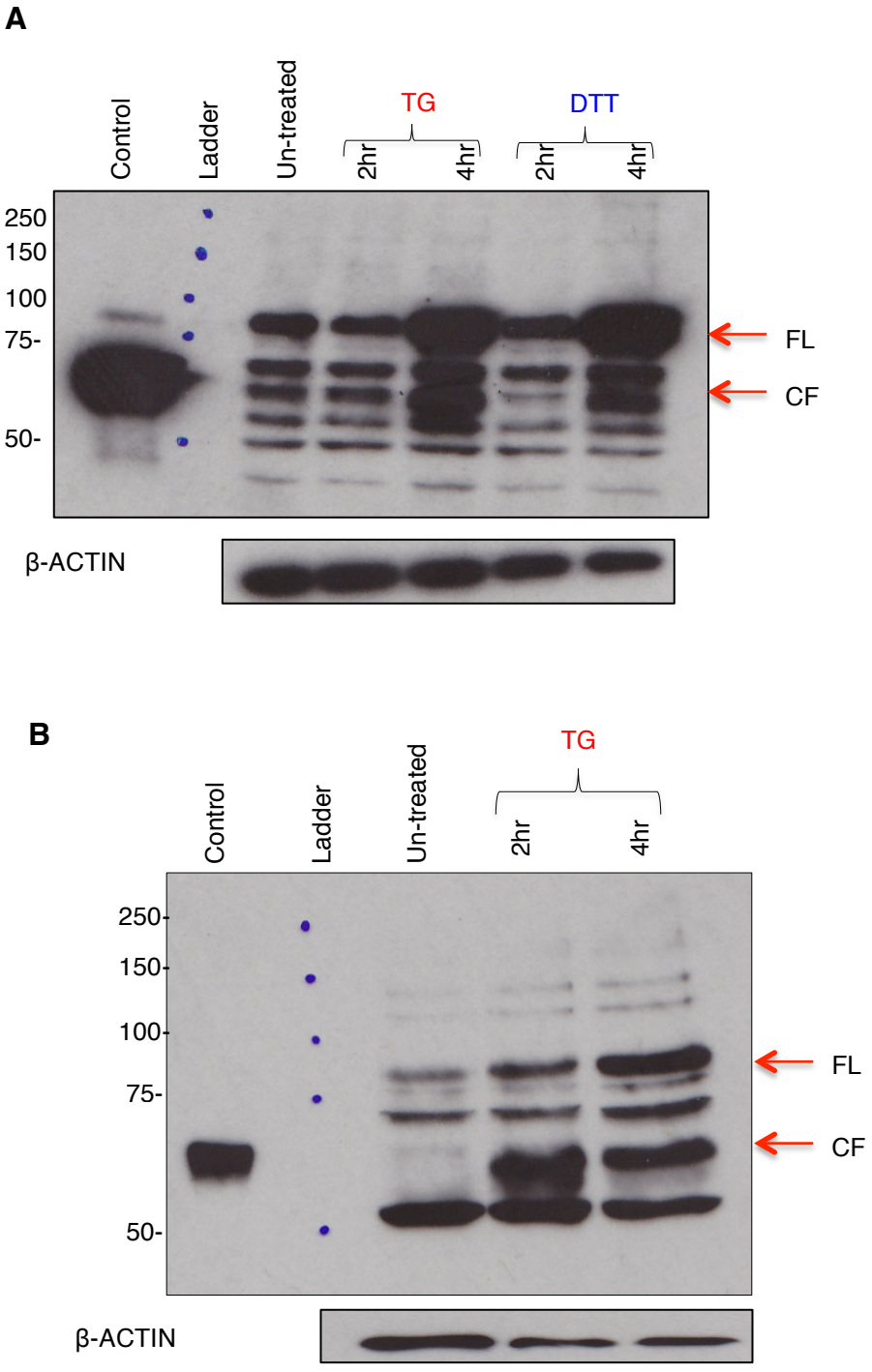


**Figure 4.3: Endogenous expression of CREB3L2 in myeloma cell lines**. **A.** U266, **B.** H929**.** Protein samples from whole cell lysates were loaded on a 10% SDS-PAGE gel and transferred to a nitrocellulose membrane. The membrane was probed by CREB3L2 antibody. The control used for the cleaved form was the N-terminus of CREB3L2 overexpressed in Hela cells. Beta-ACTIN was used as a loading control. FL, Full Length. CF, Cleaved Form.

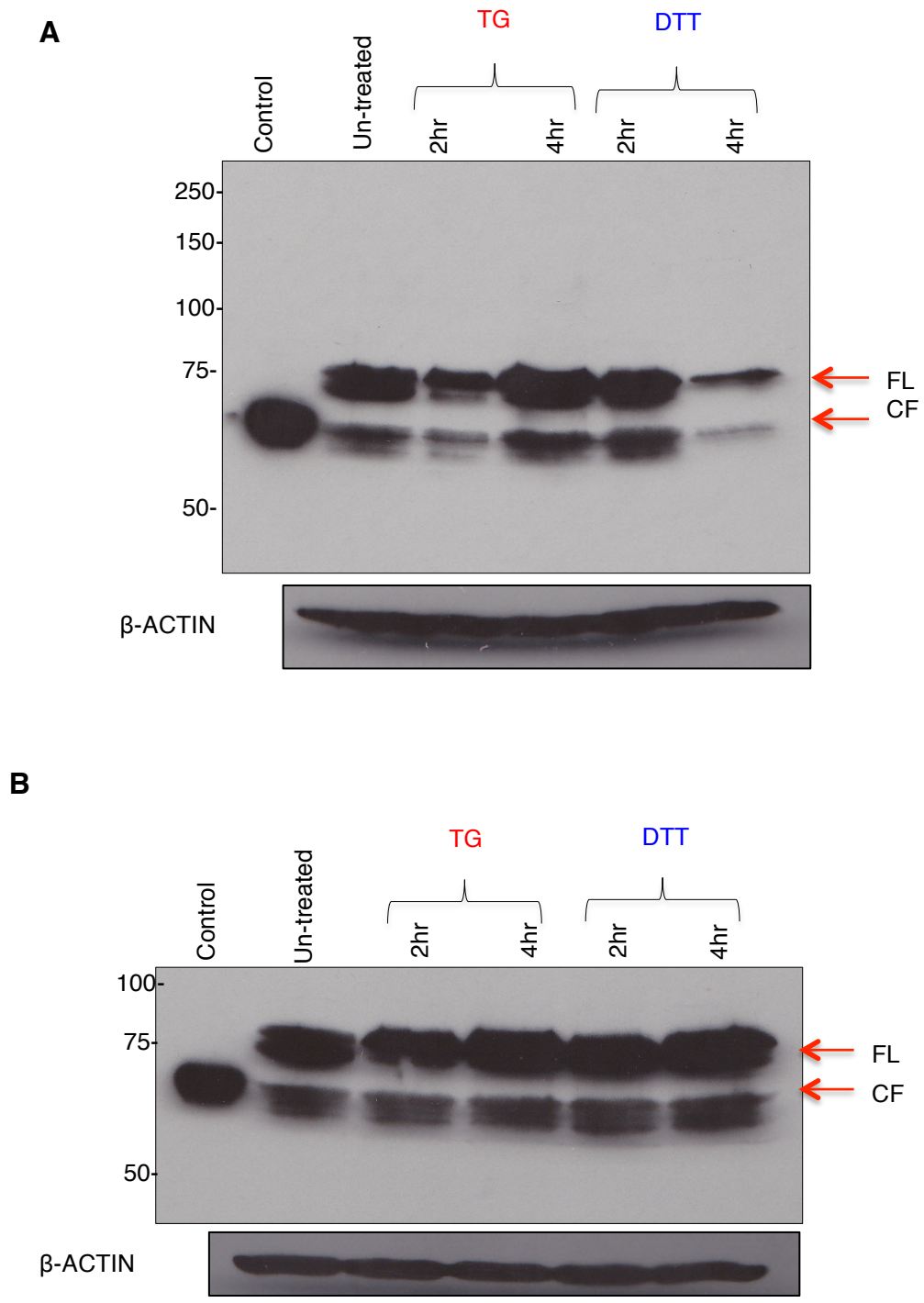


**Figure 4.4: Endogenous expression of CREB3L2 in ABC-DLBCL cell lines**. **A.** OCI-Ly3 and **B.** OCI-Ly10**.** Protein samples were loaded on a 10% SDS-PAGE gel and transferred to a nitrocellulose membrane. The membrane was probed by CREB3L2 antibody**.** The control for the cleaved form was the N-terminus of CREB3L2 overexpressed in Hela cells. β-ACTIN was used as a loading control. FL, Full Length. CF, Cleaved Form.

## 4.3 Tracking CREB3L2 expression and cleavage in human differentiated B-cells

Based on the gene expression data obtained by Cocco et al., CREB3L2 is predicted to increase as B-cells transition to antibody secreting cells, however, the active transcription factor may only be present after activation of the UPR. To determine whether the protein expression of CREB3L2 correlated with mRNA levels and differentiation stage, human B-cells were isolated from normal donors and differentiated in vitro. Protein samples were prepared at timed intervals and examined by Western blotting (Figure 4.5).

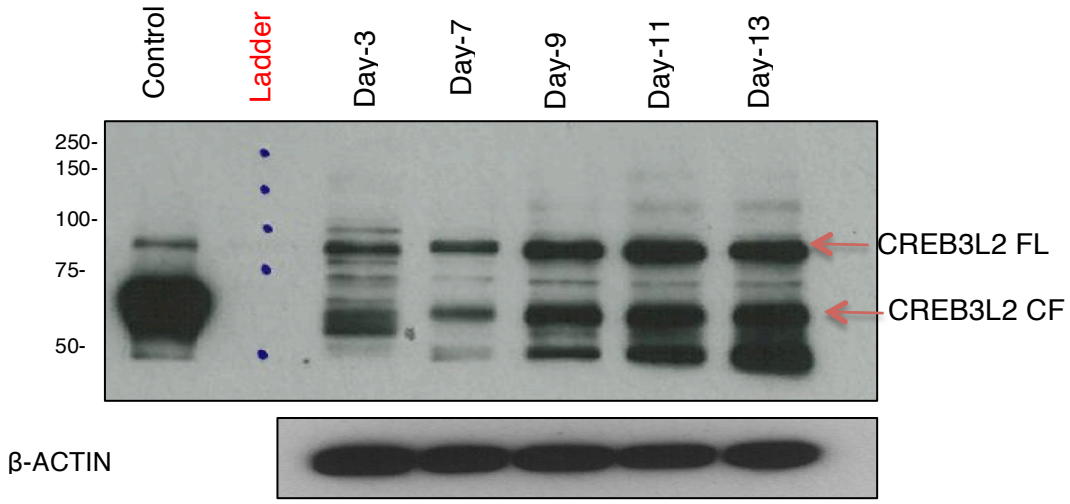


**Figure 4.5: CREB3L2 expression in human B-cells and antibody secreting cells (Day-3, -7, -9, -11 and Day-13) by Western blot.** Protein samples were loaded on a 10% SDS-PAGE gel and transferred to a nitrocellulose membrane. The membrane was probed by CREB3L2 antibody**.** The control for the cleaved form was the N-terminus of CREB3L2 overexpressed in Hela cells. β-ACTIN was used as a loading control. FL, Full Length. CF, Cleaved Form.

Figure 4.5 shows the expression pattern of CREB3L2 in human activated B-cells and during the transition to antibody secreting cells. The results revealed the presence of two bands of CREB3L2, FL (80 kDa) and CF (60 kDa), at each time point, however in Day-3 cells there is very little CF. In this particular

experiment, the Day-7 sample was taken prior to the change-over to maturation media, which includes Il-6, IFN-α and IL-21. Following transition to the new media, both CREB3L2 FL and CF were expressed increasingly to Day-13, when cells have adopted a plasma cell phenotype and are secreting large amounts of antibody.

Overall, the expression pattern agreed with the results obtained by Cocco et al (4).

Densitometry was used to quantify the bands obtained in chapter-4 to summarize the expression pattern of CREB3L2 (FL and CF) from different cell types (Figure-4.6).

A

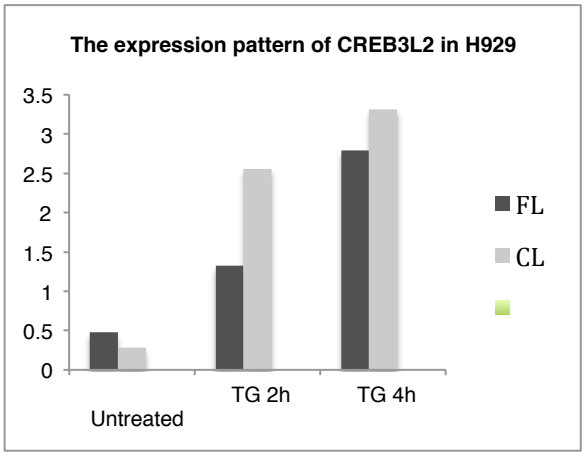


B

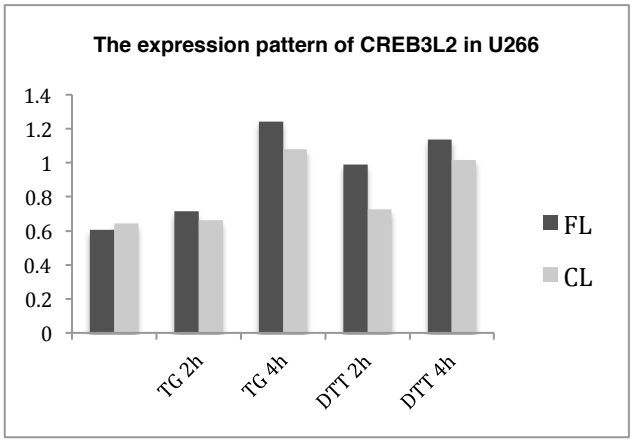


C

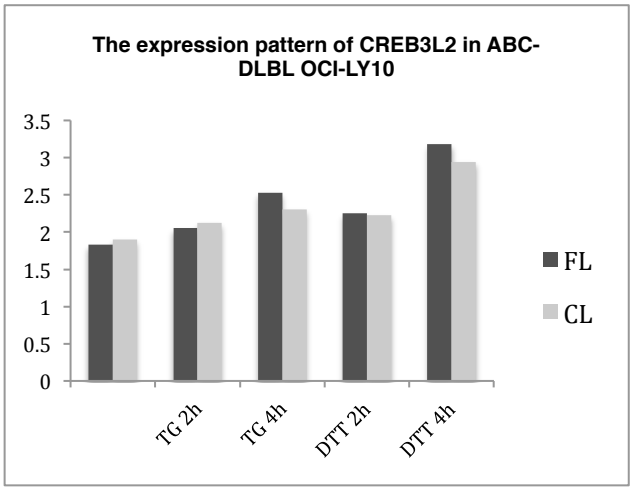


D

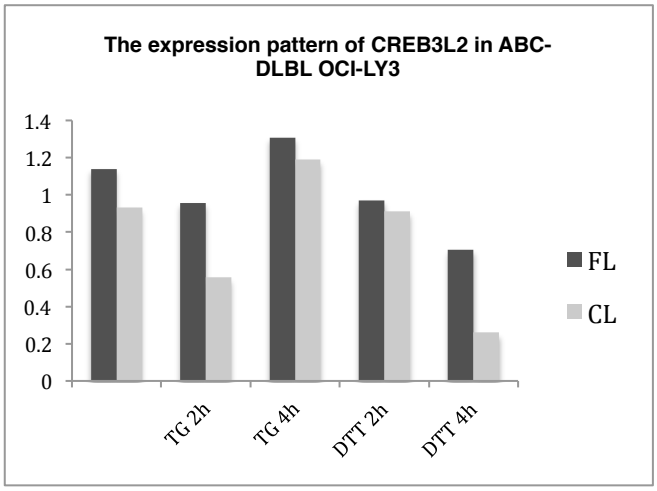


E

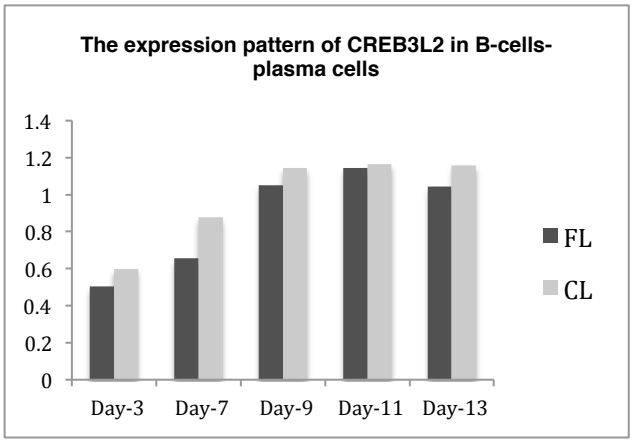


**Figure-4.6: The endogenous expression pattern of CREB3L2 (FL and CF) in different cell types using densitometry.** A. Myeloma cell lines A. H929. B. U266. ABC-DLBL cell lines. C. OCI-Ly10. D. OCI-Ly3. E. Human B cells and plasma cells. FL, Full length. CF, Cleaved Form.

## 4.4 CREB3L2 C-terminus

The vast majority of the published work on S1P/S2P regulated proteins has focussed on the transcription factors that are released from the cytoplasmic portion of the proteins. Less is known about the fate of the remaining portion that resides in the ER lumen. In 2014, Saito et al. found that upon ER-stress in chondrocytes, the C-terminus portion of CREB3L2 is secreted into the extracellular space to function as a signalling molecule through the interaction with Indian hedgehog (Ihh) and its receptor Ptch1. Hedgehog signalling is an important pathway for cell proliferation and differentiation. In addition, it is involved in the commencement and survival of many tumours such as LGFMS. In mammals, the hedgehog-signalling pathway is composed of three types, Shh (Sonic hedgehog), Dhh (Desert hedgehog) and Ihh (Indian hedgehog). The Ihh hedgehog induces the expression of PTHrP (parathyroid hormone related protein) in prehypertropic chondrocytes to stimulate the proliferation of chondrocytes (90).

Thus, CREB3L2 has dual roles: the N-terminus functions as a transcription factor and the C-terminus functions as a signalling molecule through hedgehog pathway upon ER stress (90). Interestingly, hedgehog signalling has also been implicated in the survival of myeloma cells (91). Therefore, the role of CREB3L2 C-terminus in the myeloma cell line (U266) was investigated

To determine whether the C-terminal portion of CREB3L2 could be generated under conditions of ER-stress U266 cells were treated with media alone or containing 1 μM Tg for 12 hours. At this time point tissue culture supernatants were collected for evidence of secreted protein and the cells were lysed. An isotype control or antibody against the C-terminus of CREB3L2 were then used to generate immunoprecipitates from both sources. The resulting complexes were run on SDS-PAGE, transferred to nitrocellulose and blotted with the C-terminus antibody followed by a heavy-chain specific secondary antibody (Figure 4.7).

The predicted CREB3L2 C-terminus molecular weight is 15 kDa (90). While there are a number of bands that appear to be unique to the CREB3L2 IPs, there are no bands consistent with the size of the C-terminus and relatively little difference between unstressed and stressed samples. Additionally, the blot showed a high degree of non-specific binding making interpretation difficult. Therefore, CREB3L2 full length (HA-CREB3L2-FLAG) and CREB3L2 C-terminus (CREB3L2-CTERM-FLAG) constructs were designed (Figure 4.8) and tested (Figure 4.9-4.11).

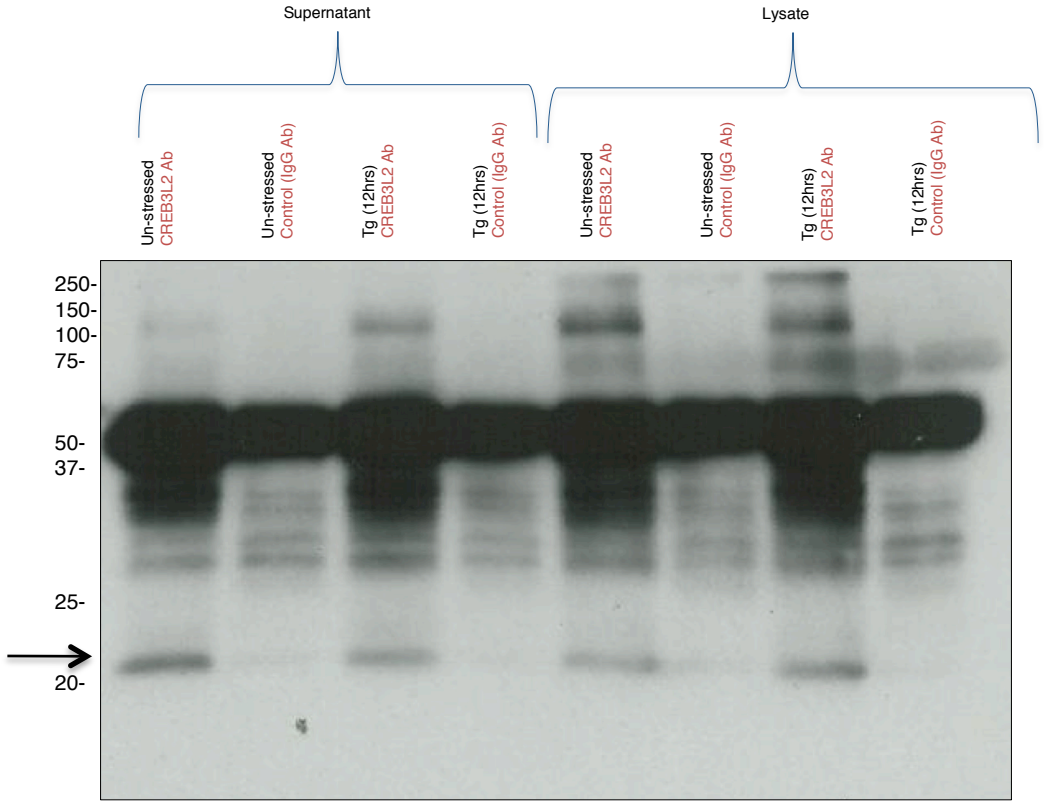


**Figure-4.7: The endogenous expression of CREB3L2 C-terminus in myeloma cell line U266.** U266 cells were incubated in media alone (unstressed) or containing 1 µM Tg (stressed) for 12 hours. Then, the lysate and supernatants were immunoprecipitated using CREB3L2 C-terminus antibody (ab102989) or IgG control antibody and analysed by Western blotting. The arrow indicates a unique protein in the CREB3L2 IPs.

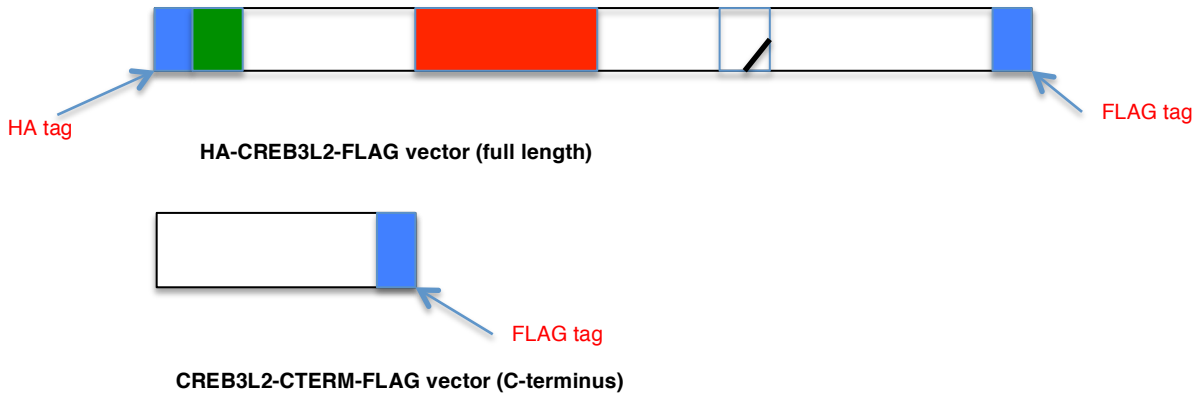


**Figure-4.8**: Diagrammatic representation of CREB3L2 full length and C-terminus vectors: HA-CREB3L2-FLAG (1-521 amino acids) and CREB3L2-CTERM-FLAG (431-521) amino acids respectively.

The full length CREB3L2 construct was designed such that an HA-tag would distinguish the N-terminus from the C-terminus marked by a FLAG-tag. Intact full-length protein would be recognised by antibodies to either, while the processed forms would only be detected by the appropriate tag. The constructs (HA-CREB3L2-FLAG and CREB3L2-CTERM-FLAG) were cloned into pIRES2-EGFP (Clonetech). Vectors containing either full length of *CREB3L2* (encoding amino acids 1-521 with amino terminal HA-tag and with C terminal FLAG-tag) or the C-terminal *CREB3L2* (encoding amino acids 431-521 with C-terminus FLAF-tag) and pIRES2-EGFP destination vector (Clontech) were digested using EcoRI and BglII (Figure 4.9A). Fragments of the correct size were purified, ligated and transformed into DH5α. DNA from the transformed cells was extracted and checked for the presence of appropriate insert by digestion with EcoRI and BglI (Figure 4.9B).

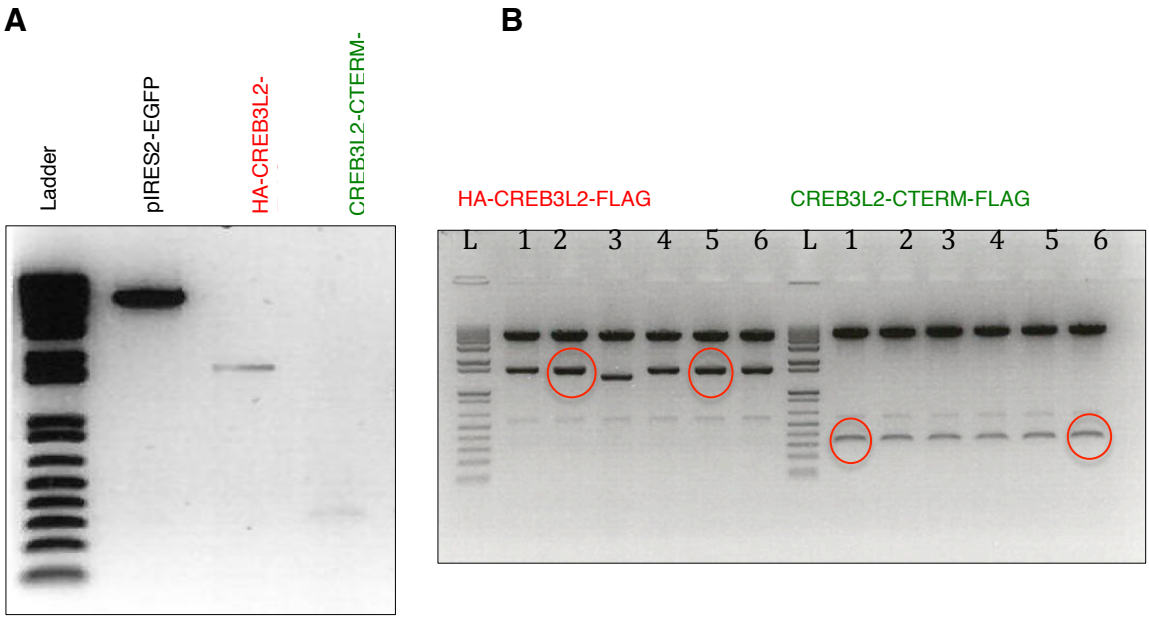


**Figure-4.9**: **Cloning of *HA-CREB3L2-FLAG and CREB3L2-CTERM-FLAG* into pIRES2-EGFP vector. A**. Preparative restriction digest of pIRES2-EGFP, HA-CREB3L2-FLAG and CREB3L2-CTERM-FLAG for cloning. **B.** HA-CREB3L2-FLAG-pIRES2EGFP and CREB3L2-CTERM-FLAG-pIRES2EGFP miniprep digestion. The expected insert sizes were 1647 bp and 318 bp, respectively. Red boxes indicate inserts of correct molecular weight. Numbering at the top indicates the designated clone number. L, molecular weight ladder.

The constructs were validated using transient transfection and Western blotting. Protein samples were prepared and run on 10% SDS-PAGE gel using HA antibody, CREB3L2 C-terminus antibody or FLAG antibody (Figure 4.10). The results show that the HA-antibody detected a protein consistent with the molecular weight of full length HA-CREB3L2-FLAG for each of the clones tested. Neither CREB3L2 C-terminus antibody nor FLAG antibody could detect CREB3L2-CTERM-FLAG as shown in Figure 4.9B. Therefore, the blot was repeated, additionally including lysates from cells transfected with the HA-CREB3L2-FLAG, which had been shown to be well expressed. Neither the positive control full-length protein nor the C-terminal fragments were detected (Figure 4.11). Given that the full-length protein was successfully expressed, it seemed likely that the problem was with the antibodies used for detection. However, this component of the project was not pursued further due to time limitations.

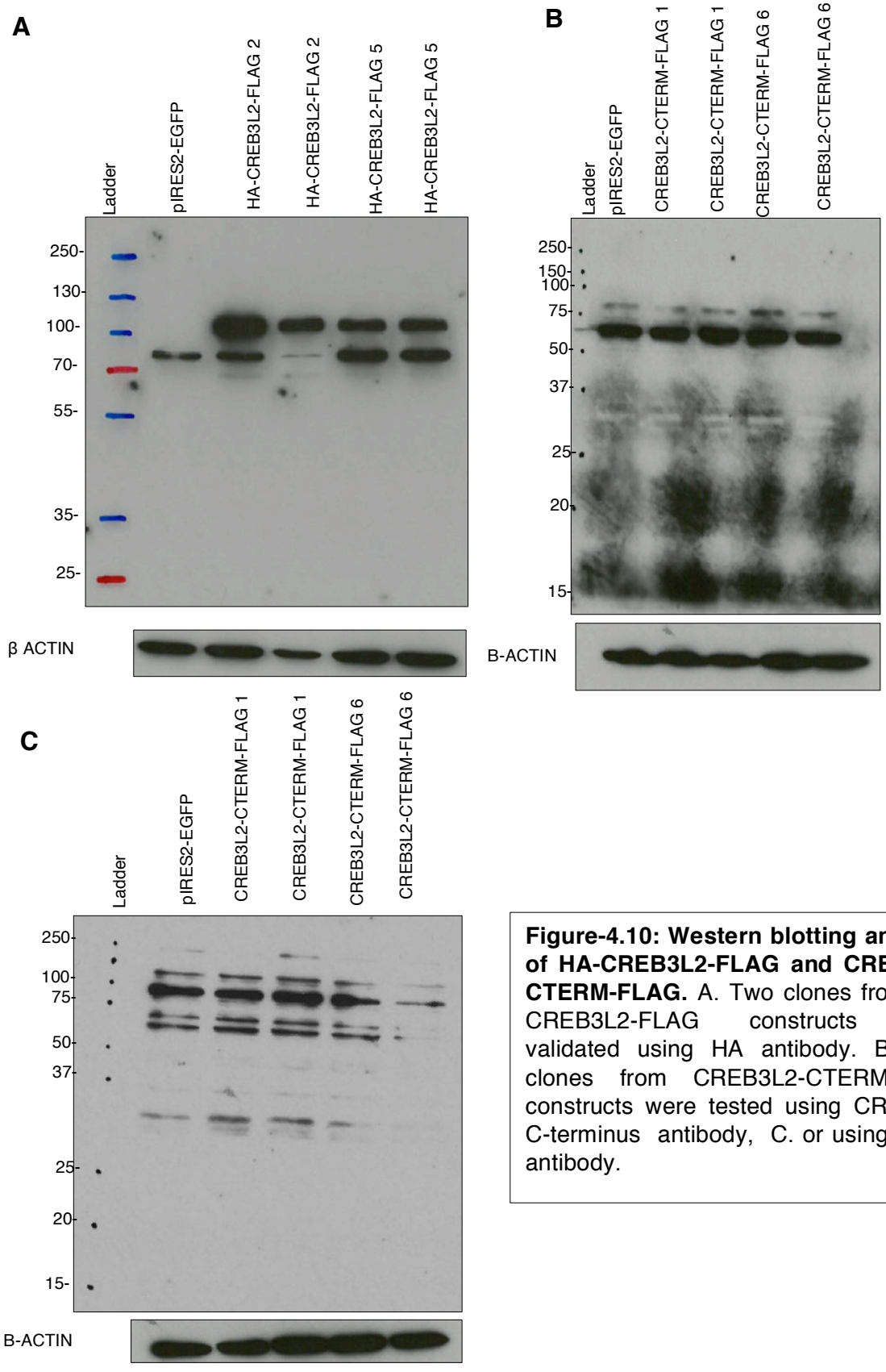


**Figure-4.10: Western blotting analysis of HA-CREB3L2-FLAG and CREB3L2-CTERM-FLAG.** A. Two clones from HA-CREB3L2-FLAG constructs were validated using HA antibody. B. Two clones from CREB3L2-CTERM-FLAG constructs were tested using CREB3L2 C-terminus antibody, C. or using FLAG antibody.

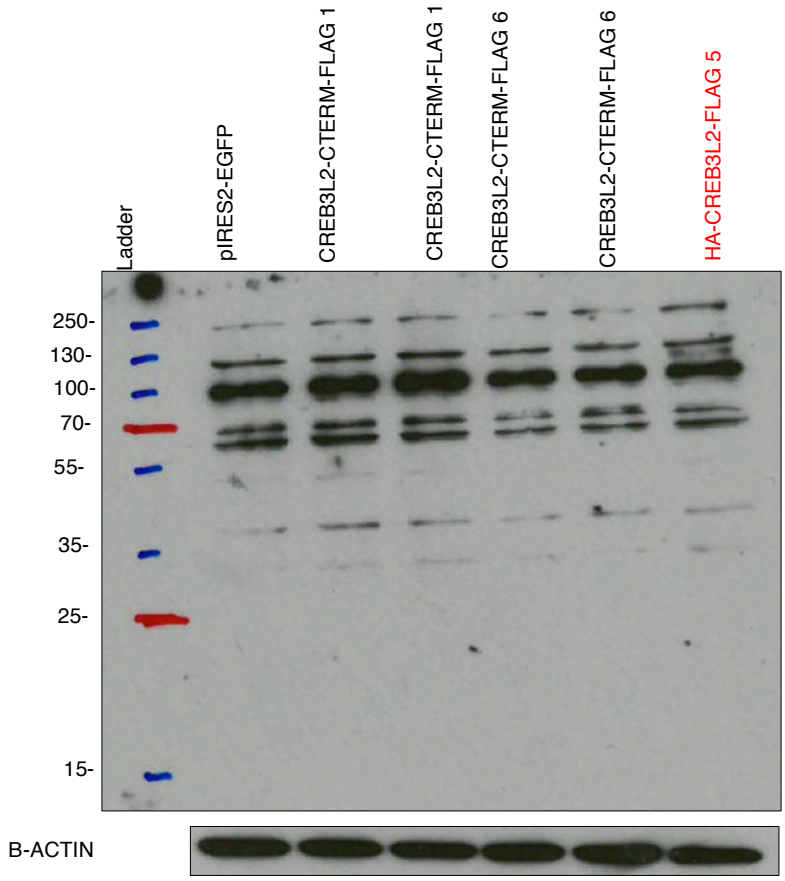


**Figure-4.11: Western blotting analysis of CREB3L2-CTERM-FLAG.** Two clones from CREB3L2-CTERM-FLAG constructs were evaluated using FLAG-antibody including HA-CREB3L2-FLAG clone 5 as a blotting control.

## 4.5 Discussion

Although it is accepted that the transition from activated B-cell to antibody secreting cell (ASC) is accompanied by a UPR, evidence suggests that this cell lineage has developed a specialised version of the response that predominantly uses the IRE1-XBP1 pathway (52). Additionally, the requirement for XBP1 occurs at later stages of the differentiation process and is not the transcription factor responsible for driving changes during the early phases of becoming an ASC (5). Work leading up to this project identified a cluster of genes displaying a co-ordinated pattern of up-regulation during plasma cell differentiation, which included not only the key PC transcription factors *PRDM1* and *IRF4*, but also *CREB3L2*. This finding was recently corroborated in study examining the transcriptional signature of murine ASCs (8).

CREB3L2 is expressed in many human tissues such as: placenta, heart, brain, and skeletal muscle. CREB3L2 has been postulated to act as a component of the UPR during chondrocyte differentiation, when the differentiating cells start to secrete extracellular matrix proteins that generate a mild ER-stress (79). In this setting CREB3L2 is cleaved in response to physiological stress and subsequently activates genes required for protein transport. In addition, Panagopoulos et al., have reported that there is an alternative *CREB3L2* transcript resulting from polyadenylation in intron-4. It is widely expressed in many human tissues and displays even stronger expression than the full length of *CREB3L2* in some tissues (75). To determine the role of the novel form encoded by BC063666, firstly, they examined whether it functions as an activator or not by co-transfection with a luciferase reporter containing a GAL4 binding domain in to Hela cells. The results revealed that BC063666 has the potential to behave as an activator, despite not having the bZIP domain. In addition, they examined whether BC063666 can regulate CRE-containing binding sites but found no evidence to support this. Moreover, the subcellular localization of the three forms of

CREB3L2 was studied using EGFP fluorescence (CREB3L2, CREB3L2ΔTM and BC063666). As anticipated the results showed that full length CREB3L2 was localised in the ER, while CREB3L2ΔTM was found in the nucleus. However, BC063666 was found in both the ER and in the nucleus suggesting that it may not be linked to ER-stress or it may have another cellular function. Thus, BC063666 is an alternative transcript of CREB3L2 that can act as a transactivator in a reporter assay; however, its cellular function remains unknown (75).

In this project, the expression of *CREB3L2* transcripts (isform-1 and isoform-2) were examined in six different cell lines derived from B-lineage tumours representative of different stages of B cell differentiation (Myeloma lines U266 and H929; ABC-DLBCL lines OCI-LY3 and OCI-LY10; Hodgkin's lymphoma lines L428 and L1236) using quantitative real-time PCR. The results revealed that both *CREB3L2* transcripts are expressed in all the six studied cell lines (U266, H929, OCI-LY3, OCI-LY10, L428 and L1236) with a single exception for OCI-LY10, which had reduced amounts of isoform 2. These results are in line with the published results, where the majority of samples tested expressed roughly equivalent levels of the two transcripts (75). It is possible that the additional form of CREB3L2 may function as a dominant-negative or plays a role in regulating the levels of total CREB3L2 protein.

To provide additional evidence that CREB3L2 is expressed from the activated B-cell stage onwards, the endogenous expression of CREB3L2 protein was examined in H929, U266, OCI-Ly3 and OCI-Ly10. Moreover, the relationship between a UPR and CREB3L2 levels was investigated using two ER-stressors. The results showed that upon ER-stress by TG or DTT, CREB3L2 FL and CF are induced and increase by time with relative ratio of approximately 2:1 for FL: CF in U266, OCI-Ly3 and OCI-Ly10 cells whereas, H929 cells expressed a relatively higher amount of CF. In addition, some additional bands were observed in the Western blots, lower than the predicted

molecular weight of FL and CF, suggesting that they could be the non-glycosylated form of FL and CF as shown by Kondo S, 2007(67).

From the gene expression profile data, the expression of CREB3L2 is predicted to increase as B-cells transition to ASCs, however, the active form of CREB3L2 may only be present after the activation of a UPR. To determine whether the protein expression of CREB3L2 correlated with mRNA levels and differentiation stage, human B-cells were isolated from normal donors and differentiated in vitro. The results revealed that the two forms of CREB3L2 (FL and CF) were expressed increasingly from Day-3 B-cells to Day-13 ASCs, suggesting that CREB3L2 is likely to play a role in the UPR signalling pathway that operates during B-cell differentiation (30). Taken together, the results from the cell lines and primary cells suggest that CREB3L2 is expressed as the cells initiate the process of differentiation and accumulate more protein as the cells mature. The presence of the processed form indicates that it is likely to be generated in response to ER-stress and its regulation and function may be similar to that observed in differentiating chondrocytes (79). It is also tempting to speculate that CREB3L2 might drive the necessary transcriptional changes to commence the expansion of the secretory machinery, prior to XBP1.

Initial attempts were also made to determine whether the hedgehog signalling-competent C-terminal portion of CREB3L2 was produced in stressed U266 cells. While the preliminary data did not provide conclusive evidence, it remains an interesting avenue to pursue. In normal B-cells, hedgehog signalling prevents apoptosis in the germinal centre and it has been linked to the survival of a number of B-cell malignancies including diffuse large B-cell lymphoma and myeloma (92-94). Establishing an additional role for CREB3L2 via hedgehog signalling would provide additional rationale for targeting this protein as a therapeutic strategy.

## 5. Site-1 protease (S1P) and site-2 protease (S2P) inhibition in myeloma cell lines and ABC-DLBCL cell lines

CREB3L2 is predicted to be a single-pass type 2 membrane-spanning protein that resides in the ER membrane until an ER stress event leads to its transport to the Golgi and subsequent proteolysis. The proteloytic cleavage involves the sequential activities of firstly S1P in an exposed luminal site and secondly S2P which catalyses an intramembrane cleavage (95). This is a conserved feature of a number of transcription factors that are released in this fashion to mediate changes in gene expression required for lipid metabolism or ER stress responses such as SREBP and ATF6. SREBPs (SREBP-1a, SREBP-1c and SREBP-2) are activated in response to sterol depletion whereas ATF6 (α and β) is activated in response to ER stress (96).

Several studies have been carried out to investigate the impact of S1P/S2P inhibition on different cell types. For example, using S1P inhibitor in HepG2 and Chines Hamster Ovary cells (CHO) blocks SREBP processing, which in turn leads to cholesterol and fatty acid depletion. Hence, SREBP has been suggested as therapeutic target for dyslipidaemia and cardio-metabolic diseases (97). In addition, Guan et al., have shown that liposarcoma cells can be targeted through inhibiting S2P, which in turn activates ER-stress, resulting in cell death (98). Thus, these studies highlight the importance of S1P/S2P inhibition.

In myeloma cell lines full-length CREB3L2 is expressed at a high level with some evidence of constitutive processing; however, there is a clear relationship between application of ER stress and the induction of both full length and processed CREB3L2 (Figure 4.3). Moreover, in differentiated human B-cells an increase in both full length and cleaved CREB3L2 is consistent with ER stress triggered by antibody production. Given that CREB3L2, and indeed other important ER stress transcription factors, is regulated by a defined mechanism involving S1P/S2P there is the potential to

modify expression using specific inhibitors. Since successful adaptation to ER stress is critical for cell survival, it is predicted that limiting the necessary transcription factors could have a profound effect. Therefore, it is important to test the impact of S1P and S2P inhibition on CREB3L2 and other UPR elements to examine its potential therapeutic intervention. Three commercially available S1P, S2P inhibitors; (4-(2-aminoethyl) benzenesulfonyl fluoride (AEBSF) and PF-429242, as S1P inhibitors and Nelfinavir as S2P inhibitor were initially tested in neoplastic B-lineage cell lines.

### 5.1 The impact of serine protease inhibitor AEBSF

AEBSF is a generic serine protease inhibitor that can target S1P. It is an irreversible serine protease inhibitor similar to phenylmethylsulfonyl fluoride (PMSF) yet it is more stable and non-toxic. It works by reacting with the hydroxyl group of the serine residue resulting in cleavage (96). In the study by Okada et al., Hela cells were pre-treated with different concentrations of AEBSF, PMSF, aprotinin or chymostatin. Then, the cells were stressed using thapsigargin and lysates analysed by Western blotting. Their results revealed that AEBSF had the greatest inhibitory impact on ATF6α and ATF6β processing among the other three studied serine protease inhibitors. Therefore, based on these results, ABC-DLBCL (OCI-Ly3 and OCI-Ly10) cell lines were treated with 300 μM of AEBSF for 1h, 6hr and 24hrs in standard culture conditions. At each time point, cells were collected for protein lysates and subsequently analysed by Western blotting (Figure-5.1). According to the proposed function of AEBSF as a S1P inhibitor, it should affect the CF of CREB3L2 only by inhibiting the cleavage, but the obtained results showed an effect on both forms of CREB3L2 that increased with time. In fact, the full-length protein appeared to diminish more rapidly. By 24hr no protein (CREB3L2) was detected despite maintenance of β-ACTIN levels. It was concluded that AEBSF might have a non-specific effect on CREB3L2 and was not used in the human differentiated B-cells-plasma cell studies.

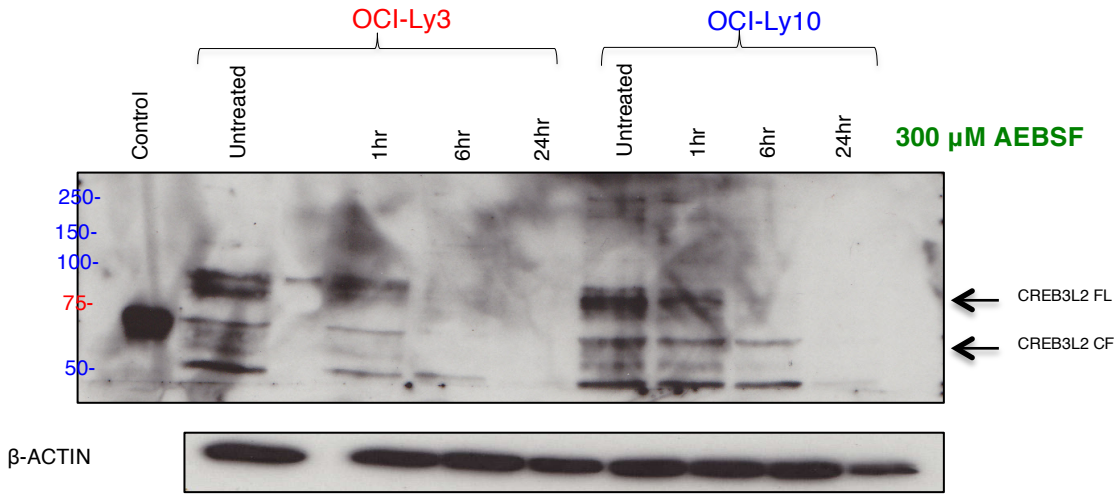


**Figure 5.1: The impact of AEBSF on CREB3L2 in ABC-DLBCL (OCI-Ly3 and OCI-Ly10) cell lines.** The cells were treated with 300 μM AEBSF for 1hr, 6hr and 24hr, protein samples generated at each time point and analysed by Western blotting. The amino terminal portion of CREB3L2 (1-375 aa) was overexpressed in Hela cells and used as a positive control for detection of the cleaved form. β-ACTIN was used as loading control. Full Length, FL. Cleaved Form, CF.

## 5.2 The impact of S1P inhibitor (PF-429242)

### 5.2.1 Dose response analysis

PF-429242 is a reversible, competitive and selective inhibitor for S1P (97). It was discovered by a Pfizer research group from a high throughput screen using purified human S1P. They generated 3 libraries to study the efficiency of different S1P inhibitors revealing PF-429242 (from the third library) to be the most selective for S1P, with an IC50 for S1P inhibition at 170 nM and no significant inhibition of proteinase, trypsin, thrombin and elastase at a concentration of 100 μM (99). In addition, PF-429242 has been shown to block SREBP processing and decrease cholesterol and fatty acids synthesis (97).

To establish the effect of selective S1P inhibition on CREB3L2, the myeloma cell line U266 was treated with different concentrations of PF-429242; 5μM, 10μM, 20μM and 50μM for 24hr (based on the published data Hawkins et al., 2008)(97) with some slight modifications. Then, the cells were collected, protein samples were prepared and analysed by Western blotting for CREB3L2 (Figure-4.2). The results revealed a reduction in the intensity of CREB3L2 cleaved form in all the studied concentrations, with slight enhancement using 10μM and 20μM PF-429242 in agreement with the published data (97). Unlike treatment with AEBSF, the loss of cleaved CREB3L2 was accompanied by an increase in the detectable full-length protein, suggesting that PF-429242 was a more effective inhibitor of S1P-mediated events.

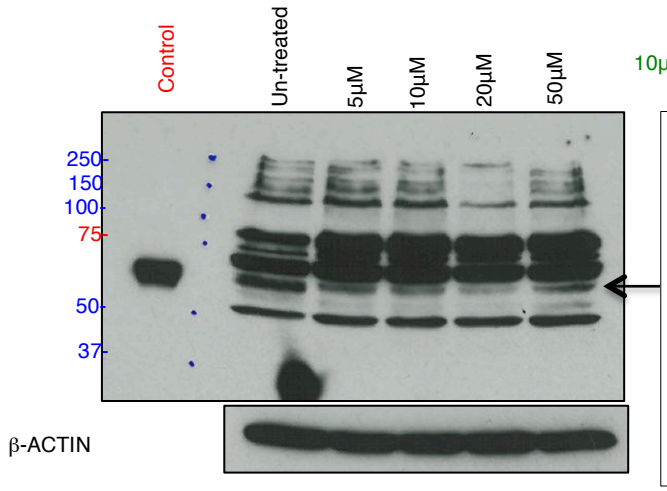


**Figure-5.2 The impact of PF-429242 on CREB3L2 in the U266 myeloma cell line.** The cells were treated with the indicated concentrations of PF-429242 for 24hrs and the protein samples analysed by Western blotting using antibody to CREB3L2. The amino terminal portion of CREB3L2 (1-375 aa) was overexpressed in Hela cells and used as a control for the cleaved form. β-ACTIN was used as loading control.

### 5.2.2 Kinetic analysis

The previous experiment suggests that treatment with 10μM PF-429242 reduced the amount of cleaved CREB3L2 by greater than 50% at a 24 hour time point. To determine whether the inhibition could be sustained or even augmented, a later time point was also assessed. The U266 cell line was treated with 10μM PF-429242 for 24 or 40hr. Then, the cells were collected and the protein samples were prepared and analysed by Western blotting for CREB3L2 (Figure-5.3). The treatment for 24hr resulted in an even more profound loss of cleaved protein (estimated 70-80%), which was accompanied by a reciprocal gain of full-length protein. Conversely, longer treatment also generated higher amounts of full-length protein but did not prevent cleavage. The failure to inhibit at 40hr could be due to decreasing efficiency of the inhibitor over time and the rate of cell growth in culture. Thus, CREB3L2 cleavage in U266 was best studied using 10μM PF-429242 for 24hrs. This agreed with other studies, such as that of Hawkins et al., where CHO cells treated with 10μM PF-429242 for 24hrs showed inhibition of endogenous SREBP
processing (97).

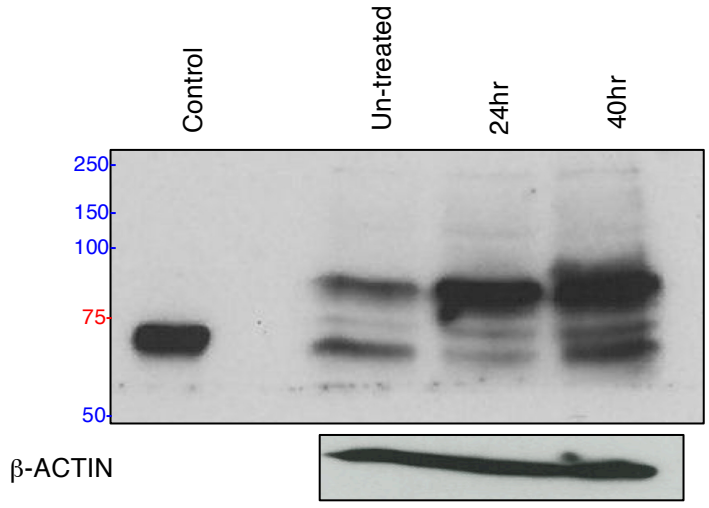


**Figure 5.3: The impact of 10μM PF-429242 on CREB3L2 in U266 for 24 and 40hr.** The cells were treated with 10μM PF-429242 for 24hr and 40hr under standard culture conditions. Protein samples were collected at each time point and analysed by Western blotting. The amino terminal portion of CREB3L2 (1-375 aa) was overexpressed in Hela cells and used as a control for the cleaved form. β-ACTIN was used as loading control.

### 5.2.3 UPR signalling pathways

Proper protein folding in the ER is an essential mechanism for secreted proteins prior to transportation to the Golgi and distribution to target organs. There are many environmental (e.g. calcium depletion), developmental (e.g. B-cell development) or pathological factors (e.g. viral infection) that can trigger the accumulation of mis-folded proteins in the ER and cause ER-stress (100). However, eukaryotic cells have evolved a physiological mechanism to overcome ER-stress called the UPR, which coordinates a transient suppression of protein translation, up-regulation of protein folding chaperones and disposal of the mis-folded proteins (101, 102). In instances where the ER-stress is not resolved, the cells will undergo apoptosis.

The UPR is composed of three signalling pathways: ATF6, IRE1 and PERK, which are normally bound to the protein folding chaperone BiP at the ER membrane. The three UPR-pathways are expressed in all cells where they become activated as BiP is titrated away in response to the accumulation of mis-folded proteins in the ER. IRE1 and PERK have similar modes of activation, where they undergo homodimerization and auto-phosphorylation in response to ER-stress. ATF6 is also released from BiP in response to the accumulation of mis-folded proteins. It then migrates to the Golgi and is cleaved via S1P and S2P, releasing the active form of ATF6, which is translocated to the nucleus to activate its target genes (30).

A number of lines of evidence suggest that there is a link between UPR and the development of plasma cells (103). During B-cell terminal differentiation, large amounts of immunoglobulins are secreted, which increase the load on ER. Hence unfolded or misfolded immunoglobulins potentially accumulate in the ER and cause ER-stress with subsequent activation of the UPR signalling pathways (104).

The initial data describing a role for XBP1 in plasma cell generation was consistent with the secretion of immunoglobulin triggering an unfolded protein response (31). Later reports suggested that XBP1 could be expressed in cells that did not secrete immunoglobulin, challenging the idea that a UPR is required (39). Unlike the proposed requirement for XBP1, available data suggest that both the PERK and ATF6 axes may be dispensable for the formation of plasma cells (51, 52). Collectively, the available evidence suggests that B-cells utilise the UPR an unconventional fashion (30). To gain a better understanding of the interplay between components of the UPR during terminal B-cell differentiation, XBP1s, ATF6 and CREB3L2 were studied in myeloma cell lines and in differentiating human B-cells.

To determine whether inhibition of S1P could be overcome by ER-stress, U266 cells were either stressed using ER-stressor thapsigargin (TG) or pre-treated with 10μM PF-429242 for 24hrs, stressed using 1μM TG for 4hrs and then evaluated for the expression of XBP1s, ATF6 and CREB3L2 (Figure-5.4). The results showed that PF-429242 treatment alone reduced the low basal expression of XBP1s. TG treatment substantially increased XBP1s, but S1P inhibitor only slightly reduced the amount in stressed cells. PF-429242 treatment leads to a marked accumulation of full length CREB3L2 accompanied by a reduction of the cleaved form in the basal state. In response to ER-stress, there is an up-regulation of both forms of CREB3L2 and S1P inhibition reduces each. However, ATF6 did not respond to either TG or 10μM PF-429242 in the cell type studied.

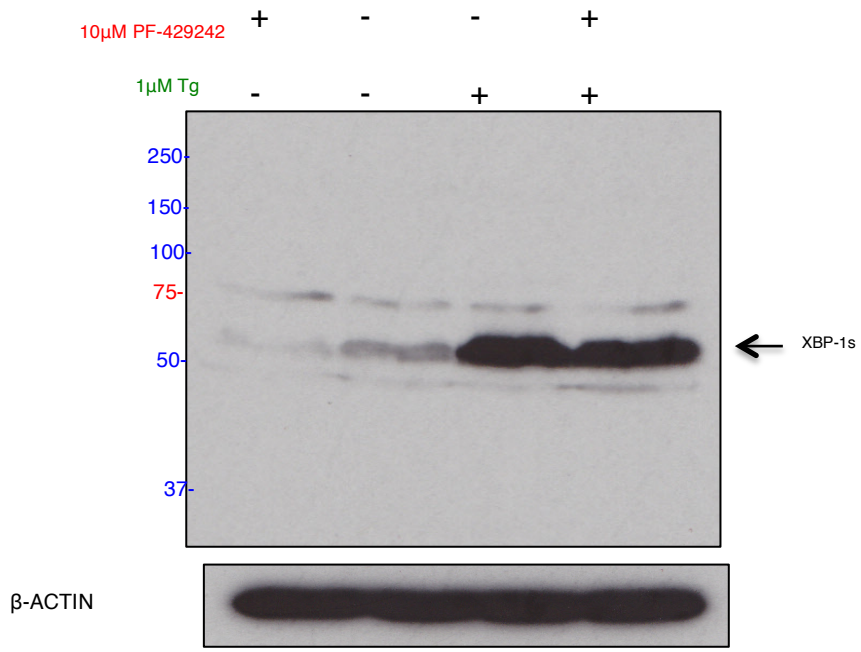


**XBP-1s**

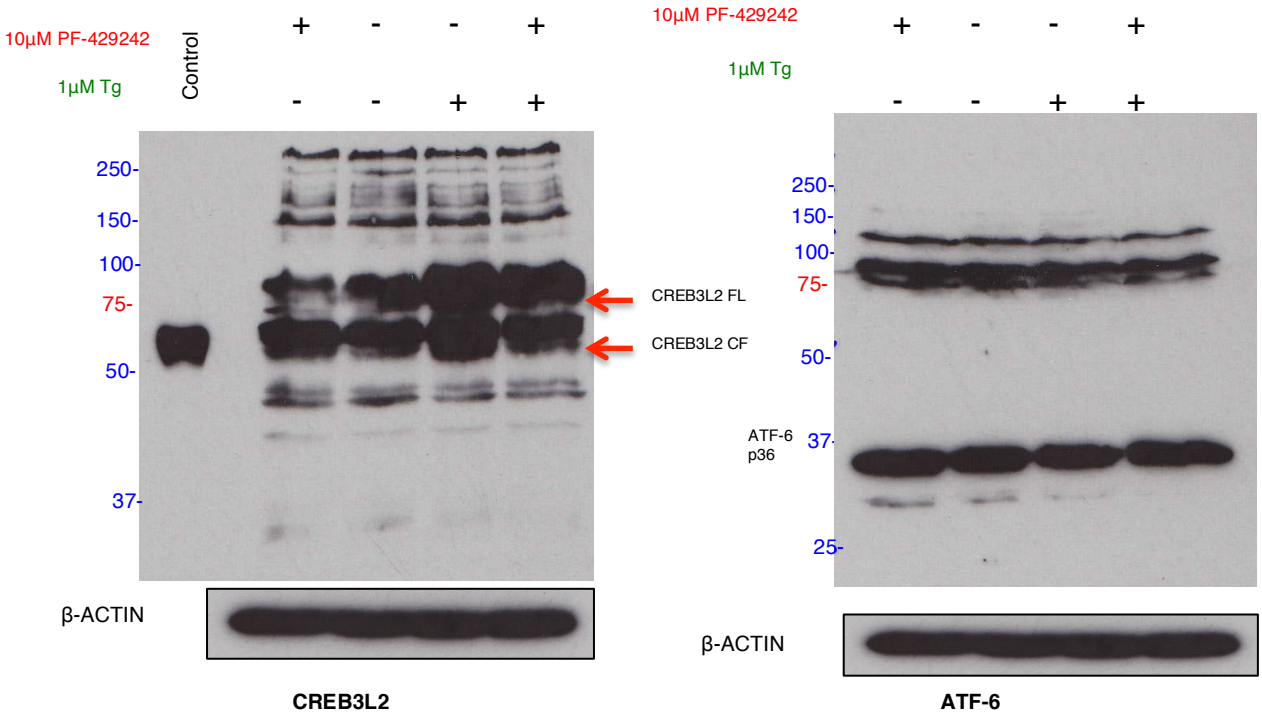


**Figure-5.4 The impact of 1μM TG and 10μM PF-429242 on CREB3L2, XBP1s and ATF6 in U266.** The cells were pre-treated with 10μM PF-429242 for 24hr and treated with TG for 4hr. Protein samples were collected and analysed by Western blotting using the indicated antibodies. 1-375 aa of CREB3L2 was overexpressed in Hela cells and used as a control for the cleaved form. β-ACTIN was used as loading control. FL, Full Length. CF, Cleaved Form.

## 5.3 **The impact of S2P inhibitor (Nelfinavir)**

Nelfinavir is used in the treatment of human immunodeficiency virus (HIV) due to its potency as an HIV-1 protease inhibitor (105). Moreover, it has been used as antiviral therapy and anticancer drug based on its ability to inhibit Akt phosphorylation, signal transducer and activating transcription factor 3 (STAT3) signalling, heat shock protein 90 (HSP90) function, cyclin-dependent kinase 2 (CDK2) function and general kinase activity, however, the exact mechanism by which it impacts on these diverse pathways has not been fully characterized (105).

In a study conducted by Guan et al., the impact of Nelfinavir and its structurally similar analogs were evaluated on Castration-Resistance Prostate Cancer cells (CRPC). Treatment of CRPC with 10 μM Nelfinavir and its analogs resulted in decreased cell proliferation and the induction of apoptosis. In addition, they showed that the structurally related compounds inhibited S2P mediated intra-membrane proteolysis that resulted in the accumulation of SREBP-1 precursor and ATF6 full-length proteins in CRPC and DU145 cells. The lack of functional SREBP1 and ATF6 generates ER-stress and an inability to resolve the UPR, thus causing the cells to undergo apoptosis (105).

Although Nelfinavir has been used to study inhibition of ATF6 cleavage (105), there appears to be a reproducible effect of Nelfinavir on the accumulation of precursor proteins only, whereas the data showing any effect of processed ATF6 or SREBP1 is less compelling. This is in contrast to the data for S1P inhibition, where gain of full-length protein is matched by loss of the cleaved form. In addition, it has been found that Nelfinavir's half-life in the context of patient treatment is 3.5-5 hours (106). Whereas, it's main metabolite, M8 is very unstable with a half-life of 0.44 h (107).

Therefore, U266 cells were exposed to Nelfinavir to check its impact on CREB3L2. U266 cells were treated with different concentrations of Nelfinavir

(5 μM, 10 μM and 20 μM) for 24hr and subsequently stressed for 4 hours using 1 μM TG. Then, the cells were collected, protein samples were prepared and analysed by Western blotting for CREB3L2 (Figure 5.5). Unexpectedly, the results showed that Nelfinavir reduced both full length and cleaved form of CREB3L2 in all studied concentrations. This could be due to secondary effects of Nelfinavir on the cells as it has been shown to have off-target, pleiotropic results in different cell types (105, 108).

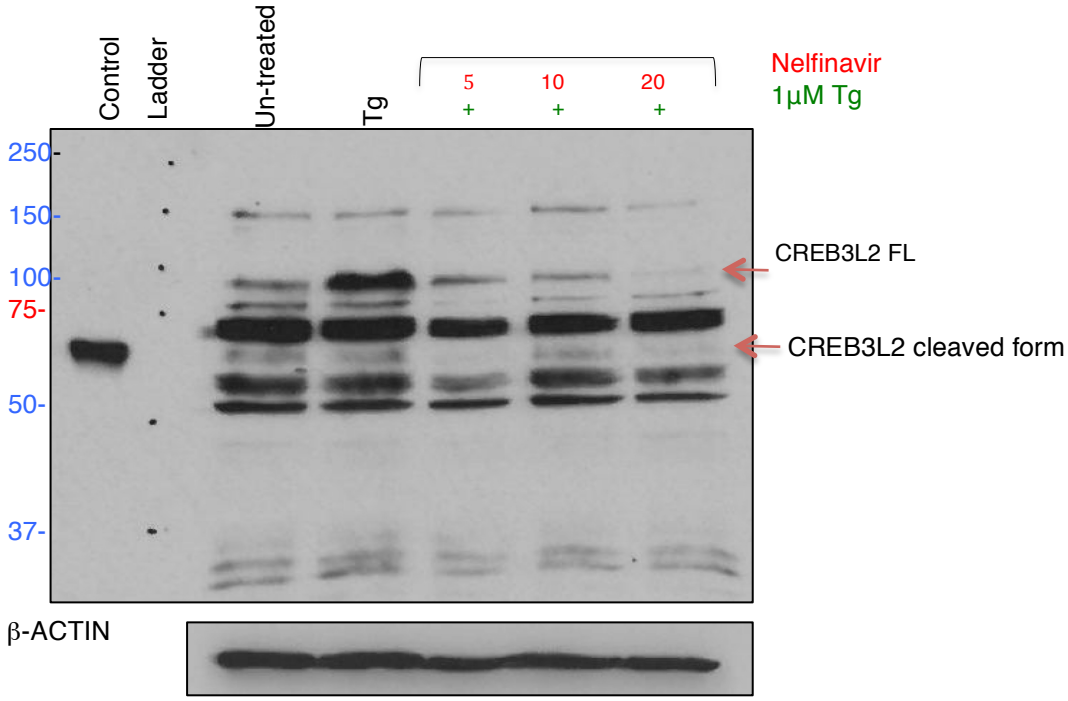


**Figure-5.5 The impact of Nelfinavir on CREB3L2 in U266.** The cells were pre-treated with different concentrations of Nelfinavir (5μM, 10μM and 20μM) for 24hr followed by stimulation with 1μM TG for 4hr. Protein samples were collected and analysed by Western blotting for CREB3L2. 1-375 aa of CREB3L2 was overexpressed in Hela cells and used as a control for the cleaved form. β-ACTIN was used as loading control.

### 5.4 A The impact of S1P and S2P inhibitors in U266

To confirm the differential impact of the S1P and S2P inhibitors, the effect of 300μM AEBSF, 10μM PF-429242 and 10μM Nelfinavir on CREB3L2 in the U266 cell line was validated (Figure-5.6). The results showed that AEBSF led to a loss of all forms of CREB3L2 suggestive of having non-specific effect, strengthening the decision to omit AEBSF as a S1P inhibitor in the human differentiated B-cells-plasma cell studies. However, the treatment with 10μM PF-429242 led to the reduction in the formation of CREB3L2 cleaved form compared to the un-treated U266 cells. On the other hand, treatment with 10μM Nelfinavir caused the accumulation of CREB3L2 cleaved form. Thus, PF-429242 and Nelfinavir treatment had an inhibitory impact on CREB3L2 processing/cleavage in the U266 cell line, which in turn may affect the cell's capability to respond to ER-stress.

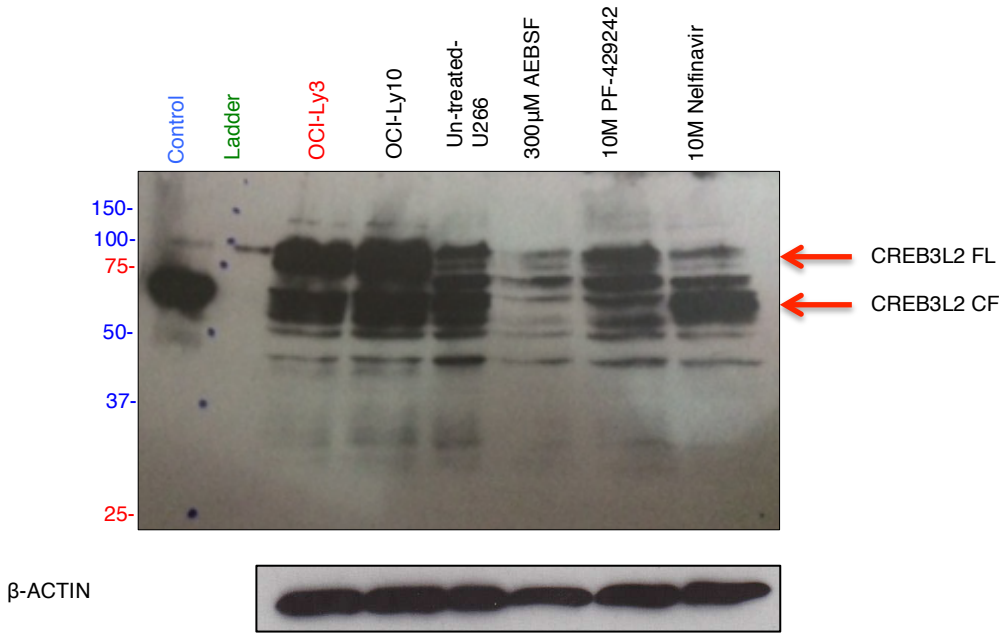


**Figure 5.6: Validating the impact of AEBSF, PF-429242 and Nelfinavir on CREB3L2 in the U266 cell line.** The cells were pre-treated with 300μM AEBSF, 10μM PF-429242 or 10μM Nelfinavir for 24hr and then stressed using 1 μM TG for 4hr. Protein samples were collected and analysed by Western blotting. 1-375 amino acids of CREB3L2 was overexpressed in Hela cells and used as a control for the cleaved form. Beta-ACTIN was used as loading control. FL, Full Length. CF, Cleaved Form.

### 5.4 B The impact of S1P and S2P inhibitors in H929

Previous results suggested that both the U266 and H929 myeloma cell lines expressed some level of CREB3L2 that could be augmented by treatment with an ER stressor, but with potentially different kinetics. Upon ER-stress (1μM TG or 1mM DTT treatment), the two forms of CREB3L2 (FL and CF) are expressed and increase by time with an approximate relative ratio of 2:1 FL: CF in the U266 cell line, whereas in H929 cells, the increase in the relative ratio was 1:1 FL: CF (Figure-4.3). Subsequently, S1P and S2P inhibitors (10 μM PF-429242 and 10 μM Nelfinavir) were shown to block CREB3L2 processing in the U266 cell line (Figure-5.6). To ascertain whether the inhibitors also functioned in H929, the cells were either stressed by 1 μM TG or pre-treated with either 10 μM PF-429242, or 10 μM Nelfinavir for 24hr and then stressed by 1 μM TG for 4hr. Then, the cells were collected and the protein samples were prepared and analysed by Western blotting for CREB3L2, XBP1s and ATF6 (Figure-5.7).

As predicted, the expression patterns of CREB3L2 and XBP1s in H929 cell line were similar in response to the ER stress stimulus (1 μM TG) as indicated by the increase in the intensity of the bands. In addition, the results have shown that 10 μM PF-429242 had a greater inhibitory impact on CREB3L2 cleavage in H929 cells, resulting in the reduction of the CF, which agreed with the results obtained in the U266 cells (Figure-5.3). Moreover, the formation of XBP1s was inhibited by 10 μM PF-429242 in H929 cells (Figure-5.7) whereas it did not alter the expression of XBP1s in U266 (Figure-5.4). ATF6 did not respond to either the ER-stressor TG or the S1P inhibitor 10 μM PF-429242, but was inhibited by the S2P inhibitor 10 μM Nelfinavir (Figure-5.7).

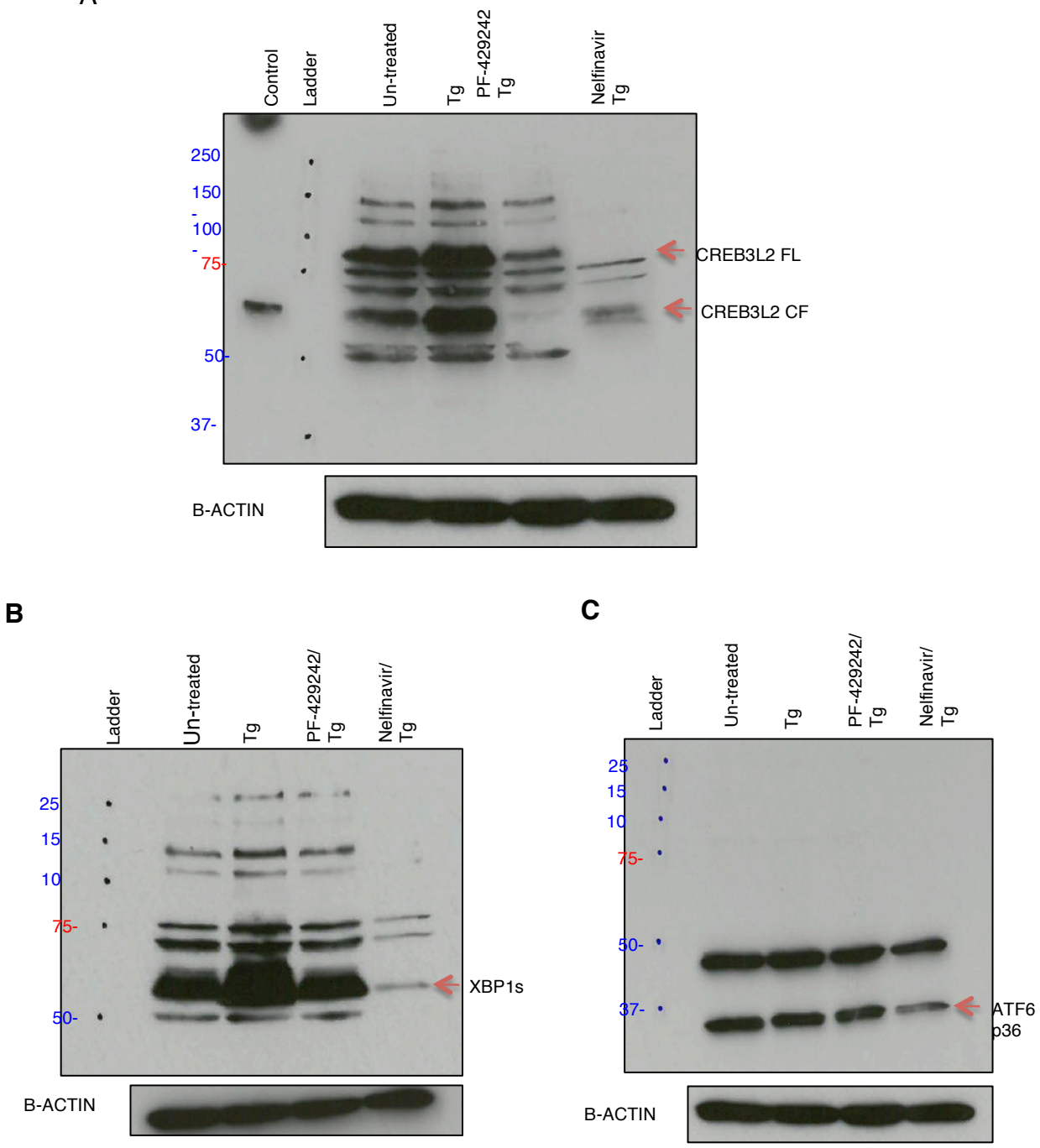


**Figure 5.7:The impact of PF-429242 and Nelfinavir on UPR components in the H929 myeloma cell line. A. CREB3L2, B. XBP1s and C. ATF6.** The cells were pre-treated with 10μM PF-429242 or 10μM Nelfinavir for 24hr and then stressed using 1 μM TG for 4hr. Protein samples were collected and analysed by Western blotting. 1-375 aa of CREB3L2 was overexpressed in Hela cells and used as a control for the cleaved form. FL, Full Length. CF, Cleaved Form. β-ACTIN was used as loading control.

### 5.5 The impact of both S1P and S2P inhibitors in H929

The results obtained have demonstrated that each inhibitor had different inhibitory impact, particularly on CREB3L2. Since the two proteases act sequentially at different sites to generate fully active cleaved proteins, it is conceivable that simultaneous application of the two inhibitors may have a more pronounced effect. Therefore, the H929 cell line was treated with different combinations of PF-429242 and Nelfinavir and the resulting levels of CREB3L2 were assessed (Figure-5.8). In this experiment, the cells were not treated with TG to allow an evaluation of the constitutive processing events. The results showed that using PF-429242 alone inhibited the formation of CREB3L2 cleaved form. However using Nelfinavir alone promoted the accumulation of the cleaved form of CREB3L2. The pattern of expression after combinatorial treatment suggests that the effect of PF-429242 is predominant, with a reduction in the observed cleavage.

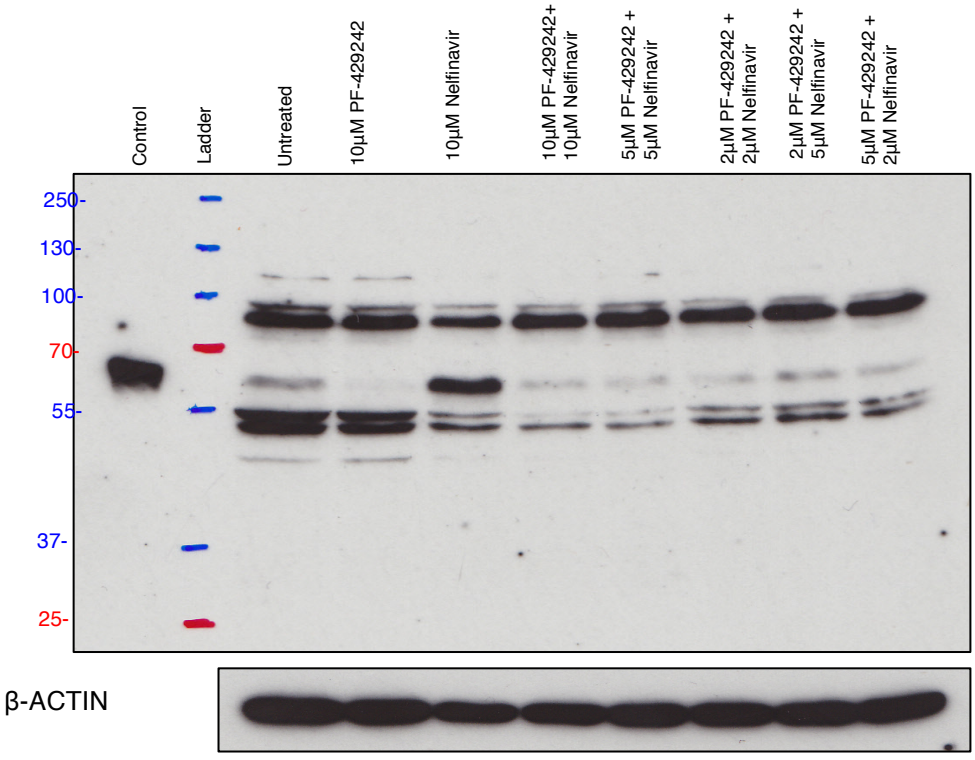


**Figure 5.8: The impact of combined PF-429242 and Nelfinavir on CREB3L2 in the H929 cell line.** The cells were treated with a combination of different concentrations of inhibitors as indicated for 24hr. Protein samples were collected and analysed by Western blotting. 1-375 aa of CREB3L2 was overexpressed in to Hela cells and used as a control for the cleaved form. β-ACTIN was used as loading control.

Densitometry was used to quantify the bands obtained in chapter-5 to summarize the impact of PF-429242, AEBSF and Nelfinavir on CREB3L2, XBP-1s and ATF6 (Figure-5.9).

A

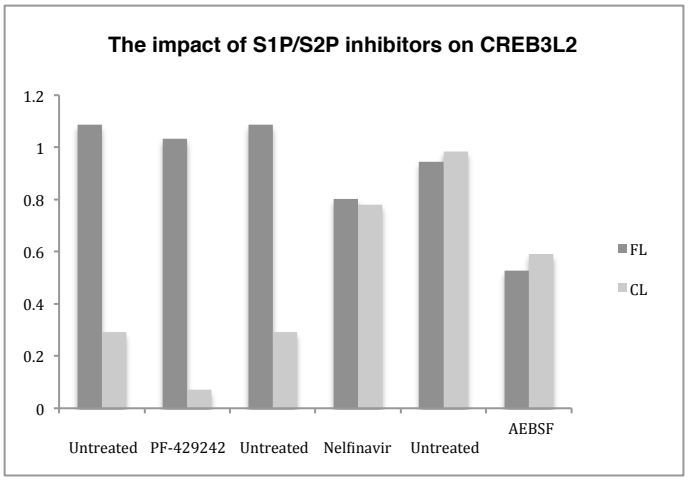


B

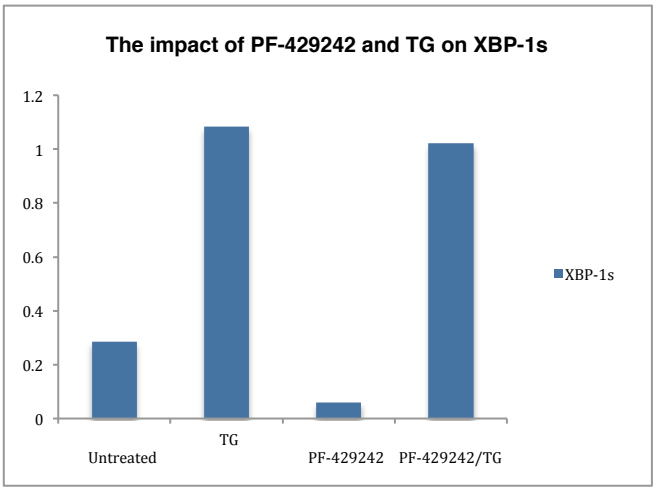


C

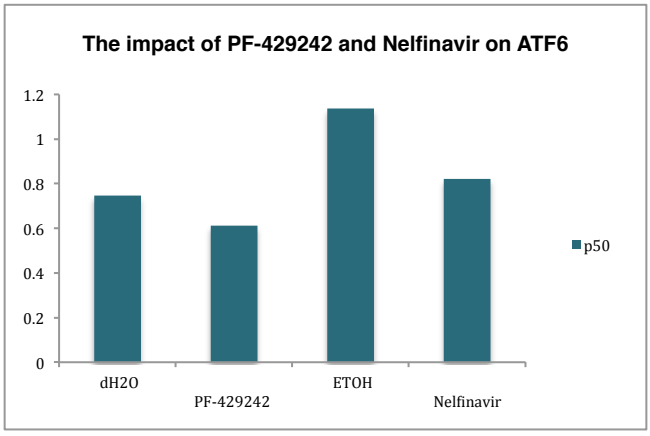


Figure-5.9: The impact of S1P/S2P inhibitors (PF-429242 and Nelfinavir) on A. CREB3L2. B. XBP-1s. And C. ATF6 using densitometry.

## 5.6 Discussion

The UPR is an important pathway protecting the cells from ER-stress by activating multiple signalling arms (IRE1, ATF6 and PERK) that work by slowing down normal protein production and up-regulating certain proteins such as chaperones to allow adaptation. Activation of ATF6 is regulated by the intramembrane proteolysis via S1P/S2P cleavage (104). However, ATF6 is not the only protein to be regulated in this fashion. Other transcription factors, including CREB3L2 are also similarly processed and are likely to make important contributions to the integrated stress response. Therefore, inhibiting the regulated intramembrane proteolysis by targeting S1P/S2P may prevent adaptation to stress and lead to cell death. Thus, the impact of S1P and S2P inhibitors on UPR signalling elements in myeloma cell lines were examined in a dose response analysis and kinetic analysis.

A series of papers had originally established that after sterol depletion, SREBPs are cleaved by intramembrane proteolysis to generate active transcription factors (109-111). The structurally related ATF6 was subsequently shown to undergo the same sort of processing (112). Two studies aimed at examining the impact of preventing this process employed the generic serine protease inhibitor (96, 113). In both instances the authors followed the effect of AEBSF on thapsigargin induced ER-stress.

Okada et al. showed that the induced cleavage of ATF6 in the Golgi following ER stress could be inhibited by AEBSF. However, the translocation of ATF6 to the Golgi remained intact, suggesting a specific effect on the proteolysis (96). In addition, Colgan et al., 2007 showed a similar effect on the generation of the active form of SREBP2 (113). In both experimental systems, downstream target genes of ATF6 and SREBP2 were altered after treatment with AEBSF.

Given these results, initially AEBSF was evaluated in ABC-DLBL cell lines (OCI-Ly3 and OCI-Ly10). If S1P is inhibited, it is predicted that the unprocessed form might accumulate in the ER. The results showed that AEBSF led to a loss of all forms of CREB3L2. In the study by Okada et al., 2003 application of AEBSF reduced the amount of processed protein, but had little effect on the level of unprocessed form. In contrast, the experiments by Colgan et al. showed similar results to those obtained in Figure 5.1, with an overall loss of SREBP2. Given that AEBSF can inhibit a wide range of serine proteases, including chymotrypsin, kallikrein, plasmin, thrombin and trypsin, it is likely to be having a broader impact than just targeting S1P (96). Thus, despite the published data showing that AEBSF can limit production of active ATF6 and SREBP2, the potential for non-specific effects makes AEBSF a less valuable tool for studying CREB3L2 and was not included in additional experiments.

Instead, compounds with higher selectivity were investigated. Another site-1 protease inhibitor (PF-429242) and a site-2 protease inhibitor (Nelfinavir) were first examined in myeloma cell lines. As mentioned above, it was predicted that using either an S1P or S2P inhibitor would inhibit the formation of the active form, which in turn will result in the accumulation of the full-length protein. In agreement with this prediction, treatment with PF-429242 led to the loss of the cleaved form accompanied by an increase in the amount of full length. However, similar to the results with AEBSF both forms of CREB3L2 were inhibited using Nelfinavir, which was not expected. In a previous report by Guan et al., treatment of the liposarcoma cell line SW872 with Nelfinavir resulted in both an increase in unprocessed ATF6 and SREBP1 and a reduction in the processed forms (98). This was accompanied by an increase in apoptosis, which the authors attributed to the accumulation of unprocessed ATF6 and SREBP1 triggering a UPR. Thus, treatment with PF-429242 or 10μM Nelfinavir may affect the cell's capability to respond to the ER-stress, but through different mechanisms.

Based on evidence from the papers cited above, ATF6 represents the prototypical target of S1P/S2P cleavage during an ER-stress response. Therefore, the impact of S1P (PF-429242) and S2P (Nelfinavir) inhibitors on ATF6 in myeloma cell lines were studied. The results showed that ATF6 did not respond to PF-429242 (S1P inhibitor) however, expression of both forms were inhibited using Nelfinavir (S2P inhibitor). While these results are unanticipated, we cannot rule out the possibility that (1) ATF6 might not localise effectively to the Golgi in these cells and (2) the effect may be attributable to off-target effects of Nelfinavir. Additionally, Aragon et al., found that ATF6α deficiency had no impact on the formation of antibody secretory cells and antibody secretion (52). The lack of requirement for ATF6 in plasma cells may be consistent with an alternative mode of activity in the B-cell lineage. In support of this, ATF6 has been shown to use a different mechanism of intracellular trafficking and stress signalling compared to CREB-H, which is structurally more similar to CREB3L2 (114).

Perhaps the most surprising result is the observed effect of S1P (PF-429242) and S2P (Nelfinavir) inhibitors on XBP1 in myeloma cell lines. mRNA encoding the XBP1 transcription factor is spliced in response to IRE1 activation by ER stress. This occurs at the same time, but independently of S1P/S2P activity on ATF6 or CREB3L2. However, a recent report provides a possible link between S1P/S2P and the expression of XBP1. Guo et al., found that ATF6 can bind to the promoter region of XBP1 and increase expression in chondrocytes (115). Although the effect of PF-429242 and Nelfinavir was not particularly pronounced, since CRE motifs allow binding of both CREB and ATF family members the XBP1 promoter might potentially also be regulated by CREB3L2.

In conclusion, PF-429242 and Nelfinavir were validated as effective inhibitors of CREB3L2 processing, but are likely to have a wider effect on additional pathways important in cells undergoing the transition to antibody secretory cells or tumours originating during this process.

# 6. Effect of site-1 protease (S1P) and site-2 protease (S2P) inhibitors on human differentiating B-cells

## 6.1 Impact of S1P inhibitor (10 μM PF-429242) on human antibody secreting cells

The regulated expression of CREB3L2 was first established in myeloma and ABC-DLBCL cell lines. Then, using the in vitro model to generate mature plasma cells, CREB3L2 expression was analysed by Western blotting. As shown in Chapter-4, CREB3L2 is expressed in human differentiated B-cells, plasmablasts and plasma cells (slightly weak expression on Day-3, stronger expression from Day-6/7 to Day-13). In both primary differentiating B-cells and B-cell lines, inhibition of S1P/S1P profoundly reduced the generation of cleaved CREB3L2, as well as other transcription factors processed in the same fashion. It is predicted that the loss of the active forms would lead to a change in the differentiation capacity or functional activity of B-cells. Therefore, the impact of S1P inhibitor (10 μM PF-429242) on ASCs was initially studied. The cells were treated with 10 μM PF-429242 and or $dH_2O$ (S1P inhibitor vehicle that acts as a control) on Day-6, Day-8 or Day-10 and analysed on Day-8, Day-10 and Day-13, respectively, for cell number, phenotype, expression of UPR-related factors and immunoglobulin production.

### 6.1.1 Cell number

The first assessment for the impact of 10 μM PF-429242 on the ASCs was the absolute cell number. After the incubation, the cells were accurately counted using CountBright ™ beads on Day-8, Day-10 and Day-13 to examine the possible impact of the inhibitor. The results revealed no changes in the cell count between the cells treated with 10 μM PF-429242 or $dH_2O$ (Figure 6.1).

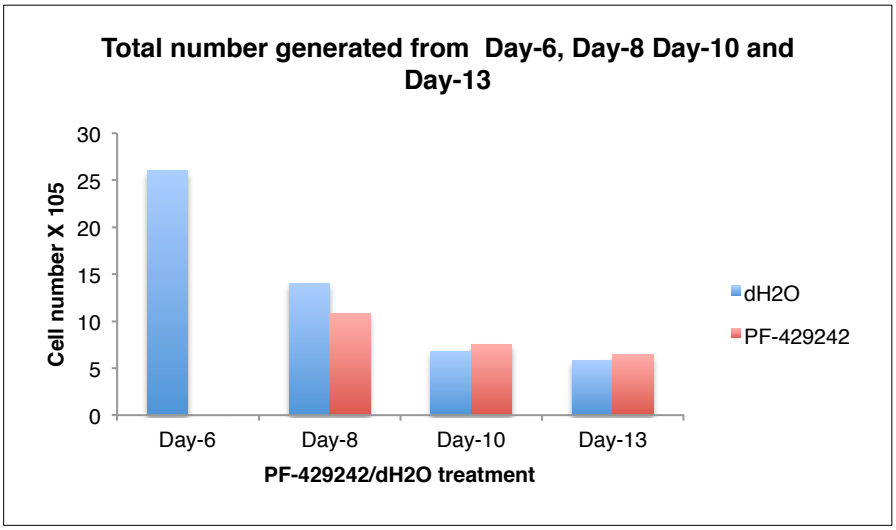


**Figure 6.1: Effect of S1P inhibitor (10 μM PF-429242) on cell number.** ASCs (Day-6, Day-8 and Day-10) were treated with 10 μM PF-429242 and or $dH_2O$ and the cells were counted at the indicated time points using CountBright ™ absolute counting. Blue bars represent the count for $dH_2O$ treated cells whereas the red bars represent the count for 10 μM PF-429242 treated cells.

### 6.1.2 Cell phenotype

The surface phenotype is a key indicator of progression through the differentiation stages. To determine whether inhibition of S1P at the plasmablast stage was sufficient to block the acquisition of full plasma cell phenotype, ASCs were treated with 10 μM PF-429242 or $dH_2O$. At each stage, the cells were stained for CD19, CD20, CD138 and CD38 and analysed by flow cytometry. The results revealed no discernable changes in expression of the evaluated markers after 10 μM PF-429242 treatment compared to its vehicle (dH2O, control) (Figure 6.2).

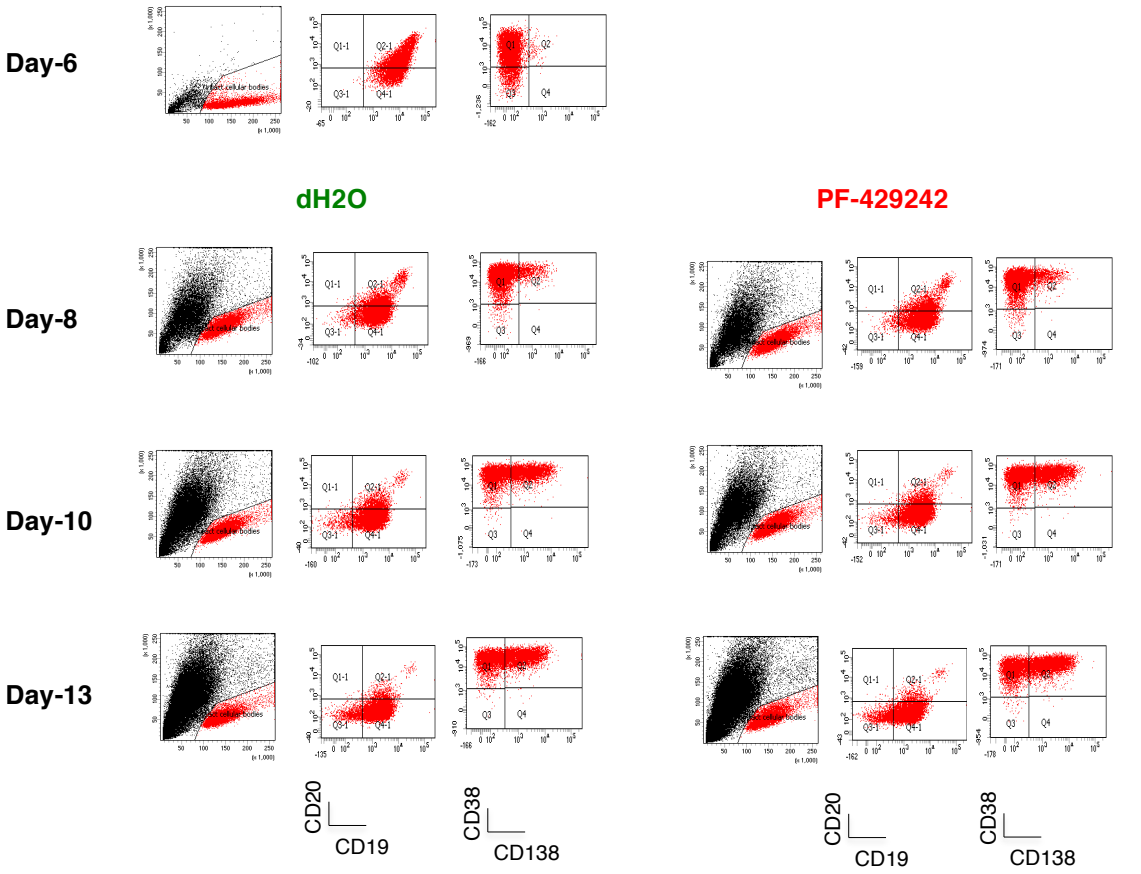


**Figure 6.2: The impact of S1P inhibitor (10 μM PF-429242) on cell surface phenotype.** ASCs (Day-6, Day-8 and Day-10) were treated with 10 μM PF-429242 or dH2O and then stained using B-cell (CD19 and CD20) and ASC markers, (CD38, and CD138) and analysed by flow cytometry at the indicated time points.

### 6.1.3 CREB3L2 expression

The expression of CREB3L2 is characterised by the presence of two forms: full-length and cleaved form in different proportions depending on the state of the cell and the stimuli (e.g ER stress stimulus; thapsigargin or the production of antibodies as the B-cells differentiate). Upon ER stress, CREB3L2 is cleaved via S1P/S2P generating the cleaved form that migrates to the nucleus to activate its target genes (67). However, using S1P/S2P inhibitors prevents the cleavage of CREB3L2, which leads to the accumulation of the full-length protein in the ER potentially triggering apoptosis. The results obtained in the previous two figures suggest that blocking conversion of CREB3L2 to the active form does not have this effect at late time points during differentiation. To confirm that inhibition of S1P was affecting protein processing, Western analysis of protein lysates was performed. The results show that the cleavage of CREB3L2 in the antibody secretory cells was strongly reduced upon the treatment with 10 μM PF-429242 compared to its vehicle ($dH_2O$) at the protein level (Figure 6.3).

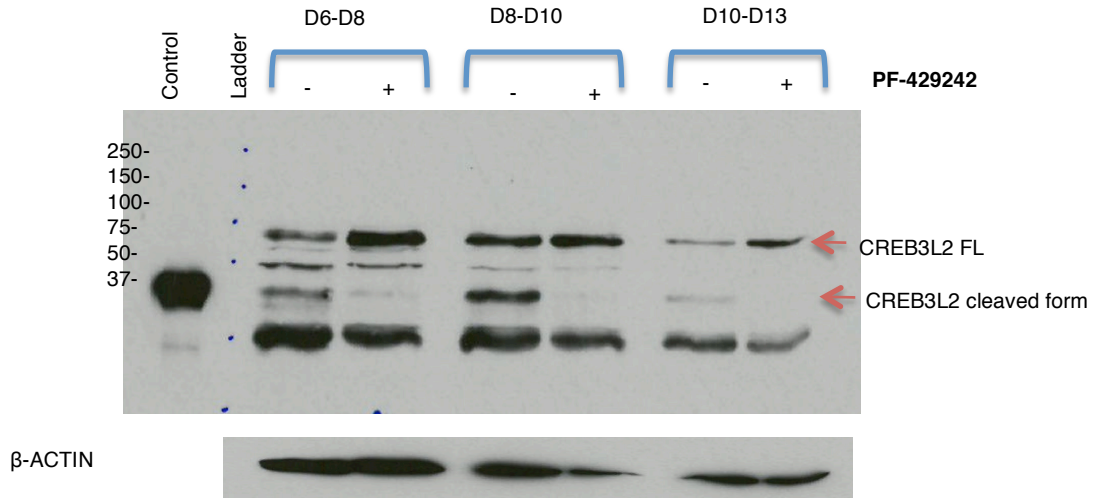


**Figure 6.3: The impact of S1P inhibitor (10 μM PF-429242) on CREB3L2 protein expression.** ASCs (Day-6, Day-8 and Day-10) were treated with 10 μM PF-429242 or $dH_2O$ for the indicated times and the cells were collected for protein preparation and analysis using 10% SDS-PAGE and Western blot. The lane labelled "Control" is loaded with lysate containing the N-terminus of CREB3L2 that has been overexpressed in Hela cells. β-ACTIN was used as a loading control.

### 6.1.4 XBP1 expression

To date, only one UPR regulator has been implicated in plasma cell differentiation, XBP1. Therefore, RNA samples collected from Day-8, Day-10 and Day-13 with and with out S1P inhibitor (10 μM PF-429242) treatment were initially tested for *XBP1* splicing by PCR. In addition, RNA sample from U266 cells that had been treated with 1μM thapsigargin for 2, 4 and 6 hours were included in the gel as a control for splicing. The results showed a slight inhibition of *XBP1* splicing upon 10 μM PF-429242 treatment compared with its vehicle (Figure 6.4) confirming the impact of S1P inhibitor (10 μM PF-429242) treatment on *XBP1* splicing. It is also worth noting that contrary to what might be expected, *XBP1* shows very little splicing in the in vitro generated antibody secreting cells, particularly at the later time points.

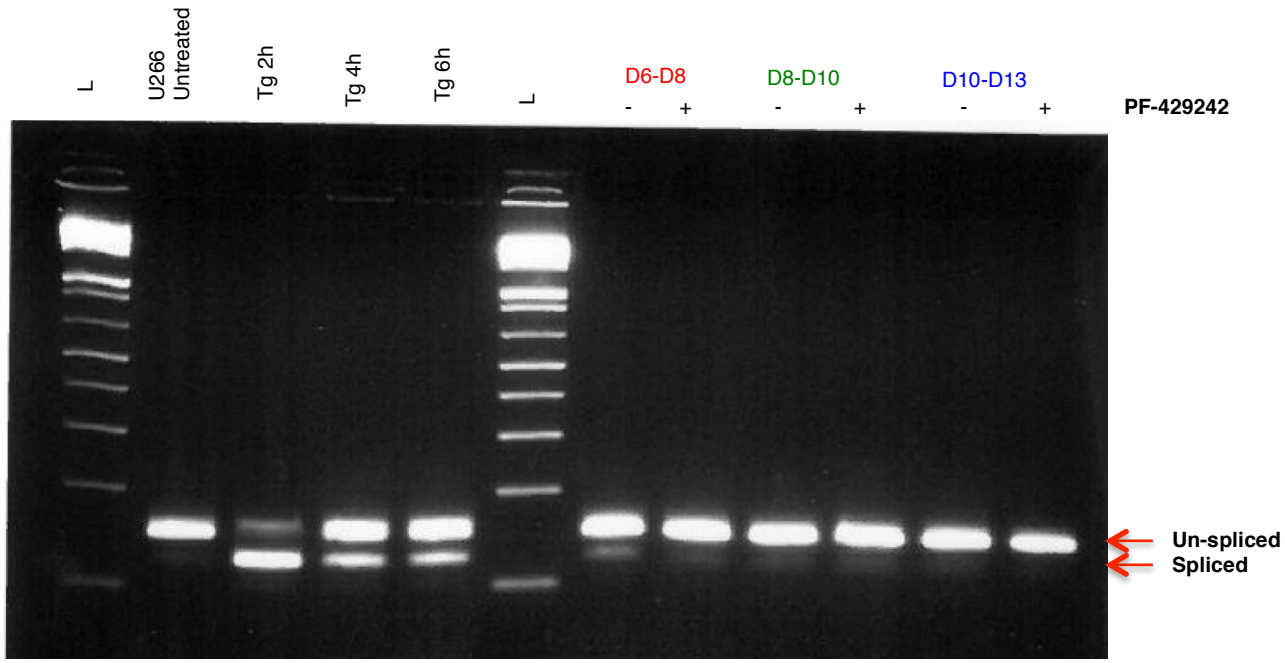


**Figure 6.4: The impact of S1P inhibitor (10 μM PF-429242) on *XBP1* splicing.** ASCs (Day-6, Day-8 and Day-10) were treated with 10 μM PF-429242 and or $dH_2O$ for the indicated time period and the cells were collected for RNA extraction and analysed using conventional RT-PCR with primers that detect both spliced and unspliced *XBP1*. L, Ladder. Tg, Thapsigargin.

### 6.1.5 Immunoglobulin secretion (IgM and IgG)

The S1P inhibitor (10 μM PF-429242) had little discernable effect on cell number or the phenotypic characteristics of ASCs (Day-8, Day-10 and Day-13); however, it is crucial to quantify the immunoglobulin (IgM and IgG) levels to determine whether this was matched by preservation of function. Thus, the supernatant were collected from the treated /untreated cells and analysed using ELISA. The results showed that there is no difference in the immunoglobulin (IgM and IgG) levels between the treated and the untreated samples suggesting that 10 μM PF-429242 does not affect secretion (Figure 6.5).

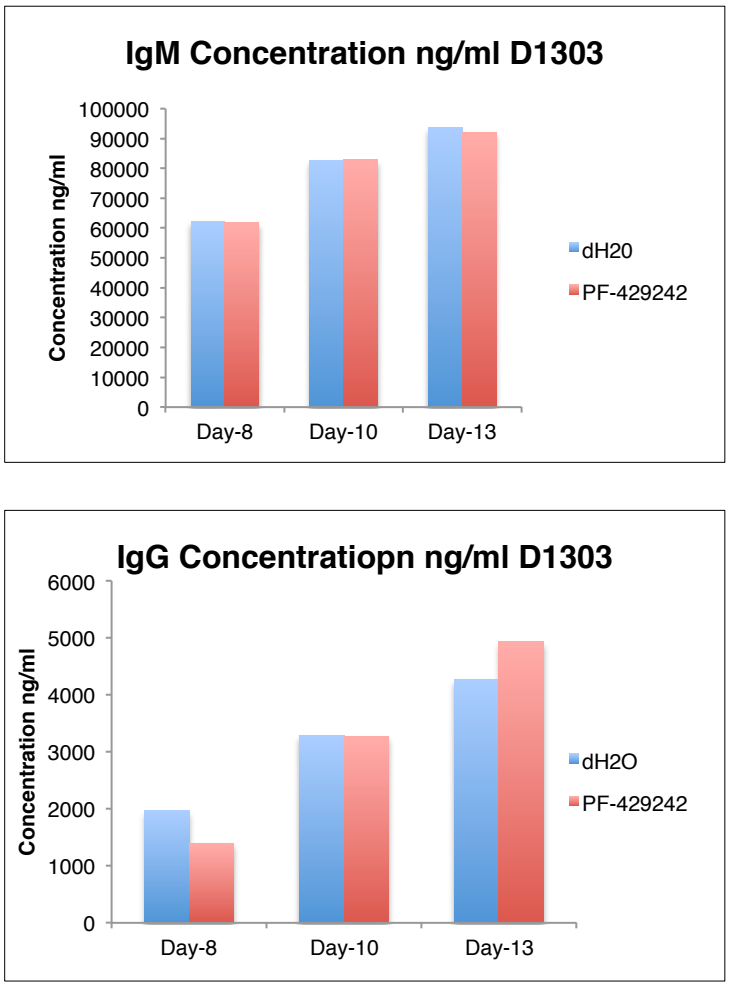


**Figure 6.5: The impact of S1P inhibitor on immunoglobulin production.** ASCs (Day-6, Day-8 and Day-10) were treated with 10 μM PF-429242 or dH2O and the supernatants were collected at the indicated time points for IgM and IgG quantifications using ELISA. Blue bars represent the amount for dH2O treated cells whereas the red bars represent 10 μM PF-429242 treated cells.

Thus, based on cell counts, cell phenotypes and immunoglobulin levels (IgM and IgG), S1P inhibitor (10 μM PF-429242) did not affect the viability or function of the human differentiated antibody secretory cells when treated on Day-6 or Day-8 or Day-10 despite having an impact on the protein level of CREB3L2 cleaved form, suggesting that CREB3L2 or other S1P-regulated transcription factors are not required for terminal differentiation.

On the other hand, meta-profile analysis of DLBCL gene expression signatures has shown that *CREB3L2* is characteristic of the activated B-cell (ABC) subset (Figure 6.6) (87). In addition, CREB3L2 protein is detectable in the human differentiated B-cells using the in vitro model (Chapter-4) at the activated B-cell stage, corresponding to Day-3. This would imply that CREB3L2 is consistently expressed and likely to function in B-cells initiating the process of plasma cell differentiation. Therefore, to determine whether CREB3L2 might play a role in starting the transition to becoming an ASC, it necessary to treat the cells with S1P inhibitor at the earlier activated B-cell stage.

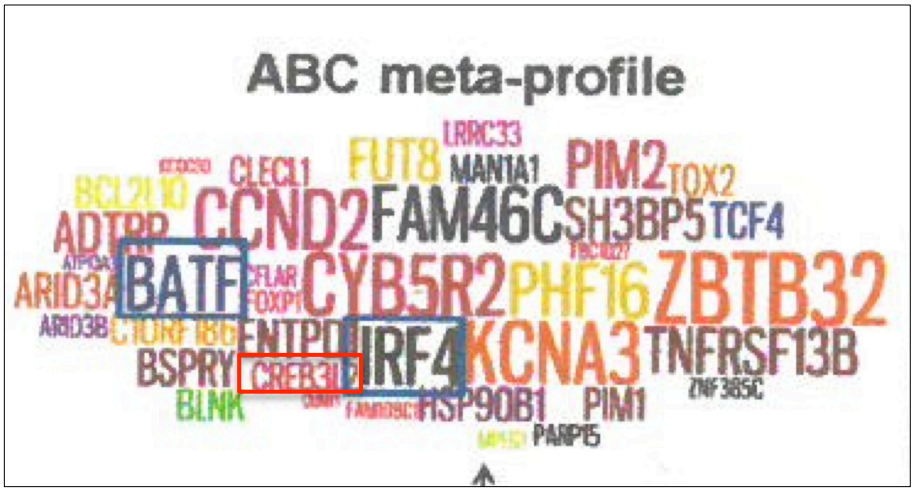


**Figure 6.6:** ABC-DLBCL meta-profile depicted as a Wordle where font size indicates degree and consistency of expression. Figure from Matt Care.

## 6.2 Impact of S1P inhibitor and S2P inhibitor on the transition from activated B-cell to ASC

Based on the results obtained by Western blotting of the endogenous expression of CREB3L2 in human differentiated B-cells (Chapter-4), the full length and cleaved form of CREB3L2 were expressed from the B-cell stage (Day-3) onwards. Since blocking S1P at the later stages of differentiation had no real impact, it was hypothesised that instead CREB3L2 and related factors may in fact be primarily operating during the initial phases. To test this, Day-3, Day-4 and Day-5 human differentiated B-cells were treated with 10 μM PF-429242/dH2O (vehicle control) or 10 μM Nelfinavir/ethanol (vehicle control) for 24 hours and analysed for the same parameters as described in the above experiments.

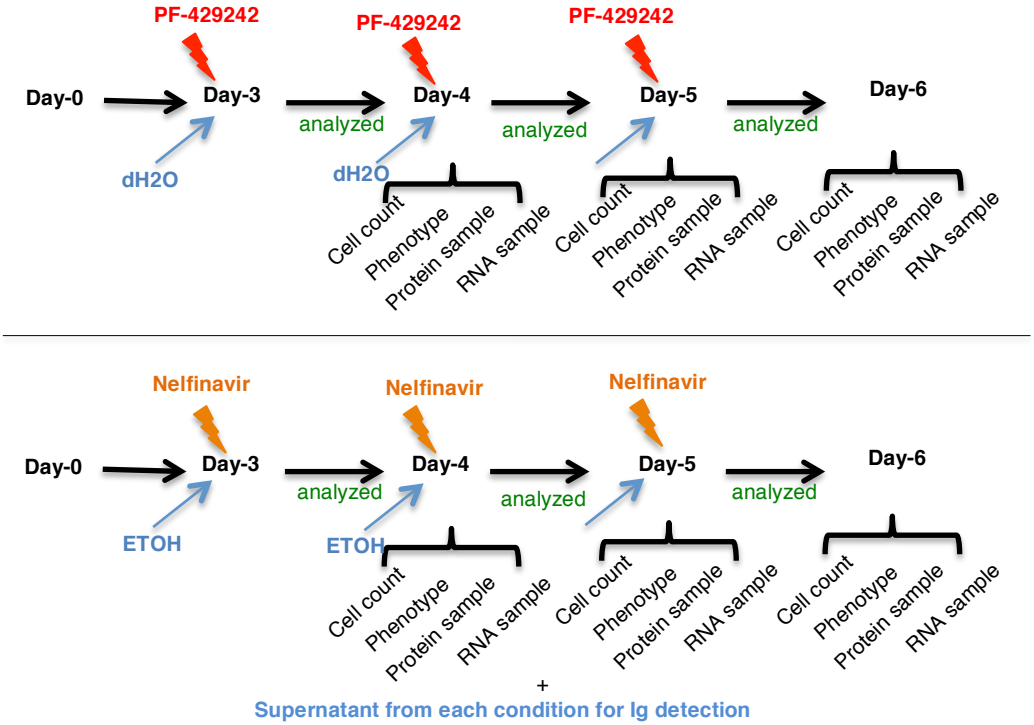


**Figure 6.7: Diagrammatic representation of experimental design to test the impact of S1P and S2P inhibitors PF-429242 and Nelfinavir on human B-cell differentiation.** The cells were treated on Day-3, Day-4 and Day-5 and analysed 24 hours post treatment for protein and RNA expression, cell count, surface phenotype and immunoglobulin secretion.

### 6.2.1 Expression of UPR-related transcription factors

The data in Chapter 5 demonstrated that S1P and S2P inhibitors not only affected CREB3L2, but also impacted on other UPR-related transcription factors in myeloma and ABC-DLBCL cell lines. To determine whether the same was true in primary cells, human differentiated B-cells and ASCs (Day-3, Day-4 and Day-5) were treated with 10 μM PF-429242/dH2O or 10 μM Nelfinavir/Ethanol for 24 hours and analysed on Day-4, Day-5 and Day-6 respectively. At each time point, cells were collected for lysate preparation and analysed by Western blotting. The results in Figure 6.8 show the impact of the inhibitors, revealing a profound inhibition by 10 μM PF-429242 on the cleavage of CREB3L2 at each of the time points assessed. In contrast, 10 μM Nelfinavir had less of an impact CREB3L2 processing, but did diminish the full-length form likely due to its multiple bioactivities (108). These results indicate that both drugs are likely to be functioning as effective inhibitors at the concentrations and times tested, but that PF-429242 might have a greater impact on CREB3L2 regulated targets.

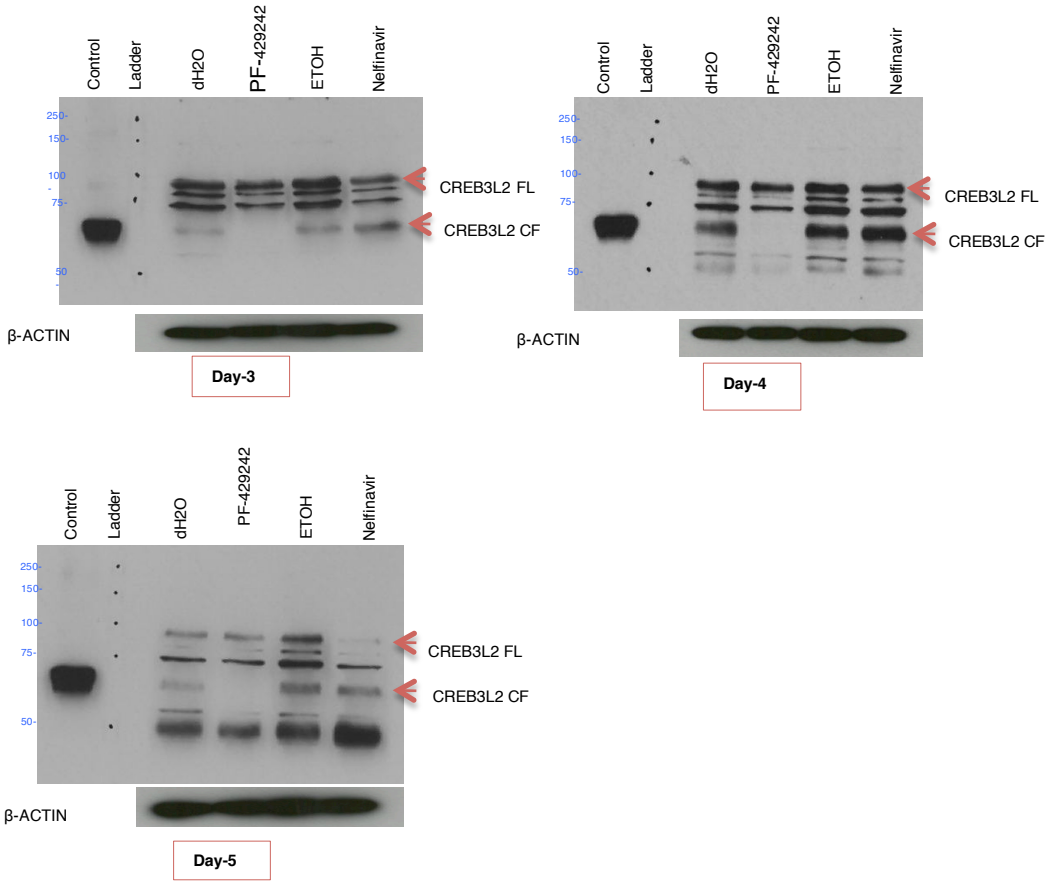


**Figure 6.8: The impact of S1P inhibitor (PF-429242) or S2P inhibitor (Nelfinavir) on CREB3L2 expression in differentiating B-cells.** Cells (Day-3, Day-4 and Day-5) were treated with 10 μM PF-429242/dH2O or 10 μM Nelfinavir/Ethanol for 24 hours and cell lysates analysed by immunoblotting. Control was the N-terminus of CREB3L2 that has been overexpressed in Hela cells. β-ACTIN was used as a loading control.

Considered to be one of the three conventional arms of the UPR, ATF6 is processed by the same step-wise proteolytic mechanisms as CREB3L2. To determine whether inhibition of S1P and S2P had a similar effect on ATF6 expression, the lysates were assessed by immunoblotting with antibody that recognised the cleaved form (Figure 6.9). Although far less pronounced than the effect on CREB3L2, treatment with PF-429242 did modestly reduce the amount of detectable ATF6 and this was similar to the reduction of ATF6 achieved with Nelfinavir.

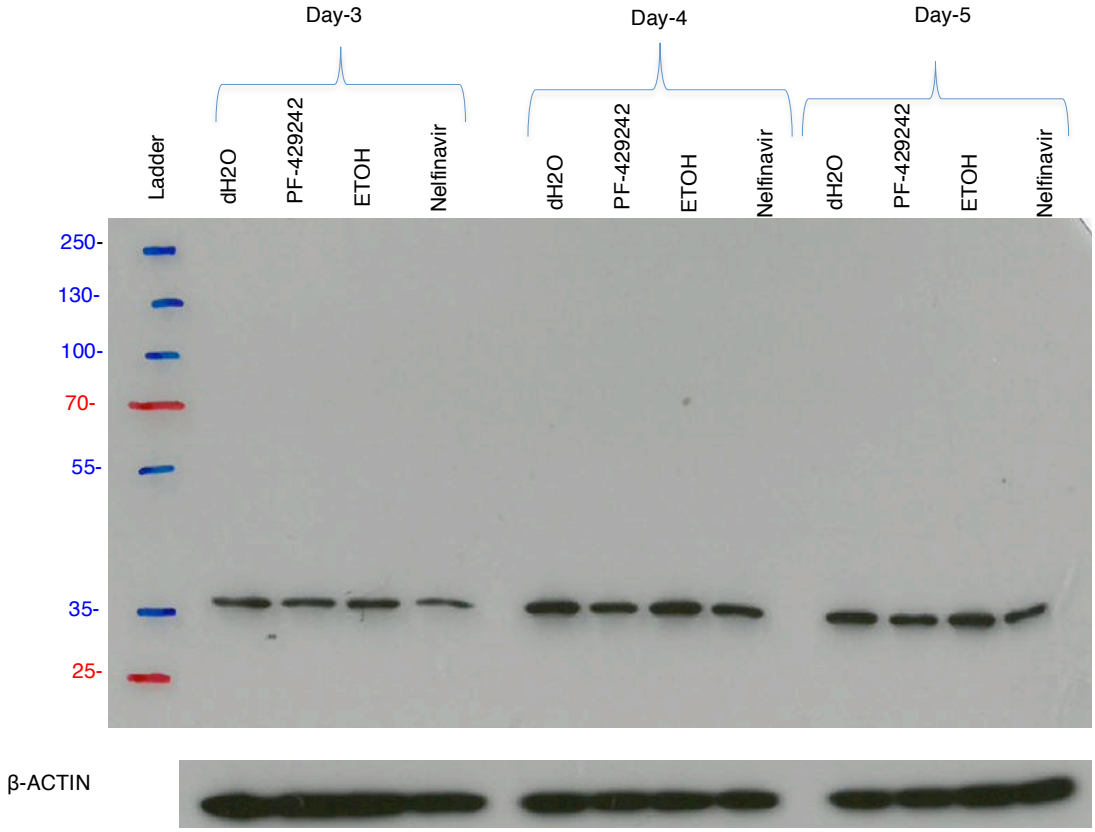


**Figure 6.9: The impact of S1P inhibitor (PF-429242) or S2P inhibitor (Nelfinavir) on ATF6 expression.** Cells (Day-3, Day-4 and Day-5) were treated with 10 μM PF-429242/dH2O or 10 μM Nelfinavir/Ethanol for 24 hours and lysates analysed by Western blot using anti-ATF6. B-ACTIN was used as a loading control.

XBP1 is an important transcription factor that has been implicated in the UPR, particularly in plasma cells. In addition, XBP1 has been postulated as potential therapeutic target for multiple myeloma (116). Given that S1P/S2P play a role in regulating multiple components of the UPR and the results obtained in Chapter-5, it was of interest to determine whether XBP1 might be affected as an indirect consequence.

Therefore Day-3, Day-4 and Day-5 cells were treated with S1P inhibitor (10 μM PF-429242) or S2P inhibitor (10 μM Nelfinavir) for 24 hours and analysed for XBP1s using Western blotting. Consistent with its role in the UPR and generation of ASC, XBP1 is not readily detected until Day-5 of the culture, when cells are phenotypically changing and beginning to secrete immunoglobulin (Figure 6.10). Interestingly, expression of XBP1s is inhibited by 10 μM PF-429242 in cells treated on Day-5; whereas its expression is inhibited by 10 μM Nelfinavir in cells treated a day earlier (Figure 6.10). Hence, although the inhibitors do not directly target it, XBP1s is also sensitive to the treatment and its loss may enhance any observed effects.

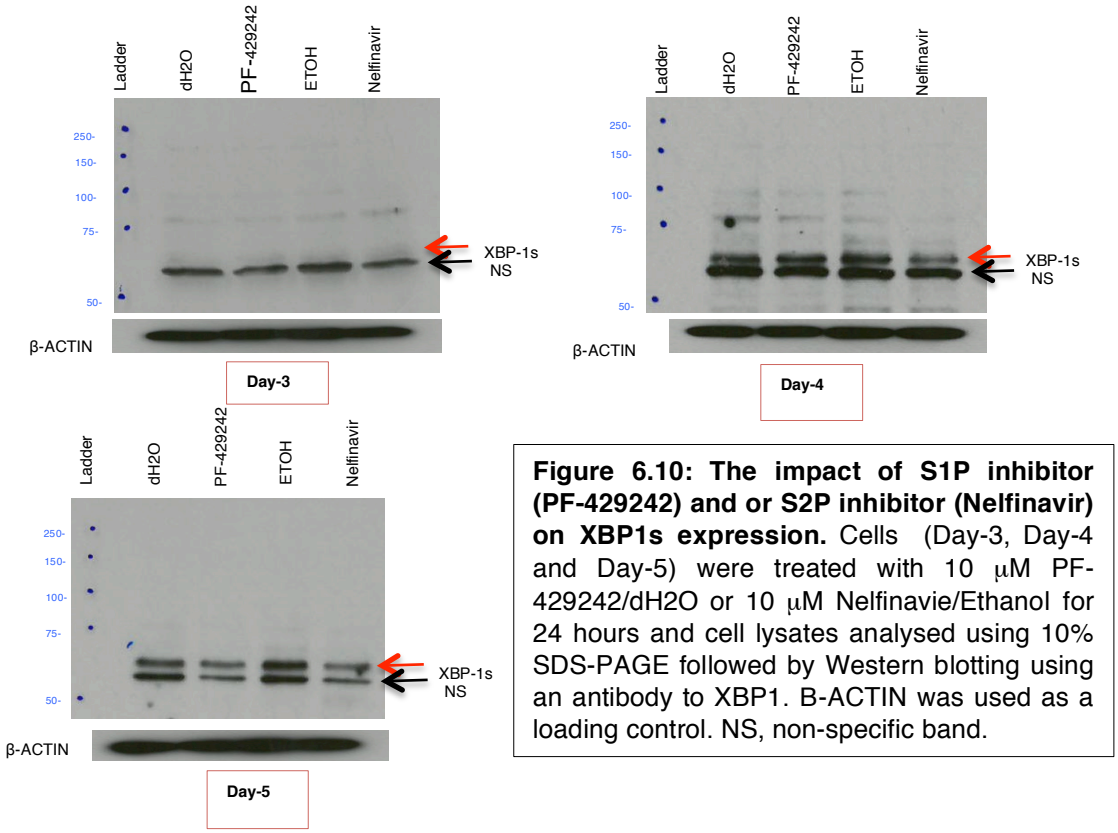


**Figure 6.10: The impact of S1P inhibitor (PF-429242) and or S2P inhibitor (Nelfinavir) on XBP1s expression.** Cells (Day-3, Day-4 and Day-5) were treated with 10 μM PF-429242/dH2O or 10 μM Nelfinavie/Ethanol for 24 hours and cell lysates analysed using 10% SDS-PAGE followed by Western blotting using an antibody to XBP1. B-ACTIN was used as a loading control. NS, non-specific band.

To determine whether the loss of detected XBP1s after treatment with S1P/S2P inhibitors was a reflection of an alteration in its splicing, RNA samples were initially tested using a PCR assay that detects both forms. In addition, RNA sample from U266 cells that have been treated with 1μM thapsigargin for 4 hours were included in the gel as a control for splicing. The results provided no clear conclusive impact of the inhibitors; however, splicing was detected from Day-5 onward, which agreed with protein expression pattern (Figure 6.11).

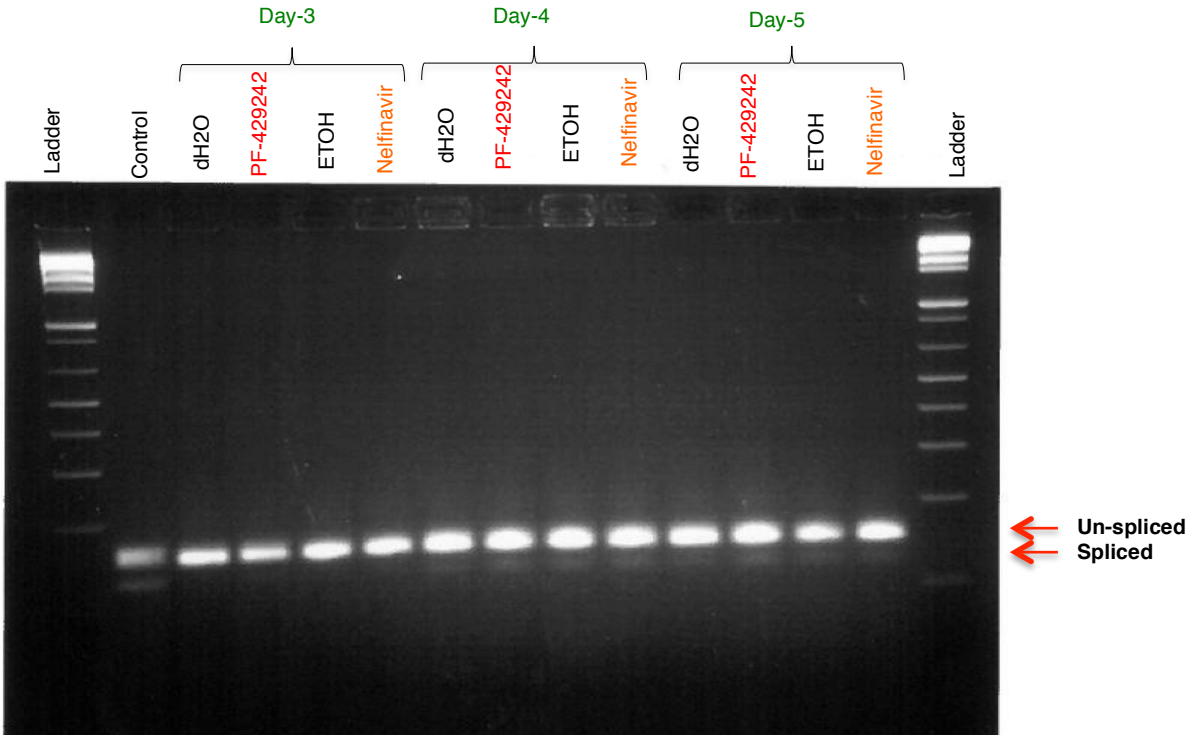


**Figure 6.11: The impact of S1P inhibitor (PF-429242) or S2P inhibitor (Nelfinavir) *XBP1* splicing.** Cells (Day-3, Day-4 and Day-5) were treated with 10 μM PF-429242/dH2O or 10 μM Nelfinavir/Ethanol for 24 hours and splicing evaluated by RT-PCR. Control is an RNA sample from U266 cells that have been treated with 1μM Tg for 4 hours**.** Tg, Thapsigargin.

### 6.2.2 Cell count

At the activated B-cell stage, the cells are undergoing rapid proliferation, with as many as 3 divisions within the space of 24 hours (117). From Day-3 to Day-6 the cells continue to divide prior to completing terminal differentiation, which is accompanied by exit from cell cycle. To determine whether S1P/S2P regulated proteins would affect the expansion of activated B-cells, cells were treated with 10 μM PF-429242 or 10 μM Nelfinavir for 24 hours. After the incubation, the cells were enumerated on Day-4, Day-5 and Day-6. The results revealed minimal changes in the cell counts between the cells treated with 10 μM PF-429242/dH2O or 10 μM Nelfinavir/Ethanol (Figure 6.12) suggesting that within the time-frame of the experiment neither proliferation or cell viability are dependent on S1P/S2P-regulated pathways.

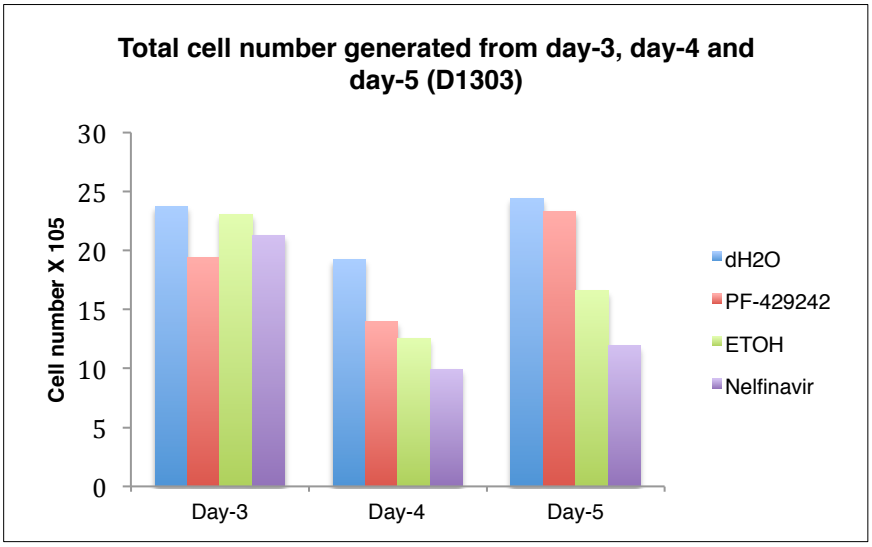


**Figure 6.12: The impact of S1P inhibitor (PF-429242) and S2P inhibitor (Nelfinavir) on B-cell expansion.** Activated B-cells (Day-3, Day-4 and Day-5) were treated with 10 μM PF-429242/dH2O or 10 μM Nelfinavir/Ethanol for 24 hours and the cells were counted using CountBright ™ absolute counting. Blue bars represent the count for dH2O treated cells, red bars represent cell count for 10 μM PF-429242 treated cells, green bars represent the count for ethanol treated cells, purple bars represent cell count for 10 μM Nelfinavir treated cells.

### 6.2.3 Cell phenotype

The results above suggest that S1P/S2P inhibitors do not profoundly alter cell cycle regulation of differentiating activated B-cells. As the decision to become an ASC has been linked to proliferative capacity (118), it was important to determine whether there were any differences in the accompanying changes in surface phenotype. Cells were examined on Day-3 (untreated), Day-4, Day-5 and Day-6 treated for expression of CD19, CD20, CD138 and CD38. The results revealed no changes on cell phenotype between treated (either with 10 μM PF-429242 nor 10 μM Nefinavir) and untreated (control; treated with dH2O or ethanol) cells (Figure 6.13), consistent with the cell number data.

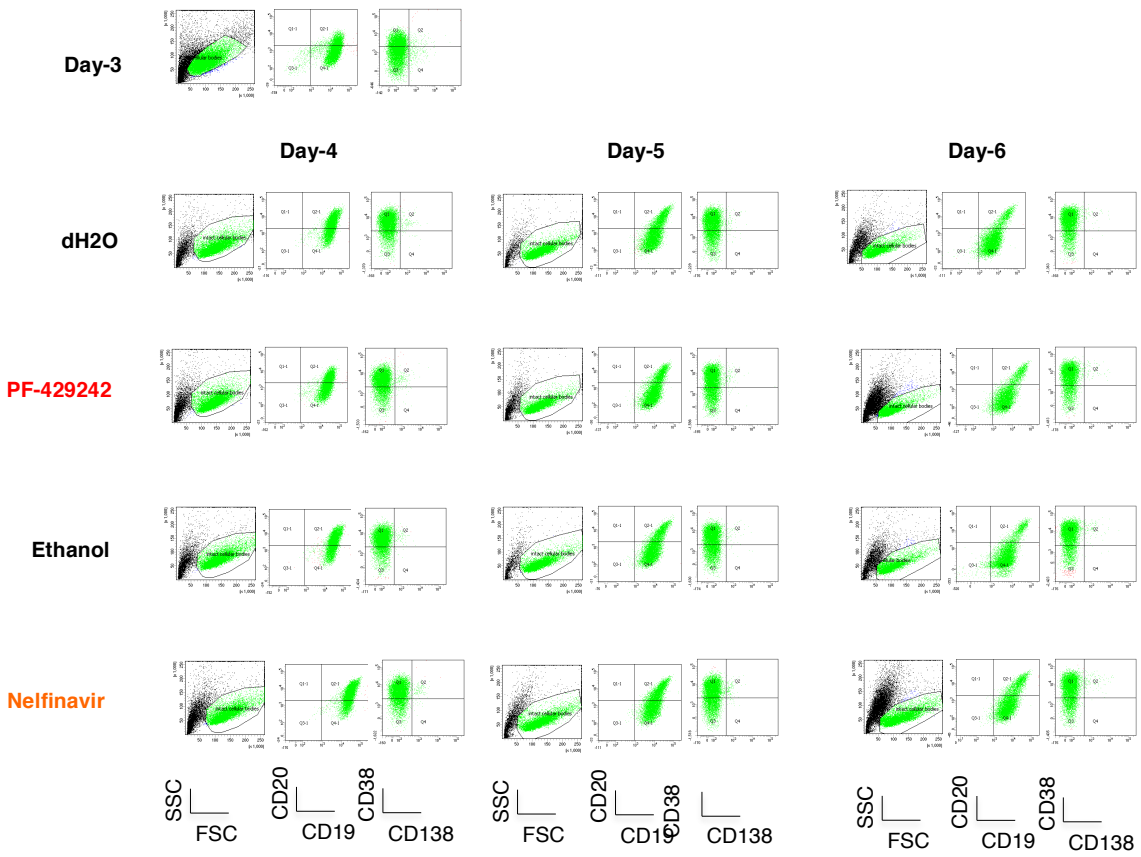


**Figure 6.13: The impact of S1P inhibitor (PF-429242) and S2P inhibitor (Nelfinavir) on cell phenotype.** In vitro differentiated cells (Day-3, Day-4 and Day-5) were treated with 10 μM PF-429242/dH2O or 10 μM Nelfinavir/Ethanol for 24 hours and subsequently stained using B-cell markers (CD19 and CD20) and ASC markers (CD38 and CD138) and analysed using flow cytometry.

### 6.2.4 Immunoglobulin levels

Although, phenotypically the cells appeared to be differentiating normally, it was still possible that inhibition of S1P/S2P could affect the function of ASCs. Therefore, the cell culture supernatants were collected from the treated /untreated cells and analysed using ELISA. In the single donor that was evaluated in this experiment, it appeared that both inhibitors caused a slight reduction in secretion of IgG, with a more pronounced effect on IgM after treatment with Nelfinavir (Figure 6.14).

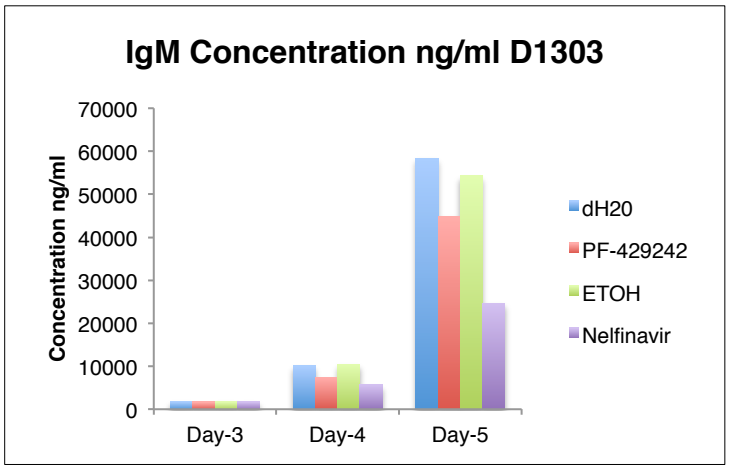


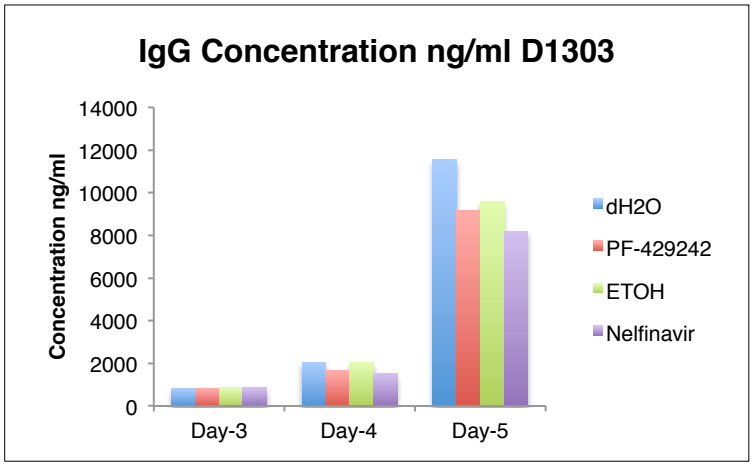


**Figure 6.14: The impact of S1P inhibitor (PF-429242) and S2P inhibitor (Nelfinavir) on immunoglobulin production.** Cells (Day-3, Day-4 and Day-5) were treated with 10 μM PF-429242/dH2O and or 10 μM Nelfinavir/Ethanol for 24 hours and the supernatants were collected for IgM and IgG quantifications using ELISA. Blue bars represent dH2O treated cells, red bars represent 10 μM PF-429242 treated cells, green bars represent ethanol treated cells and purple bars represent 10 μM Nelfinavir treated cells.

### 6.3 Day-3 to Day-6

While the impact of 10µM PF-429242 or 10µM Nelfinavir on cells during the activated B-cell to plasmablast transition was minimal in terms of cell number and phenotype, the results of Figure 6.14 suggested that the inhibitors could alter the functionality of ASC. The experiments conducted thus far only examined the cells after 24 hours of treatment. It was plausible that a greater effect might be observed after prolonged exposure to the drugs. Therefore, the cells were treated with the inhibitors for longer time: either with one dose on Day-3 and analysed on Day-6 (72 hours) or by re-treating the cells every 24 hours until Day-6 (Figure 6.15).

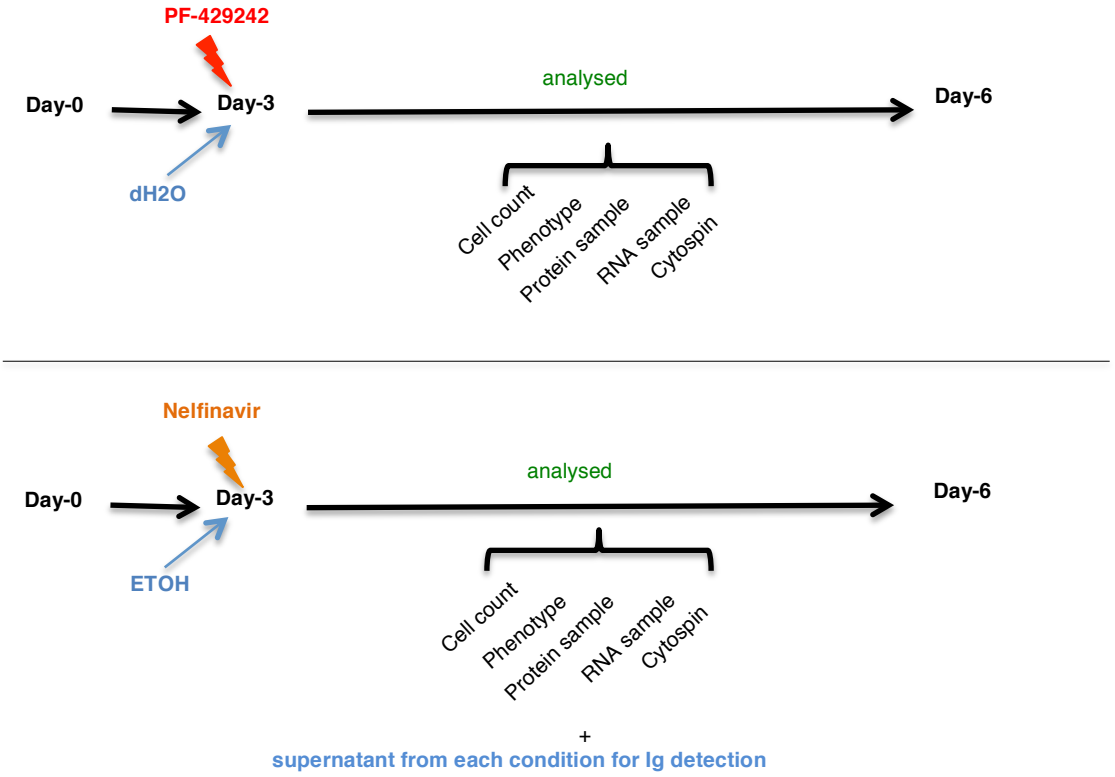


**Figure 6.15: Diagrammatic representation of experiments to detect the impact of S1P and S2P inhibitors.** The cells were treated on Day-3 for 72 hours and analysed on Day-6 for cell number, cell phenotype, protein expression, RNA expression and immunoglobulin levels.

### 6.3.1 Day-3 to Day-6 (One dose)

#### 6.3.1.1 Cell count

To determine whether extended exposure to S1P/S2P inhibitors might result in a reduction of proliferation or enhanced cell death, activated Day-3 cells were treated with 10 μM PF-429242/dH2O or 10 μM Nelfinavir/Ethanol for 72 hours. On Day-6, the cells were accurately counted using CountBright™ absolute counting to examine the possible impact of the inhibitors. The results revealed an 80% reduction in the number of treated B-cells compared to their controls, confirming that inhibiting S1P/S2P regulated pathways had an impact on cell viability (Figure-6.16).

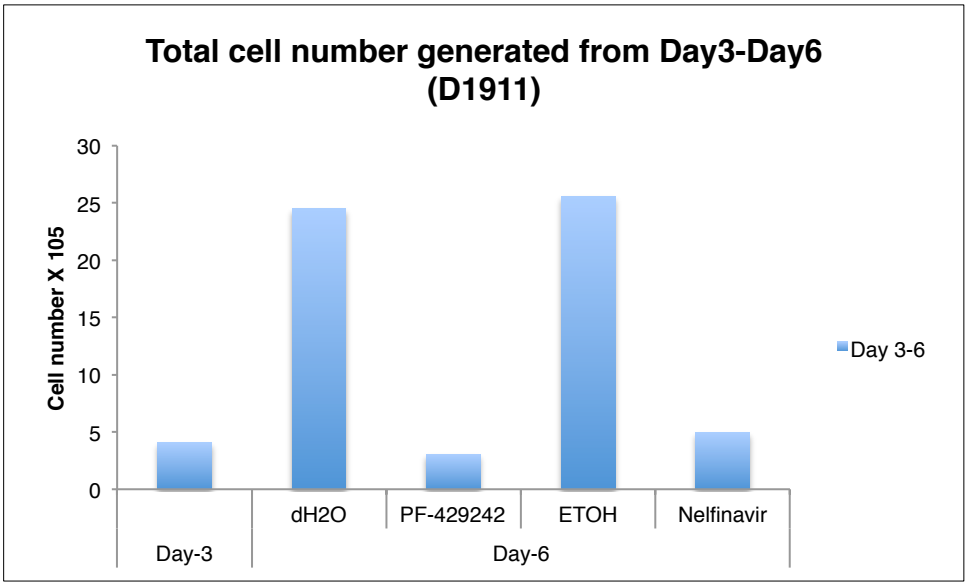


**Figure 6.16: The impact of S1P inhibitor (PF-429242) and S2P inhibitor (Nelfinavir) on cell number.** Day-3 B-cells were treated with 10 μM PF-429242/dH2O or 10 μM Nelfinavir/Ethanol for 72 hours and analysed on Day-6 using CountBright ™ absolute counting.

### 6.3.1.2 Cell phenotype

The ability of cells to down-modulate B-cell associated markers while acquiring a PC phenotype is an essential component of the differentiation process. To investigate whether inhibiting S1P/S2P could interrupt this change, Day-3 cells were treated with 10 μM PF-429242/dH2O or 10 μM PF-429242 10 Nelfinavir/Ethanol and the surface expression patterns were examined on Day-6 by flow cytometry.

The results showed a slight change in cell phenotype upon inhibitor treatment, by decreasing the plasmablast formation (CD38) and retaining B cell markers (CD20) compared to the control (dH20 and Ethanol) (Figure 6.17).

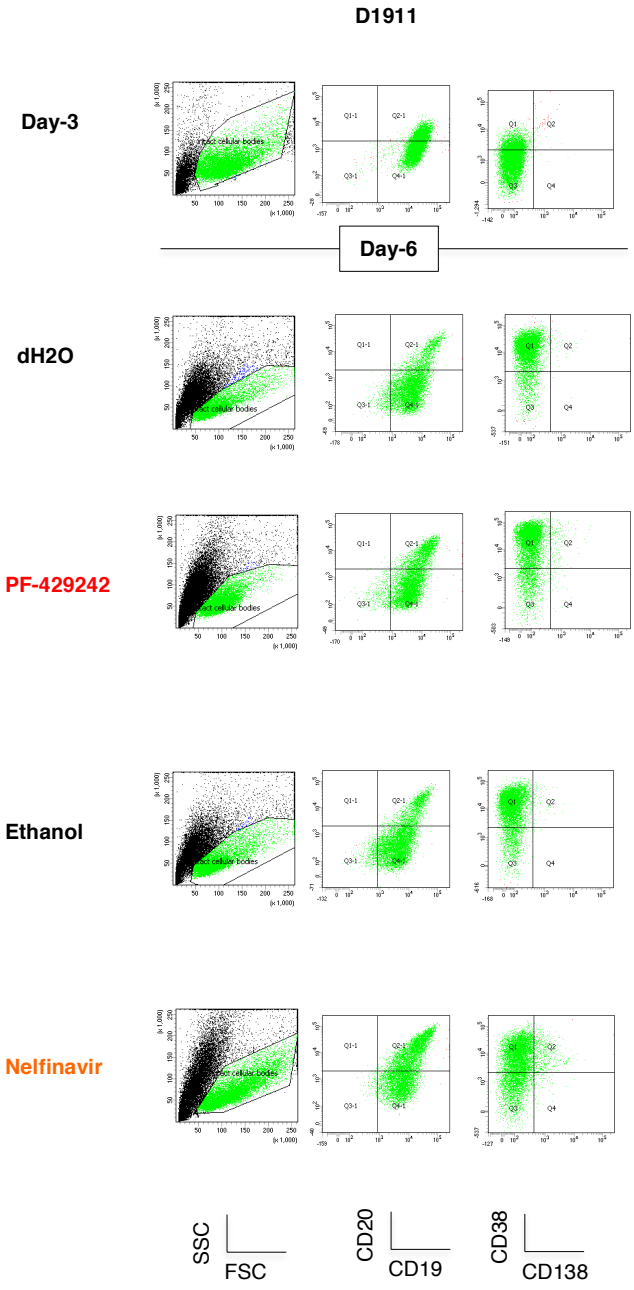


**Figure 6.17: The impact of S1P inhibitor (PF-429242) and S2P inhibitor (Nelfinavir) on cell phenotype during differentiation.** Human B-cells (Day-3) were treated with 10 μM PF-429242/dH2O or 10 μM Nelfinavir/Ethanol for 72 hours. On Day-6, the cells were stained using B-cell (CD19 and CD20) and ASC markers (CD38 and CD138) and analysed by flow cytometry.

### 6.3.1.3 Expression of UPR-related transcription factors

The previous experiments suggested that the inhibitor treatment lead to a marked reduction of CREB3L2 and loss of ATF6 and XBP1s. To confirm that that the loss of protein was maintained over the extended period of incubation, Day-3 cells were treated with 10 μM PF-429242/dH2O or 10 μM Nelfinavir/Ethanol for 72 hours and protein expression examined. As before, there was a profound inhibition of S1P-mediated cleavage using 10 μM PF-429242 on CREB3L2 and XBP1, but less of an effect on ATF6 (Figure 6.18). However, 10 μM Nelfinavir had an impact on CREB3L2 (both forms), XBP1s and ATF6.

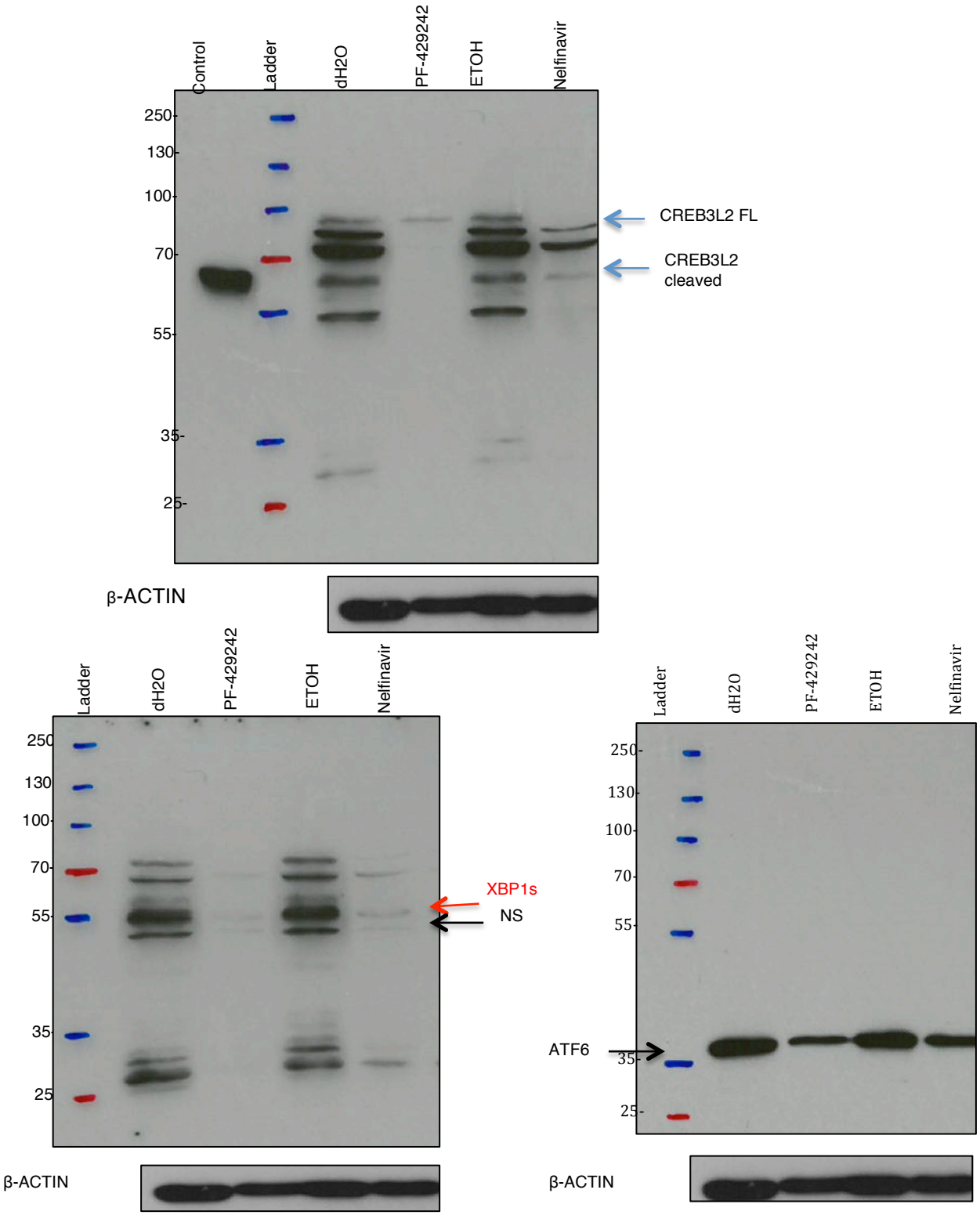


**Figure 6.18: The impact of S1P inhibitor (PF-429242) or S2P inhibitor (Nelfinavir) on CREB3L2, XBP1s and ATF6 after 72 hr treatment.** Day-3 B-cells were treated with 10 μM PF-429242/dH2O or 10 μM Nelfinavir/Ethanol for 72 hours and cell lysates analysed by Western blot. Migrations of TFs are indicated by arrows. Control was the N-terminus of CREB3L2 that has been overexpressed in Hela cells. B-ACTIN was used as a loading control.

### 6.3.1.4 Immunoglobulin levels

The results in Figure 6.14 suggested that inhibiting S1P/S2P might prevent the secretion of antibody. To ascertain whether the effect was more pronounced with an extended incubation, the supernatants were collected from the treated /untreated cells and analysed using ELISA. The results show almost a complete elimination of IgM in the treated samples compared with the control (Figure 6.19). On the other hand, IgG levels were reduced by 75-90%. These results suggest that prolonged exposure to 10 μM PF-429242 and 10 μM Nelfinavir severely cripples immunoglobulin production.

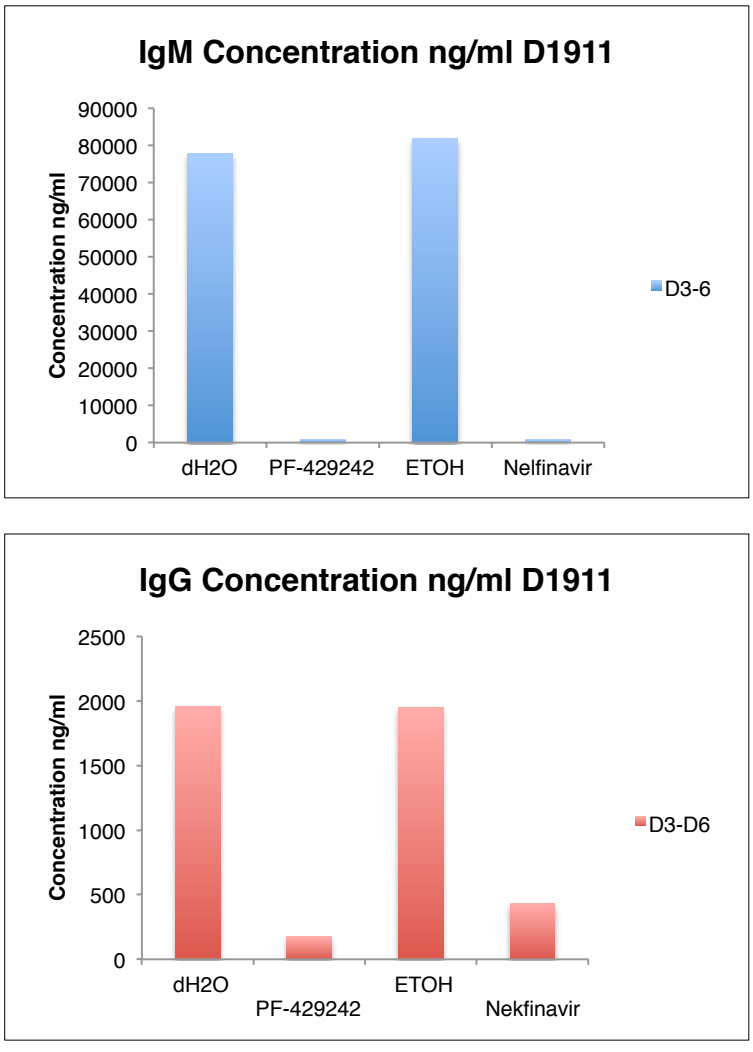


**Figure 6.19: The impact of S1P inhibitor (PF-429242) and S2P inhibitor (Nelfinavir) on immunoglobulin production after 72 hrs of treatment.** Day-3 B-cells were treated with 10 μM PF-429242/dH2O or 10 μM Nelfinavir/Ethanol for 72 hours and the supernatant were collected for IgM and IgG quantifications using ELISA. Blue bars represent IgM levels whereas the red bars represent IgG levels.

### 6.3.1.5 Cell morphology

The data in Figure-6.16 clearly shows a dramatic drop in cell number after treatment with 10 μM PF-429242 or 10 μM Nelfinavir, whereas the surviving cells were able to show phenotypic maturation. Interestingly, Nelfinavir also generated a population of cells that had increased FSC/SSC compared to other cells at Day-6 (Figure-6.17). To further investigate the impact of S1P or S2P treatment on plasmablasts, cytospin samples were assessed for morphological differences (Figure-6.20). Unexpectedly, cells treated with Nelfinavir exhibited polyploidy. In control cells, 94% had 1 nuclear lobe, 4.6% had 2 nuclear lobes and 1.4% had >2. In contrast, after 72 hours of Nelfinavir exposure 69% of cells had a single nuclear lobe, 22% had 2 lobes and 9% featured more than 2 nuclear lobes in a single cell. Treatment with PF-429242 generated vacuolated cells, consistent with increased cell death.

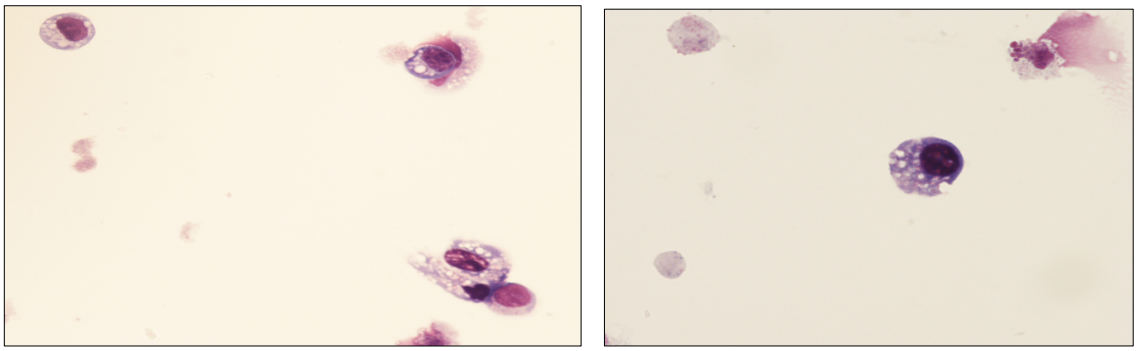

10 μM PF 429242

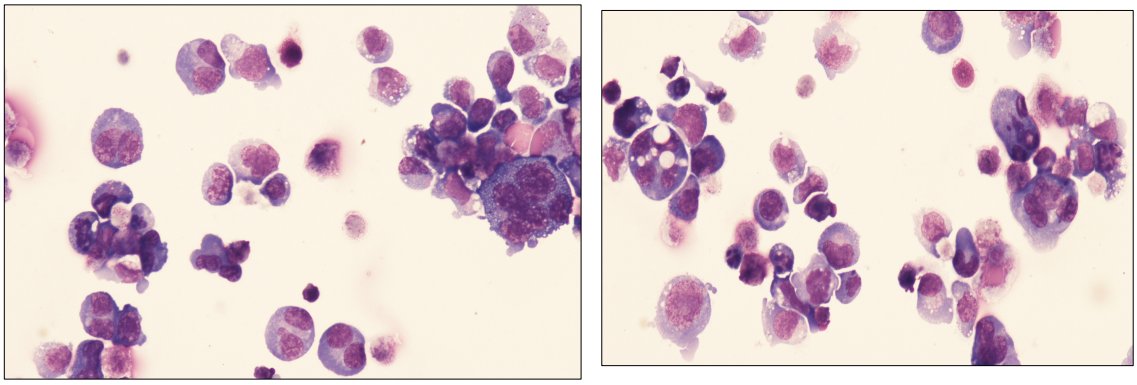

10 μM Nelfinavir

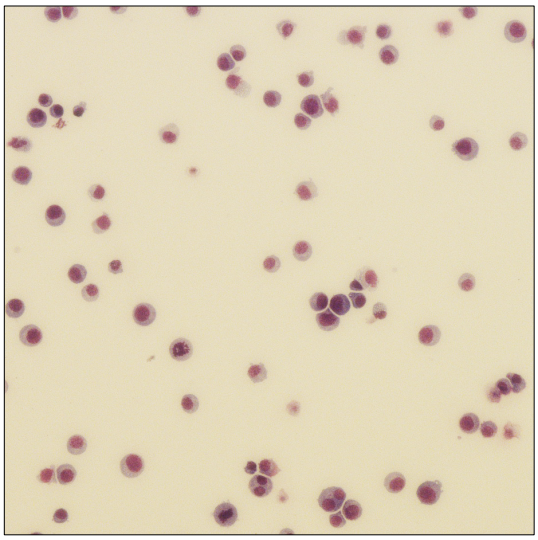

Control

**Figure 6.20: The impact of S1P inhibitor (PF-429242) and S2P inhibitor (Nelfinavir) on the morphology of human differentiated B-cells.** Day-3 B-cells were treated with 10 μM PF-429242/dH2O or 10 μM Nelfinavir/Ethanol for 72 hours. After incubation, the cells were stained using Geimsa stain.

### 6.3.2 Day-3 to Day-6 (Multiple doses)

The impact of S1P and S2P inhibitors was further investigated by repeating the treatment with the inhibitors. Thus, Day-3 B-cells were treated with 10µM PF-429242/dH2O or 10µM Nelfinavir/Ethanol, the cells were re-seeded and re-treated with the inhibitors on Day-4 and Day-5 and analysed on Day-6 (Figure- 6.21) for protein and RNA expression, cell count, cell phenotype and immunoglobulin production.

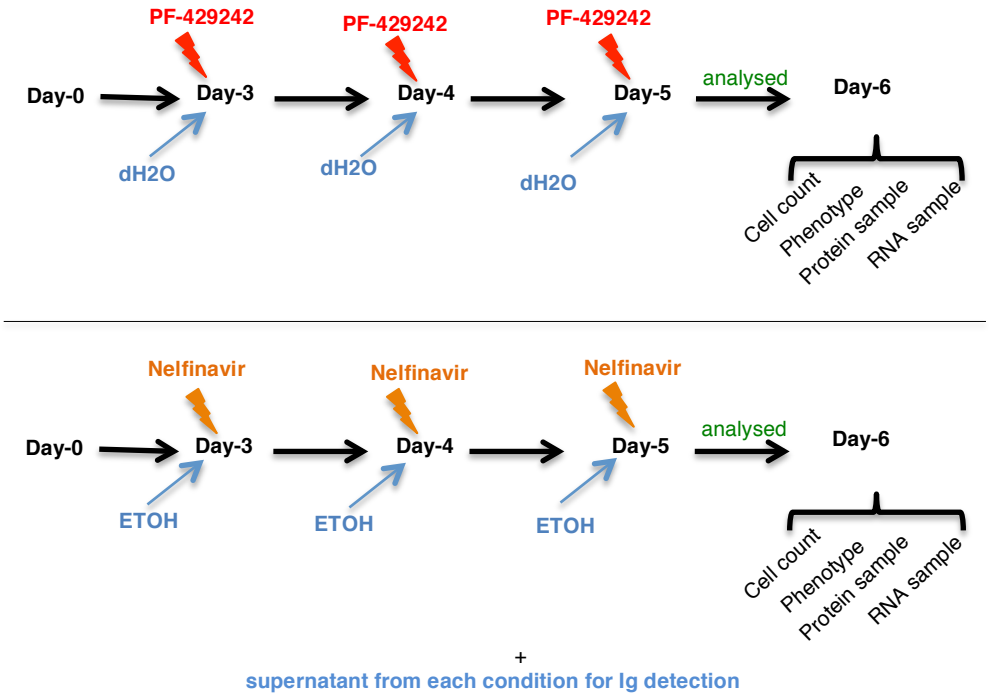


**Figure 6.21: Diagrammatic representation of experimental design to test the impact of S1P and S2P inhibitors administered in multiple doses.** The cells were treated on Day-3, and re-treated on Day-4 and Day-5. Then the cells were analysed on Day-6 for cell number, cell phenotype, protein and RNA expression and immunoglobulin levels.

#### 6.3.2.1 Expression of UPR-related transcription factors

The single dose of S1P or S2P inhibitor applied at Day-3 was able to abolish CREB3L2 and XBP1 expression at Day-6 and dampen expression of ATF6. To determined whether multiple doses might further reduce protein expression, patterns of the three UPR elements; CREB3L2, XBP1s and ATF6 were checked after the triple dose of inhibitors. As before, both forms of CREB3L2 were lost as was XBP1s (Figure 6.22). Furthermore, multiple doses more effectively reduced the levels of ATF6.

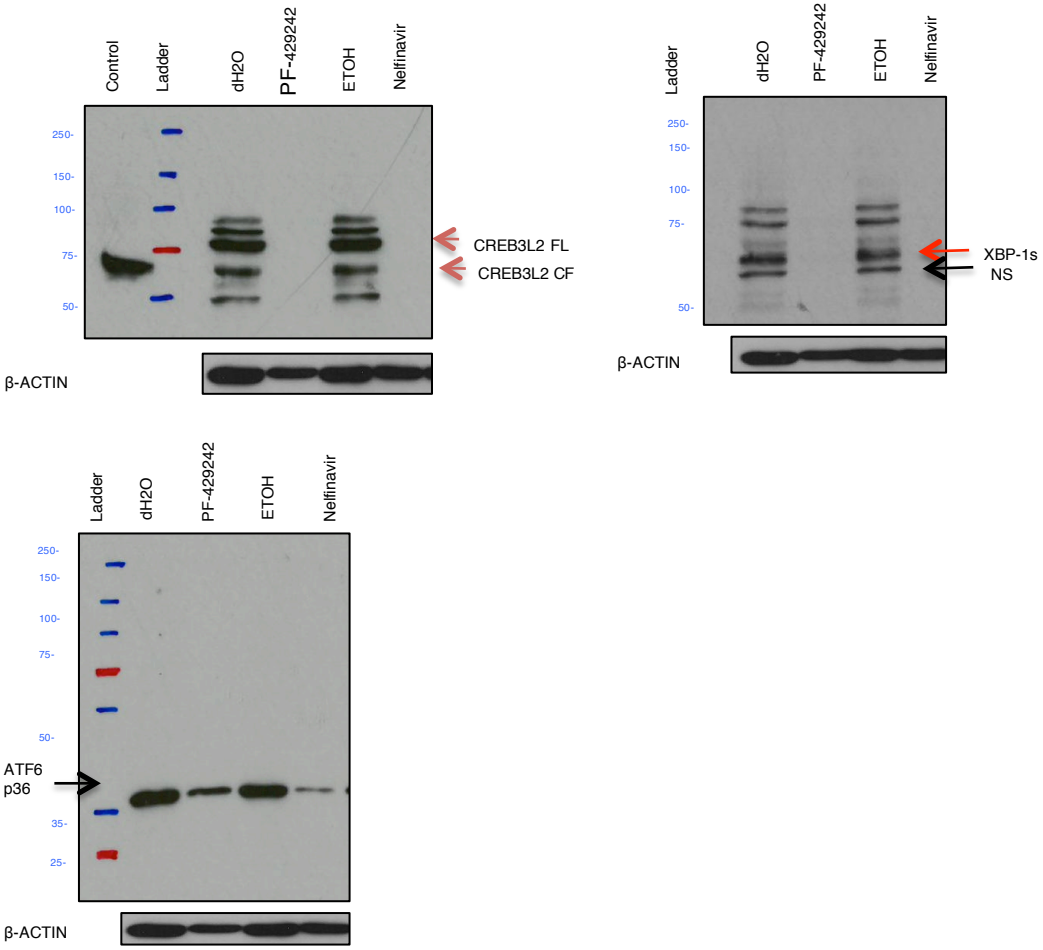


**Figure 6.22: The impact of multiple doses of S1P inhibitor (PF-429242) and or S2P inhibitor (Nelfinavir) on CREB3L2, XBP1s and ATF-6 expression.** B-cells were treated repeatedly with 10 μM PF-429242/dH2O or 10 μM Nelfinavir/Ethanol on Day-3, Day-4 and Day-5 and the cells were collected for protein analysis by Western blotting on Day-6. Migrations of TFs are indicated by arrows. Control was the N-terminus of CREB3L2 that has been overexpressed in Hela cells. β-ACTIN was used as a loading control. NS, non-specific band.

### 6.3.2.2 Cell count

On Day-6, the cells were accurately counted using CountBright ™ absolute counting to examine the effect of treating the cells repeatedly with S1P and S2P inhibitors during the activated B-cell to plasmablast transition. The results demonstrated more than 90% reduction in the number of treated B-cells compared to their controls, confirming that S1P inhibitor (10 μM PF-429242) and S2P inhibitor (10 μM Nelfinavir) had a profound impact on cell viability during the early stages of becoming an ASC (Figure-6.23).

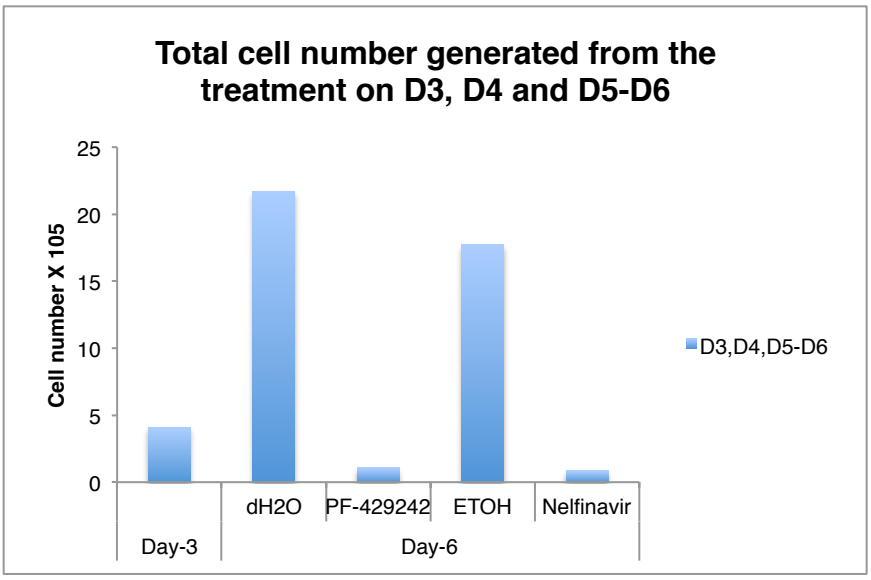


**Figure 6.23: The impact of repeated doses of S1P inhibitor (PF-429242) and S2P inhibitor (Nelfinavir) on cell number.** Day-3 B-cells were treated with 10 μM PF-429242/dH2O or 10 μM Nelfinavir/Ethanol for 24 hours and then re-treated with the same inhibitors on Day-4 and Day-5 and analysed on Day-6 using CountBright ™ absolute counting.

### 6.3.2.3 Cell phenotype

The impact of multiple treatments on both the expression of CREB3L2, XBP1 and ATF6 and cell survival was compelling. To determine whether this extended to preventing phenotypic alterations, the cells were repeatedly treated on Day-3, Day-4 and Day-5 with 10 μM PF-429242/dH2O or 10 μM PF-429242 10 Nelfinavir/Ethanol and analysed on Day-6. The cells were stained with CD19, CD20, CD138 and CD38 and evaluated using flow cytometry. The results showed that there is an increase in CD38 high population from PF-429242 treated samples compared to the control. However, CD20 is retained in PF-429242 treated samples compared to the control (dH20 and Ethanol) (Figure 6.24).

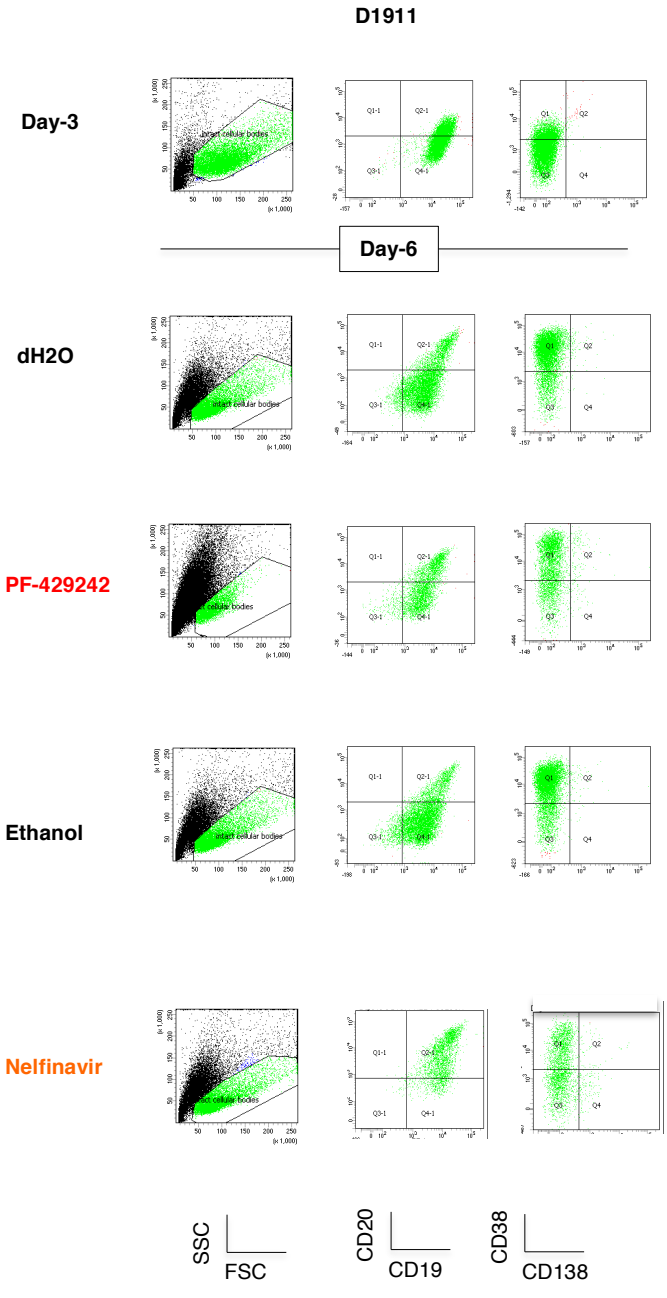


**Figure 6.24: The impact of repeated doses of S1P inhibitor (PF-429242) and S2P inhibitor (Nelfinavir) on cell phenotype during the transition from activated B-cell to plasmablast.** B-cells (Day-3) were treated with 10 μM PF-429242/dH2O or 10 μM Nelfinavir/Ethanol for 24 hours and then the cells were re-treated with the same inhibitors on Day-4 and Day-5 and analysed on Day-6. On Day-6, the cells were stained using B-cell markers (CD19 and CD20) and ASC markers (CD38 and CD138) and analysed using flow cytometry.

### 6.3.2.4 Immunoglobulin levels

The previous results using a single dose showed that the cells were unable to produce much immunoglobulin, despite evidence for phenotypic changes associated with the plasmablast stage. To further investigate the impact of multiple doses of S1P and S2P inhibitors on immunoglobulin (IgM and IgG) production, the supernatants were collected from the treated /untreated cells and analysed using ELISA. In this experiment both IgM and IgG were reduced by greater than 90% after repeated exposure to the inhibitors (Figure 6.25).

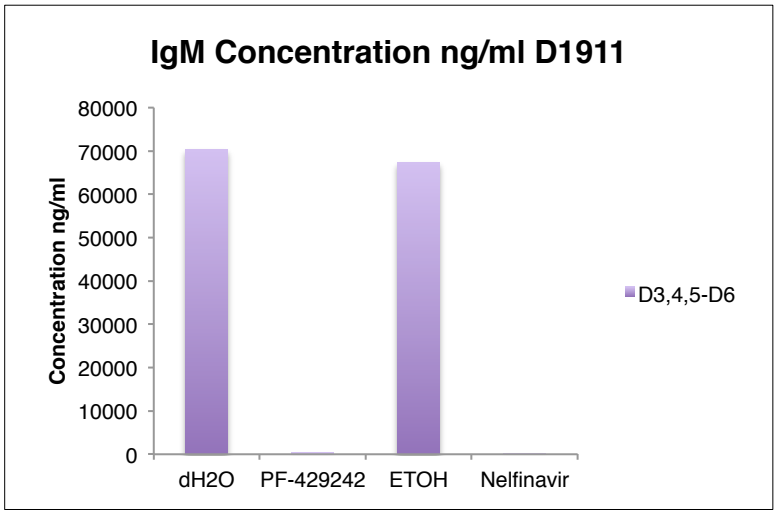


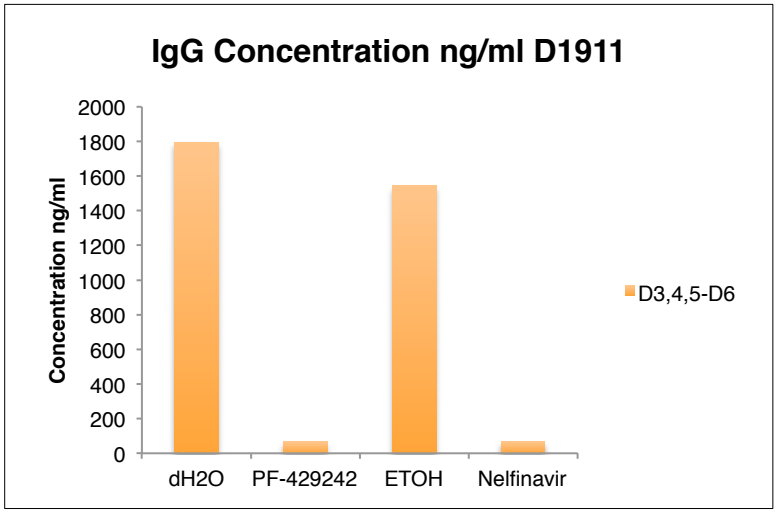


**Figure 6.25: The impact of multiple doses of S1P inhibitor (PF-429242) and S2P inhibitor (Nelfinavir) on IgM and IgG levels.** Day-3 B-cells were treated with 10 μM PF-429242/dH2O or 10 μM Nelfinavir/Ethanol for 24 hours and then re-treated with the same inhibitors on Day-4 and Day-5 and analysed on Day-6. The supernatants were collected and the immunoglobulins (IgM and IgG) were quantified using ELISA.

## 6.4 Validation of S1P/S2P Inhibitor Single Application on Day3 with Evaluation on Day6

The preliminary set of experiments described above suggested that the optimum condition for evaluating the impact of S1P and S2P inhibitors on the UPR elements (CREB3L2, XBP1s and ATF6) in differentiating human B-cells was using a single dose of inhibitor on Day-3 activated cells followed by evaluation 3 days later when the cells had progressed to the plasmablast stage. A total of 7 donors were assessed for protein expression (Figure 6.26), cell count (Figure 6.27), cell phenotype (Figure 6.28), and IgM and IgG levels (Figure 6.29) following treatment with 10 μM PF-429242 or 10 μM Nelfinavir.

Initially, protein samples were evaluated to confirm that S1P/S2P inhibitors were producing the appropriate effect on the expression of CREB3L2, XBP1s and ATF6 in each of the 7 donors. The results showed a consistent inhibition of both forms of CREB3L2 by PF-429492 and Nelfinavir, with a near complete loss of protein upon treatment with the S1P inhibitor. Interestingly, one donor (D704) had a prominent band detected by the anti-CREB3L2 at approximately 50 kDa that was also affected by the inhibitor. This band was variably observed in different donors, but never to the extent as seen in this particular experiment. There are several predicted ESTs for *CREB3L2*; it is possible that the B-cells in this differentiation expressed a particular isoform containing the epitope recognised by the antibody. This sample was also relatively resistant to Nelfinavir treatment. Furthermore, the expression of both XBP1s and ATF6 appeared to closely mirror that of CREB3L2 (Figure 6.26).

## A. CREB3L2



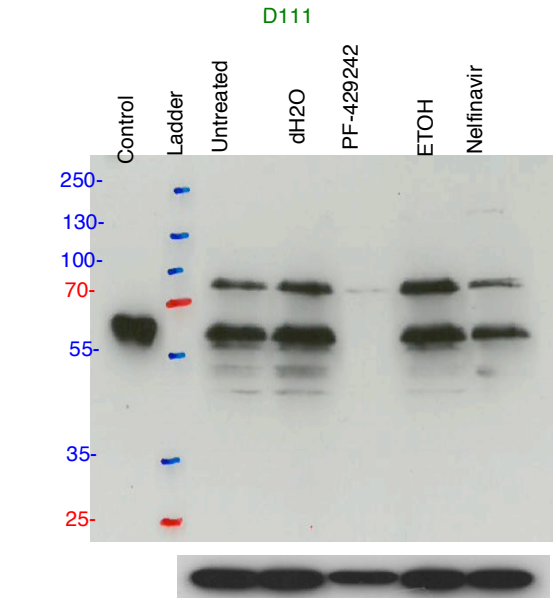


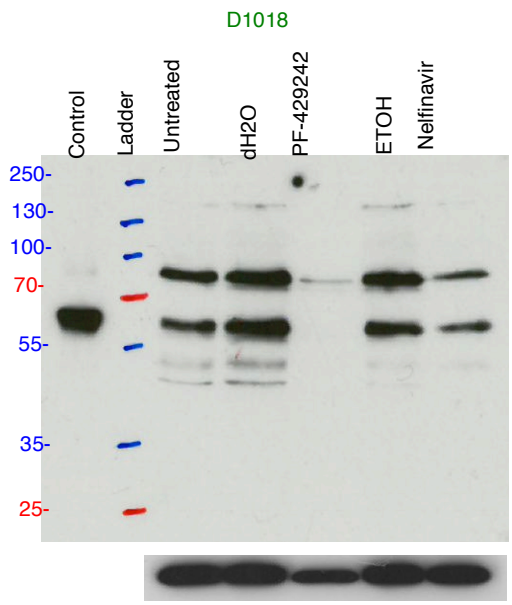


β-ACTIN

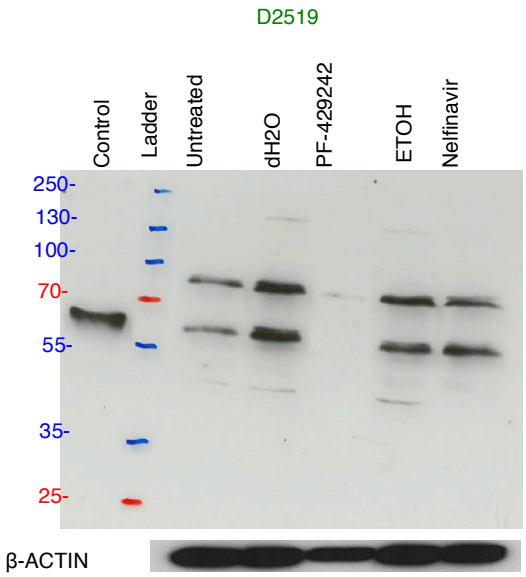


β-ACTIN

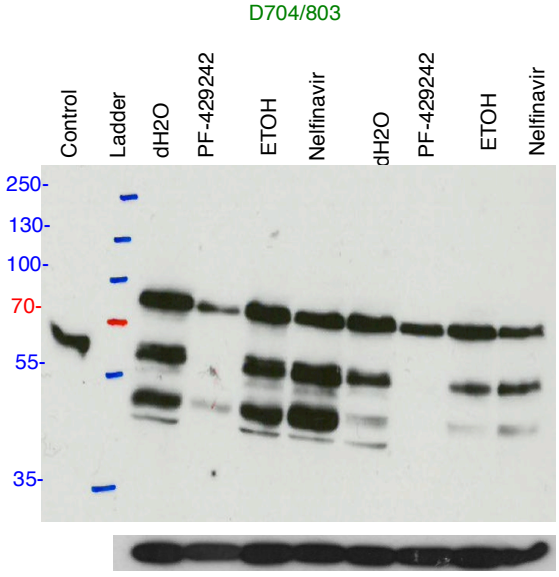


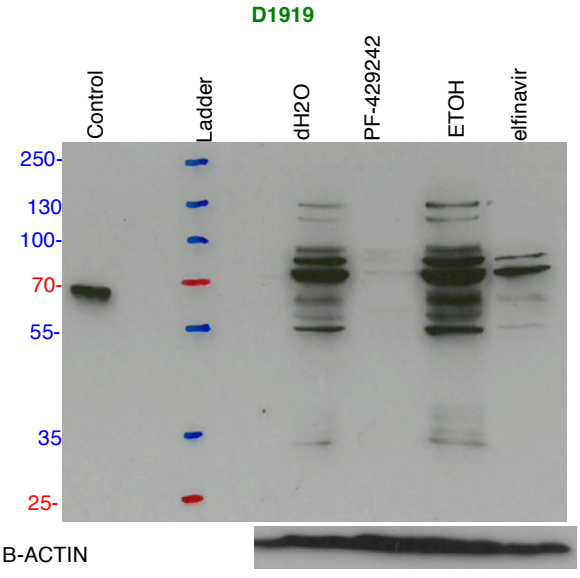


B-ACTIN

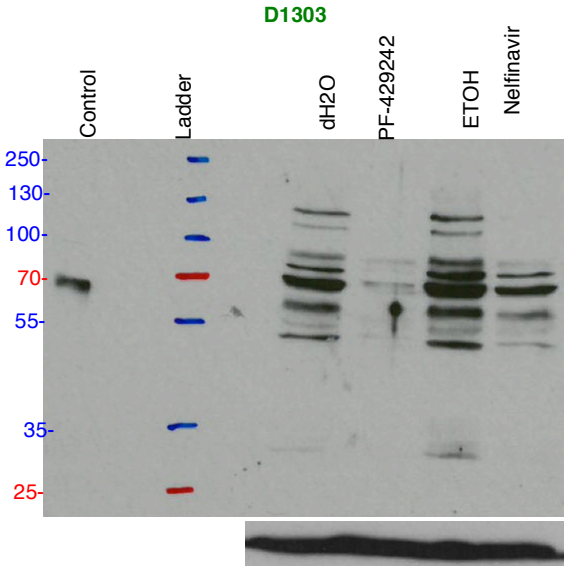

**B. XBP1s**

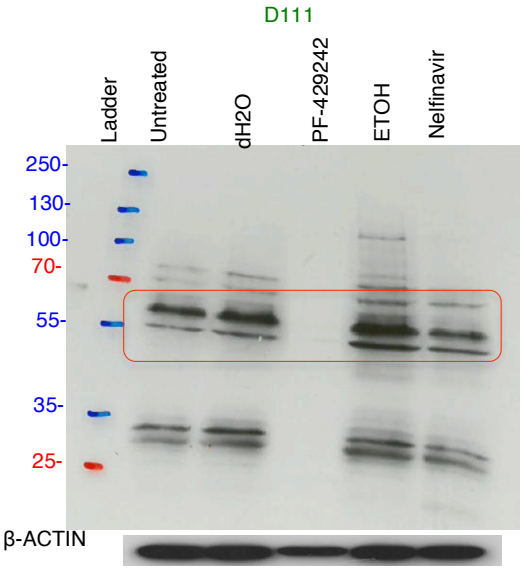
D111
Ladder
Untreated
dH2O
PF-429242
ETOH
Nelfinavir
250-
130-
100-
70-
55-
35-
25-
β-ACTIN

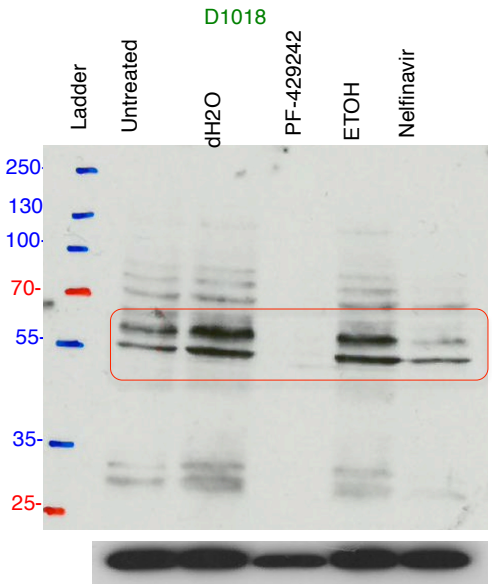
D1018
Ladder
Untreated
dH2O
PF-429242
ETOH
Nelfinavir
250-
130-
100-
70-
55-
35-
25-

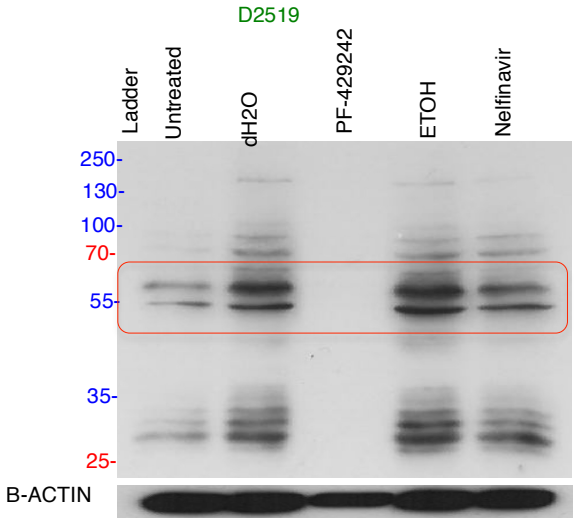
D2519
Ladder
Untreated
dH2O
PF-429242
ETOH
Nelfinavir
250-
130-
100-
70-
55-
35-
25-
B-ACTIN

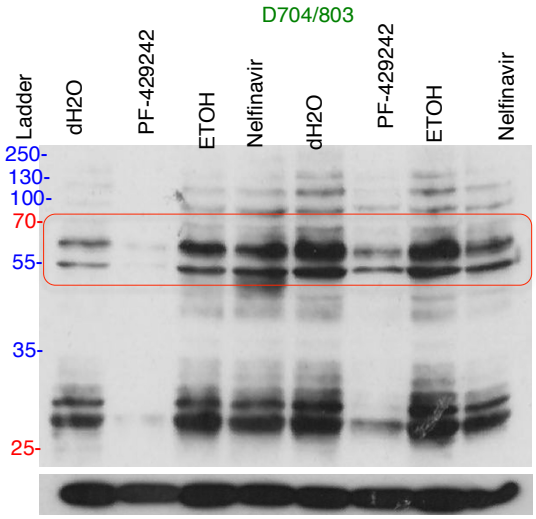
D704/803
Ladder
dH2O
PF-429242
ETOH
Nelfinavir
dH2O
PF-429242
ETOH
Nelfinavir
250-
130-
100-
70-
55-
35-
25-

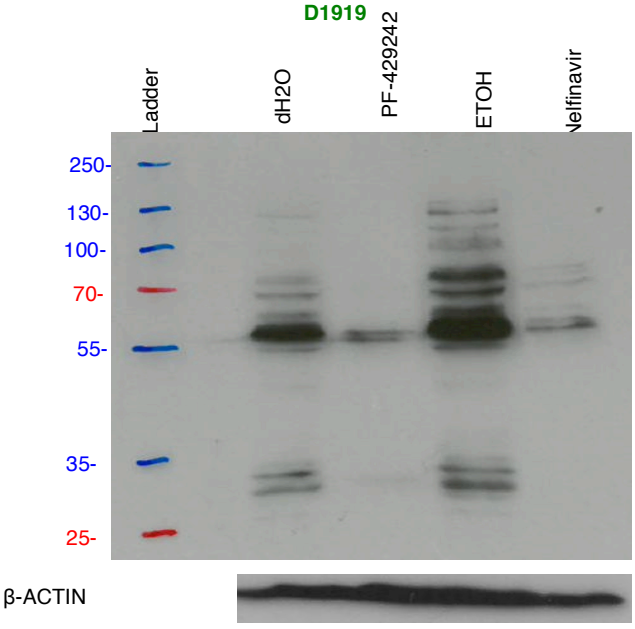
D1919
Ladder
dH2O
PF-429242
ETOH
Nelfinavir
250-
130-
100-
70-
55-
35-
25-
β-ACTIN

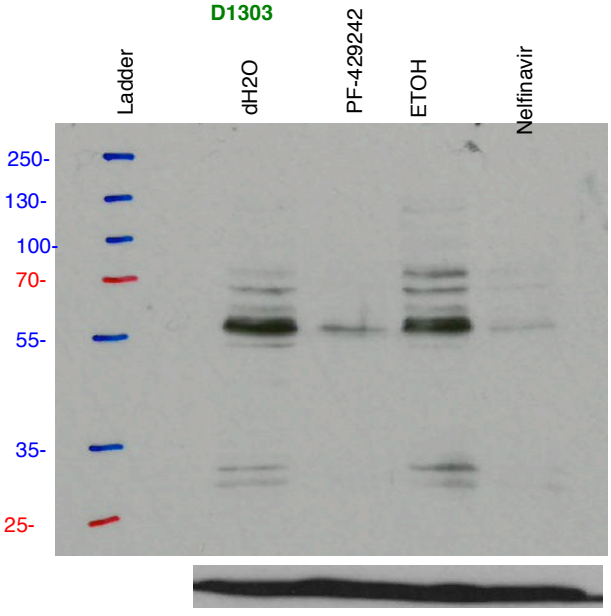
D1303
Ladder
dH2O
PF-429242
ETOH
Nelfinavir
250-
130-
100-
70-
55-
35-
25-

## C. ATF-6

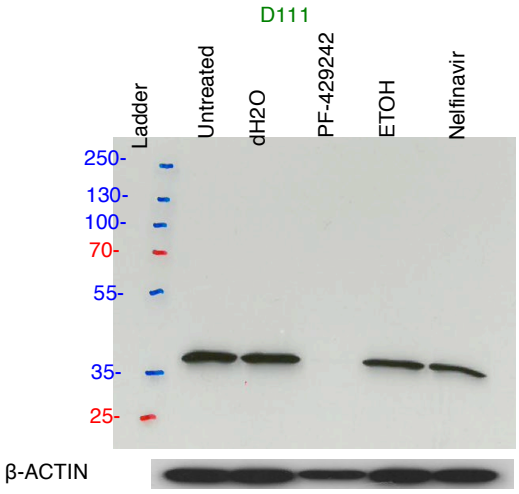
D111
Ladder
Untreated
dH2O
PF-429242
ETOH
Nelfinavir
250-
130-
100-
70-
55-
35-
25-
β-ACTIN

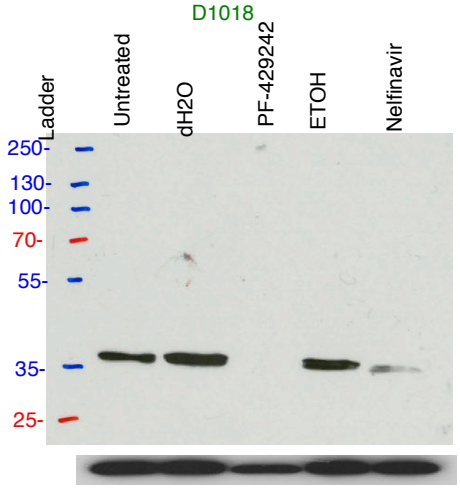
D1018
Ladder
Untreated
dH2O
PF-429242
ETOH
Nelfinavir
250-
130-
100-
70-
55-
35-
25-

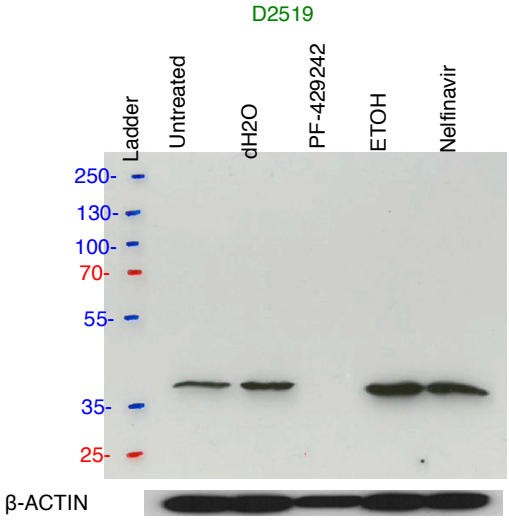
D2519
Ladder
Untreated
dH2O
PF-429242
ETOH
Nelfinavir
250-
130-
100-
70-
55-
35-
25-
β-ACTIN

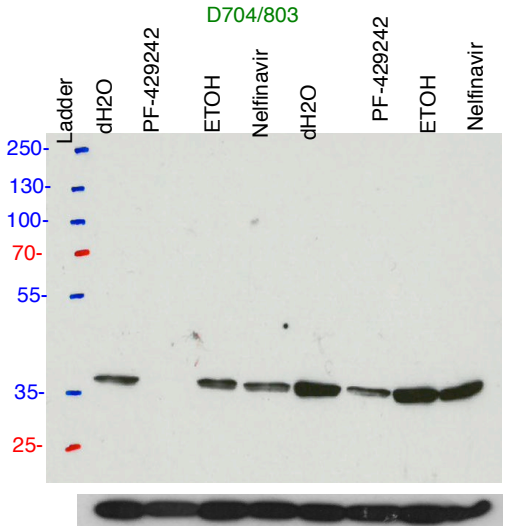
D704/803
Ladder
dH2O
PF-429242
ETOH
Nelfinavir
dH2O
PF-429242
ETOH
Nelfinavir
250-
130-
100-
70-
55-
35-
25-

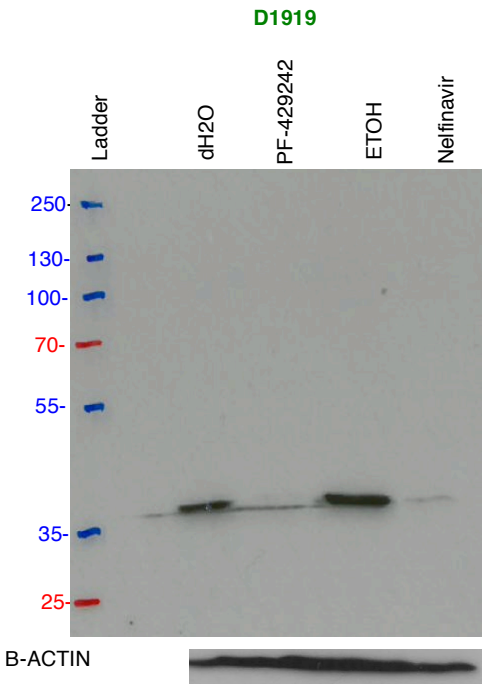
D1919
Ladder
dH2O
PF-429242
ETOH
Nelfinavir
250-
130-
100-
70-
55-
35-
25-
B-ACTIN

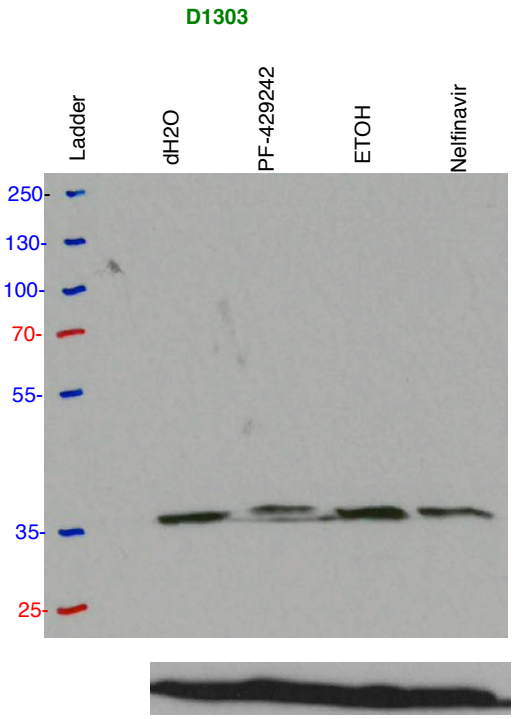
D1303
Ladder
dH2O
PF-429242
ETOH
Nelfinavir
250-
130-
100-
70-
55-
35-
25-

**Figure 6.26 Validating the impact of S1P inhibitor (PF-429242) or S2P inhibitor (Nelfinavir) on the endogenous protein expression of CREB3L2, XBP1s and ATF6.** Day-3 B-cells from 7 human donors were treated with 10 μM PF-429242/dH2O or 10 μM Nelfinavir/Ethanol for 72 hours. Cell were collected for protein preparation and analysis using 10% SDS-PAGE followed by Western blot for (A) CREB3L2, (B) XBP1 and (C) ATF6. Control was the N-terminus of CREB3L2 that has been overexpressed in Hela cells. β-ACTIN was used as a loading control. Individual donors are indicated at the top of each blot.

The impact of S1P and S2P inhibitors on the accumulation of active UPR-related transcription factors indicated that the drugs were effectively targeting the expected pathways. To ascertain whether this would be accompanied by a change in other attributes, a range of assays were performed. Figure 6.27 depicts the absolute counts of cells obtained after 3 days of culture in media containing either PF-429242 or Nelfinavir. Consistent with the previous results, counts obtained from 7 human donors gave fewer cells after S2P inhibition and showed a severe reduction in response to S1P inhibition.

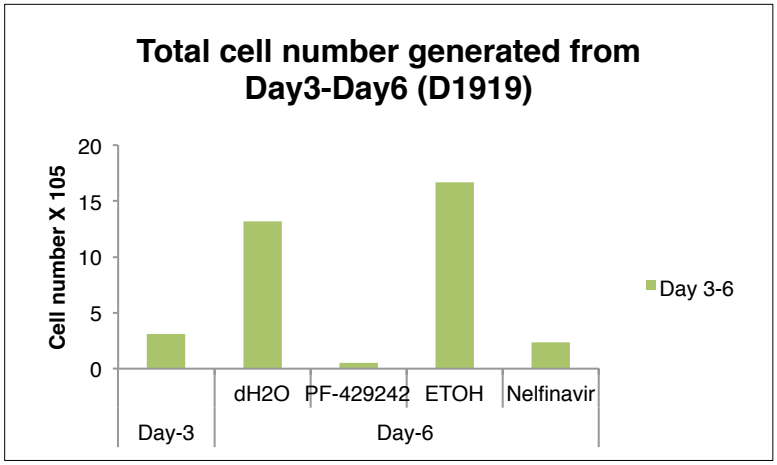


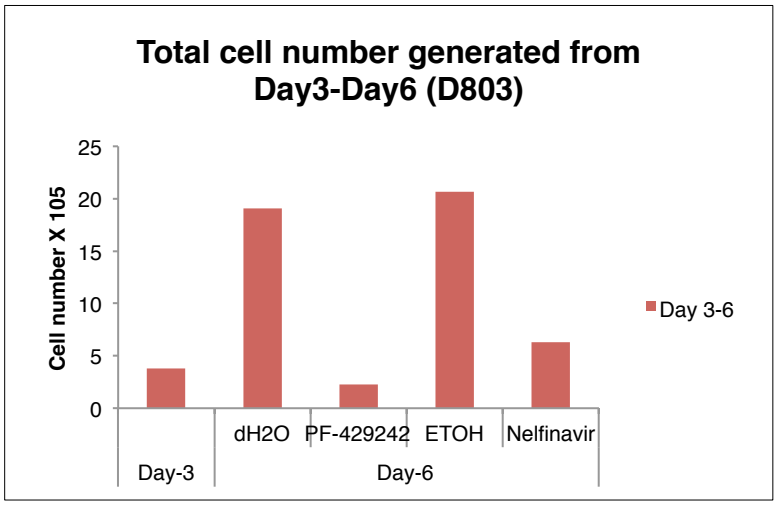

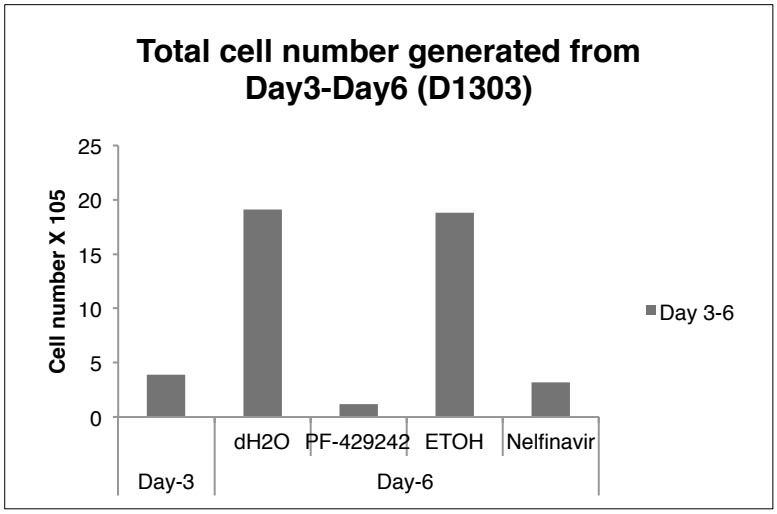
Total cell number generated from Day3-Day6 (D1303)
Cell number X 105
25
20
15
10
5
0
dH2O
PF-429242
ETOH
Nelfinavir
Day-3
Day-6
Day 3-6

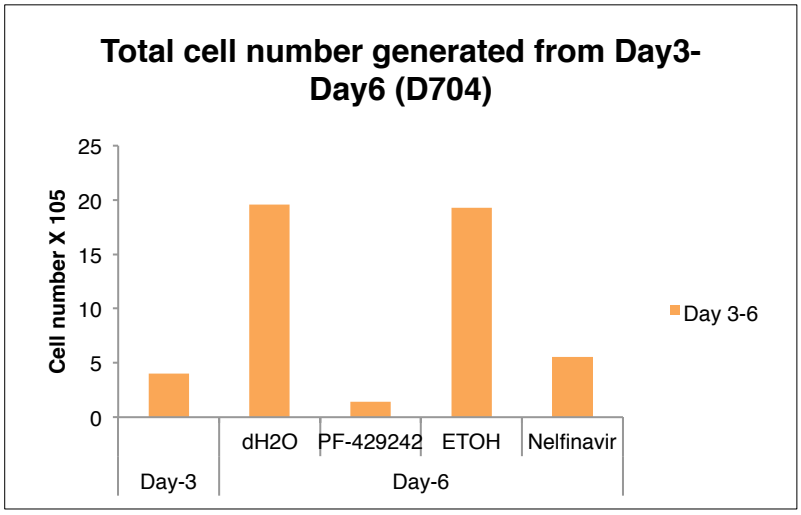
Total cell number generated from Day3-Day6 (D704)
Cell number X 105
25
20
15
10
5
0
dH2O
PF-429242
ETOH
Nelfinavir
Day-3
Day-6
Day 3-6

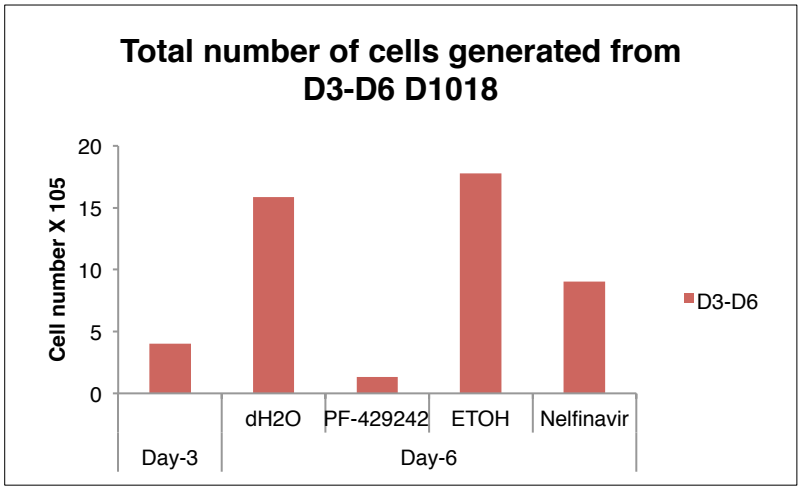
Total number of cells generated from D3-D6 D1018
Cell number X 105
20
15
10
5
0
dH2O
PF-429242
ETOH
Nelfinavir
Day-3
Day-6
D3-D6

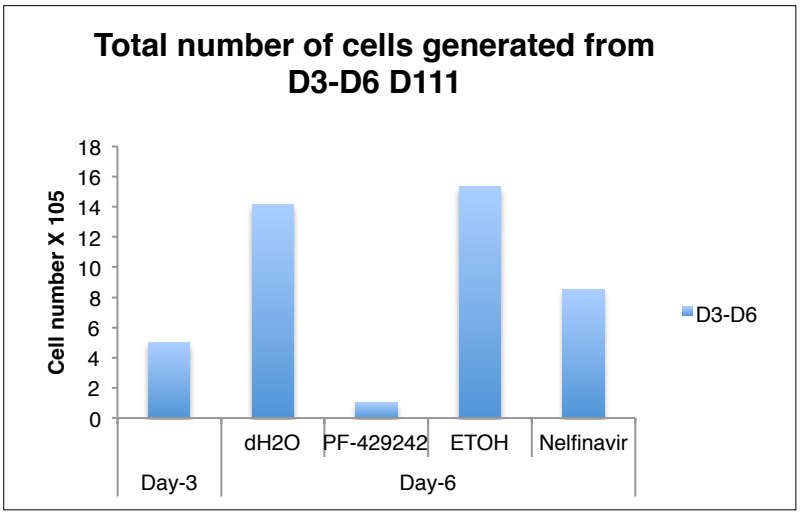


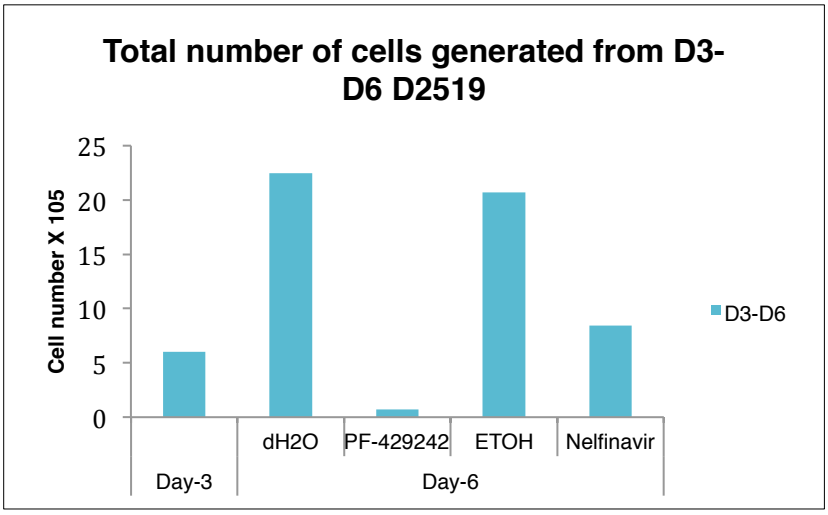


**Figure 6.27 Validating the impact of S1P inhibitor (PF-429242) and S2P inhibitor (Nelfinavir) on cell viability.** Day-3 B-cells were treated with 10 μM PF-429242/dH2O or 10 μM Nelfinavir/Ethanol for 72 hours and analysed on Day-6 for cell number using CountBright ™ absolute counting. Counts for individual donors are depicted in each graph.

The impact of S1P and S2P inhibitors on the transition from B-cells to more mature antibody secretory cells based on cell phenotype was validated as well using flow cytometry (Figure 6.28). The results from 7 donors showed that PF-429242 and Nelfinavir appeared to cause retention of CD20 (B-cells) while delaying the acquisition of CD38 (plasmablast) compared with the control (dH2O and Ethanol), which are the same results obtained earlier.

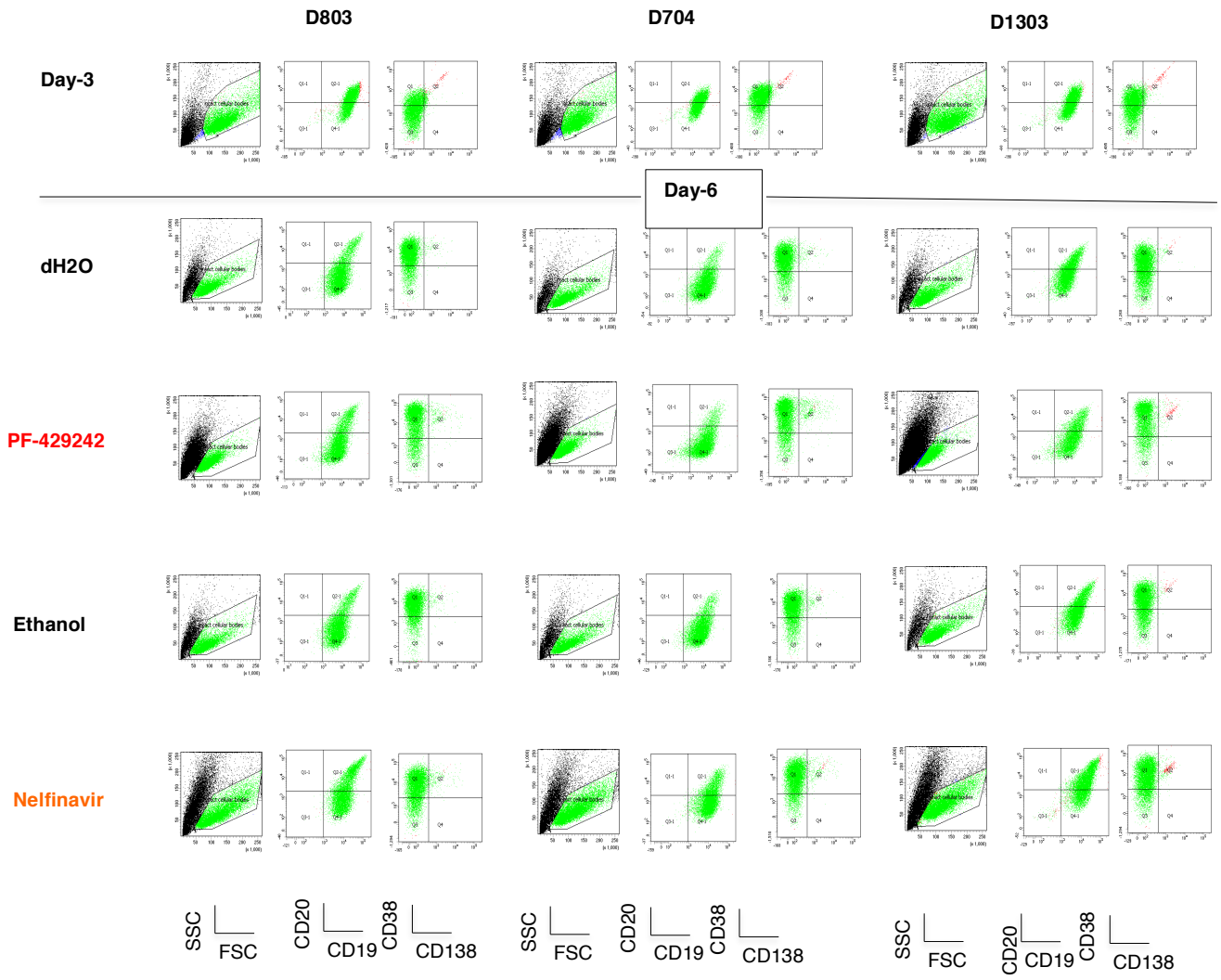

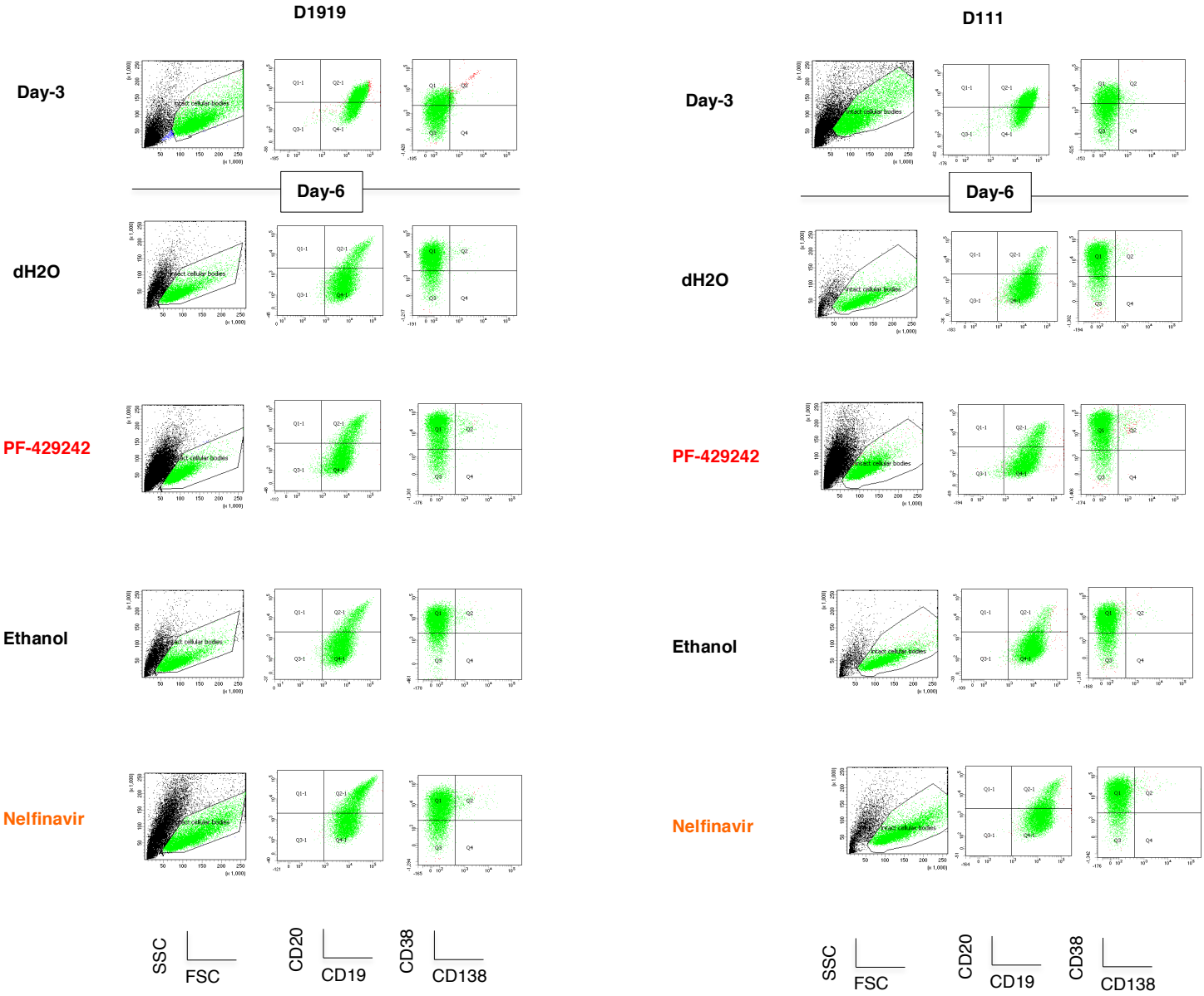
D1919
D111
Day-3
Day-6
dH2O
PF-429242
Ethanol
Nelfinavir
Intact cellular bodies
SSC
FSC
CD20
CD19
CD38
CD138

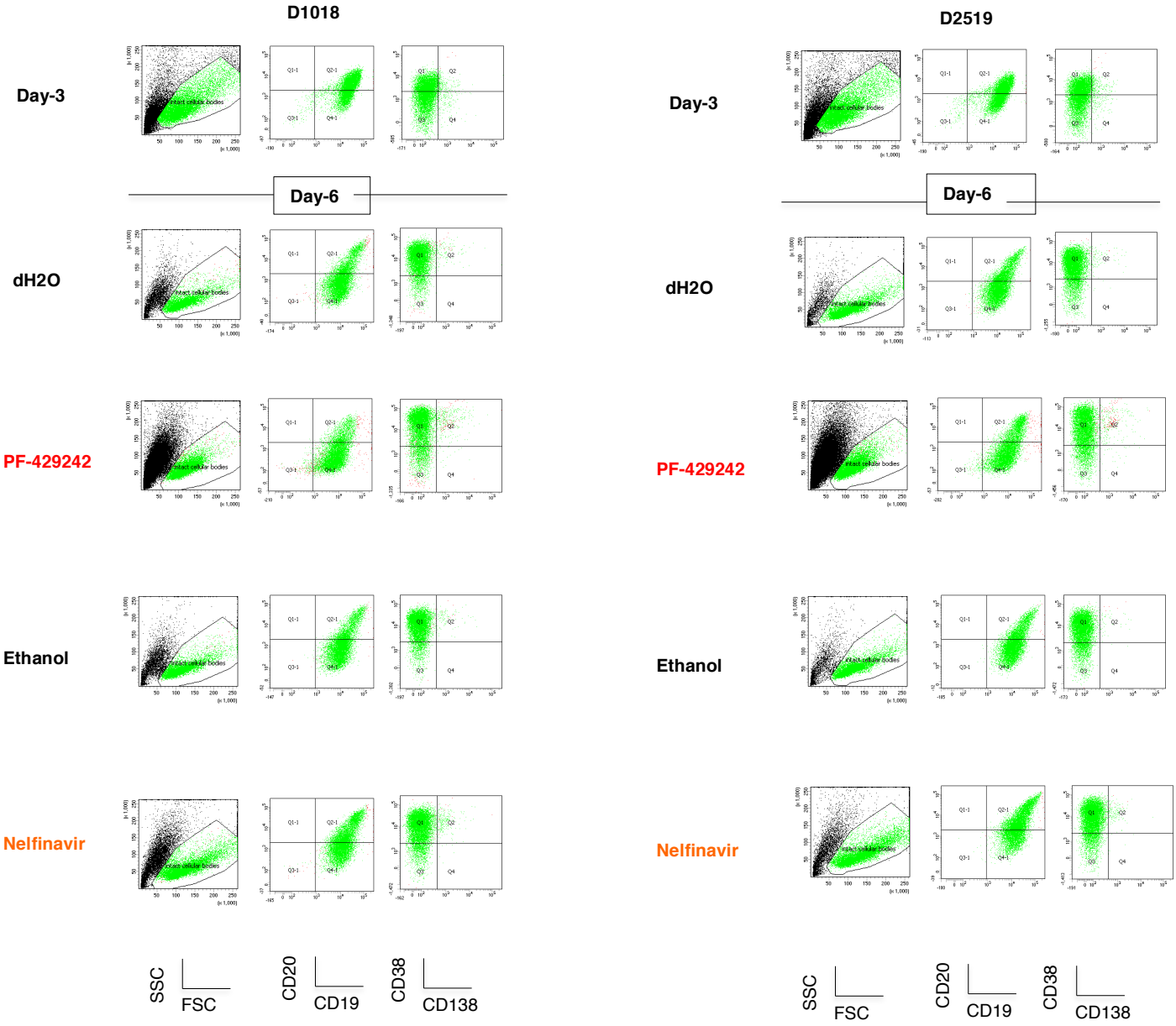


**Figure 6.28 Validating the impact of S1P inhibitor (PF-429242) and S2P inhibitor (Nelfinavir) on cell surface phenotype.** Human activated B-cells (Day-3) were treated with 10 μM PF-429242/dH2O or 10 μM Nelfinavir/Ethanol for 72 hours. On Day-6, the cells were stained for CD19, CD20, CD38 and CD138 and analysed using flow cytometry. Donor numbers are shown at top.

Moreover, using the supernatant samples from the 7 donors, IgM and IgG levels were quantified by ELISA. The results provide evidence for substantial reduction in the IgM and IgG levels in the treated samples compared to the control suggesting that the protease inhibitors not only affect the cell viability but also the immunoglobulin secretion (Figure 6.29). Of interest, the donor (D704) who was characterised by the presence of a potentially new form of CREB3L2 showed relative resistance in the ability to secrete IgG.

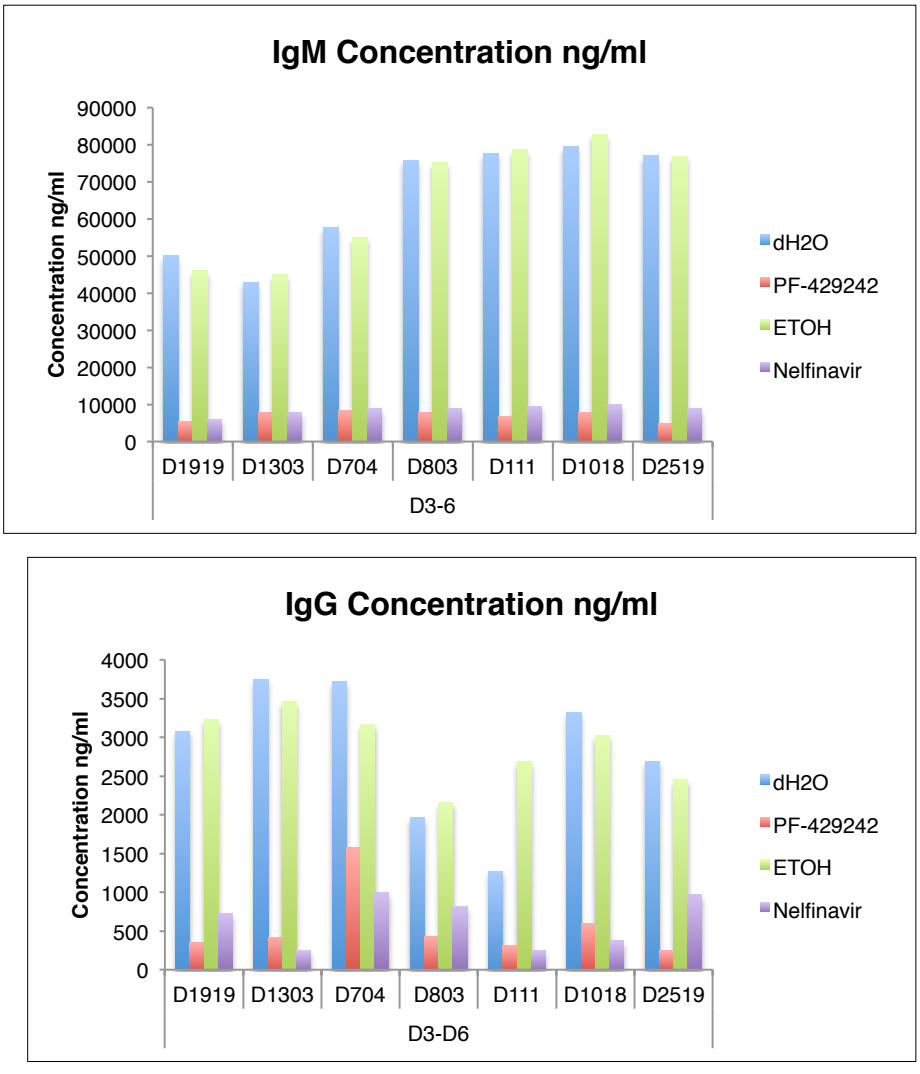


**Figure 6.29 Validating the impact of S1P inhibitor (PF-429242) and S2P inhibitor (Nelfinavir) on immunoglobulin secretion.** Day-3 B-cells from 7 human donors were treated with 10 μM PF-429242/dH2O or 10 μM Nelfinavir/Ethanol for 72 hours and analysed on Day-6. The supernatants were collected and the immunoglobulins (IgM and IgG) were quantified using ELISA.

### 6.5 Gene expression profile

The changes in the various characteristics described above suggest that inhibition of S1P or S2P might have a profound impact on the gene expression programs governing plasma cell differentiation or survival. While many of the pathways have been described, the full extent of the requirements for generating ASC populations is unknown. To determine the potential role that S1P/S2P-regulated pathways might play in this process, RNA samples were prepared from cells that had been treated from Day-3 for 72 hours with PF-429242, Nelfinavir or vehicle and processed for evaluation of global gene expression by microarray. Figure-6.30 depicts select genes that show greater than 1.4-fold difference in the conditions tested. Amongst these, genes such as *ALDOC* and *ABCA1* were downregulated by both inhibitors, but there were clear differences in the patterns of expression following the two types of treatment.

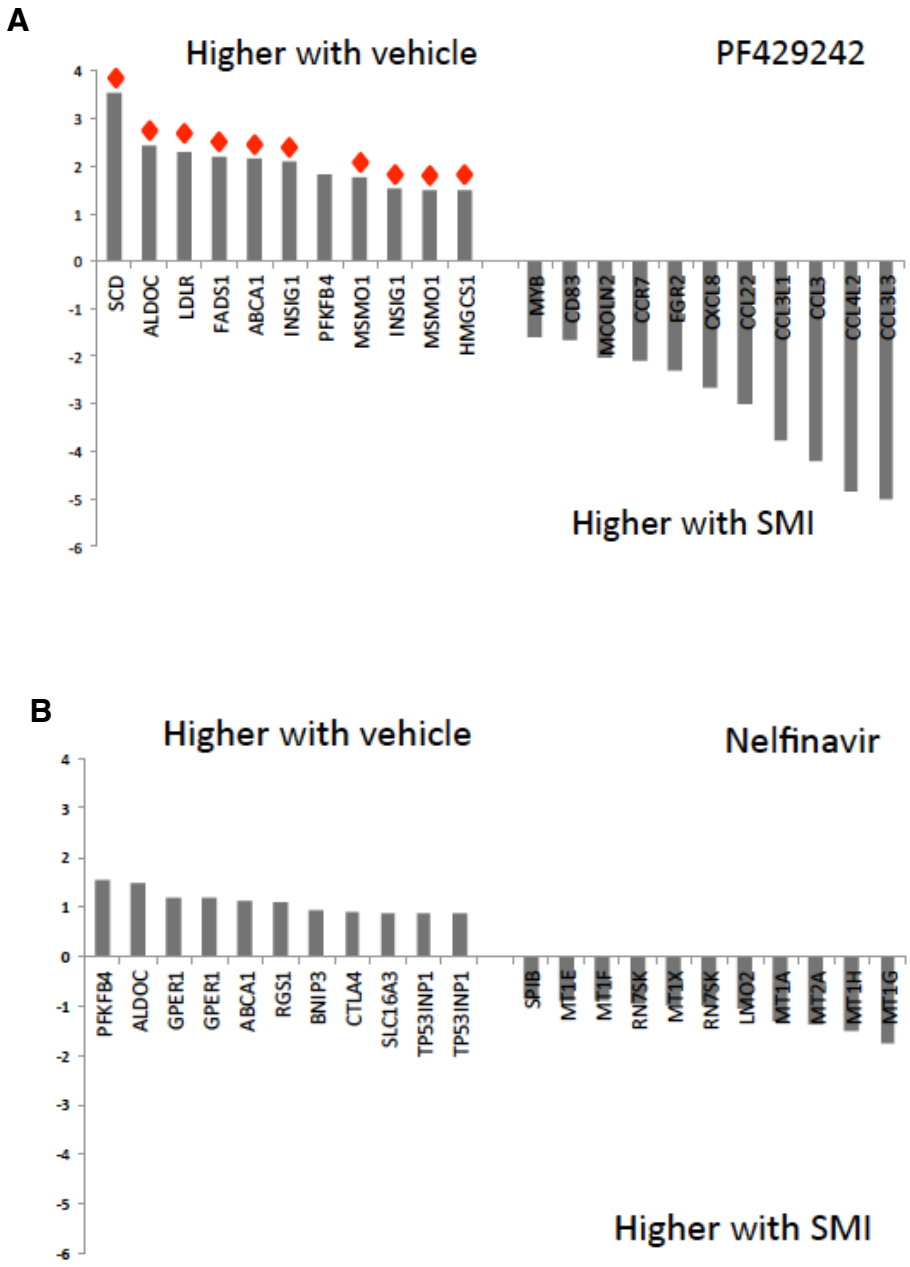


**Figure-6.30: Impact of S1P/S2P inhibition on plasmablast gene expression.** Day-3 B-cells from 3 donors were treated with (A) 10 μM PF-429242 or (B) Nelfinavir and analysed on Day-6 using Illumina bead arrays. Selected genes showing greater than 1.4-fold change in expression are depicted. The red diamonds indicate genes contributing to gene ontology terms in Figure-6.31.

To better understand the how the groups of genes might be impacting of ASC behaviour, gene signature and ontology analysis was performed using over 28,000 signatures (Figure-6.31). Remarkably, the signatures most significantly associated with the downregulated genes after PF-429242 treatment were related to SREBP and lipid metabolism, suggesting that a substantial proportion of the change in gene expression might be attributable to the loss of processed SREBP. The most prominent signature associated with downregulated genes in the Nelfinavir treated cells was hypoxia/HIF related and this was additionally observed in the PF-429242 samples.

**A**

Top 10 enriched signatures - Higher in vehicle vs PF

| Gene Signature | GeneSet | FDR |
|---|---|---|
| SREBP1a&2_up_Scap_dep | SignatureDB | 4.42E-16 |
| HALLMARK_MTORC1_SIGNALING | MSigDB_H | 1.80E-14 |
| Small molecule biosynthetic process | GeneOntology_BP | 1.80E-14 |
| GARY_CD5_TARGETS_UP | MSigDB_C2 | 2.17E-13 |
| Sterol metabolism | UniProt-Keyword | 9.43E-13 |
| HORTON_SREBF_TARGETS | MSigDB_C2 | 1.05E-12 |
| Cholesterol biosynthetic process | GeneOntology_BP | 2.26E-12 |
| SCHMIDT_POR_TARGETS_IN_LIMB_BUD_UP | MSigDB_C2 | 2.53E-12 |
| Lipid metabolism | UniProt-Keyword | 2.54E-12 |
| Sterol biosynthetic process | GeneOntology_BP | 5.01E-12 |

**B**

Top 10 enriched signatures - Higher in vehicle vs NEL

| Gene Signature | GeneSet | FDR |
|---|---|---|
| ELVIDGE_HIF1A_AND_HIF2A_TARGETS_DN | MSigDB_C2 | 0.00025843 |
| ELVIDGE_HIF1A_TARGETS_DN | MSigDB_C2 | 0.00025843 |
| FARDIN_HYPOXIA_11 | MSigDB_C2 | 0.00034742 |
| ELVIDGE_HYPOXIA_BY_DMOG_UP | MSigDB_C2 | 0.00042195 |
| ELVIDGE_HYPOXIA_UP | MSigDB_C2 | 0.00132249 |
| HALLMARK_HYPOXIA | MSigDB_H | 0.00200085 |
| WIERENGA_STAT5A_TARGETS_UP | MSigDB_C2 | 0.00350715 |
| MODULE_84 | MSigDB_C4 | 0.00457632 |
| Human Breast_Nuyten06_123genes_hypoxia ( | GeneSigDB | 0.00457632 |
| Human Breast_Chi06_123genes (16417408-Fi | GeneSigDB | 0.00532246 |

**Figure-6.31: Impact of S1P/S2P inhibition on plasmablast gene expression signatures.** Day 3 B-cells from 3 donors were treated with (A) 10 μM PF-429242 or (B) Nelfinavir and analysed on day 6 using Illumina bead arrays. Gene ontology/signature enrichment was evaluated using 28,000+ signatures and ontology terms. The terms highlighted in red are linked to the genes marked by red diamonds in Figure-6.30. Signature analysis conducted by Matthew Care.

An integrated signature enrichment analysis revealed several additional ontology terms of interest (Figure-6.32). Inhibition of S1P in differentiating B-cells also affected serine/AA synthesis, fatty acid metabolism, mTOR signalling and targets associated with regulation by IRF4. Collectively, these results suggest that inhibition of S1P/S2P results in a substantial change in genes associated with metabolic process that are likely to explain the loss of cell function and viability.

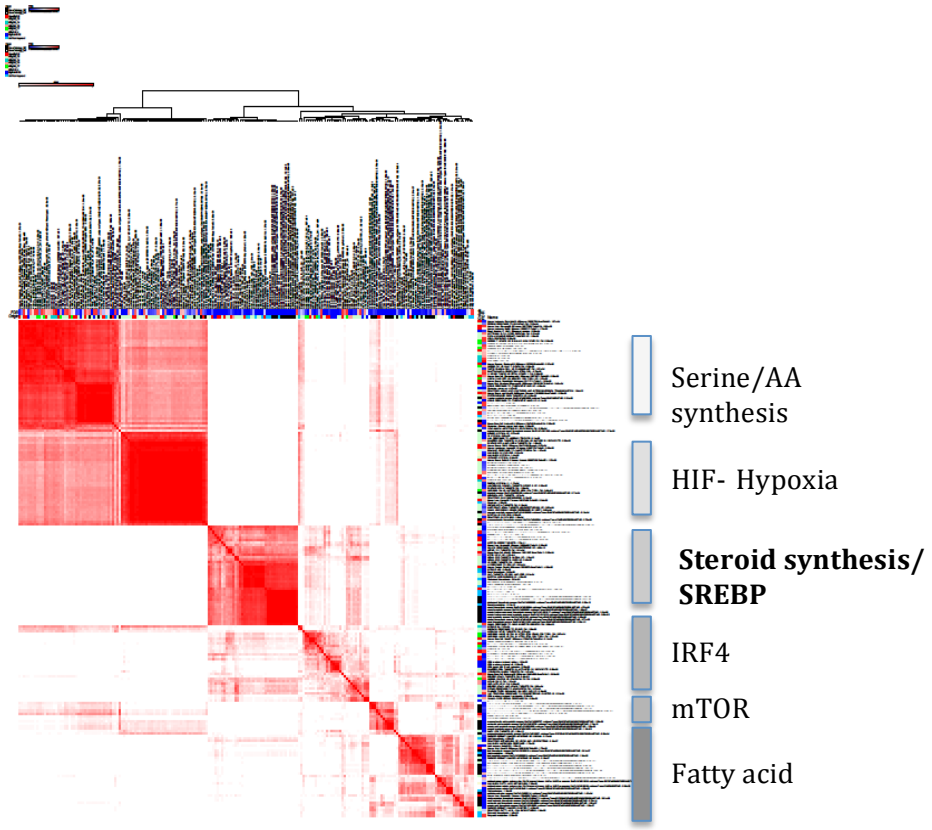


**Figure-6.32: Hierarchical clustering of gene signature and ontology terms enriched amongst genes downregulated in PF-429242 treated plasmablasts**. Enrichment of gene signatures was determined using a hypergeometric test against a curated set of 28,000+ signatures and ontology term associations. Enriched signatures and ontologies were clustered according to genes contributing to enrichment, and summary labels are shown on the right. Analysis conducted by Matthew Care.

### 6.5.1 SREBP-1 (Sterol Regulatory Element Binding Protein-1)

Based on the gene expression profile results, SREBP-1 was one of the most highly differentially expressed and affected by PF-429242. Therefore, it was further investigated. Two antibodies (a rabbit polyclonal and mouse monoclonal) were tested revealing that the monoclonal recognised specific bands of the appropriate molecular weight for both the full length and the processed form of SREBP-1 whereas, the rabbit SREBP-1 antibody had many non-specific interactions (Figure 6.33).

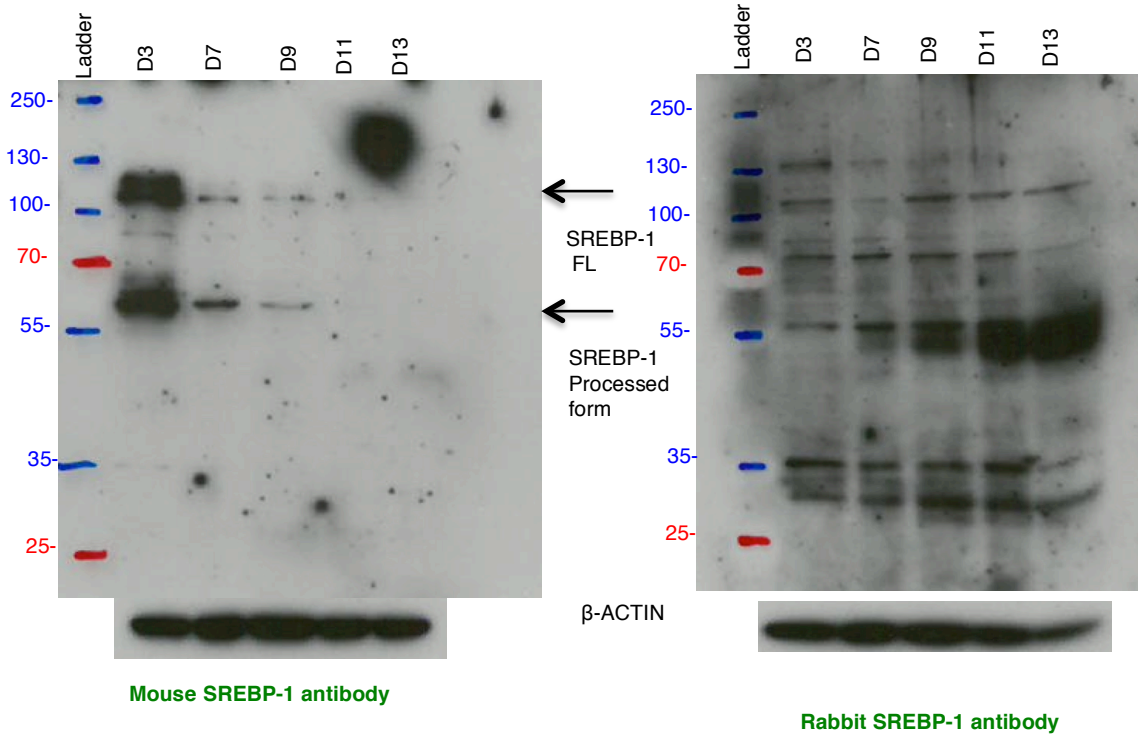


**Figure 6.33 Evaluation of SREBP-1 antibodies.** Two commercially available antibodies against SREBP-1 were tested on lysates from human differentiated B-cells and ASCs Day-3, -7, -9, -11 and -13 using Western blotting.

Thus, the mouse monoclonal SREBP-1 antibody was used to study protein expression in cells treated with PF-429242 and Nelfinavir for 12 hours from Day-3 to Day-6 (total of 72 hours) (Figure 6.34). The results showed that SREBP-1 inhibition started 36 hours post treatment with PF-429242 and Nelfinavir and continued until 72 hours. The degree of inhibition of SREBP-1 by PF-429242 is much greater than Nelfinavir.

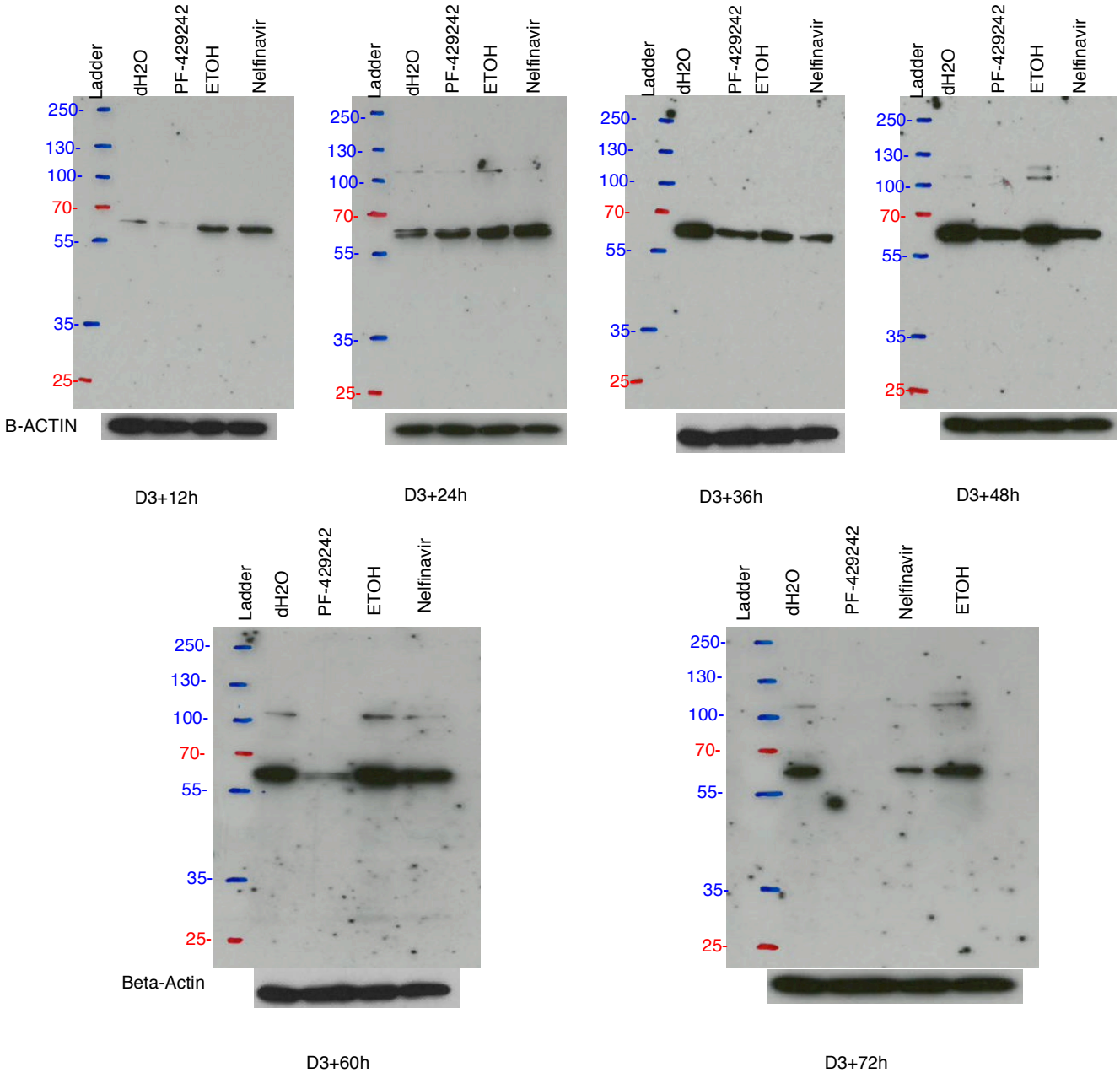


**Figure 6.34 The impact of S1P and S2P inhibitors on SREBP-1 protein expression.** The cells were treated with 10 μM PF-429242/dH2O or 10 μM Nelfinavir/Ethanol from Day-3 and collected every 12 hours to examine the impact of the inhibitors on SREBP-1 protein expression.

### 6.5.2 CD40L Expression

The gene expression profile results showed that *CD40L* is expressed upon PF-429242 treatment (data not shown). Therefore, surface CD40L expression was examined on differentiating human B-cells from 3 donors after treating Day-3 cells with PF-429242/dH2O or Nelfinavir/Ethanol for 12 hours until Day-6. At each time point, cells were collected and stained for CD154 (CD40L) and CD20 and the phenotype was checked using flow cytometry (Figure 6.35). The flow cytometry plots show that CD40L expression is enhanced upon PF-429242 treatment on Day3+60 hours and Day3+72 hours compared to the control (dH2O), suggesting that CREB3L2 has an inhibitory impact on CD40L expression.

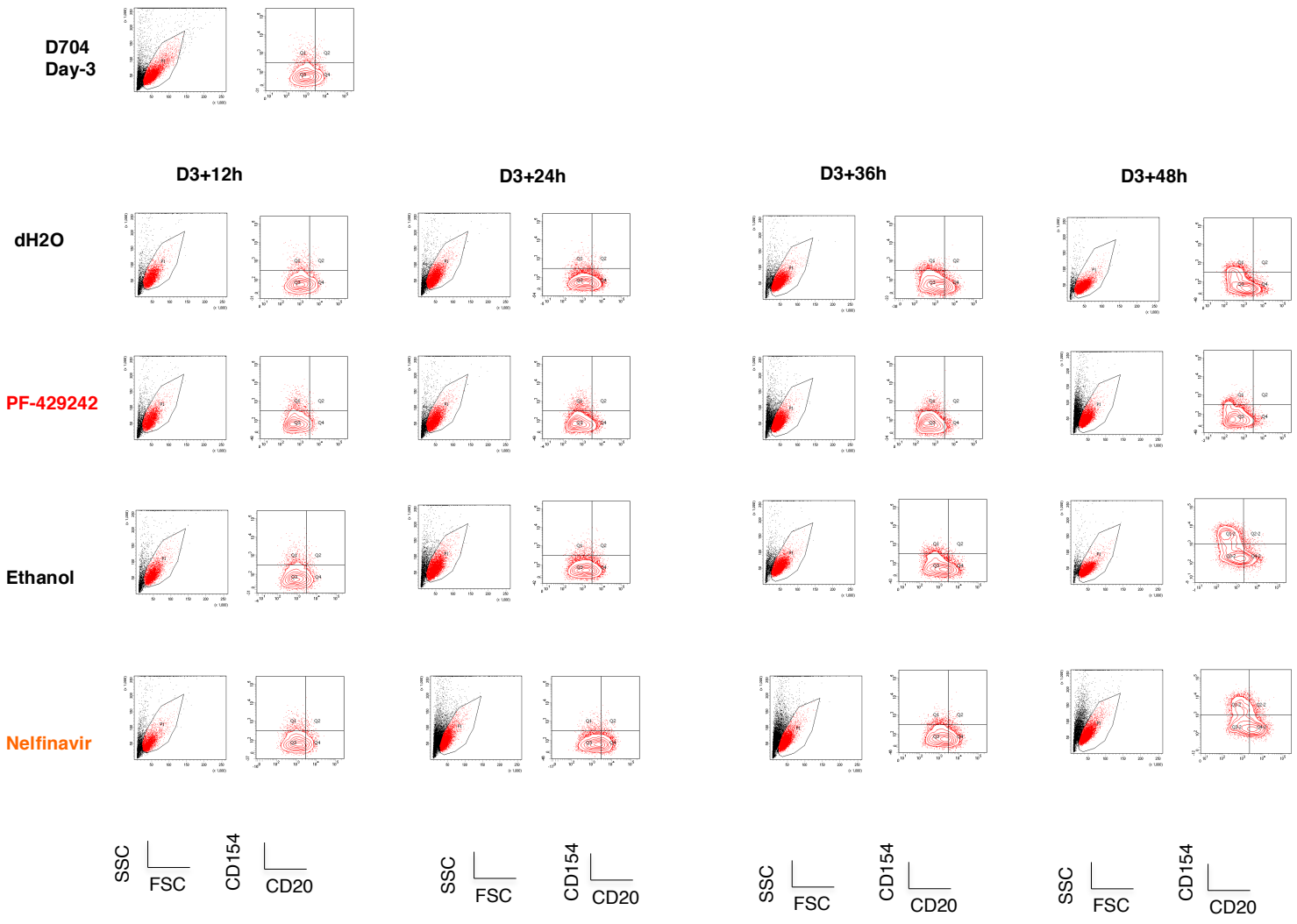

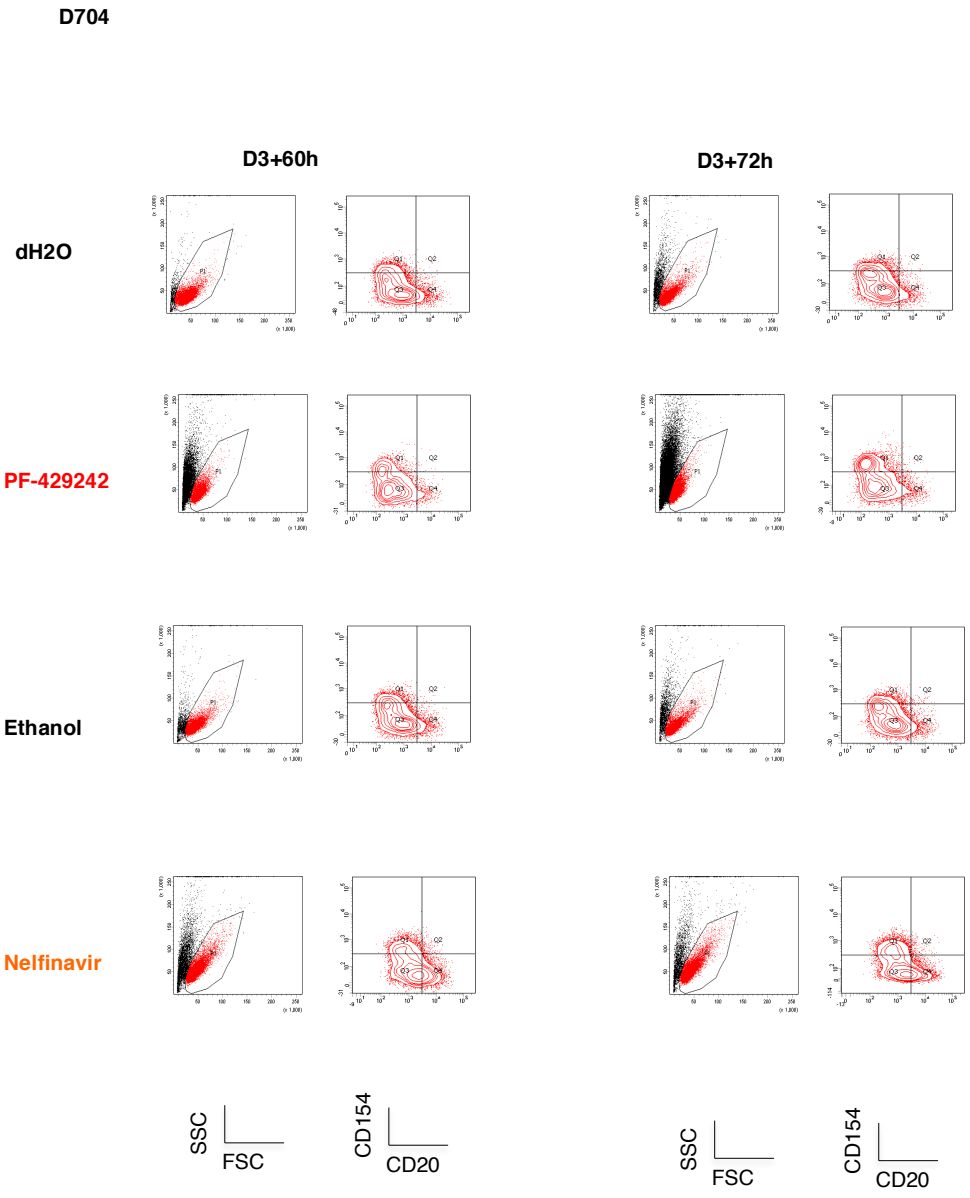
D704
D3+60h
D3+72h
dH2O
PF-429242
Ethanol
Nelfinavir
SSC
FSC
CD154
CD20
SSC
FSC
CD154
CD20

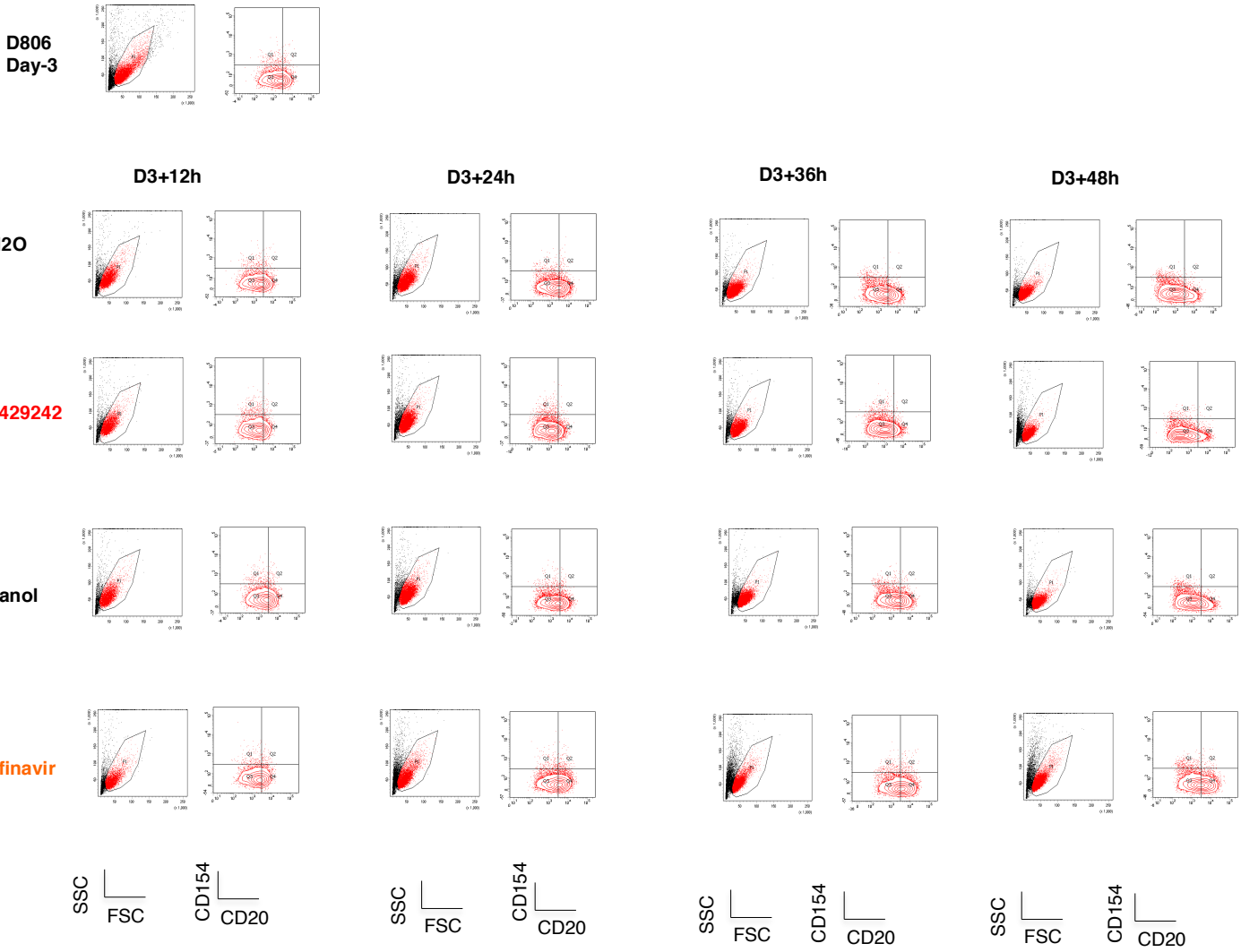
D806
Day-3
D3+12h
D3+24h
D3+36h
D3+48h
dH2O
PF-429242
Ethanol
Nelfinavir
SSC
FSC
CD154
CD20

**D806**

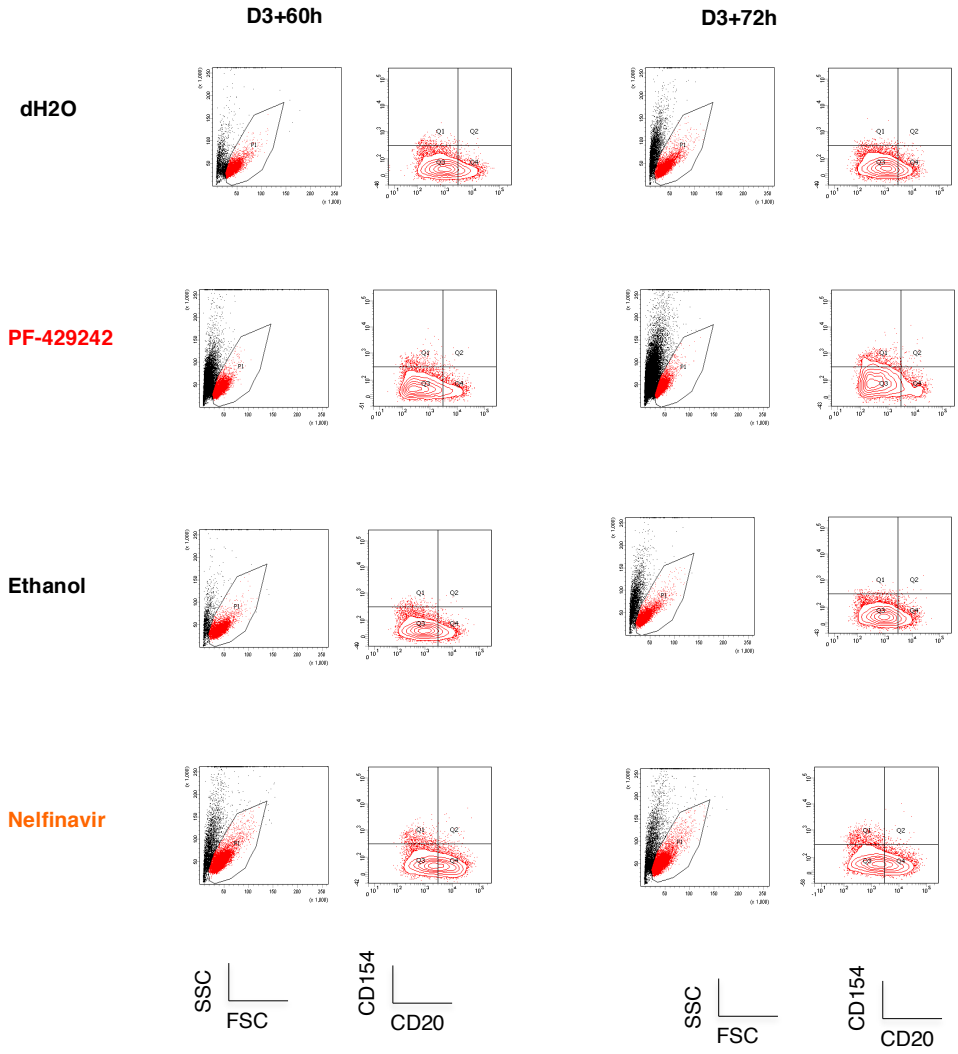
D3+60h
D3+72h
dH2O
PF-429242
Ethanol
Nelfinavir
SSC
FSC
CD154
CD20
SSC
FSC
CD154
CD20

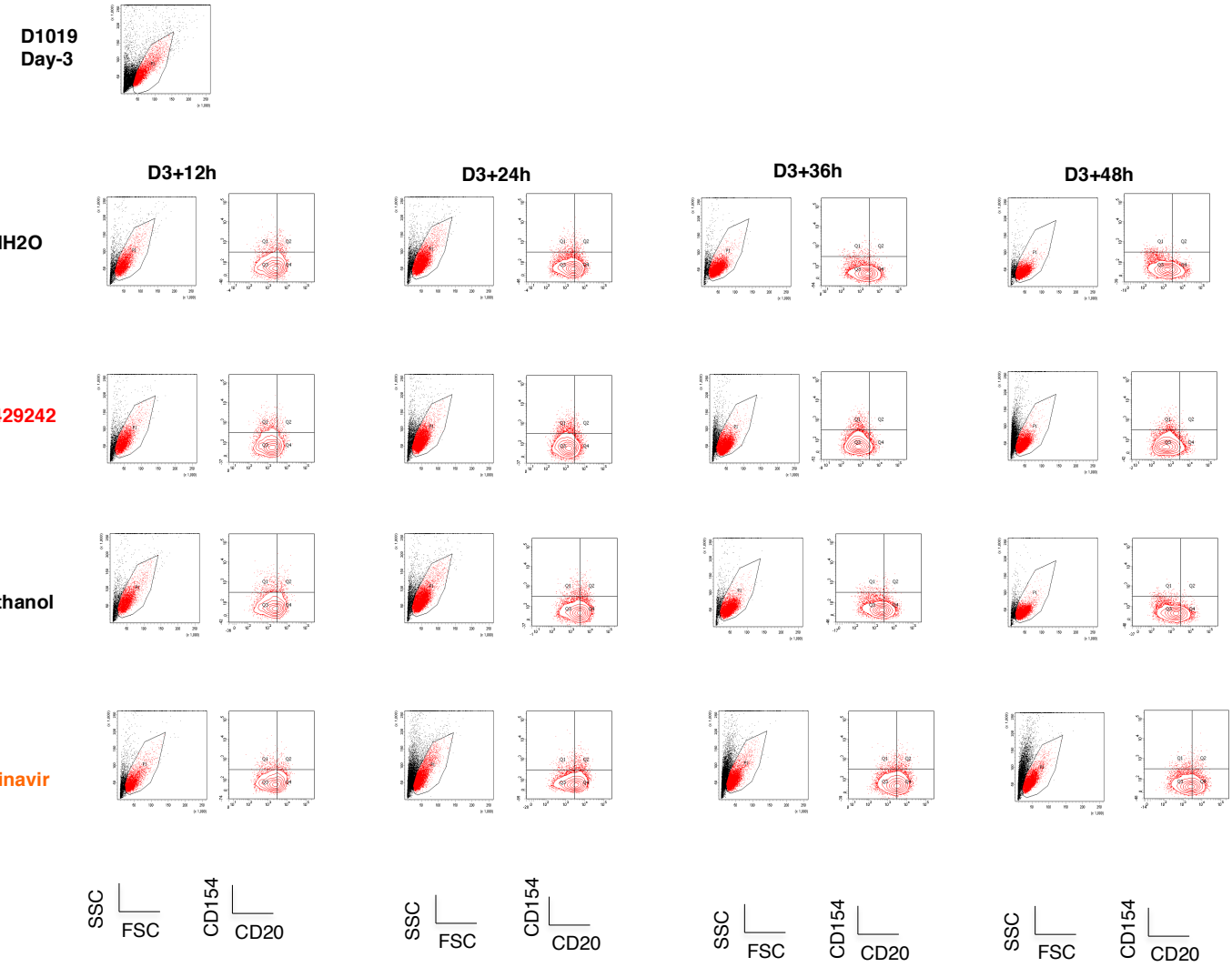
D1019
Day-3
D3+12h
D3+24h
D3+36h
D3+48h
dH2O
PF-429242
Ethanol
Nelfinavir
SSC
FSC
CD154
CD20

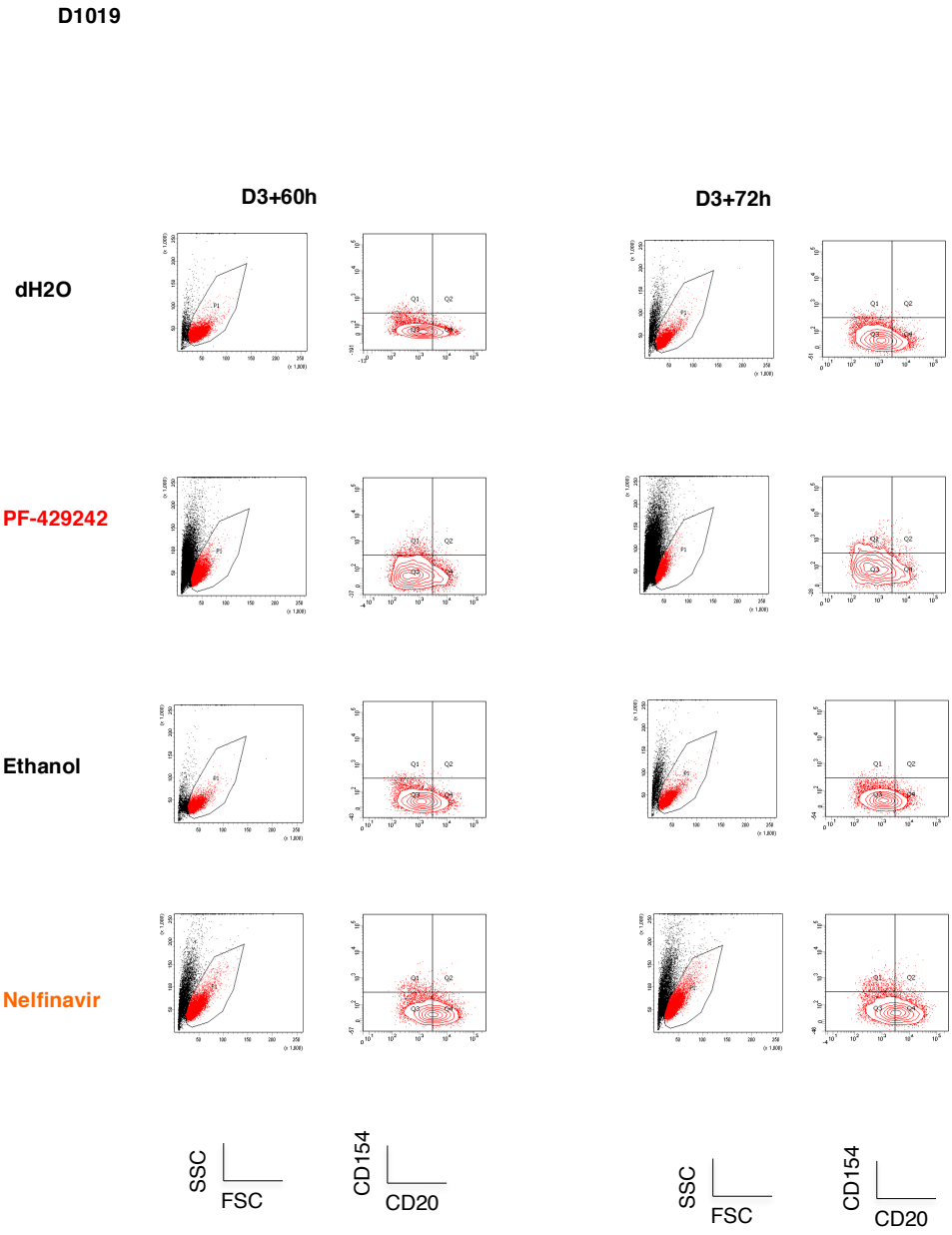


**Figure 6.35 The impact of PF-429242 and Nelfinavir on CD40L expression on differentiating human B-cells.** Human activated B-cells (Day-3) cells from 3 donors were treated with 10 μM PF-429242/dH2O or 10 μM Nelfinavir/Ethanol for 12-hour intervals up to Day-6. At each time point, the cells were collected and stained for CD154 (CD40L) and CD20 (B-cells).

### 6.6 A The impact of S1P and S2P inhibitors on human plasma cells (Day-13)

The impact of S1P and S2P inhibitors on the initial stages of plasma cell differentiation encompassing the activated B-cell stage (Day-3) to plasmablast stage (Day-6) have been evaluated and validated in (6.1-6.4). Initial experiments also examined the effect of the inhibitors during the transition from plasmablast (Day-6) to plasma cell (Day-13). Neither PF-429242 nor Nelfinavir affected the cell viability of ASCs when treated after Day-5, but multiple aspects of cell biology are affected when the cells treatment start from Day-3 where the expression of CREB3L2 begins.

Since CREB3L2 is highly expressed in human plasma cells (Day-13) as shown in Chapter-4 it was of interest to determine the longer-term effects of reducing CREB3L2 along with other affected transcription factors. Thus, the impact of S1P and S2P inhibitors on human plasma cells was evaluated by treating the cells starting from Day-3, re-treating the cells on Day-6 and then evaluating on Day-13 (which is plasma cell stage) for cell count (Figure 6.36), cell phenotype (Figure 6.37) and IgM and IgG levels (Figure 6.38).

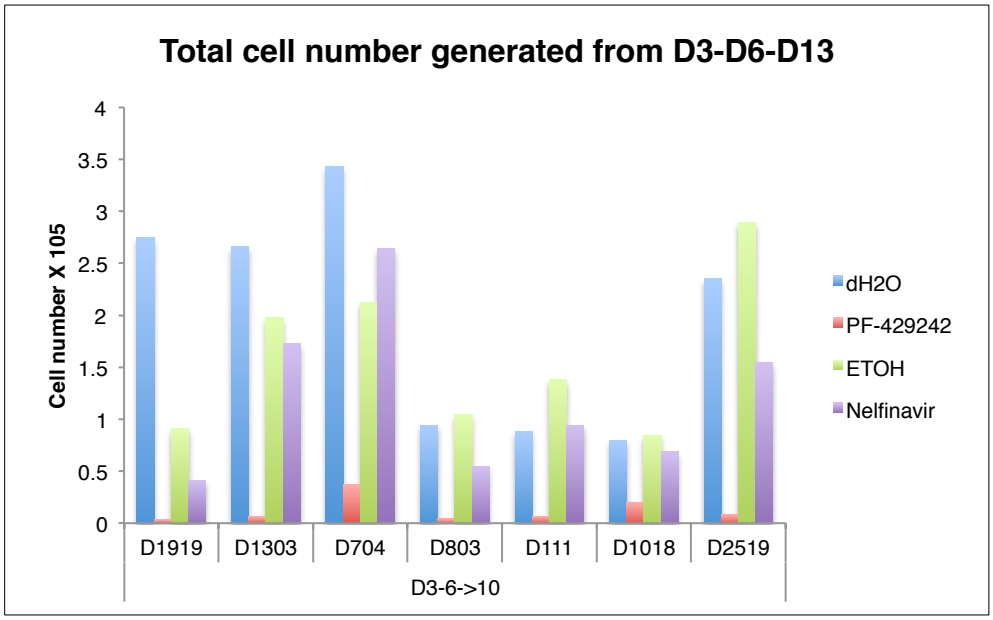


**Figure 6.36 The impact of S1P inhibitor (PF-429242) and S2P inhibitor (Nelfinavir) on plasma cell number.** Human activated B-cells (Day-3) from 7 donors were treated with 10 μM PF-429242/dH2O or 10 μM Nelfinavir/Ethanol for 72 hours. On Day-6, the cells were re-treated with the inhibitors and incubated up to Day-13. After the culture period the cells were enumerated using CountBright™ absolute counting.

The total cell number on Day-13 from the 7 donors generated from Day-3 and Day-6 treatment, showed around 90% reduction in cell number of PF-429242 treated samples whereas, the impact of Nelfinavir varied from donor to donor.

In addition, the cell phenotype of Day-13 cells was examined revealing minimal change in phenotype compared with the control (dH2O and Ethanol), in the Nelfinavir treated cells (Figure 6.35). Although treatment with PF-429242 severely diminished cell viability, some cells with a phenotype consistent with plasma cells ($CD38^{hi}$ CD138+) did emerge. In addition, according to the MFI values, it appears that PF-429242 treatment can promote plasma cell differentiation (Figure-6.52).

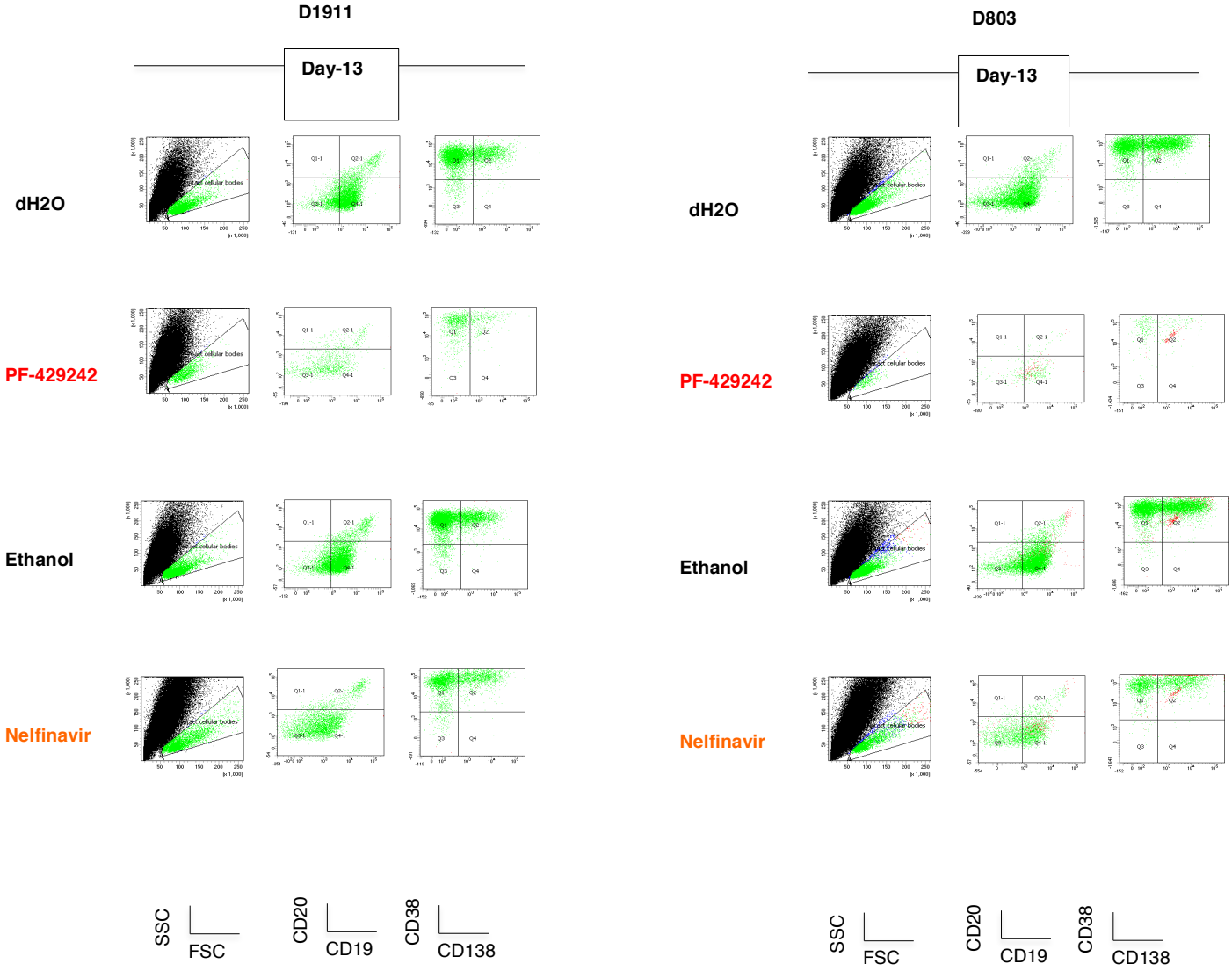
D1911
Day-13
dH2O
PF-429242
Ethanol
Nelfinavir
SSC
FSC
CD20
CD19
CD38
CD138
D803
Day-13
dH2O
PF-429242
Ethanol
Nelfinavir
SSC
FSC
CD20
CD19
CD38
CD138

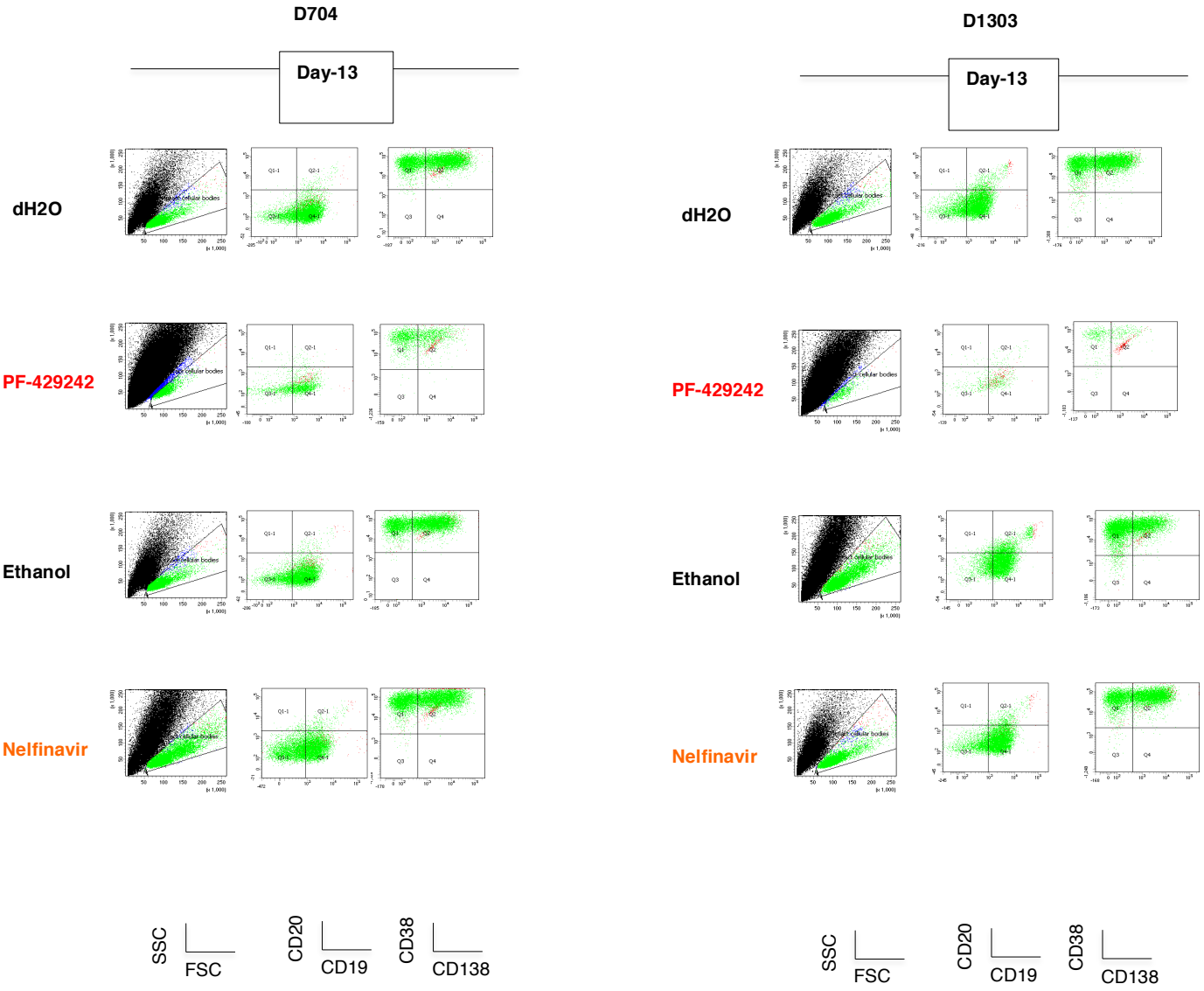
D704
Day-13
dH2O
PF-429242
Ethanol
Nelfinavir
SSC
FSC
CD20
CD19
CD38
CD138
D1303
Day-13
dH2O
PF-429242
Ethanol
Nelfinavir
SSC
FSC
CD20
CD19
CD38
CD138

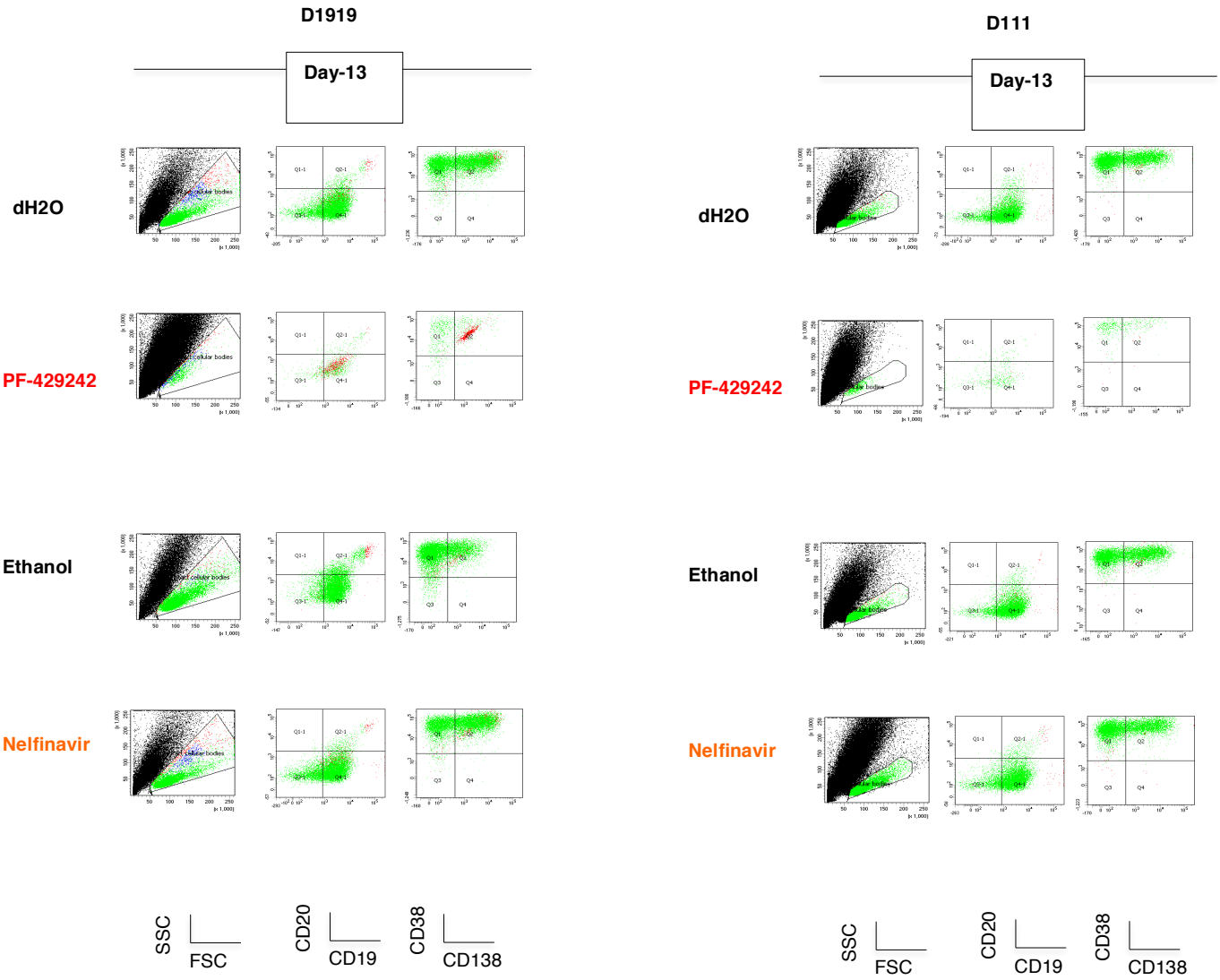
D1919
Day-13
dH2O
PF-429242
Ethanol
Nelfinavir
SSC
FSC
CD20
CD19
CD38
CD138
D111
Day-13
dH2O
PF-429242
Ethanol
Nelfinavir
SSC
FSC
CD20
CD19
CD38
CD138

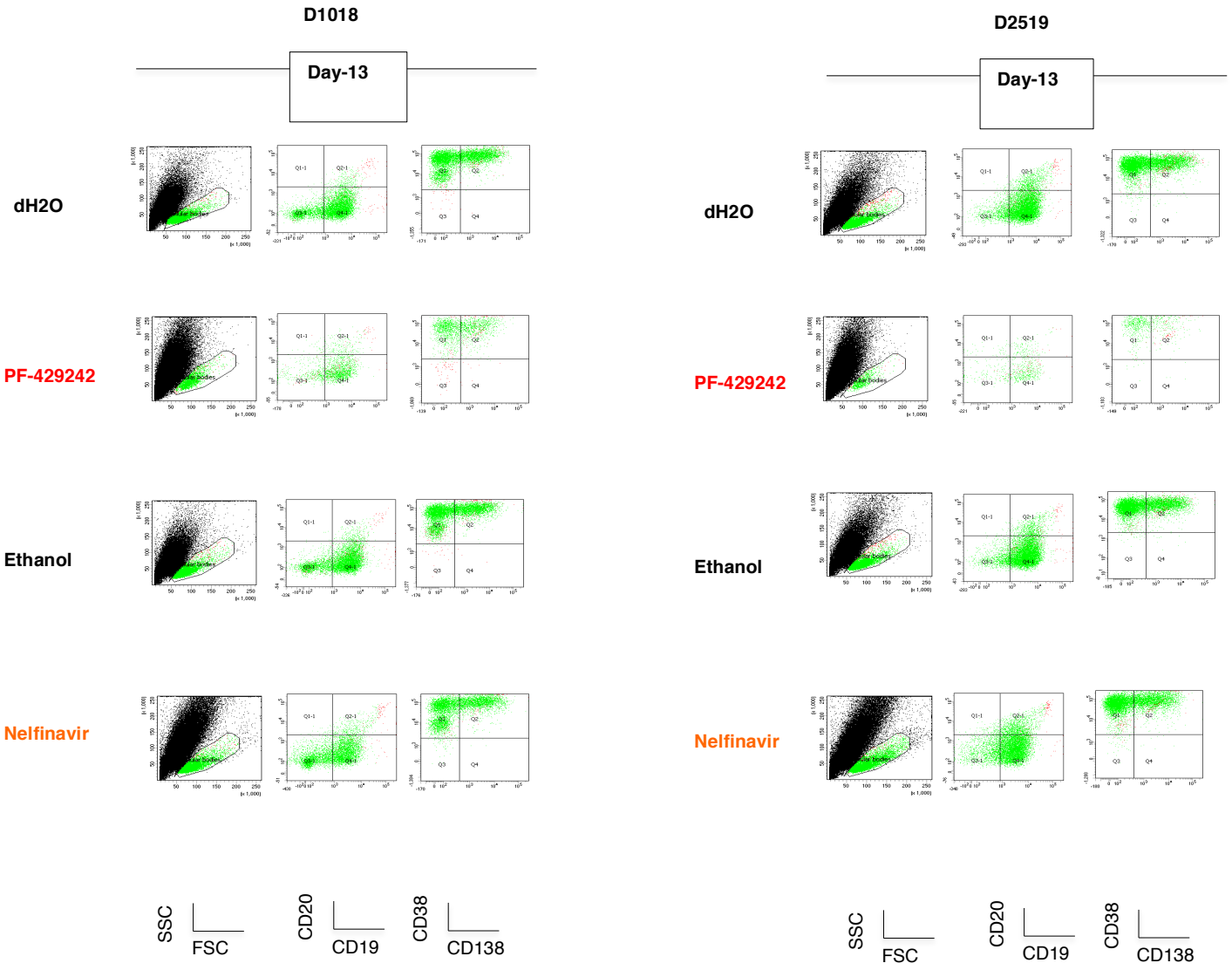


**Figure 6.37 The impact of S1P inhibitor (PF-429242) and S2P inhibitor (Nelfinavir) on plasma cell phenotype.** Human activated B-cells from 8 donors (Day-3) were treated with 10 μM PF-429242/dH2O or 10 μM Nelfinavir/Ethanol for 72 hours. On Day-6, the cells were re-treated with the inhibitors and incubated up to Day-13. After culture, the cells were stained for CD19, CD20, CD38 and CD138 and analysed by flow cytometry.

To provide further evidence that inhibition of S1P/S2P might have a lasting effect on plasma cell function, tissue culture supernatants were harvested to evaluate the levels of secreted immunoglobulin. As expected, treatment with PF-429242 almost completely abrogated the production of antibody (Figure 6.38). In contrast to the relatively modest effect on cell number and phenotype, Nelfinavir had a more pronounced effect on Ig secretion, particularly IgG.

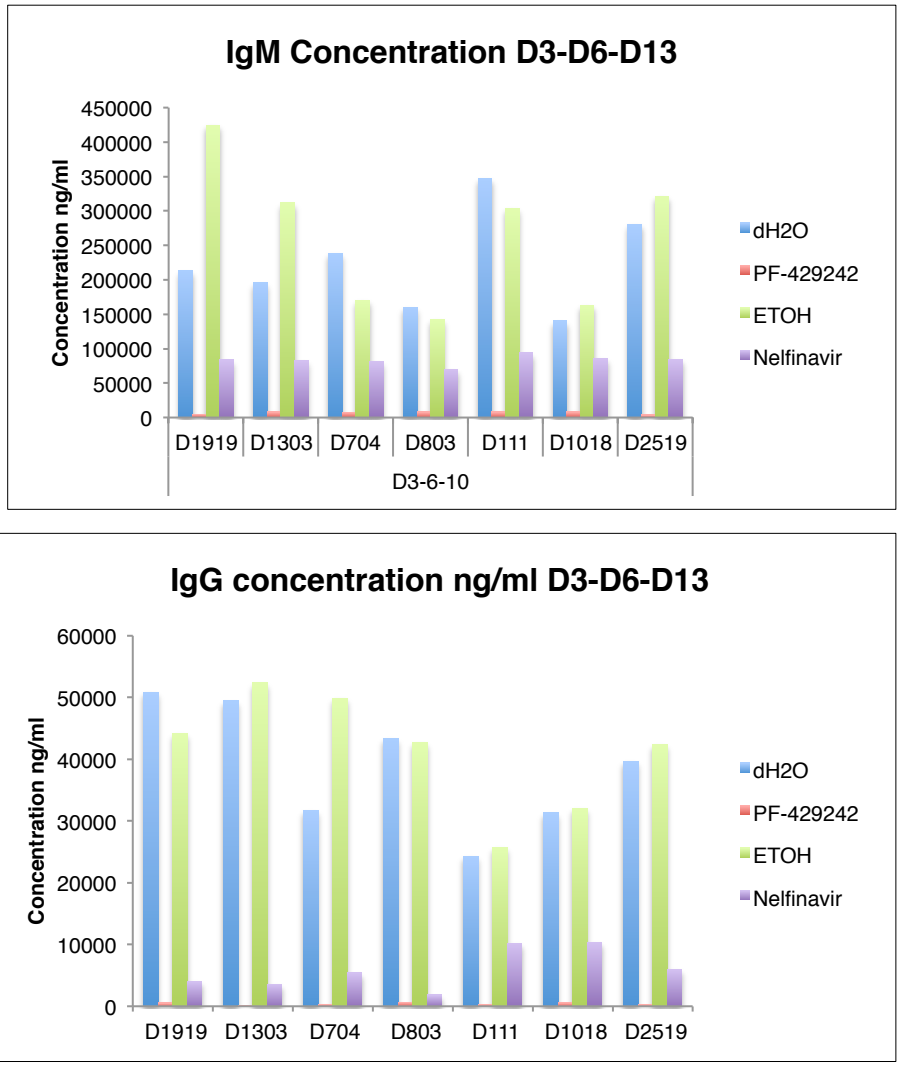


**Figure 6.38 The impact of S1P inhibitor (10 μM PF-429242) and S2P inhibitor (10 μM Nelfinavir) on plasma cell secretion.** Human activated B-cells (Day-3) (7 donors) were treated with 10 μM PF-429242/dH2O or 10 μM Nelfinavir/Ethanol for 72 hours. On Day-6, the cells were re-treated with the inhibitors and incubated up to Day-13. After culture, the supernatants were collected and IgM and IgG were quantified using ELISA.

## 6.6 B The impact of transient application of S1P and S2P inhibitors on human ASCs

PF-429242 and Nelfinavir had an inhibitory affect on the cleavage and processing of the UPR elements CREB3L2, XBP1s and ATF6, which was accompanied by a change in the biological characteristics of the differentiating populations. Since both drugs act as reversible, competitive inhibitors, it may be that cells cultured after transient exposure may re-express the relevant factors and regain some functionality. Therefore, to examine whether the inhibitory affect can be rescued cells were treated on Day-3 with PF-429242 or Nelfinavir for 72 hours. After the incubation, the cells were re-seeded with the Day-6 standard condition (IMDM/10%FCS, amino acids, Il-6, Il-21, TX-HYB, lipids) and analysed on Day-13 for cell count (Figure 6.39) and cell phenotype (Figure 6.40). The results validated the inhibitor effect of PF-429242 and Nelfinavir on Day-6 antibody secretory cells. In addition, the results show that the inhibitory effect of PF-429242 is not fully rescued even if the cells are provided with the necessary mix of cytokines required to support differentiation (without the PF-429242). However, the inhibitor effect of Nelfinavir can be rescued, generating cells that had grown normally in count and phenotype compared to the control (Ethanol) (Figure 6.36 and 6.37). These results enhance the importance of PF-429242 as a potential therapeutic drug for B-cell and ASC disorders.

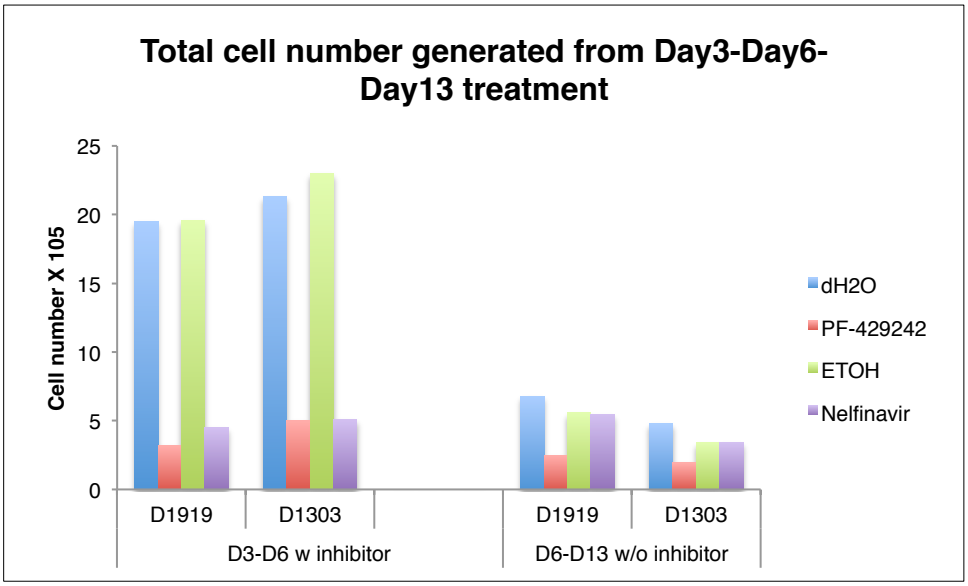


**Figure 6.39 The impact of transient S1P inhibitor (PF-429242) and S2P inhibitor (Nelfinavir) on ASC number.** Human activated B-cells (Day-3) from 2 donors were treated with 10 μM PF-429242/dH2O or 10 μM Nelfinavir/Ethanol for 72 hours. On Day-6, the cells were re-seeded with the Day-6 standard condition (without the inhibitors) and incubated up to Day-13 to examine the possible rescue levels. On Day-13, the cells were collected and counted using CountBright™ beads.

In the previous experiment (Figure 6.37) PF-429242 had affected plasma cell phenotype by increasing CD138 expression compared to the control (dH2O) and this was also observed after attempted rescue (Figure 6.40). However, Nelfinavir had less of an impact on plasma cell phenotype consistent with the restoration of cell count in the presence of appropriate nutrients.

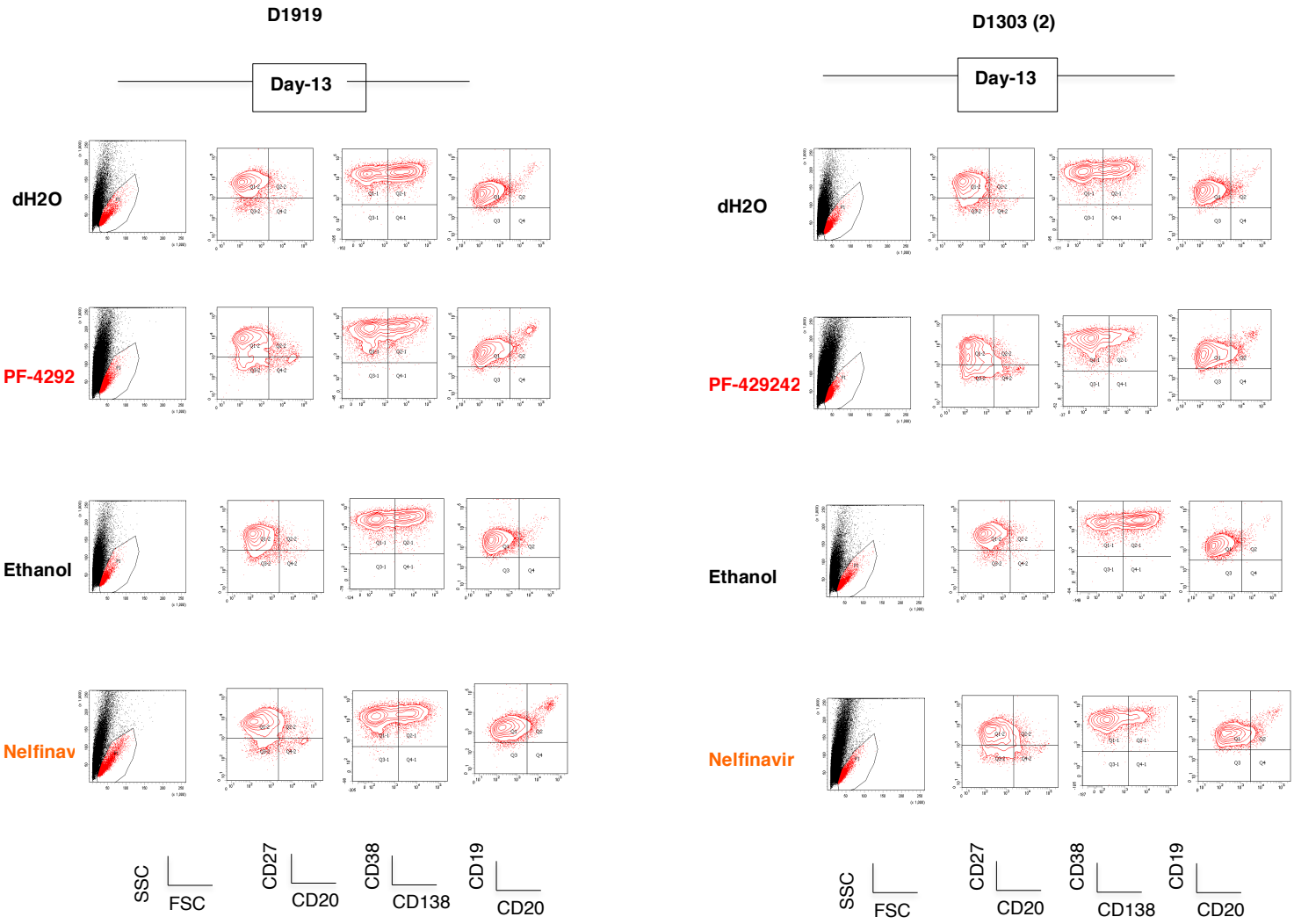


**Figure 6.40 The impact of transient S1P inhibitor (PF-429242) and S2P inhibitor (Nelfinavir) on plasma cell phenotype.** Human activated B-cells from 2 donors (Day-3) were treated with 10 μM PF-429242/dH2O or 10 μM Nelfinavir/Ethanol for 72 hours. On Day-6, the cells were re-seeded with Day-6 standard conditions (without the inhibitors) and incubated up to Day-13. After incubation, the cells were stained for CD19, CD20, CD38, CD138 and CD27 and evaluated by flow cytometry.

## 6.7 Testing the impact of S1P and S2P inhibitors on B cell proliferation (Day-3 to Day-6)

The experiments detailed above have indicated that treatment with S1P/S2P inhibitors has a marked impact on cell number. A body of evidence suggests that the ability to differentiate to an ASC is increased as the cells divide (16). CFSE (CarboxyFluorescein Succinimidyl Ester) is a dye used to track cell proliferation and the formation of the multiple generations by flow cytometry. To determine whether the inhibitors altered the proliferative capacity of differentiating B-cells, 24 hours post isolation the cells from three donors were labelled with 5mM CFSE. 24hours later, the staining was assessed compared to a negative control (Day-0). On Day-3, the cell proliferation was checked and then cultures treated with 10 µM PF-429242/dH2O or 10 µM Nelfinavir/Ethanol and incubated for 72 hours. After the incubation, the cells were collected and analysed for the CFSE using flow cytometry (Figure 6.41). The results revealed that PF-429242 and Nelfinavir treatment delayed the proliferation compared to the controls (dH2O and Ethanol, respectively). Despite that, the formation of the multiple generations was not clear due to the rapid division. Therefore, to improve the resolution of generations, CFSE has to be evaluated in a shorter time point between Day-3 and Day-6.

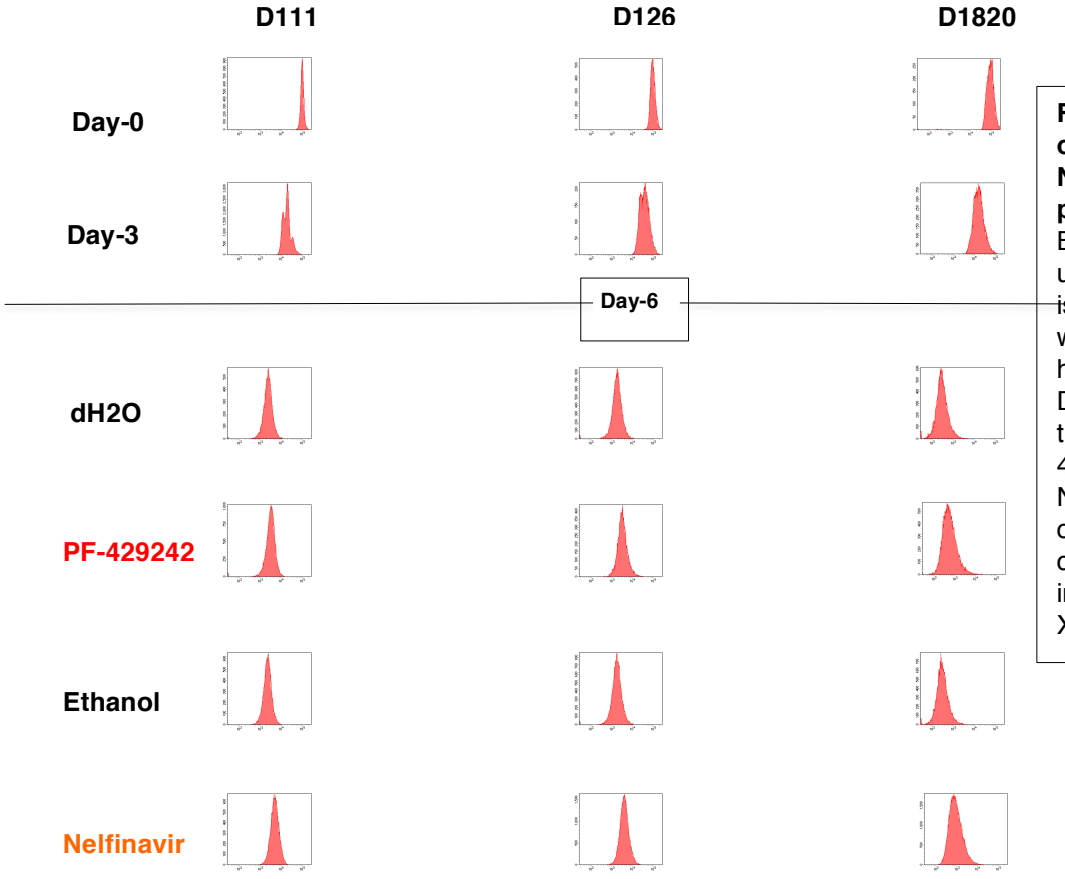


**Figure 6.41 The impact of PF-429242 and Nelfinavir on cell proliferation.** Human B-cells were isolated using the memory B-cell isolation kit and labelled with 5mM CFSE 24 hours post isolation. Day-3 B-cells were treated with 10 µM PF-429242 and 10 µM Nelfinavir and analysed on Day-6 using flow cytometry. CFSE intensity appears on the X-axis of each plot.

## 6.8 Evaluation of the role of autophagy in response to PF-429242 and Nelfinavir

Autophagy is a lysosomal degradation process initiated by forming an autophagosome that fuses with endolysosmal vesicles leading to degradation of the contents. It occurs in response to nutrient starvation and accumulation of unfolded protein in the ER. In addition, it may occur during differentiation, development, infections and cancer. There are three known autophagy processes; chaperone mediated autophagy (CMA), macro- and microautophagy (1). CMA has only been described in mammals whereas micro and macroautophagy have been detected in plant, fungi and mammals. Autophagy is controlled by number of autophagy-related genes (Atg proteins) (Figure 6.42). The process starts with the membrane nucleation, which requires Atg6 and PI3K followed by an elongation step. The membrane elongation requires two ubiquitin-like conjugation systems; Atg8-PE (LC3-II) and Atg5-Atg12 thus, forming the autophagosome that fuse with the lysosome to form the autophagolysosome hence its degradation. The membrane elongation causes the conversion of LC3 (Light Chain 3 known as Atg8 in fungi) from LC3I to LC3II, which is used as a marker for autophagy (1).

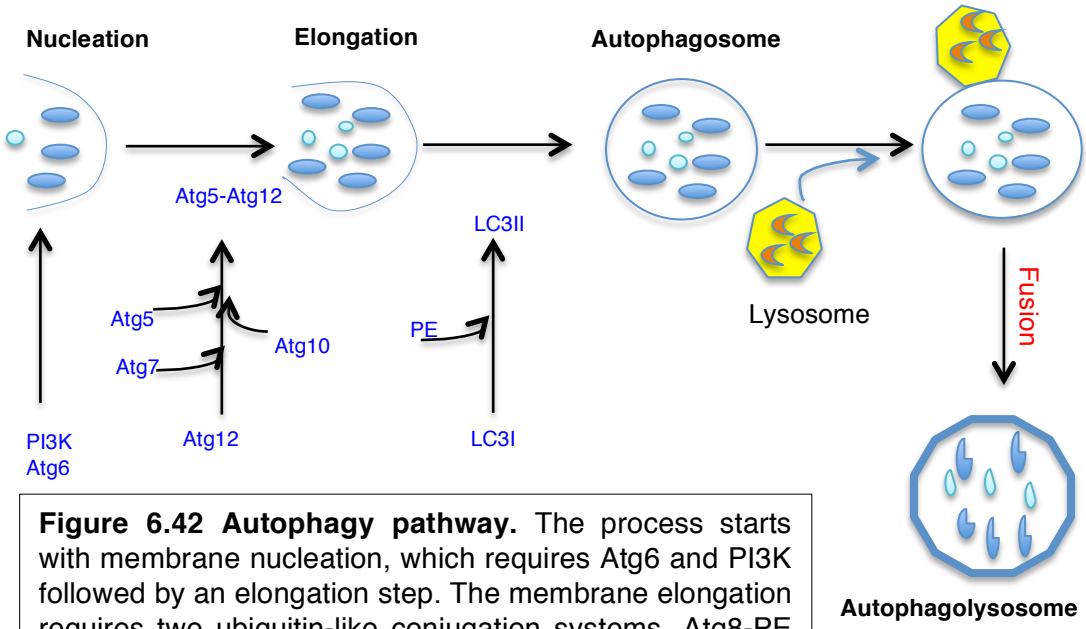


**Figure 6.42 Autophagy pathway.** The process starts with membrane nucleation, which requires Atg6 and PI3K followed by an elongation step. The membrane elongation requires two ubiquitin-like conjugation systems, Atg8-PE (LC3-II) and Atg5-Atg12, which form the autophagosome that fuses with the endosome and lysosome to generate an autolysosome that is subsequently degraded (1).

The accumulation of mis-folded proteins in the ER increases the ER load and folding capacity leading to ER-stress. The UPR is a mechanism by which prokaryotic and eukaryotic cells attempt to resolve ER-stress. A component of the UPR includes proteasome-mediated degradation of mis-folded proteins. If the level of mis-folded proteins exceeds the proteasome capacity, autophagy will be trigged. In addition, it has been shown by Ogata et al. that autophagy inhibits cell death mediated by ER-stressors (tunicomycin or thapsigargin) (119). Thus, autophagy can be considered a mechanism that promotes cell survival by removing the aggregates that form due to ER-stress (120).

Although autophagy has been proposed to act in a positive fashion to preserve optimal secretory activity in plasma cells, failure to restrict the level of autophagy may lead to cell death. To determine whether the failure to increase cell numbers in human differentiating B-cells treated with S1P and S2P inhibitors was related to autophagy, protein samples were examined for LC3I/LC3II by Western blotting. LC3 is the mammalian homologue to Atg and is considered to be the most reliable marker for autophagosome detection and monitoring autophagy (1). The results show that PF-429242 treatment was associated with enhanced autophagy due to the conversion of LC3I to LC3II compared to the control (dH2O), whereas, the other autophagy markers did not show any conclusive results. On the other hand, Nelfinavir did not show any changes (Figure 6.43).

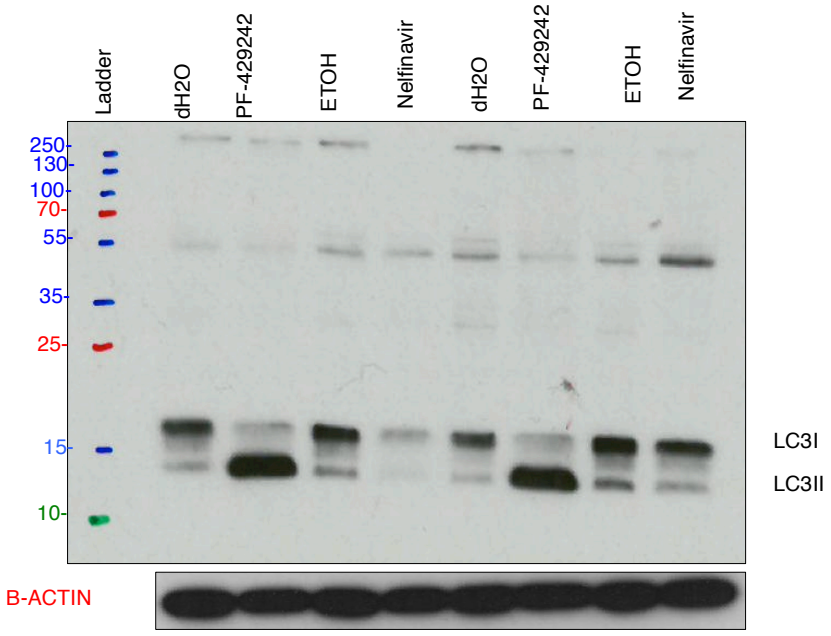


**Figure 6.43 Investigation of the impact of PF-429242 and Nelfinavir on autophagy.** Day-3 human activated B-cells were treated with 10 µM PF-429242 or 10 µM Nelfinavir and incubated for 72 hours then analysed on Day-6 for autophagy using markers ATG7, ATG3 (not shown) and LC-III.

## 6.9 Detailed kinetic analysis of the effect of S1P and S2P inhibition during the transition between activated B-cell and plasmablast stage

Human differentiated B-cells (Day-3) treated with PF-429242/dH2O and Nelfinavir/Ethanol for 72 hours have been assessed by multiple parameters, including evaluation by microarray to check their impact on gene expression. While this assessment provided an insight into the changes that occurred at the time when the cells had reached a relatively homogeneous stage in differentiation, it was of interest to determine how inhibition of S1P/S2P was affecting the cells as they progressed through this phase. Thus, Day-3 B-cells were treated with PF-429242/dH2O and Nelfinavir/Ethanol for a series of shorter time points. Samples were collected every 12 hours from Day-3 until Day-6 for protein expression by Western blotting, RNA samples for expression profiling, cell count using CountBright ™ absolute counting (C36950, Life technology), cell phenotype for CD19, CD20, CD38 and CD138 and supernatant for IgM and IgG quantification (Figure 6.44).

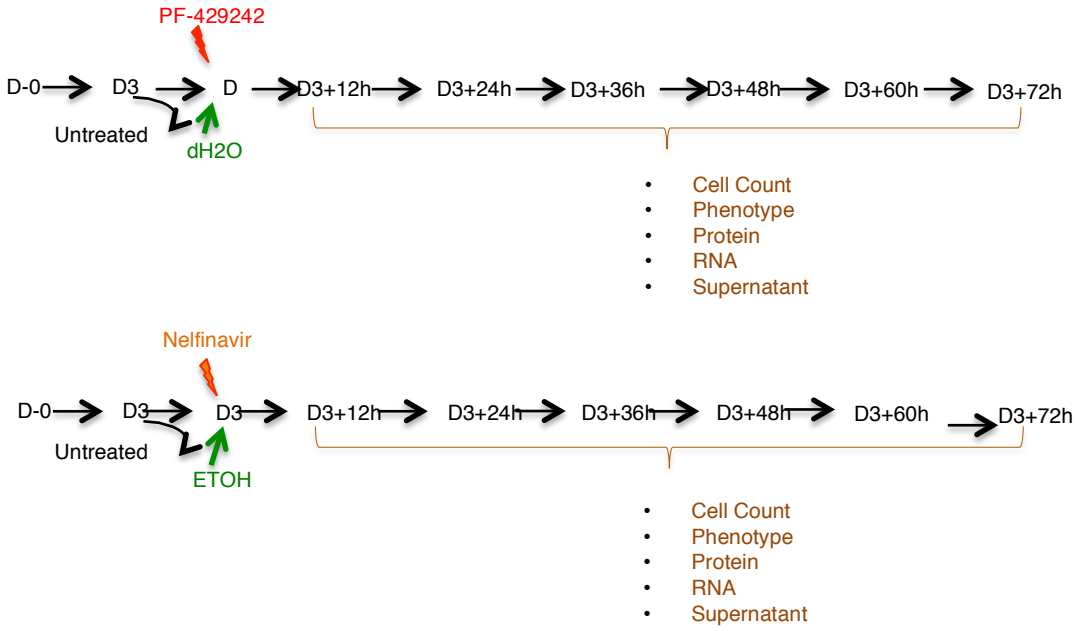


**Figure 6.44 Diagrammatic representation of the experimental design to test the temporal effect of S1P and S2P inhibitors.** Activated B-cells were treated with the indicated drug and harvested every 12 hours starting from Day-3 until Day-6. At each time point, samples were collected for cell count, surface phenotype, protein expression, RNA expression and immunoglobulin (IgM and IgG levels) quantification.

### 6.9.1 Expression and processing of CREB3L2

Careful monitoring of protein expression is important to verify that the S1P/S2P inhibitors are targeting the transcription factors likely to be acting on the underlying molecular changes accompanying plasma cell differentiation. During the kinetic evaluation, inhibition of CREB3L2 cleavage by PF-429242 accompanied by an increase in full-length protein was first detected 24 hours post-treatment (Figure 6.45). Nelfinavir also showed potency at 24 hours, but predominantly led to a loss of full-length protein. By 72 hours, PF-429242 had abrogated expression of CREB3L2, but in this experiment the effect of Nelfinavir was transient with the re-emergence of CREB3L2.

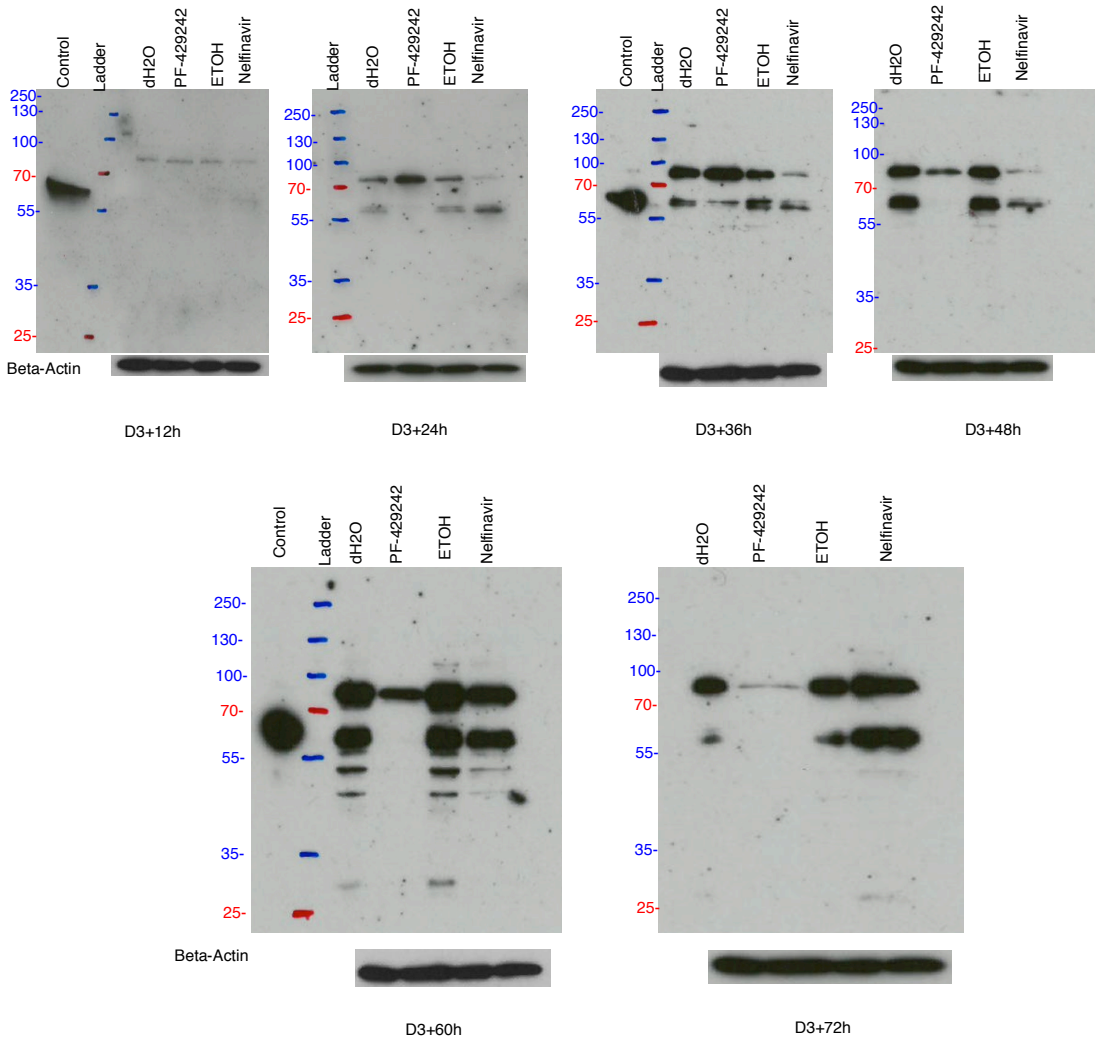


**Figure 6.45 Kinetic analysis of the impact of S1P inhibitor (PF-429242) and S2P inhibitor (Nelfinavir) on CREB3L2 expression.** Day-3 B-cells were pre-treated with 10 μM PF-429242/dH2O and or 10 μM Nelfinavir/Ethanol for 12-hour intervals until Day-6. At each time point, lysates were evaluated by Western blotting.

### 6.9.2 Cell count

The detailed kinetic analysis have confirmed the importance of studying the impact of PF-429242 and Nelfinavir on differentiating B-cells between Day-3 and Day-6 and revealed when the drugs first show an effect on cell number and when the difference is at its peak. From the cell count (Figure 6.46), the PF-429242 and Nelfinavir appear to start impacting on the B-cells 36 hours from the treatment with increasing activity up to 72 hours (Day-6).

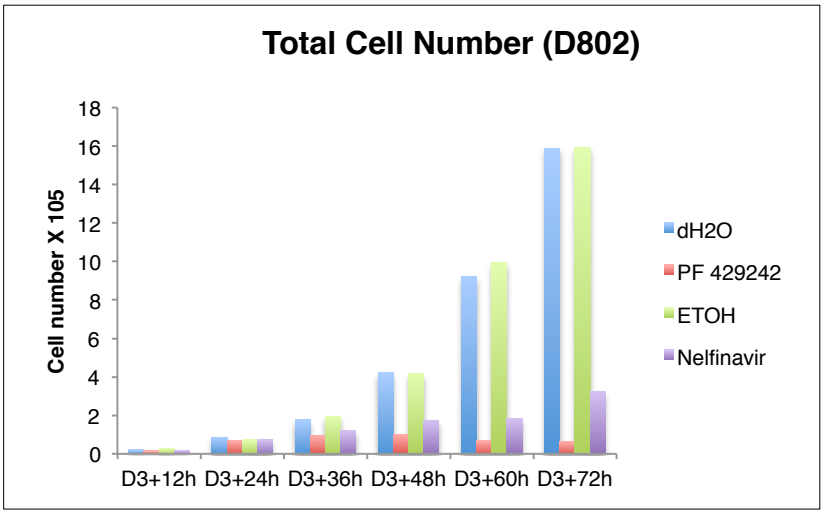


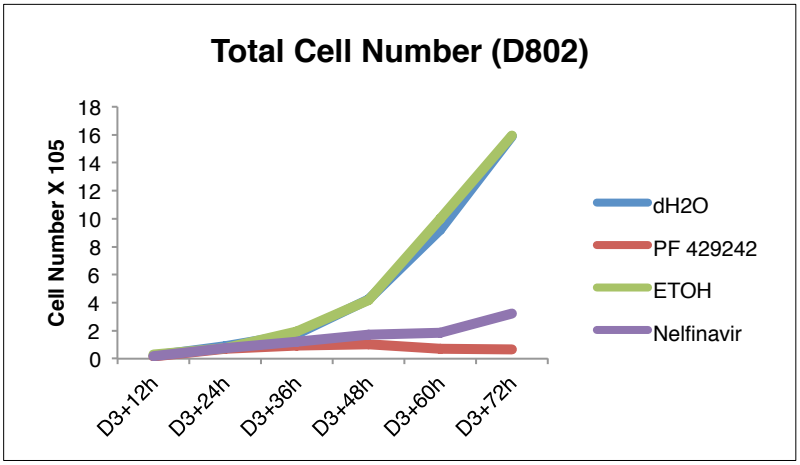


**Figure 6.46 Kinetic analysis of the impact of S1P inhibitor (PF-429242) and S2P inhibitor (Nelfinavir) on differentiating B-cell number.** Day-3 B-cells were treated with 10 μM PF-429242/dH2O or 10 μM Nelfinavir/Ethanol for 12-hour intervals until Day-6. At each time point, the cells were collected for counting using CountBright ™ beads.

### 6.9.3 Cell phenotype

The detailed examination of the impact of S1P/S2P inhibitors provides comprehensive information on the critical window where the affected transcription factors are most likely to be exerting an influence on the underlying change in gene expression. To determine whether the timing of the reduction in cell number was accompanied by other changes, surface phenotype was evaluated.

Consistent with the cell number observation, PF-429242 started affecting cell phenotype 36 hours after the treatment, revealing a reduction of CD20 expression compared to the control (dH2O) and increase in CD38 population in PF-429242 treated sample clearly at D3+72h (Figure 6.47). These changes in cell phenotype increased over time until 72 hours post treatment where culture with PF-429242 generated two populations ($CD38^{high}$ and $CD38^{low}$) whereas the control had only one cell population ($CD38^{high}$).

On the other hand, the impact of Nelfinavir on cell phenotype was different. Although Nelfinavir also affected cell count as early as 36 hours post treatment, its effect on cell phenotype was delayed. 48 hours post-Nelfinavir treatment CD20 expression was increased compared to its control (Ethanol), with no changes observed in CD38/CD138 expression (Figure 6.47).

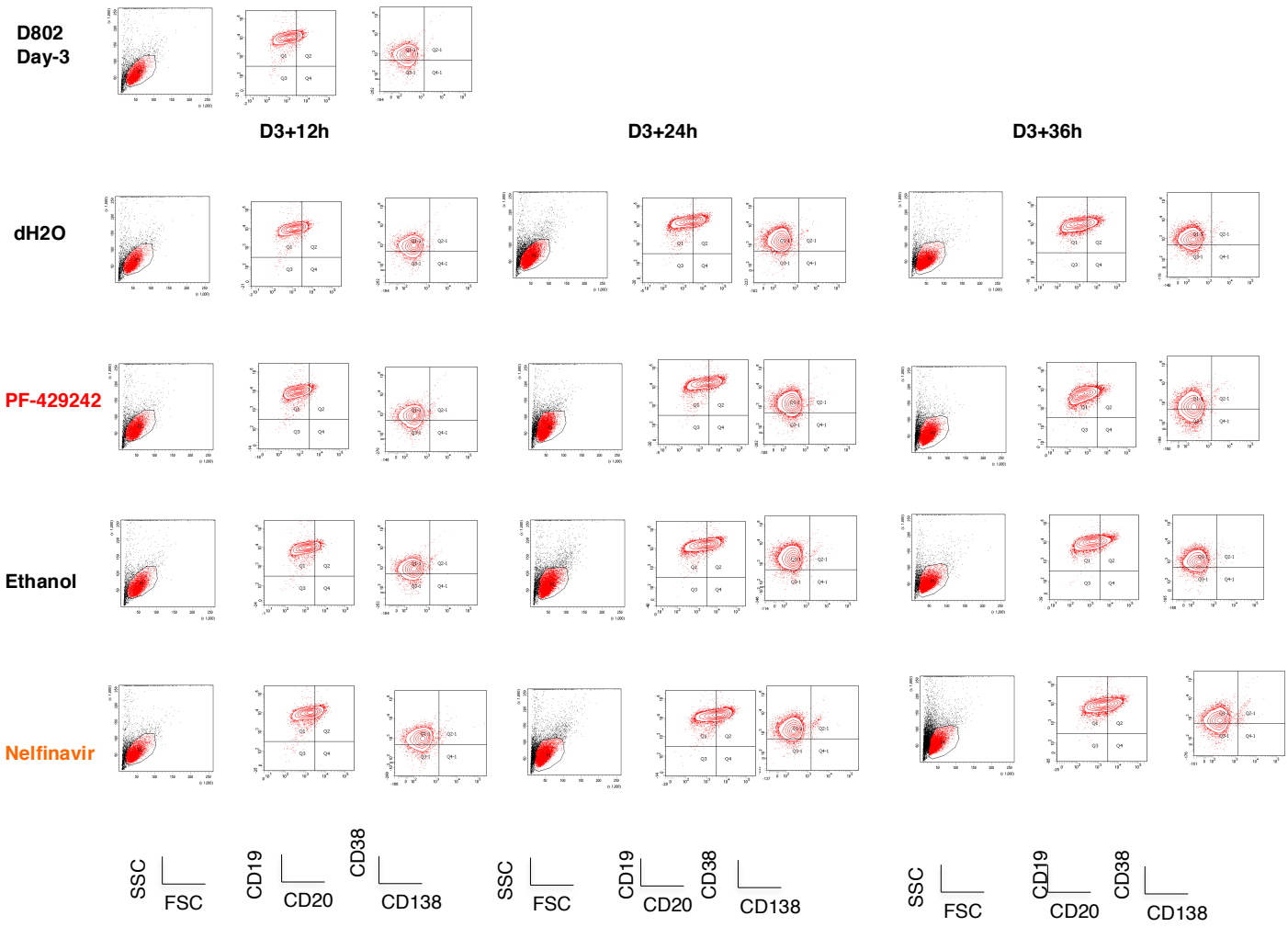
D802
Day-3
D3+12h
D3+24h
D3+36h
dH2O
PF-429242
Ethanol
Nelfinavir
SSC
FSC
CD19
CD20
CD38
CD138

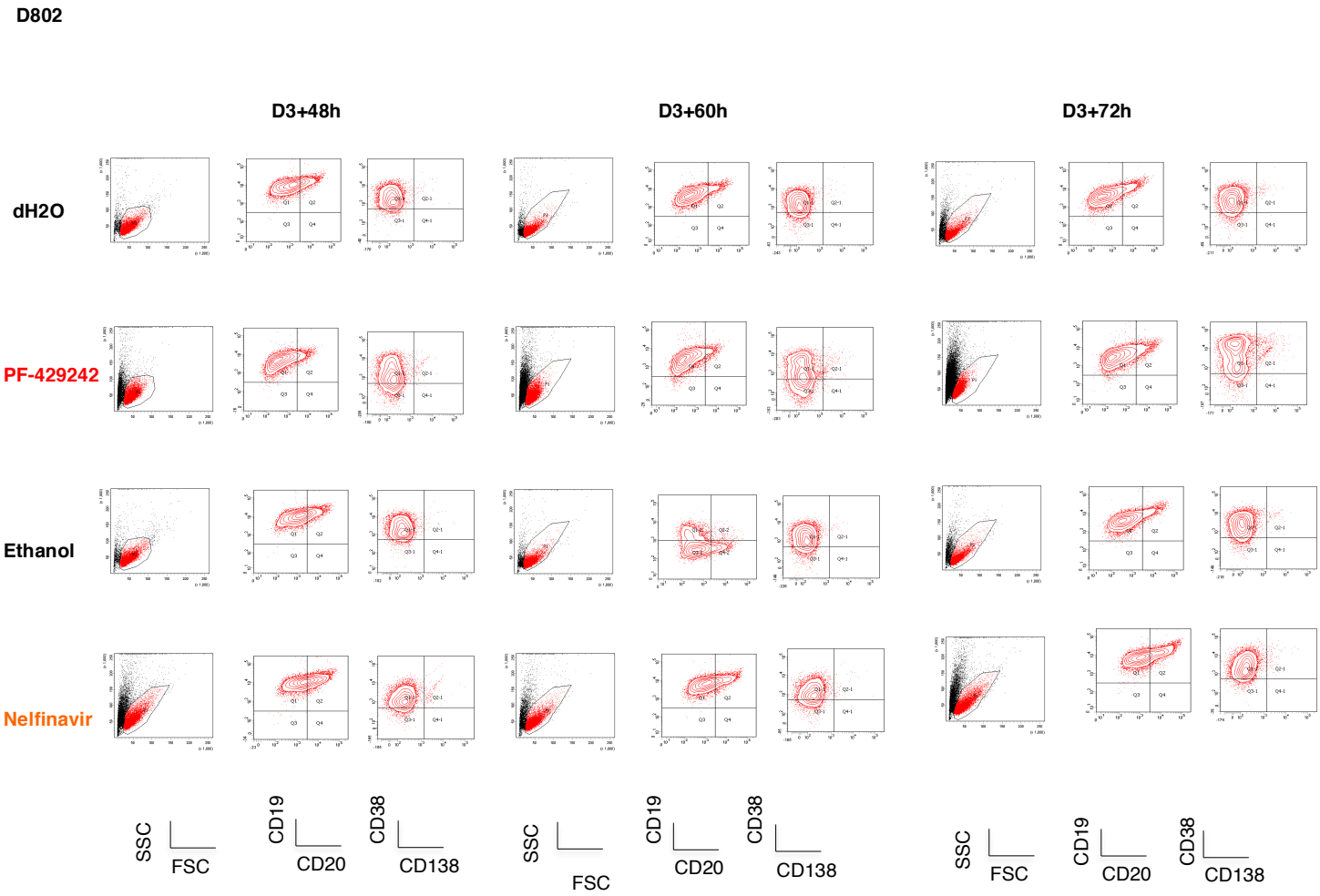


**Figure 6.47 Kinetic analysis of the impact of S1P inhibitor (PF-429242) and S2P inhibitor (Nelfinavir) on cell phenotype.** Day-3 B-cells were treated with 10 μM PF-429242/dH2O or 10 μM Nelfinavir/Ethanol for 12-hour intervals until Day-6. At each time point, the cells were stained for CD19, CD20, CD38 and CD138 and analysed by flow cytometry.

### 6.9.4 Immunoglobulin levels

The ability to secrete immunoglobulin should accompany the phenotypic changes associated with becoming an ASC. To determine whether the impact of S1P inhibitor and S2P inhibitor on phenotype was matched by secretory output, it was important to quantify the immunoglobulin (IgM and IgG) levels. Thus, at each time point, the supernatants were collected and analysed using ELISA. The results revealed a profound reduction in the IgM and IgG levels (more than 90%), which was first detectable 36 hours post treatment in the treated samples compared with the control (Figure 6.48). The exception was Nelfinavir at 72 hours where the inhibition was less (same results in the protein expression, Figure 6.45) that needs to be repeated for validation. Thus, 10 μM PF-429242 and 10 μM Nelfinavir had an inhibitory affect on the secreted IgM and IgG levels from ASCs that were in agreement with the previous observations using these samples.

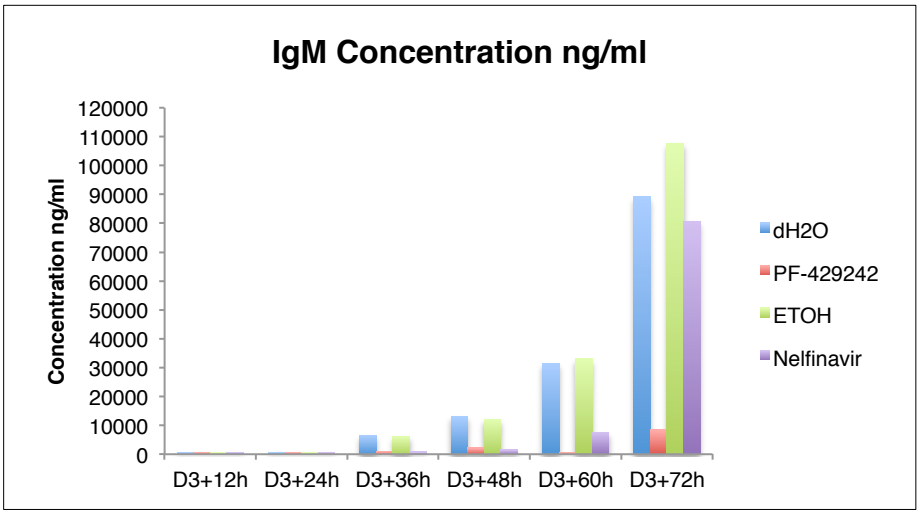


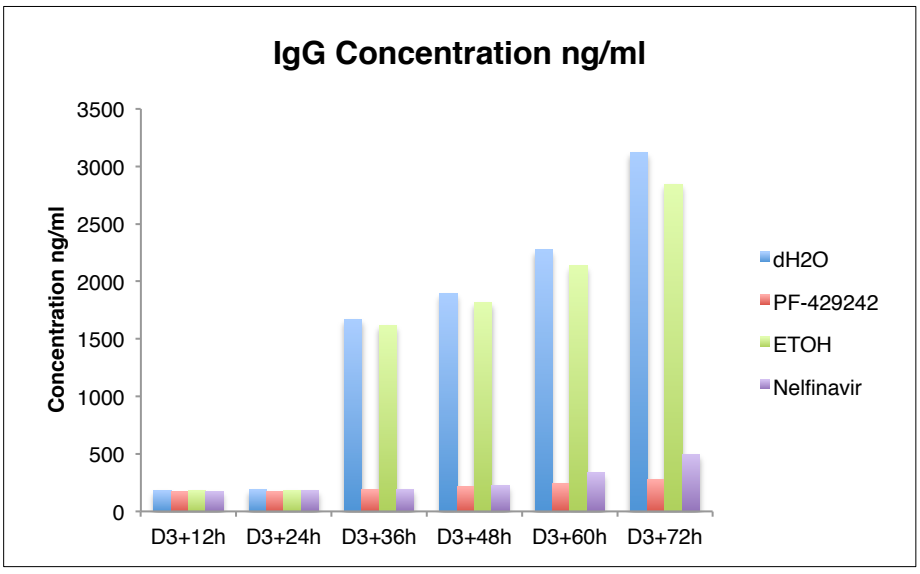


**Figure 6.48 Kinetic analysis of the impact of S1P inhibitor (PF-429242) and S2P inhibitor (Nelfinavir) on IgM and IgG levels.** Day-3 B-cells were treated with 10 μM PF-429242/dH2O or 10 μM Nelfinavir/Ethanol for 12-hour intervals until Day-6. At each time point, the supernatants were collected and the immunoglobulins (IgM and IgG) were quantified using ELISA.

## 6.10 Validation of kinetic analysis of PF-429242 and Nelfinavir treatment on differentiating B-cells

### 6.10.1 Protein expression

The detailed investigation on the impact of PF-429242 and Nelfinavir on the human differentiated B-cells and antibody secretory cells has the potential to provide us with a better understanding of the pathways regulated by these inhibitors. To ascertain whether CREB3L2 processing was uniformly affected, the impact on CREB3L2 protein expression was validated using three additional donors. The results showed that the inhibitory affect of PF-429242 and Nelfinavir started as early as 12-24 hours until 72 hours post-treatment (Figure 6.49), which matches the results obtained before.

**A**

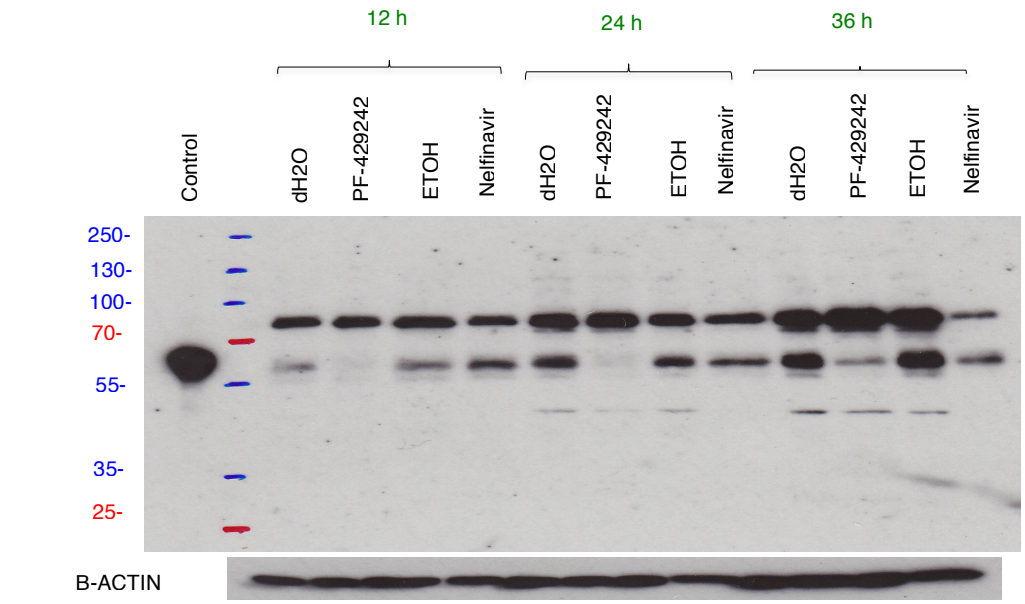
12 h
24 h
36 h
Control
dH2O
PF-429242
ETOH
Nelfinavir
dH2O
PF-429242
ETOH
Nelfinavir
dH2O
PF-429242
ETOH
Nelfinavir
250-
130-
100-
70-
55-
35-
25-
B-ACTIN

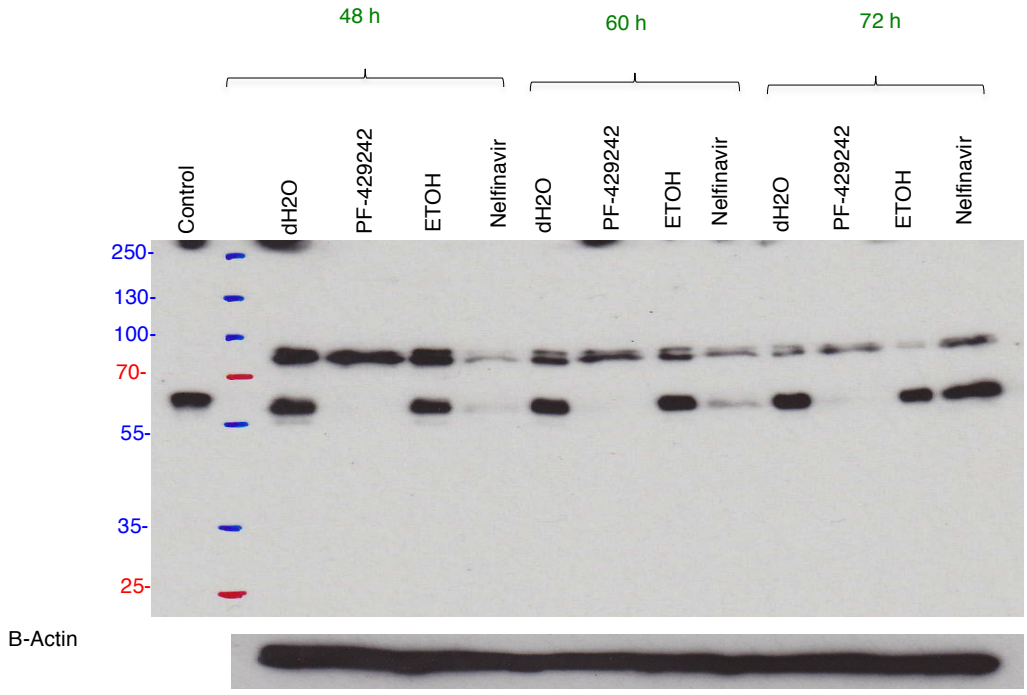
48 h
60 h
72 h
Control
dH2O
PF-429242
ETOH
Nelfinavir
dH2O
PF-429242
ETOH
Nelfinavir
dH2O
PF-429242
ETOH
Nelfinavir
250-
130-
100-
70-
55-
35-
25-
B-Actin

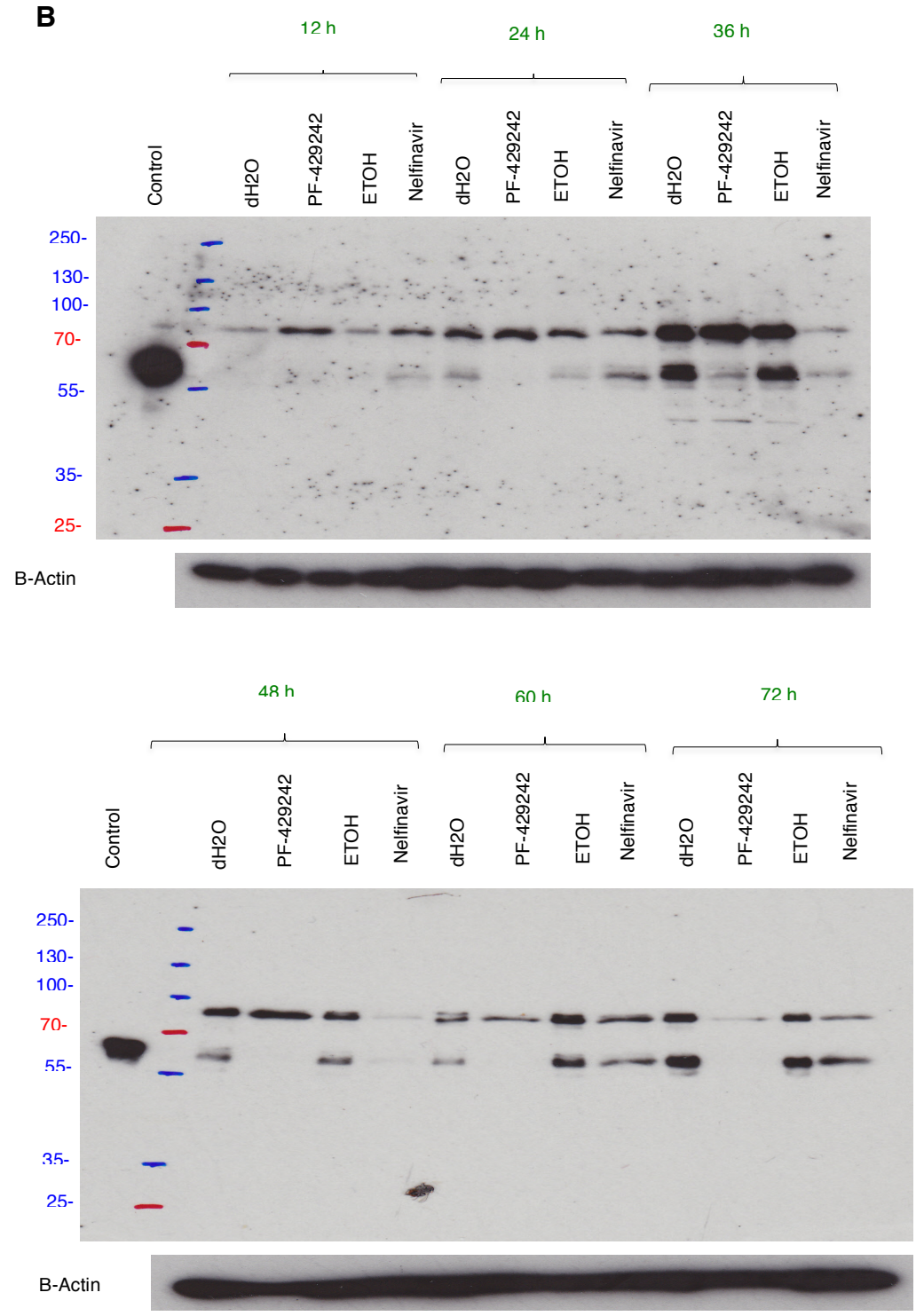


**Figure 6.49 Validation of the impact of S1P inhibitor (PF-429242) and S2P inhibitor (Nelfinavir) on CREB3L2 protein expression during the activated B-cell to plasmablast transition.** Day-3 B-cells from two donors, (A) D806 and (B) D704, were treated with 10 μM PF-429242/dH2O or 10 μM Nelfinavir/Ethanol for 12 hour-intervals until 72 hours (Day-6). At each time point, the cells were collected and prepared for protein examination by Western blotting.

### 6.10.2 Cell count

The impact of PF-429242 and Nelfinavir on differentiating B-cells was validated using three donors. The results depicted in Figure 6.48 show a profound inhibitory affect of PF-429242 on cell count that started 36 hours post treatment and continued increasing until 72 hours (Day-6). On the other hand, the impact of Nelfinavir on the cell count was variable between the three donors. Its inhibitory effect started 24 hours post treatment in one donor with slight decrease in the other two donors, which escalated until 72 hours (Day-6) (Figure 6.50). Thus, the inhibitory impact of PF-429242 and Nelfinavir on cell number during the transition period between activated B-cell and plasmablast has been confirmed.

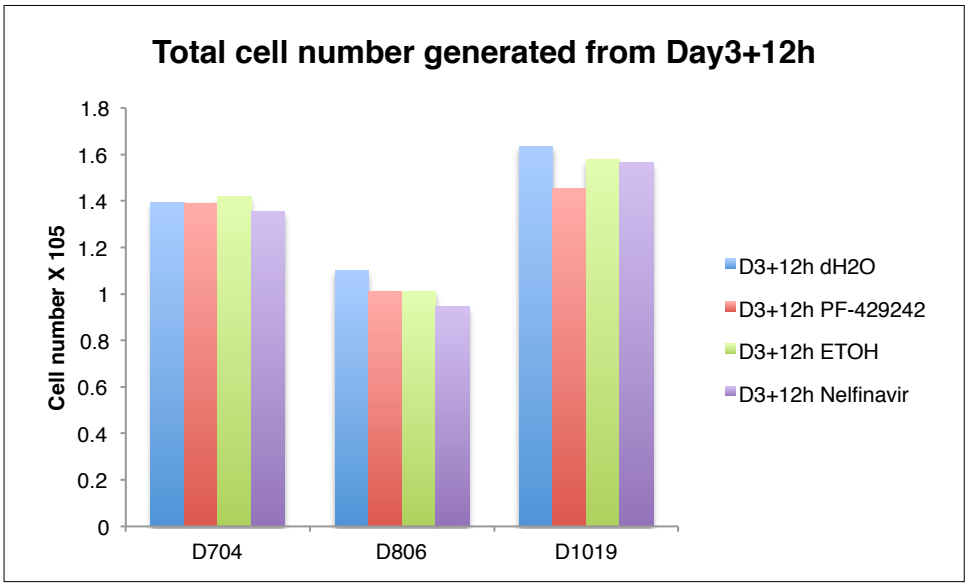


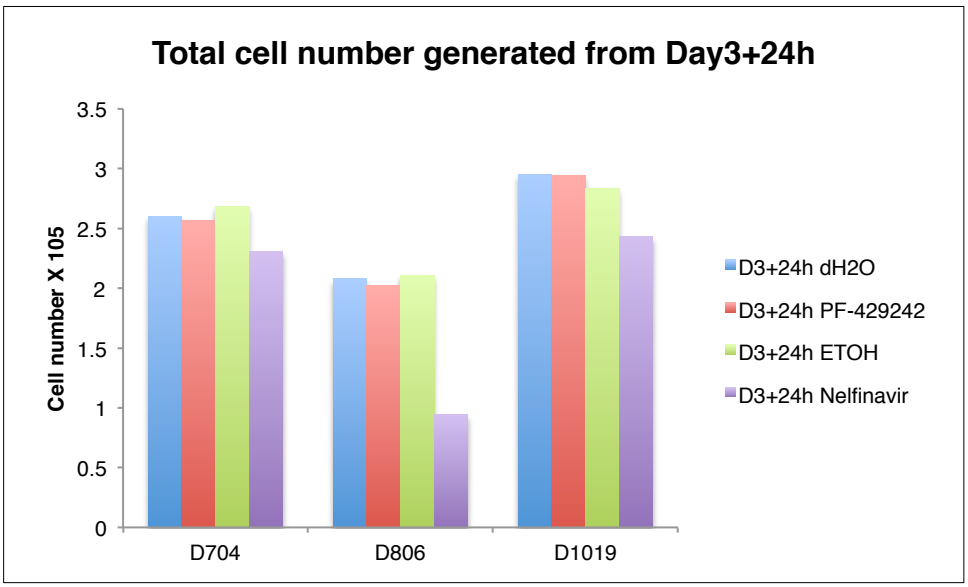

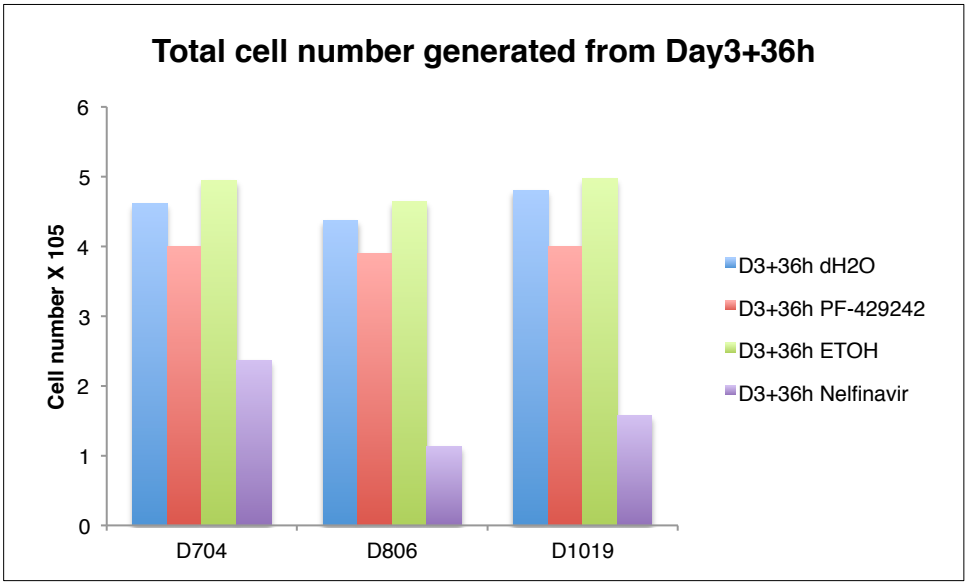
Total cell number generated from Day3+36h
Cell number X 105
0
1
2
3
4
5
6
D704
D806
D1019
D3+36h dH2O
D3+36h PF-429242
D3+36h ETOH
D3+36h Nelfinavir

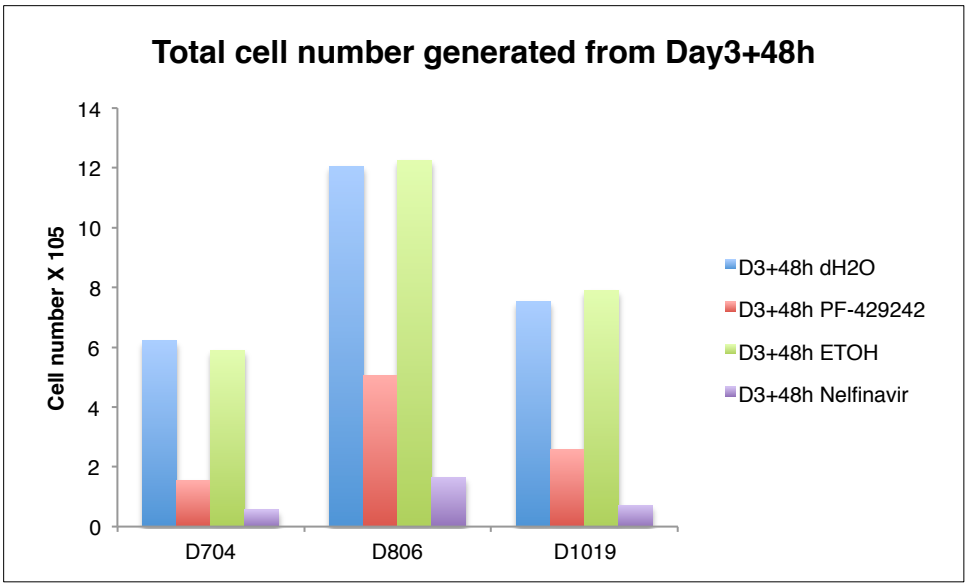
Total cell number generated from Day3+48h
Cell number X 105
0
2
4
6
8
10
12
14
D704
D806
D1019
D3+48h dH2O
D3+48h PF-429242
D3+48h ETOH
D3+48h Nelfinavir

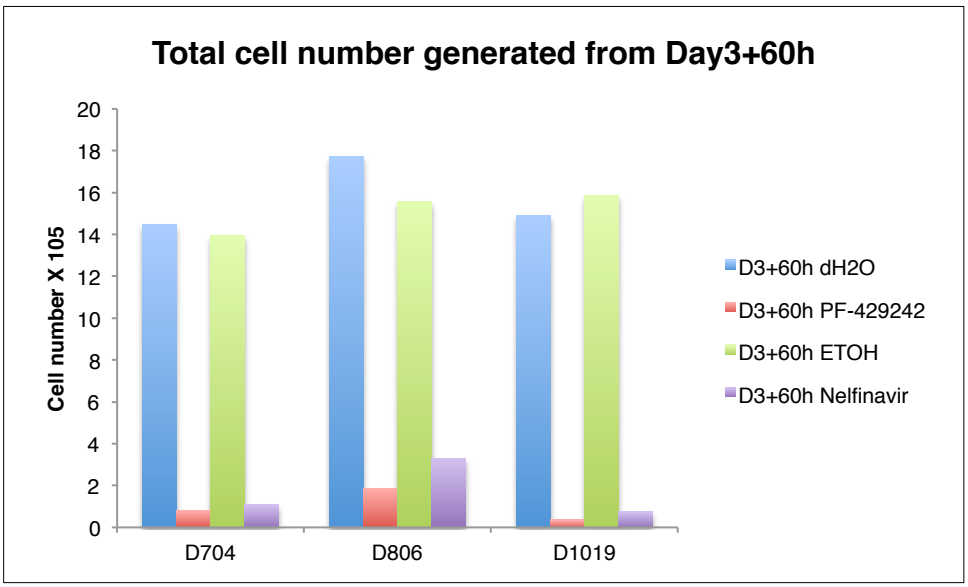
Total cell number generated from Day3+60h
Cell number X 105
0
2
4
6
8
10
12
14
16
18
20
D704
D806
D1019
D3+60h dH2O
D3+60h PF-429242
D3+60h ETOH
D3+60h Nelfinavir

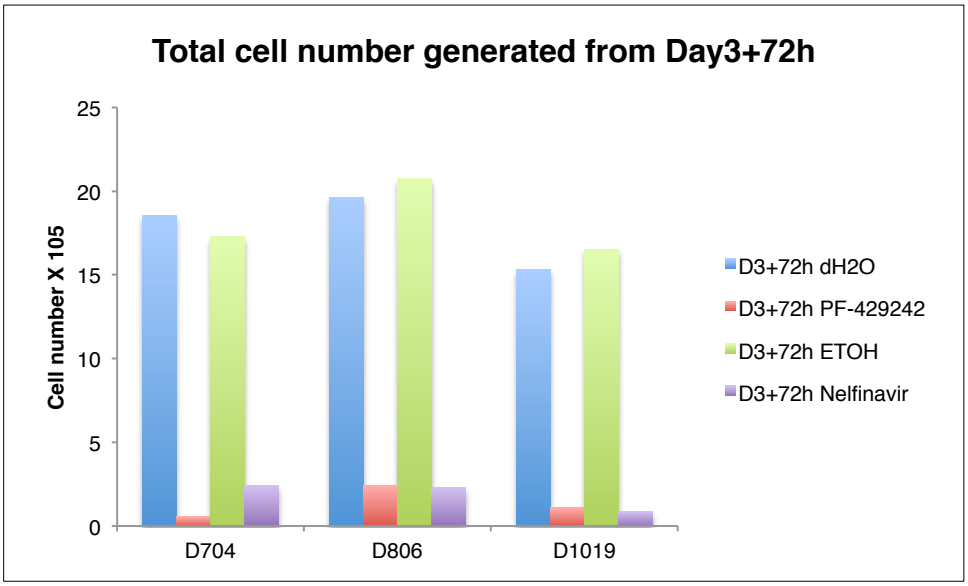


**Figure 6.50 Validating the impact of S1P inhibitor (PF-429242) and S2P inhibitor (Nelfinavir) on cell count during activated B-cell to plasmablast transition.** Day-3 B-cells (from three donors) were treated with 10 μM PF-429242/dH2O or 10 μM Nelfinavir/Ethanol for 12-hour intervals until Day-6. At each time point, the cells were counted using CountBright ™ technology.

### 6.10.3 Cell phenotype

The impact of PF-429242 and Nelfinavir surface phenotype was validated using cells from three donors. Based on the results obtained in the previous experiment, PF-429242 treatment lead to the formation of two cell populations based on CD38 ($CD38^{high}$ and $CD38^{low}$). Previous studies have identified $CD38^{-/low}$ cells capable of secreting immunoglobulin that can be identified by the expression of CD27 (121). Moreover, the acquisition of CD27 prior to CD38 has been postulated to identify the "pre-plasmablast" stage (122). Therefore CD27 staining was included in the study to investigate whether PF-429242 altered formation of pre-plasmablasts. The results showed that PF-429242 treatment lead to the delayed the acquisition of CD27 beginning at 36 hours, suggesting a possible effect on the commitment to becoming an ASC. In addition, in respect to the impact of PF-429242 on CD38 and CD20, similar results were obtained as in the previous experiment confirming its effect on the plasmablast population.

Furthermore, the impact of Nelfinavir on cell phenotype was similar among the three donors. Its impact started at 36 hours post treatment with a slight retention of CD20 expression, but no changes in CD27 expression in the treated cells compared to its control (Ethanol) (Figure 6.51).

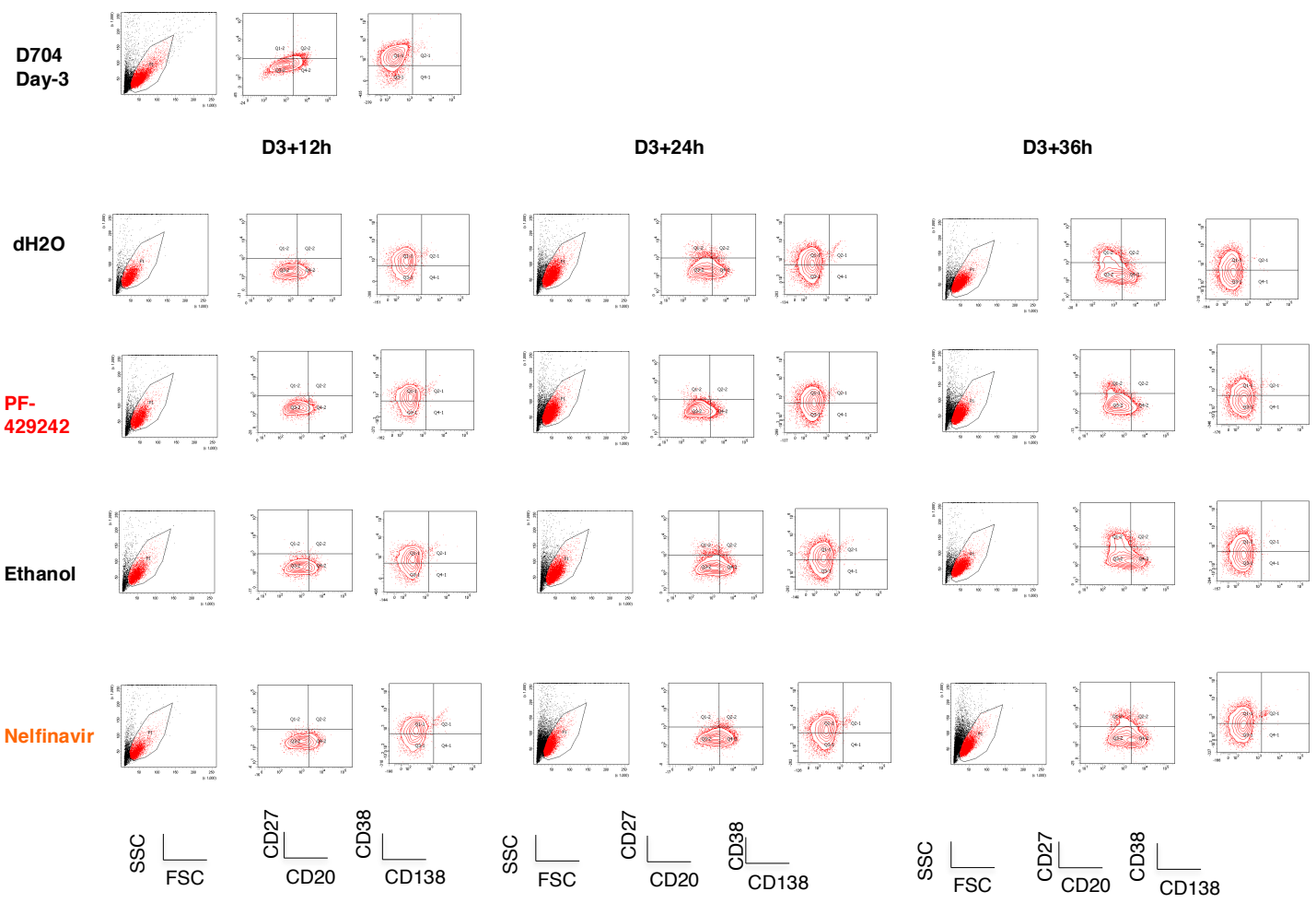
D704
Day-3
D3+12h
D3+24h
D3+36h
dH2O
PF-
429242
Ethanol
Nelfinavir
SSC
FSC
CD27
CD20
CD38
CD138

D704

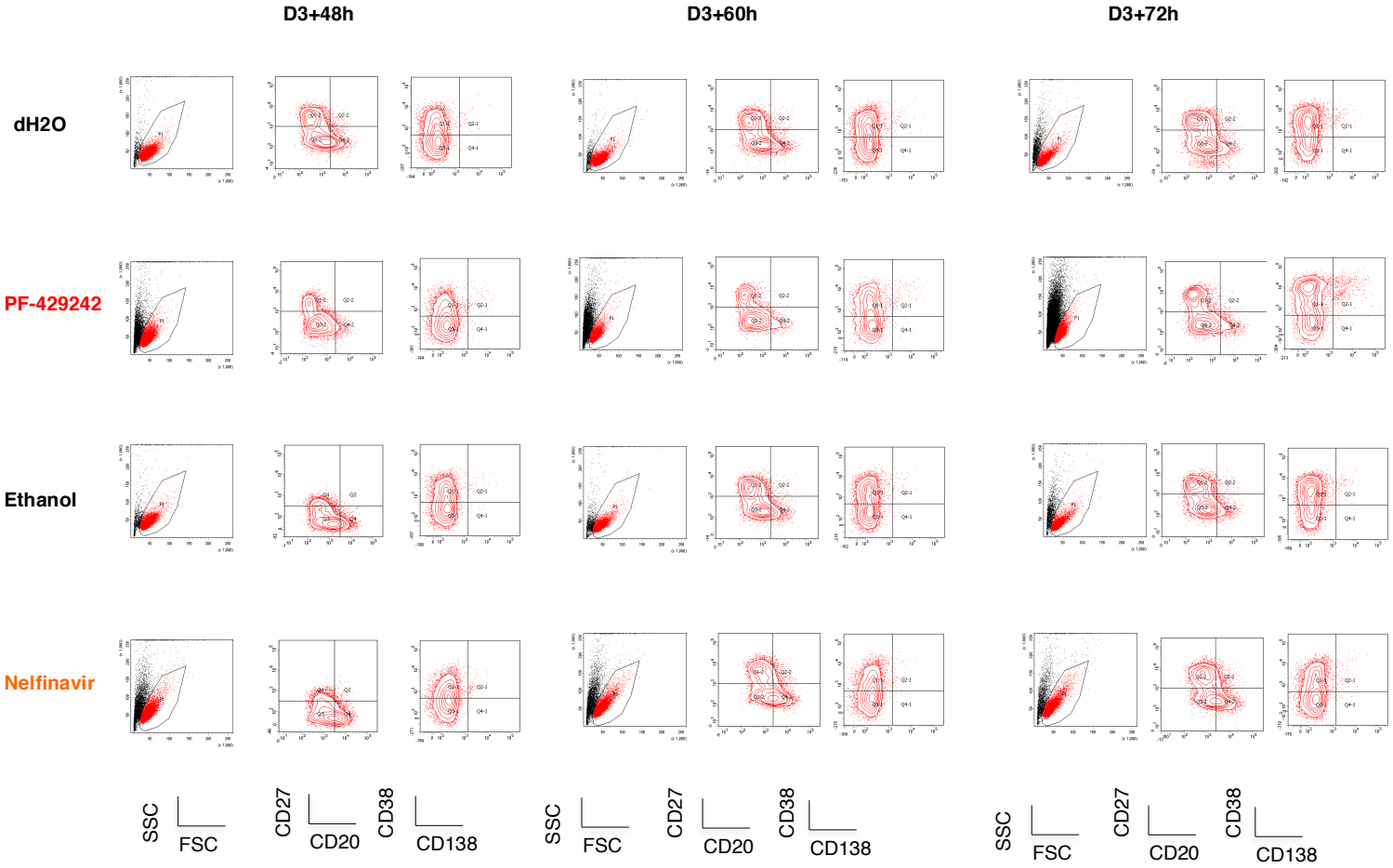
D3+48h
D3+60h
D3+72h
dH2O
PF-429242
Ethanol
Nelfinavir
SSC
FSC
CD27
CD20
CD38
CD138

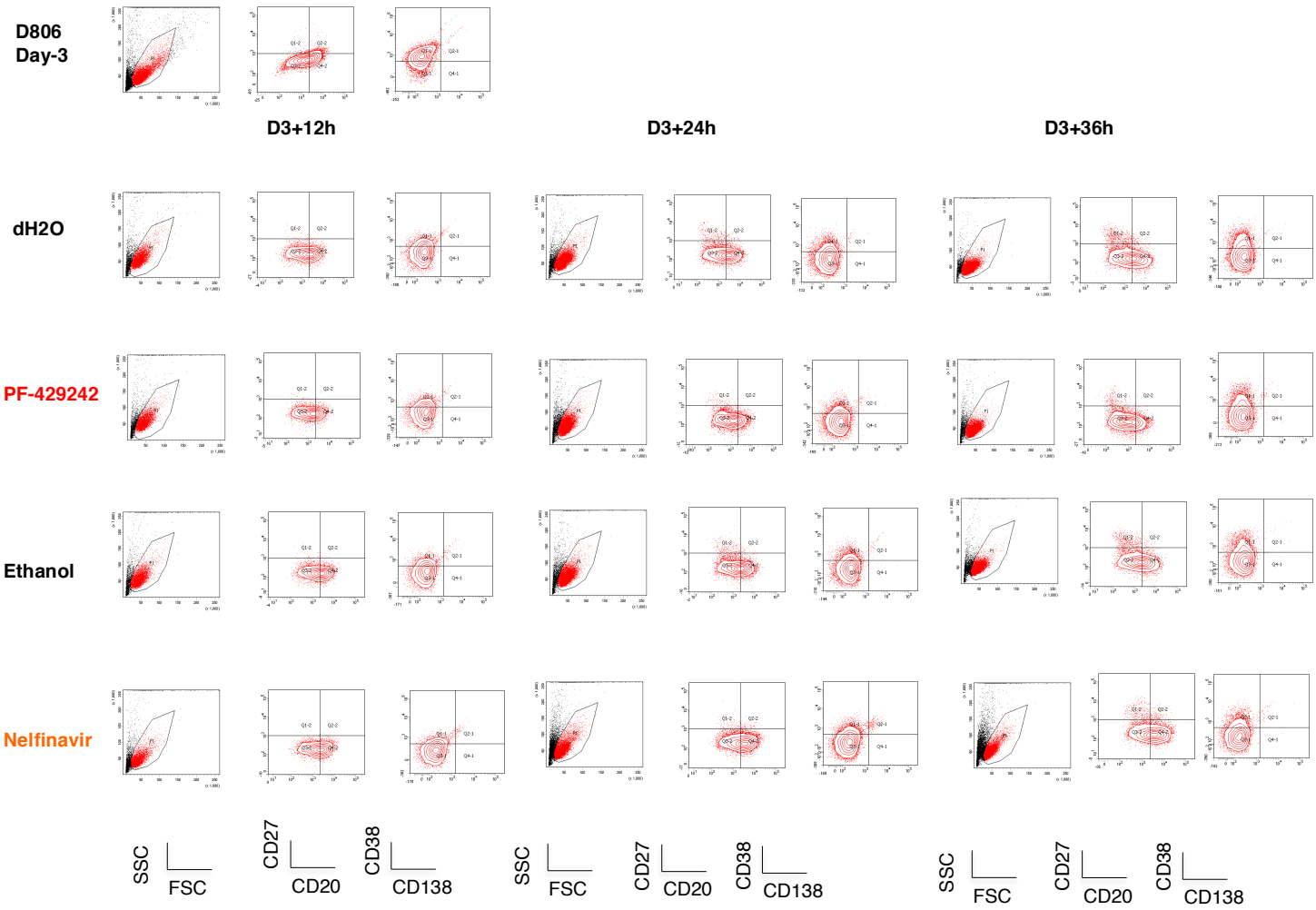
D806
Day-3
D3+12h
D3+24h
D3+36h
dH2O
PF-429242
Ethanol
Nelfinavir
SSC
FSC
CD27
CD20
CD38
CD138

**D806**

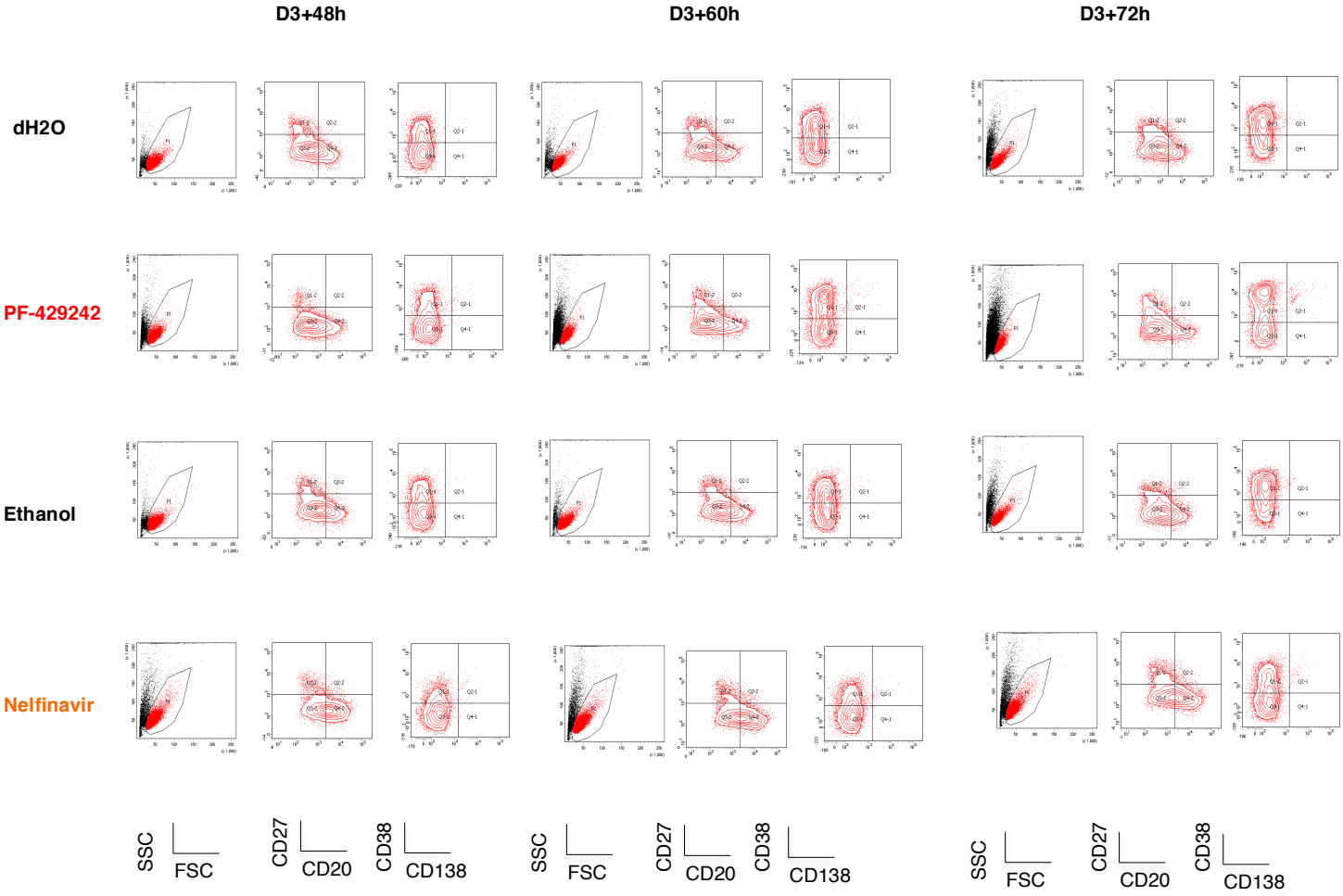
D3+48h
D3+60h
D3+72h
dH2O
PF-429242
Ethanol
Nelfinavir
SSC
FSC
CD27
CD20
CD38
CD138

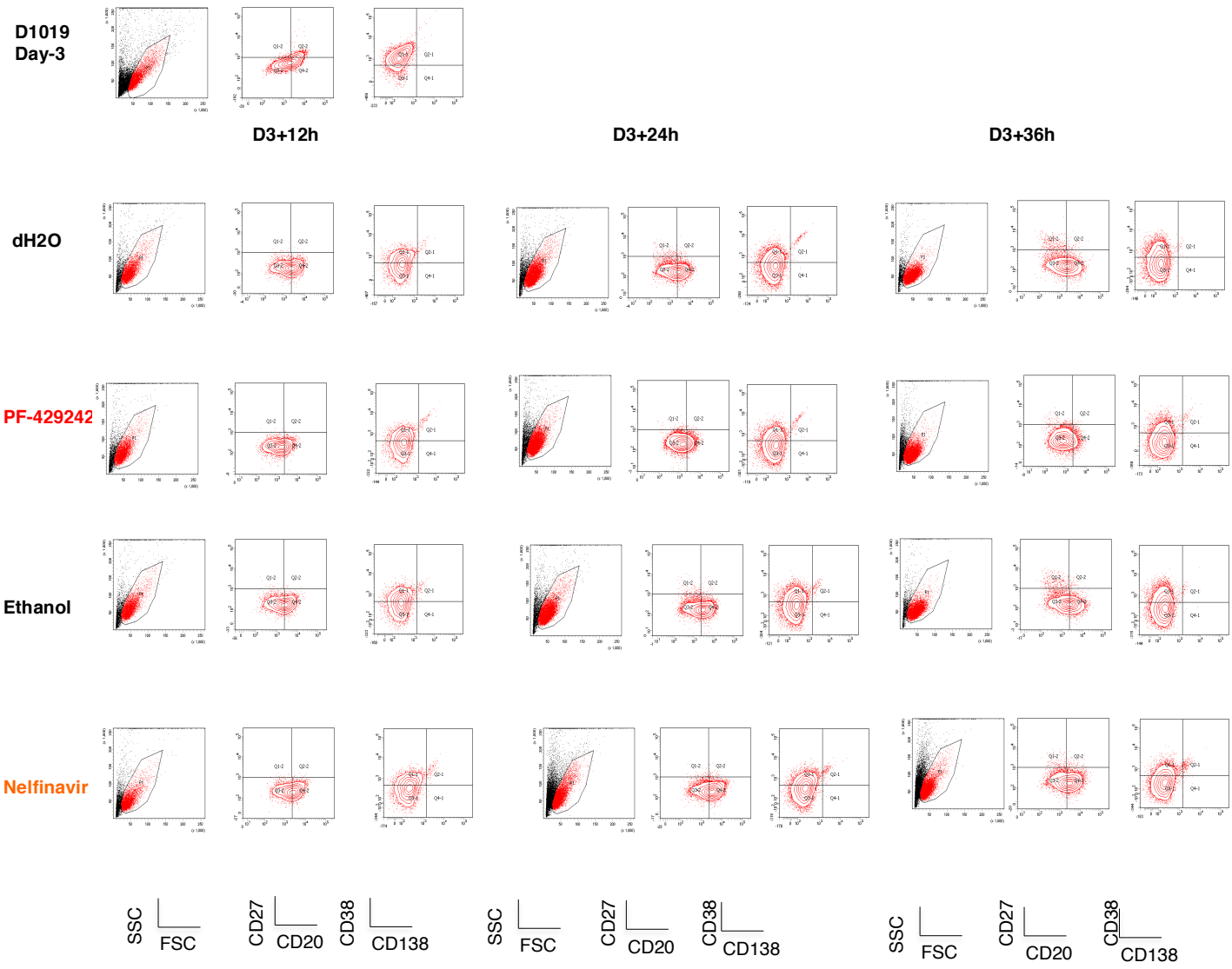
D1019
Day-3
D3+12h
D3+24h
D3+36h
dH2O
PF-429242
Ethanol
Nelfinavir
SSC
FSC
CD27
CD20
CD38
CD138

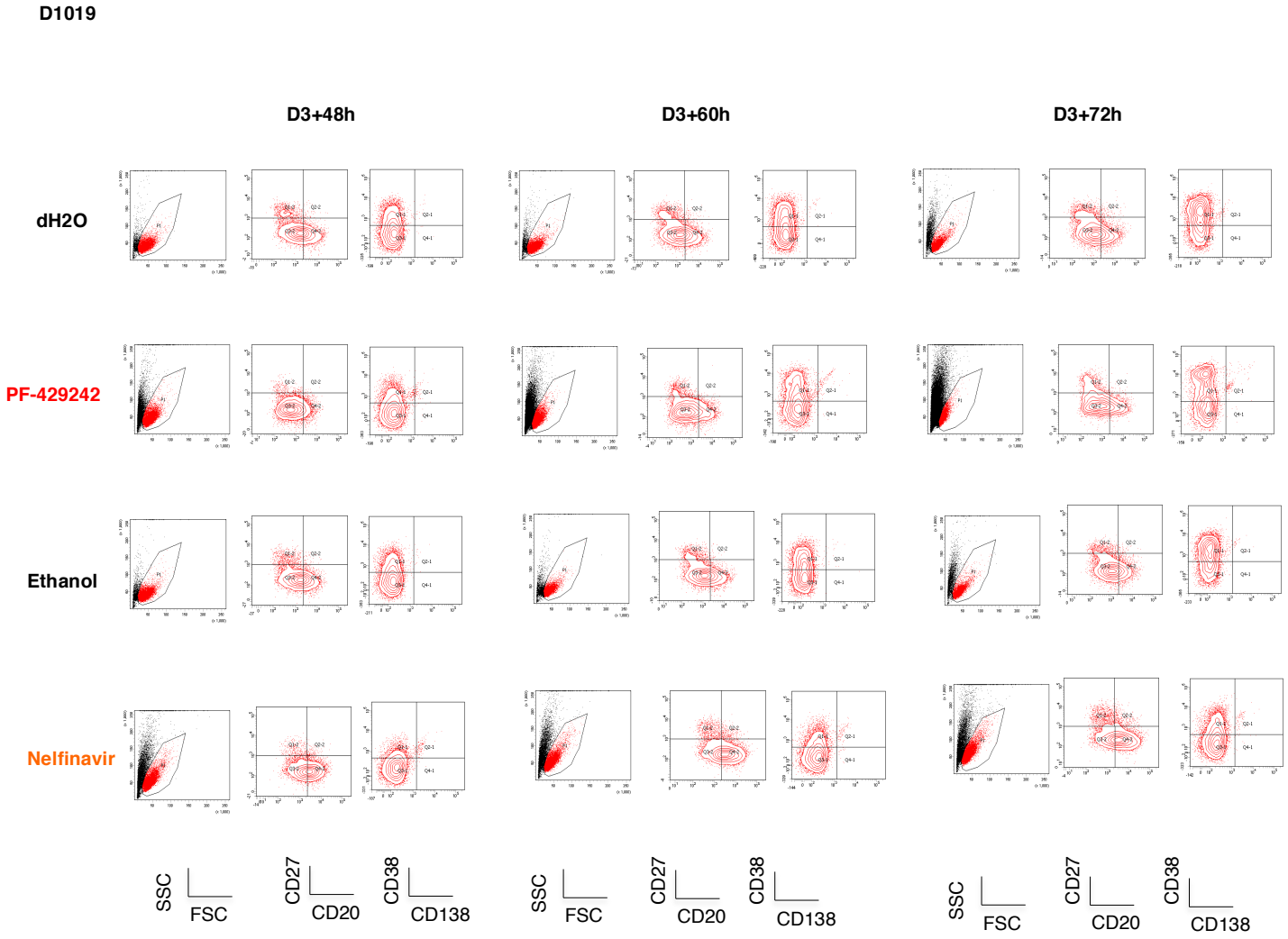


**Figure 6.51 Validating the impact of S1P inhibitor (PF-429242) and S2P inhibitor (Nelfinavir) on phenotypic changes prior to the plasmablast stage.** Day-3 B-cells (from three donors) were treated with 10 μM PF-429242/dH2O or 10 μM Nelfinavir/Ethanol for 12-hour intervals until Day-6. At each time point, the cells were collected and stained for CD27, CD20, CD38 and CD138 and analysed by flow cytometry.

In summary, the impact of PF-429242/dH2O and Nelfinavir/ETOH on B-cells (Day-6) were evaluated by calculating the significance of difference between the groups in CD38-, CD38+ and CD138+ fractions (Figure-6.52). It revealed that, PF-429242 treatment generated significant difference in the level of CD38 expression and appeared promote plasma cell differentiation compared to the control. The increase in autophagy after PF-429242 treatment may have allowed a small number of cells to successfully adapt and become more mature.

A

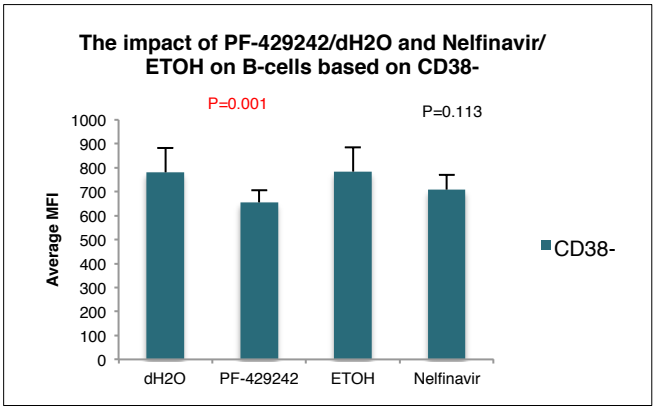


B

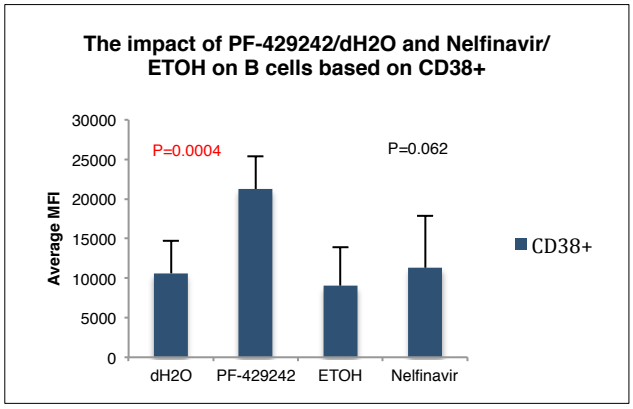


C

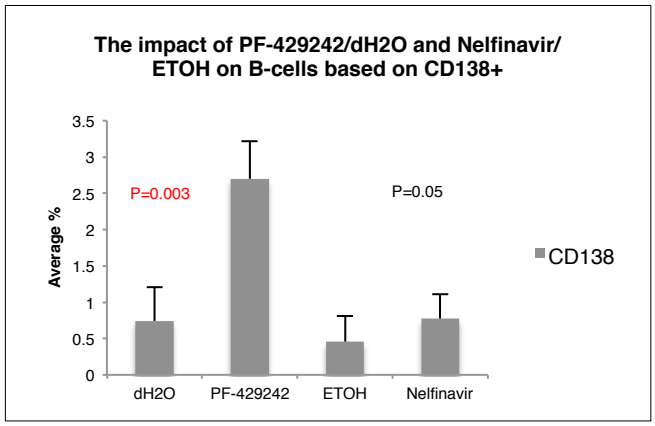


**Figure-6.52:** Summary on the impact of PF-429242/dH2O and Nelfinavir/ETOH on B-cells (Day-6) based on A. CD38-. B. CD38+ and C. CD138+. The significance difference between the tested groups (dH2O/PF-429242 and ETOH/Nelfinavir) was tested using t-test and P values were calculated ($P<0.05$ is significant, $P>0.05$ is not significant).

## 6.11 Determination of ASC formation by ELISpot (Enzyme-Linked Immunospot)

The results shown in Figure 6.49 indicated that treatment of activated B-cells with the S1P inhibitor PF-429242 resulted in a delay in the acquisition of CD27 and the generation of distinct $CD38^{high}$ and $CD38^{low}$ populations at Day-6. These findings suggested that blocking S1P-regulated pathways might impede commitment to ASC formation or differentially affect naïve vs memory precursor populations. Since the defining feature of ASCs is the ability to secrete antibodies, a sensitive ELISpot assay was employed to measure active Ig production from purified cells. B-cells were extracted from three donors and treated with PF-429242 on Day-3 (Figure 6.53) for 72 hours.

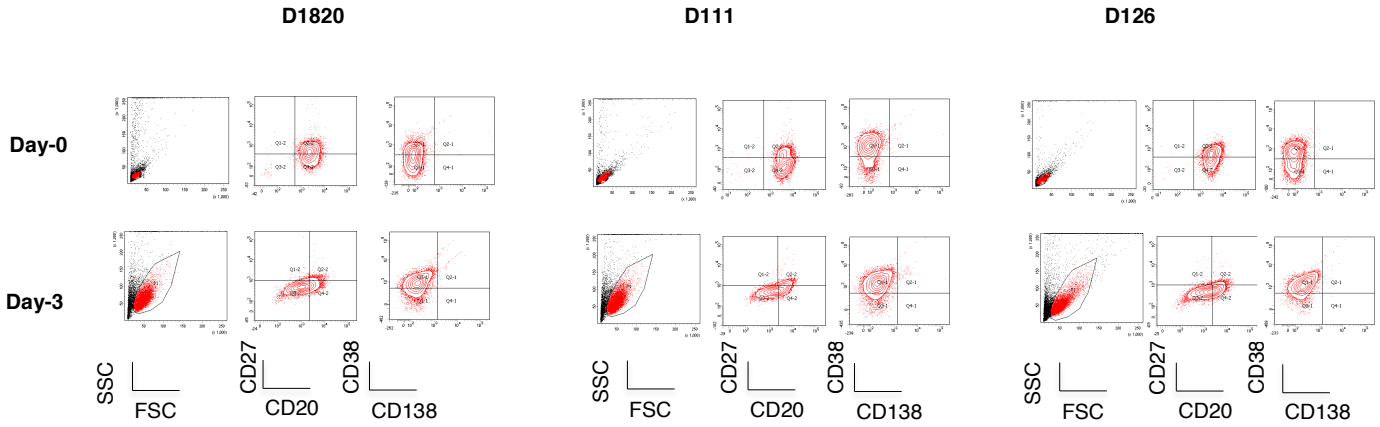


**Figure 6.53 Phenotypic characterisation of activated B-cells.** B-cells were extracted from three healthy donor blood samples. The cell phenotypes were checked before PF-429242 treatment.

On Day-6, $1X10^6$ cells were sorted based on CD38 expression levels ($CD38^{high}$ and $CD38^{low}$) following treatment with PF-429242 or the control with dH2O (Figure 6.54).

**D1820 (dH2O)**

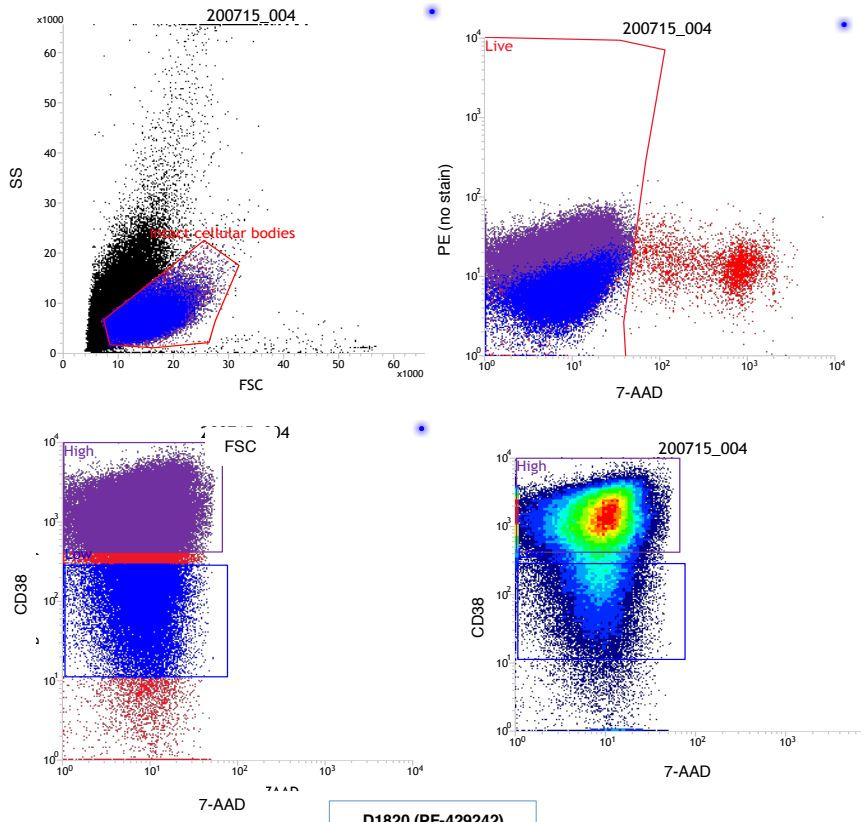


**D1820 (PF-429242)**

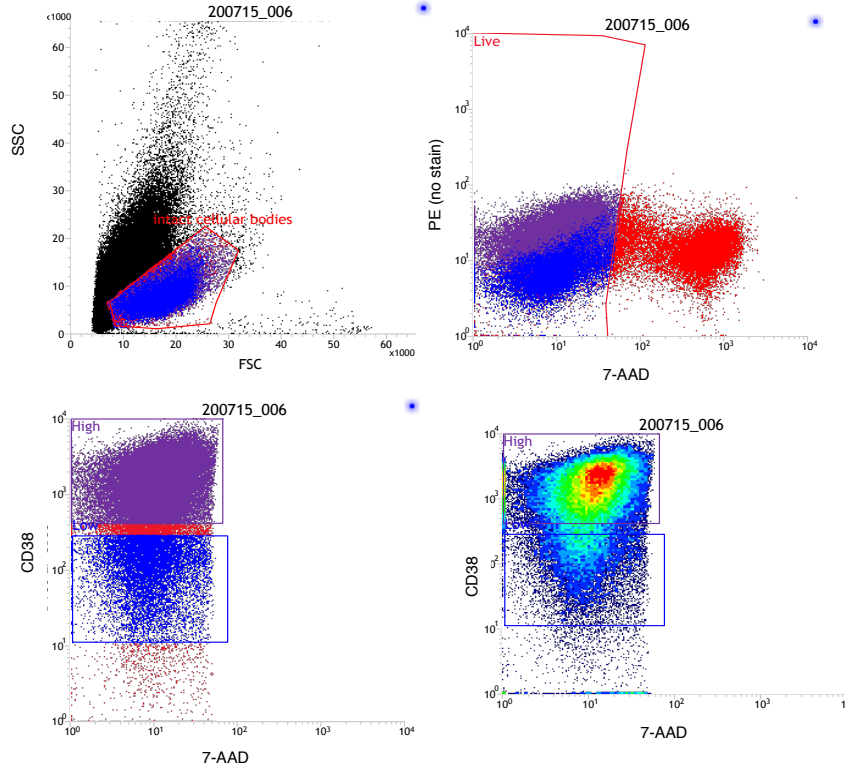

D111 (dH2O)

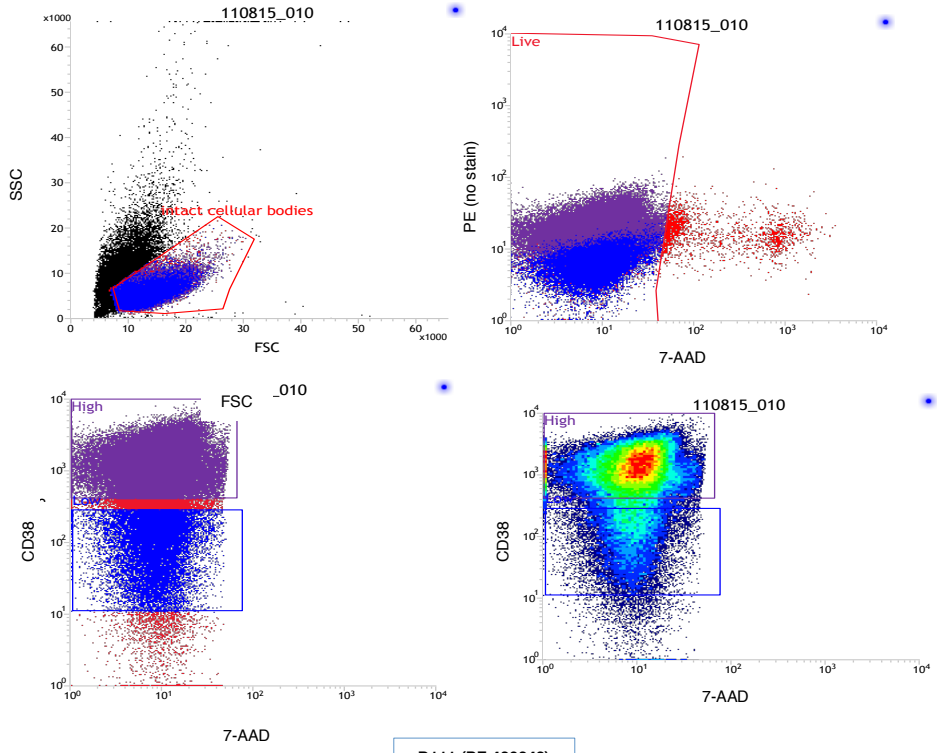


D111 (PF-429242)

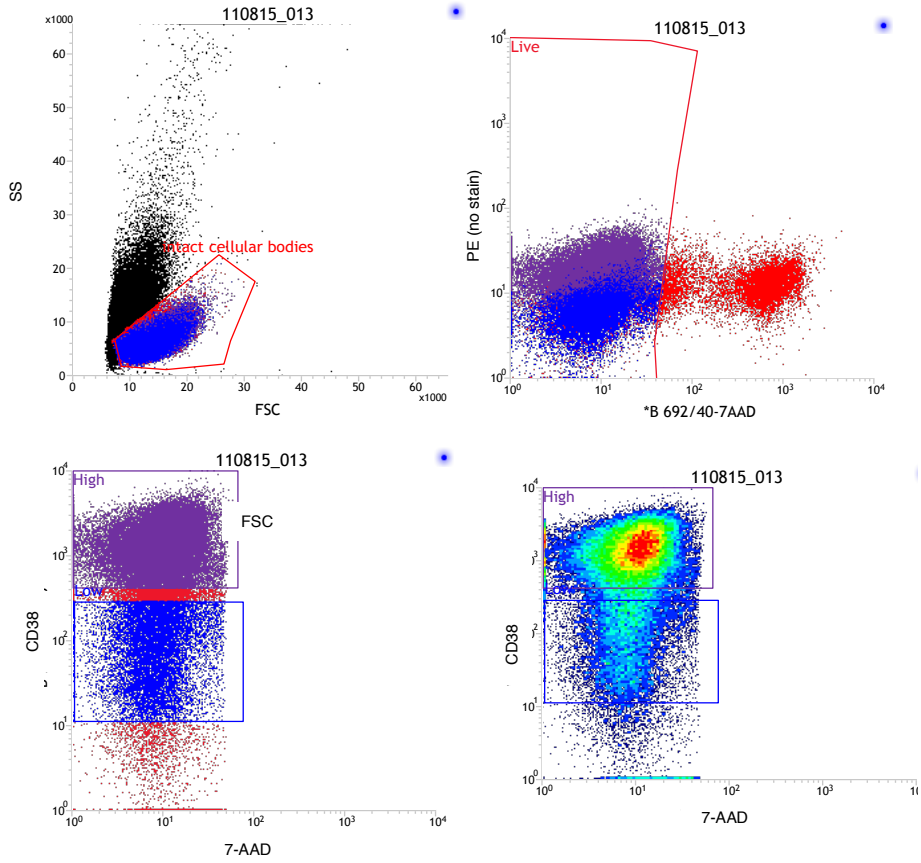

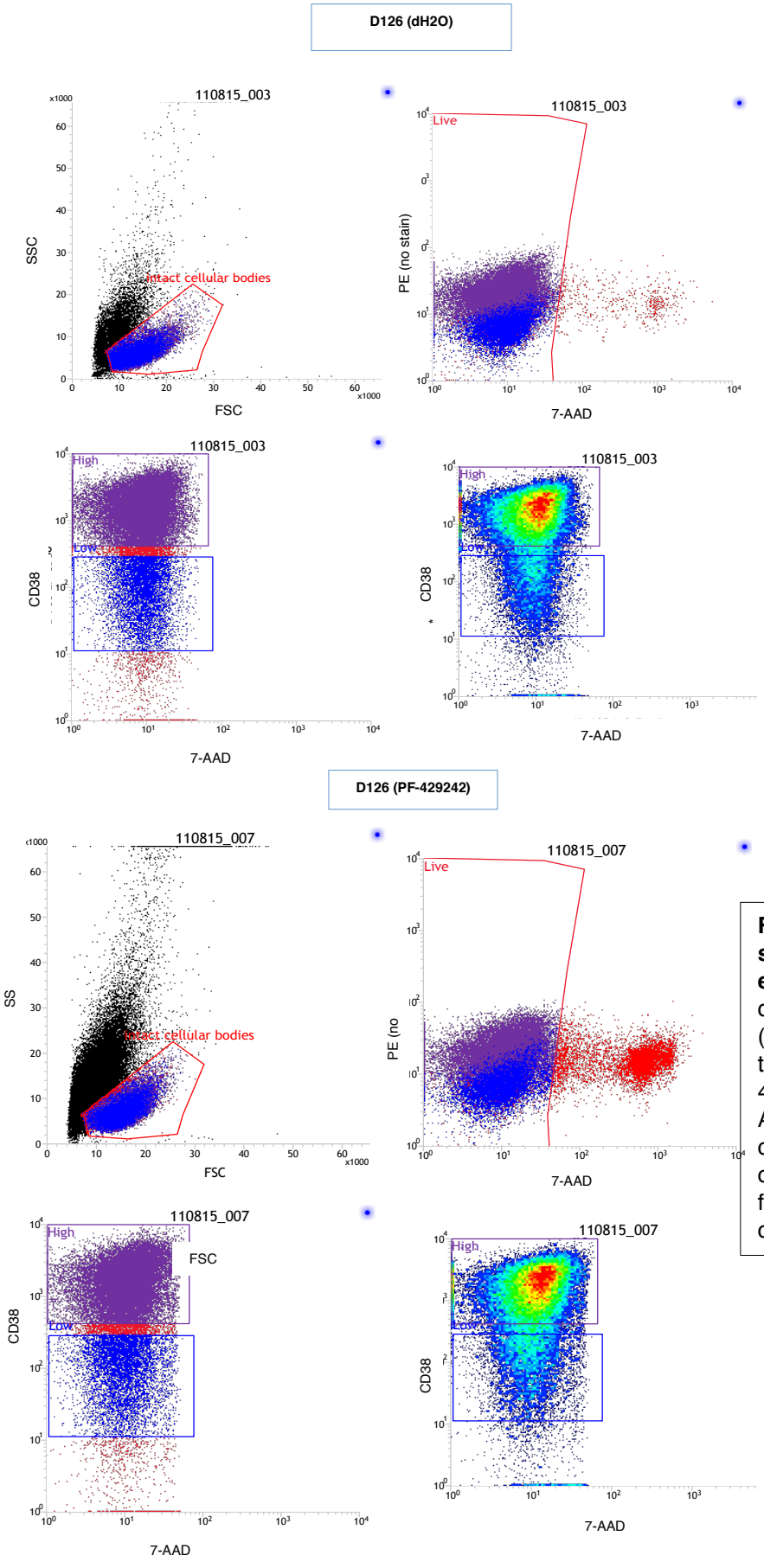


**Figure 6.54 Sorting strategies for ELIspot examination.** Human differentiated B-cells (from three donors) were treated with 10 µM PF-429242 for 72 hours. After the incubation, the cells were sorted based on CD38 (high and low) for treated cells and the control (dH2O).

An equal amount (2,000 cells or 5,000 cells) of the sorted cells ($CD38^{high}$, $CD38^{low}$ from either PF-429242 treatment or dH20 control) were seeded into each well of a 96-well plate and the IgM and IgG secretory cells were enumerated using ELIspot technique (Figure 6.55).

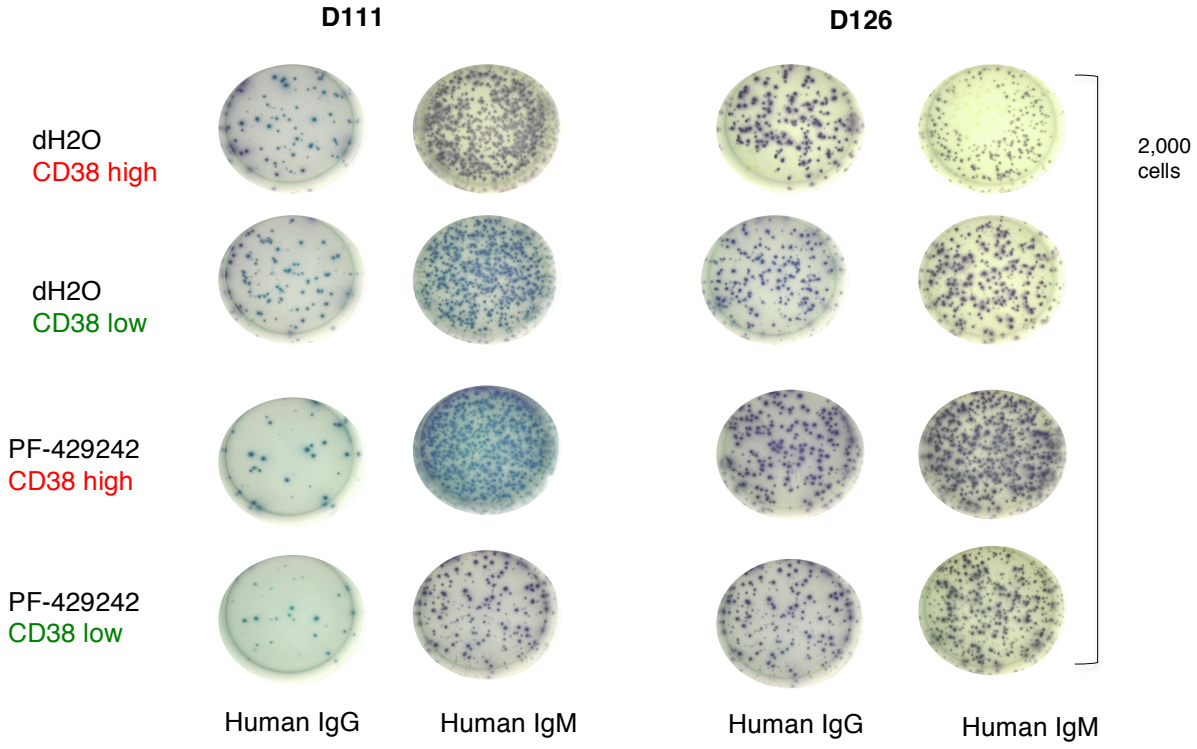


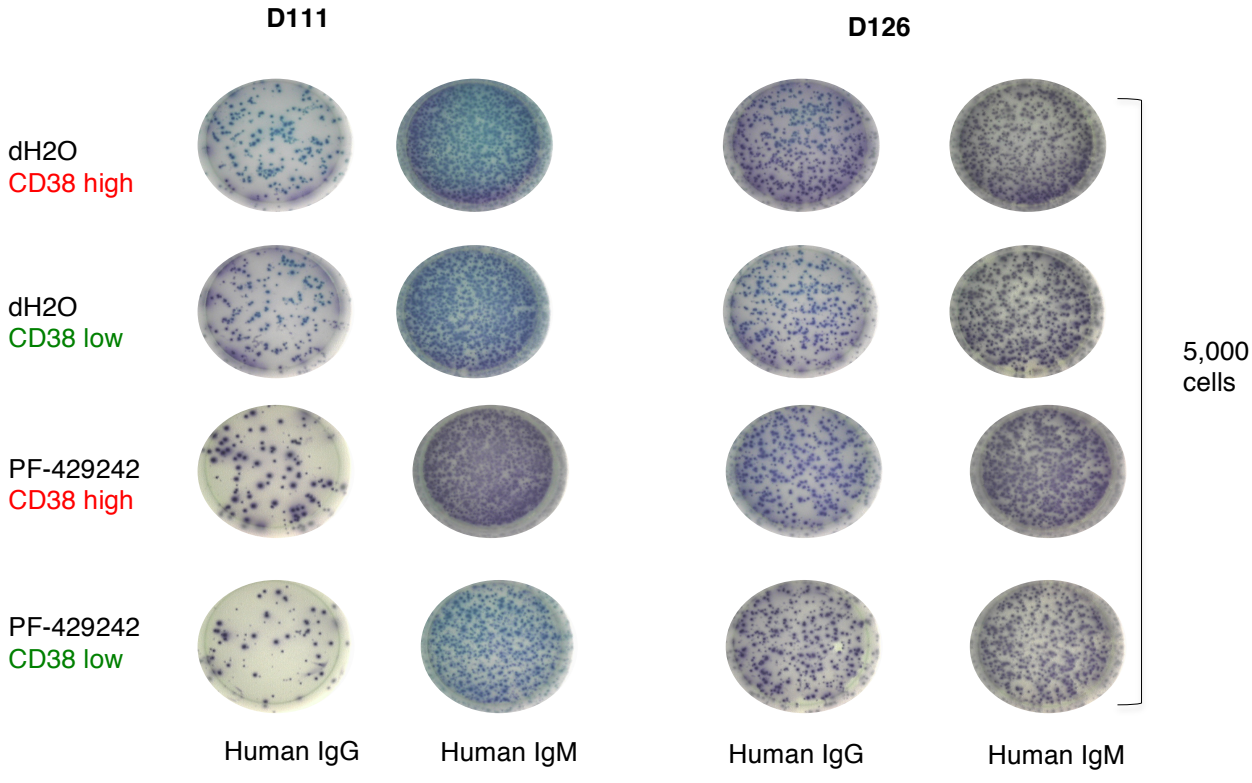

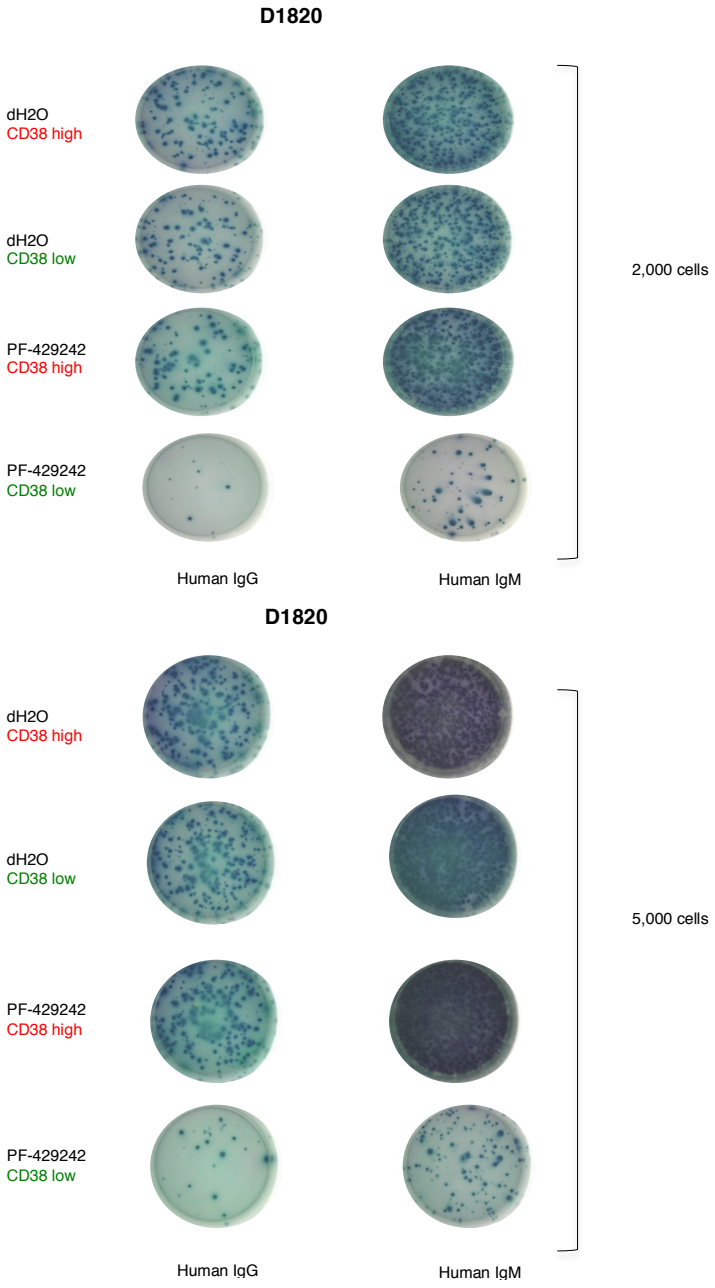


**Figure 6.55 Quantification of IgM and IgG secretory cells by ELIspot.** Human differentiated B-cells (from three donors) were treated with 10 M PF-429242 or dH2O for 72 hours. After the incubation, the cells were sorted based on CD38 expression (high and low). An equal number of the sorted cells (2,000 cells or 5,000 cells) were used to quantify the secretory cells after culturing in the presence of PF-429242 or dH2O using ELIspot technique.

The results revealed an interesting distribution of secretory capacity. In control cultures an equal number of cells from both $CD38^{high}$ and $CD38^{low}$ sorts were capable of secreting IgM, whereas the number of IgG secreting cells was slightly lower in the $CD38^{low}$ population. In terms of PF-429242 treatment, the number of IgM-secreting cells in the $CD38^{high}$ group was comparable to that observed in the control. The number of IgM-secreting cells derived from $CD38^{low}$ was reduced by 2-fold or greater. The most profound effect of PF-429242 was on the generation of IgG-secreting cells. The number of IgG-producing $CD38^{high}$ cells was lower than the control and $CD38^{low}$ production of IgG was severely reduced. Thus, the capacity to secrete immunoglobulin tallied well with the phenotypic characteristics of the cells and treatment with PF-429242 showed a preferential effect on the ability of $CD38^{low}$ to secrete Ig. Furthermore, the capacity to secrete IgG was more profoundly altered by PF-429242, suggesting either a differential effect on naïve versus memory B-cells or a role for S1P in class switching.

## 6.12 Discussion

When B-cells encounter antigen they undergo a process of terminal differentiation to become effector cells that secrete antibodies, which provide protective humoral immunity. This is a step-wise process, during which first the B-cells become activated and start proliferating. The cells then start to lose the B-cell phenotype and acquire changes compatible with antibody secretion. These changes are coordinated by TFs that prepare the cells for high-level secretion. As the cells produce large amounts of immunoglobulin, the UPR becomes activated to cope with the amount of protein transiting the ER. To date, the only branch of the UPR that has been shown to participate is IRE1-XBP1(123). However, results presented in the previous chapters have shown that the ER-stress activated TF CREB3L2 is expressed in myeloma and ABC-DLBCL cell lines. In addition, CREB3L2 is expressed as cells differentiate from activated B-cells to ASCs using the in vitro model. The data presented in Chapter-5 established that S1P/S2P inhibitors could prevent the expression of active CREB3L2. Moreover, these inhibitors also reduced the expression of ATF6 and XBP1. The loss of these proteins would be predicted to have an impact on the generation, maintenance or function of ASCs.

Since CREB3L2 expression is highest in ASCs, initially S1P/S2P inhibitors were tested on cells that had reached the plasmablast or plasma cell stage. To confirm that inhibition of S1P/S2P was affecting protein processing, Western analysis of protein lysates was performed. The results show that the cleavage of CREB3L2 in the ASCs was strongly reduced upon the treatment with inhibitor compared to vehicle at the protein level. Despite this, the inhibitors did not affect the cell counts, cell phenotypes or immunoglobulin levels (IgM and IgG), indicting that inhibition of S1P/S2P did not affect the viability or function of the human differentiated antibody secretory cells when treated on Day-6 or Day-8 or Day-10, suggesting that CREB3L2 or other S1P/S2P-regulated transcription factors are not required for final stages of terminal differentiation.

Although CREB3L2 is most highly expressed in plasma cells, meta-profile analysis of DLBCL gene expression signatures has shown that *CREB3L2* is characteristic of the activated B-cells (ABC) subset (87). Additionally, both the full length and cleaved form of CREB3L2 proteins were detected at low levels in the Day-3 activated B-cells. During the early stages of ASC commitment, IRF4 is the predominant TF that initiates the process, driving transcription of *BLIMP1* and *ZBTB20* that together control the ASC gene network(124, 125). XBP1 is activated later and recent evidence suggests that it is not required to generate ASCs, but does contribute to the production of immunoglobulin(5, 6, 39). Combined, these data indicated that CREB3L2 might actually be operating in the early phases of ASC development, prior to the requirement for XBP1.

The first experiment designed to test this applied PF-429242 or Nelfinavir on Days-3, 4 or 5 during which time the cells are rapidly proliferating. Assessment was made 24 hours post treatment of the drug. Using these conditions there was a marked decrease in the protein levels of CREB3L2, ATF6 and XBP1, but the reduction in *XBP1* splicing observed earlier was not reproduced. There was little change in cell count or phenotype, but some reduction in immunoglobulin production. This was interpreted to mean that the drugs were likely to be having an effect, but the time point was too soon to see much of an impact. Consequently, the test conditions were altered such that cells treated on Day-3 were analysed 72 hours later on Day-6, when the B-cells should have adopted a plasmablast phenotype. In contrast to the earlier results, allowing the cells to undergo several rounds of cell division in the presence of the S1P/S2P inhibitors had a dramatic effect on cell number with an accompanying drop in the level of immunoglobulin production. There was also a change in the phenotype with retention of CD20 and a delay in the upregulation of CD38. These results were repeated on a total of 8 donors.

Work by Hodgkin and colleagues have demonstrated that the probability of becoming a plasma cell increases with cell division(126, 127). After receiving

the appropriate stimulus, the cells start to divide and stochastically decide to undergo further division, ASC differentiation or death. The data obtained with PF-429242 and Nelfinavir suggest that S1P/S2P regulated pathways can alter the output during this phase of expansion. To better understand how this might be happening, gene expression analysis was undertaken.

Strikingly, the genes that were differentially regulated by the drugs contributed to a group of cohesive gene ontology signatures. Focussing on the signatures associated with treatment of PF-429242, there is a clear connection to metabolic regulation. The signatures include multiple aspects of metabolism, such as amino acid synthesis, steroid synthesis, and lipid/cholesterol biosynthetic processes. For example, one of genes that was downregulated by both PF-429242 and Nelfinavir is *ABCA1 (128).*It has been recognised as the gatekeeper for removing excess cholesterol and phospholipids from the tissue to the liver. In macrophages, ABCA1 is part of a complex that maintains cholesterol homeostasis and helps to balance the production of inflammatory cytokines (129). Another gene showing altered expression is *INSIG1*, which also plays a role in cholesterol regulation, as well as lipogenesis and glucose homeostasis (130). Interestingly, INSIG1 binds to SCAP and prevents the transit of SREBP to the Golgi, which is a pre-requisite for SREBP activation, suggesting that there may be a feedback loop for maintaining levels of active SREBP in plasma cells.

These data are in keeping with the prediction that S1P/S2P regulated pathways might be altering the ability of differentiating cells to upregulate the necessary building blocks to expand organelles and cope with increased protein production. Moreover, recent evidence confirms that metabolic programming is essential for plasma cell survival. Upon the encountering T-cell dependent antigen, B-lymphocytes either form short-lived plasma cells that can live for a few days, or enter the germinal centre and undergo somatic hypermutation and CSR forming long-lived plasma cells that can live for years. There are many metabolic pathways that are utilised during B-cell

differentiation however; it is not known which might distinguish between long-lived and short-lived plasma cells. A new study by Lam et al. has now established the metabolic properties associated with survival of long-lived cells. Through examining oxygen consumption rates (OCR), they found that long-lived plasma cells had higher respiratory capacity than the short-lived ones. In addition, long-lived plasma cells are able to persist due to the uptake of glucose and the import of pyruvate (131). It is conceivable that targets of CREB3L2 or other S1P/S2P regulated TFs contribute to this metabolic switch.

Another signature that was identified was mTOR (mammalian Target Of Rapamycin), which is an important signalling mechanism for cell proliferation, differentiation and survival. In the context of B-cells, mTOR is activated in response to the stimulation of BCR or Toll like receptor. Downstream signalling to PI3K/Akt inhibits the negative regulator TSC, resulting in activation of mTOR. mTOR is required to control protein synthesis by the phosphorylation of 4E-BP1 and p70S6K1, which in turn increase cell growth and protein synthesis (123).

Benhamron et al. studied the relationship between mTOR and UPR using XBP1-KO, TSC-KO and DKO mice. They have found that higher immunoglobulin levels were obtained in the DKO mice compared to the XBP1-KO. In addition, they have identified Ly6C as an mTOR target that contributes to the high immunoglobulin level in DKO mice. Moreover, by studying morphology using electron microscopy, they found that the ER is less collapsed in the DKO compared to the XBP1-KO due to the constitutive activation of mTOR. These results suggest that cross talk between mTOR and UPR contribute to the maintenance of ER morphology (123).

Another study has provided further confirmation for a link between the UPR and mTOR, with an additional contribution from BLIMP1. Tellier et al. found that BLIMP1 is not required for maintaining plasma cell identity once it is fully established, which is in fact similar to the results presented in this chapter

showing that S1P/S2P regulated TFs do not appear to be required by mature plasma cells (132). BLIMP1 had previously been shown to act upstream of XBP1 (58). This paper now places BLIMP1 upstream of ATF6 and other UPR components. Moreover, BLIMP1 helps maintain active mTOR by inducing the expression of amino acid supply carriers such as CD98 and preventing sestrin-AMPK mediated inhibition (132). The data from this chapter suggest that S1P/S2P regulated TFs might act in parallel with BLIMP1 to ensure that mTOR remains active to help regulate immunoglobulin production.

The papers described above have added to our knowledge of two of the key transcription factors that play roles in the transition from B-cells to plasma cell formation. However, initiation of the process and maintenance of plasma cell identity are dependent on IRF4 (27, 28). In the GC, IRF4 is expressed in centrocytes but not centroblasts, consistent with an important role in the choice between memory B-cell versus plasma cell formation (27). In addition, it has been found that IRF4 has a dose dependent function. At low concentration, it induces GC formation and CSR through activating *AID* whereas, at high concentration, IRF4 activates *BLIMP1* thus, promoting plasma cell formation (12).

Moreover, IRF4 play an important role in class switch recombination (CSR). Klein et al., have studied the impact of deleting *Irf4* in B-cells on CSR upon CD40 and IL-4 stimulation. They have found that *Irf4*$^{-/-}$ B-cells showed no IgG detected compared to the normal CSR in the wild type suggesting that IRF4 is required for CSR. Moreover, IRF4 induces the expression of number of CSR encoding genes including *Aicda*, *Pou2af1* and *Bcl6*. Therefore, the deletion of *Irf4* leads to the reduced expression of CSR encoding genes and hence reduced production of alternative isotypes (28, 118).

Thus, the association of IRF4 targets with PF-429242 treatment has the potential to help explain two aspects of the changes observed with the drug:

the apparent block in early commitment and possible interference with class switching.

In addition to the highlighted biological processes, treatment with PF-429242 was also found to alter the transcript levels of *CD40LG*. This effect was verified at the protein level, with increased expression of CD154 detected on the surface of B-cells exposed to PF-429242. There is an extensive literature demonstrating that CD40 signalling blocks differentiation of plasma cells, promoting an intermediate memory-like state until removal of the signal allows terminal differentiation to proceed (133-135). Most recently, Basu et al., found that a high level of *Blimp1* is observed in B-cells from $CD40^{-/-}$ mice compared to the wild type in part explaining the inhibitory effect of CD40 on plasma cell formation. In addition, they found that CD40 signalling prevents the early stages of the UPR by reducing the expression of IRE1α via HRD1 (ER resident protein), which is involved in ubiquitination and degradation of unfolded proteins in ER (136). Thus, CD40 acts on multiple levels to restrict plasma cell differentiation and the expression of CD154 on PF-429242 treated B-cells may reinitiate CD40 signalling coupled to abortive differentiation.

The cessation of differentiation upon treatment with either drug was accompanied by reduced proliferation and increased cell death. The observation that PF-429242 treated cells had increased vacuoles (Figure 6.20) suggested that mechanistically the reduction in cell number might be linked to increased autophagy (137). The fact that autophagy markers, in particular LC3, were induced in PF-429242 treated samples compared to the control provided support to this theory. During B-cell activation, autophagy is induced and is required for B-cell differentiation (138). Disturbing the balance of ER stress and autophagy are likely promote apoptosis, as observed in the PF-429242 treated samples.

In contrast to the PF-429242 treated samples, B-cells treated with the S2P inhibitor Nelfinavir generated an abnormally high number of cells with multiple

nuclear lobes or polyploidy. Polyploidy is characterised by the presence of multiple diploids in a cell and can arise through the process of endoreplication, such that the DNA undergo multiple rounds of replications with out cell division (139). Endoreplication usually results in cells with genomic instability and has two forms: endocycle and endomitosis. Endocycle is composed of only two phases; G and S phase and lack the M phase and therefore no cell division. On the other hand, endomitosis is composed of G1, S and G2 but it is characterised by the re-entry in to the S phase from G2 without cell division. Endoreplication inhibits mitosis and also affects cytokinesis, which in turn may cause either cell death or neoplastic proliferation. A recent publication has linked the ER-Golgi trafficking protein RINT1 with genomic stability, ER stress and autophagy (140). It may be that targets affected by Nelfinavir similarly intersect in the regulation of these pathways.

In vivo, cell division is important for generating big pools of B-cell clones in response to cognate antigen. It is linked to CSR, which changes the class of the antibody to enable specialised function. Initiation of CSR can be cytokine dependent, driven by transforming growth factor (TGF-β), interferon-γ (INF-γ) and IL-4 or cytokine independent as exemplified by LPS stimulation(118). In addition, the link between cell division and CSR is cytokine dependent in so far as more cell divisions occur before CSR at low cytokine concentrations. Moreover, cell division is linked with ASC differentiation, with an association between increased number of divisions and the increased probability of becoming an ASC. Cycling B-cells undergo CSR, once they become ASC, CSR ceases. The proliferation (CFSE) and ELispot results in this chapter are likely to be related to the link between B-cell fate with cell division and CSR. S1P/S2P inhibitors delayed proliferation compared with the controls and detailed investigation of the impact of PF-429242 on antibody secretion revealed a greater impact on the production of IgG.

Combined, the results presented in this chapter provide additional evidence that early commitment to ASC fate requires a coordinated process of cell

division, metabolic reprogramming and adaptation to demands of immunoglobulin production. The results additionally provide novel insight into the role that S1P/S2P regulated TFs play in these processes.

# 7. CREB3L2 Function

The data so far highlight the importance of CREB3L2 in human B-cells and ASCs. Given the expression pattern of CREB3L2, It is also anticipated that it is likely to be fulfilling a similar role in ABC-DLBCL. Therefore determining the exact nature CREB3L2 function in the B-cell context is essential.

In this project, several studies have been conducted to study the expression and cleavage of CREB3L2 in myeloma cell lines, ABC-DLBL cell lines and in human differentiating B-cells. In addition, the impact of S1P and S2P inhibition in the studied cell types has been examined. The results have shown that CREB3L2 is highly expressed in each of the cell types and that expression is responsive to ER-stress. Moreover, inhibiting S1P and S2P had a profound inhibitory impact on CREB3L2, which in turn affected cell viability, likely through initiating autophagy. Furthermore, the impact of S1P and S2P inhibition was studied using a gene expression profile experiment. While the results suggest a major effect on cellular metabolism, it is difficult to attribute the change in gene expression to a particular component downstream of S1P/S2P. Therefore, to specifically determine the function of CREB3L2, a combination of loss-of-function using knockdown and ChIP-seq to examine CREB3L2 target genes that are likely to contribute to the metabolic gene signature described in Chapter-6 were conducted.

## 7.1 siRNA mediated knockdown of CREB3L2

The obtained results have shown that CREB3L2 is expressed and cleaved in cell lines representative of post-germinal centre B-cell neoplasms and in the normal B-lineage counterparts generated in vitro. In addition, the generation of the transcriptionally active form of CREB3L2 can be inhibited using site-1 and site-2 protease inhibitors (PF-429242 and Nelfinavir, respectively). However, the inhibitors have a more far-reaching effect than the inhibition of active CREB3L2 and potentially block several arms of the ER-stress response, including XBP1, ATF6 and SREBP. To determine the specific effect of

CREB3L2 on differentiating B-cells knockdown experiments were attempted using two different types of *CREB3L2* siRNA, alone or in combination.

### 7.1A CREB3L2 knockdown in myeloma cell lines

Initially, the ability to use siRNA to achieve knockdown of CREB3L2 was tested in myeloma cell lines H929 and U266 using two different *CREB3L2* siRNA#1 and #2 (cat No 4392420 siRNA ID No s34890, s34891 respectively). *CREB3L2* siRNA#1 targets both *CREB3L2* isoforms (the long and short); however, *CREB3L2* siRNA#2 targets only one isoform (the long one) (Figure-7.1).

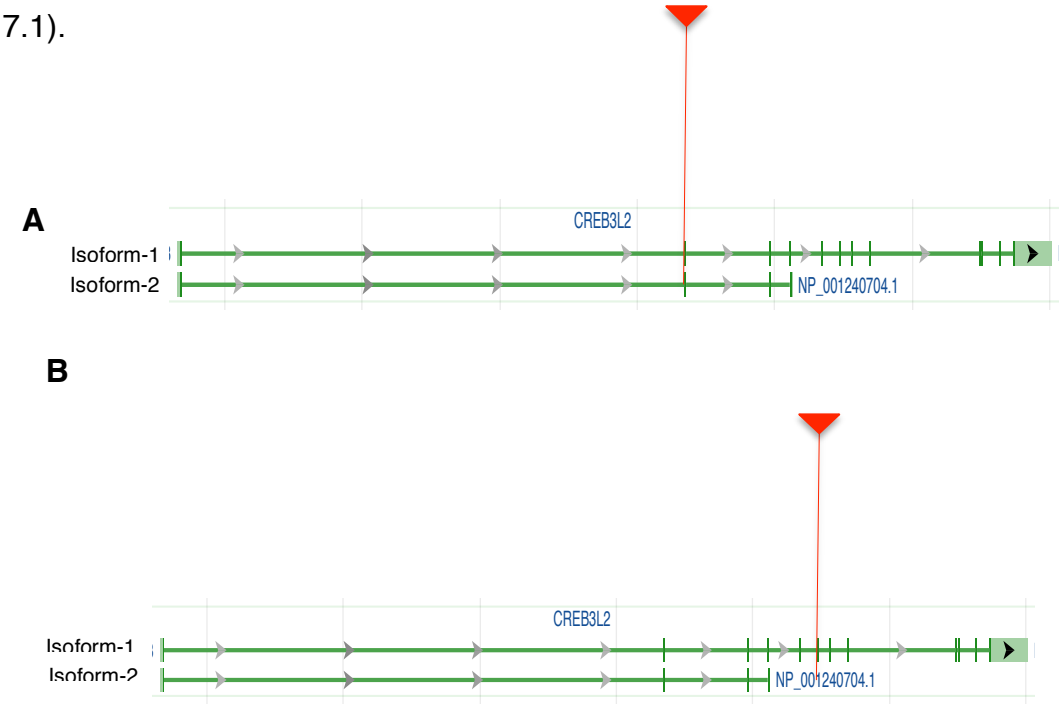


**Figure 7.1: Targeting of *CREB3L2* by siRNA.** A. Diagrammatic representation of the location of *CREB3L2* siRNA#1 on the two isoforms of CREB3L2. B. Diagrammatic representation of the location of *CREB3L2* siRNA#2 on the two isoforms of CREB3L2. The diagram shows the intron/exon structure of *CREB3L2* isoforms modified from the NCBI entry. The red line shows where the siRNAs bind to *CREB3L2*.

H929 and U266 were transfected with 400 pmoles of *CREB3L2* siRNA#1 as a first dose to knockdown CREB3L2 for 24hr or 48hr. At each time point, cells were collected and stored for protein and RNA preparation. By using *CREB3L2* siRNA#1 that is predicted to target *CREB3L2* isoform 1 and 2, the results revealed around 90% of CREB3L2 knockdown in both H929 and U266 cell lines, at both 24 hours and 48 hours post transfection. To control for non-specific effects two conditions were used: firstly, untransfected cells (H929 or U266: UnTr) were included to measure the effect of nucleofection on the cells to avoid false negative interpretation and secondly non-targeting, scrambled siRNA which acts as negative control for CREB3L2 was transfected in a separate tube. In H929 cells there appeared to be fairly substantial reduction in the amount of CREB3L2 in the scramble treated cells as compared to the cells that were not exposed to siRNA (Figure-7.2). This was more pronounced at 24h. At the 48h time point, both cell lines had fairly comparable amounts of CREB3L2 for both Untr and the scramble control, suggesting that this may be a better time point for evaluation. In both cell lines, additional bands between 50-55kDa were observed, but these do not correspond to the full length or cleaved form of CREB3L2 and were not affected by the *CREB3L2* siRNA (Figure-7.2).

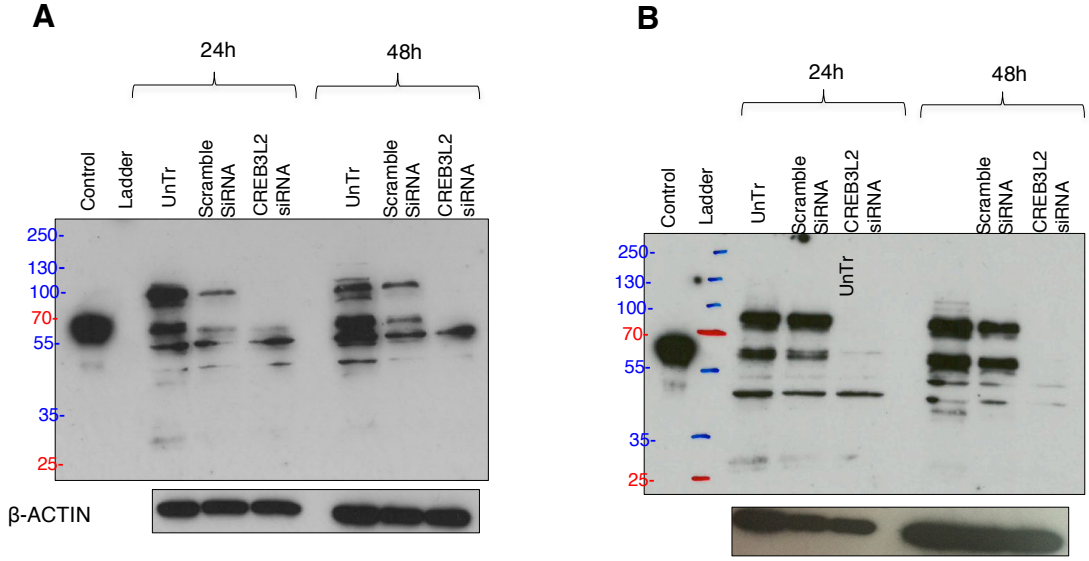


**Figure 7.2: Testing CREB3L2 knockdown efficacy in myeloma cell lines using siRNA#1. A**. H929 cells were transfected using siRNA#1 for 24hr and 48hr. **B**. U266 cells were transfected using siRNA#1 for 24hrs and 48hrs. Protein lysates were assessed by Western blot for CREB3L2. CREB3L2 (1-375 a.a.) was overexpressed in Hela cells and used as control for the cleaved form. UnTr, Untransfected myeloma cells. β-ACTIN was used as loading control.

Although there are potentially two isoforms of *CREB3L2*, the function of the short form remains speculative and only the longer form encodes a protein with the documented activity of a transcription factor. To provide additional evidence that changes observed after knockdown were linked to the long isoform, H929 and U266 were transfected with 400 pmoles of *CREB3L2* siRNA#2 (100µM stock) for 12hr (not shown), 24hr or 48hr. Moreover, it is recommended in knockdown experiments to use more than one siRNA to increase the effectiveness of testing and to minimize any off-target effects.
At each time point, cells were collected and stored for protein and RNA testing. Using *CREB3L2* siRNA#2, which targets CREB3L2 isoform1 only revealed around 70-80% of CREB3L2 knockdown in H929 cell line, at 24 and 48 hours (Figure-7.3). As observed in the previous experiment, transfection with the scrambled control resulted in a loss of CREB3L2 at the 24hr time point, but at 48hr the levels of CREB3L2 in Untr versus scrambled were very similar.

Although high levels of knockdown were achieved using individual siRNAs, since the two target distinct regions it was possible that combined introduction of both siRNAs might lead to a more profound CREB3L2 deficiency. To test this H929 cells were transfected with a pool of *CREB3L2* siRNA#1and siRNA#2 and cultured for 24hr or 48hr. At each time point, cells were collected and stored for protein and RNA testing.

By simultaneously using *CREB3L2* siRNA#1 and *CREB3L2* siRNA#2 (pool) that target both CREB3L2 isoforms, CREB3L2 was virtually undetectable in the H929 cell line (Figure-7.3). Thus, although siRNA#1 was highly efficient, a combination of the two siRNAs resulted in a complete loss of protein.

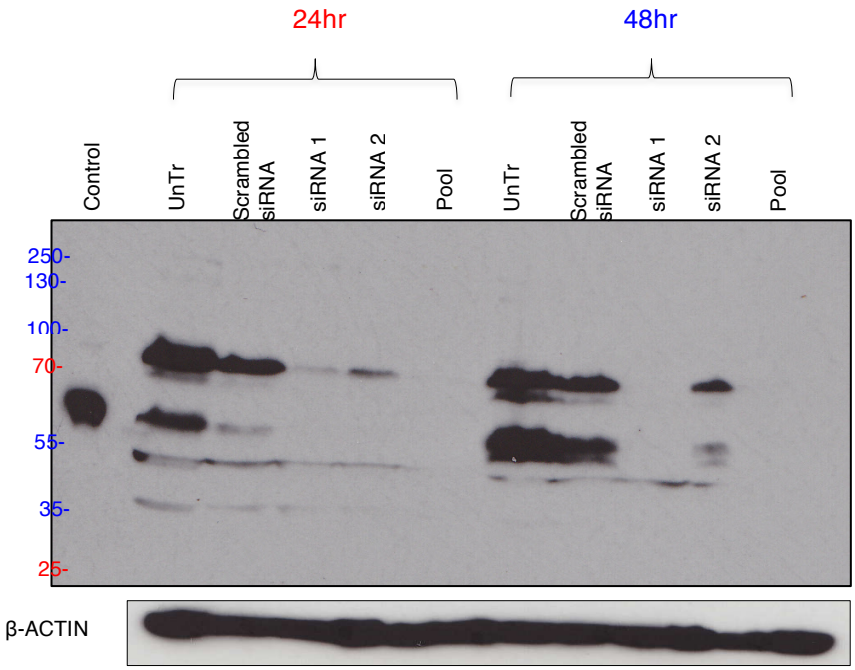


**Figure 7.3: Testing CREB3L2 function in myeloma cell lines (H929) using siRNA#1, #2 and pool (siRNA#1 and #2).** H929 cells were transfected with either siRNA#1 or siRNA#2 or pool for 24hrs and 48hrs and then assessed for CREB3L2 expression levels by Western blot. CREB3L2 (1-375 a.a) was overexpressed in to Hela cells and used as control for the cleaved product of CREB3L2. UnTr, Untransfected myeloma cells. β-ACTIN was used as loading control.

### 7.1 B CREB3L2 knockdown in human differentiated B-cells

The results in Figure-4.5 have shown that CREB3L2 is expressed in activated human B-cells, increasing as the cells progress to the plasma cell stage (Day-3 to Day-13). In addition, it has been shown that high expression of *CREB3L2* is a characteristic feature of ABC-DLBCL, which share a similar gene expression signature to the activated B-cells obtained at Day-3 during the in vitro differentiation process. The removal of Day-3 activated B-cells from CD40L-expressing cells is key to initiating differentiation and results in a rapid acquisition of new phenotype and underlying gene expression which accompany the development of antibody secretion. Therefore, Day-3 B-cells were deemed to be the best stage to prevent CREB3L2 function in human differentiated B-cells. Thus, CREB3L2 knockdown was performed in human

differentiated B-cells (Day-3) using the same siRNAs that have been used in myeloma cell line knockdown studies.

Day-3 cells were transfected with 400 pmoles of *CREB3L2* siRNA#1 to knockdown CREB3L2 for 12hr, 24hr and 48hr. At each time point, cells were collected and stored for protein examination and RNA testing using gene expression profile analysis. Similar to the H929 experiment, the introduction of scrambled siRNA lead to some reduction of the processed form of CREB3L2 at 24hr, but if anything increased full-length CREB3L2 at the 48hr time point (Figure-7.4). Approximately 40-50% CREB3L2 knockdown was observed at all time points, which was considered to be suboptimal for evaluating the impact of CREB3L2 deficiency.

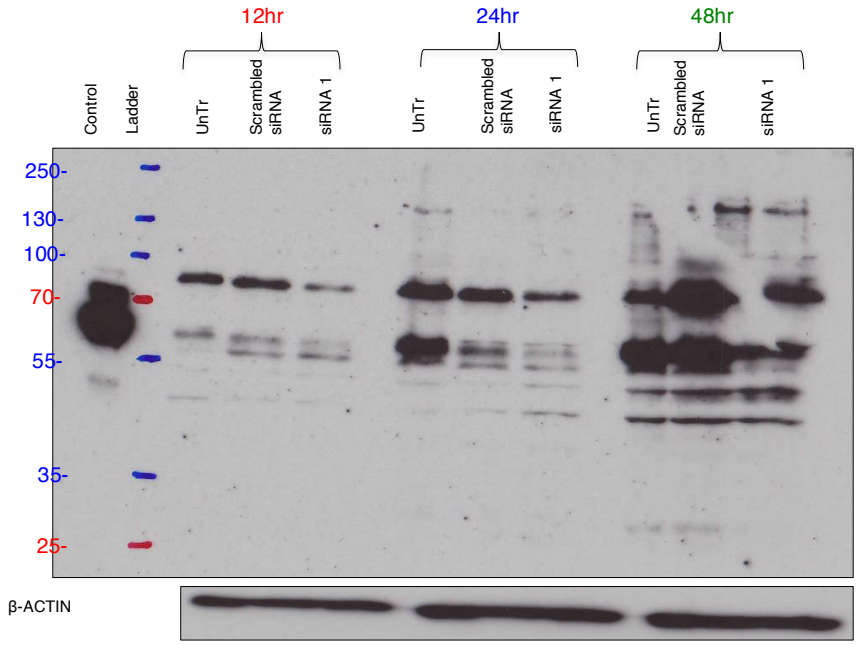


**Figure 7.4: Testing CREB3L2 knockdown in human differentiated B-cells (Day-3) using 400pmoles of siRNA#1.** Day-3 B-cells were transfected with 400pmoles of siRNA#1 and cultured for 12hr, 24hr or 48hr. Lysates were analysed by Western blot for CREB3L2 expression. CREB3L2 (1-375 a.a) was overexpressed in Hela cells and used as control for the cleaved product of CREB3L2. UnTr, Untransfected human B-cells. β-ACTIN was used as loading control.

### 7.1.B2 600 pmoles siRNA#1

In an attempt to achieve a higher degree of knockdown, 600 pmoles of siRNA#1 was used to transfect Day-3 B-cells from two donors and then evaluated at 24hr or 48hrs. Transfection with a higher level of control scrambled siRNA had no detectable effect on the full length CREB3L2, but did appear to result in lower amounts of the processed from, particularly at the earlier time point in both donors (Figure-7.5). However, both donors showed approximately 80-90% of CREB3L2 knockdown. The knockdown was greater at the 24hr time point, but still substantial at 48hr.

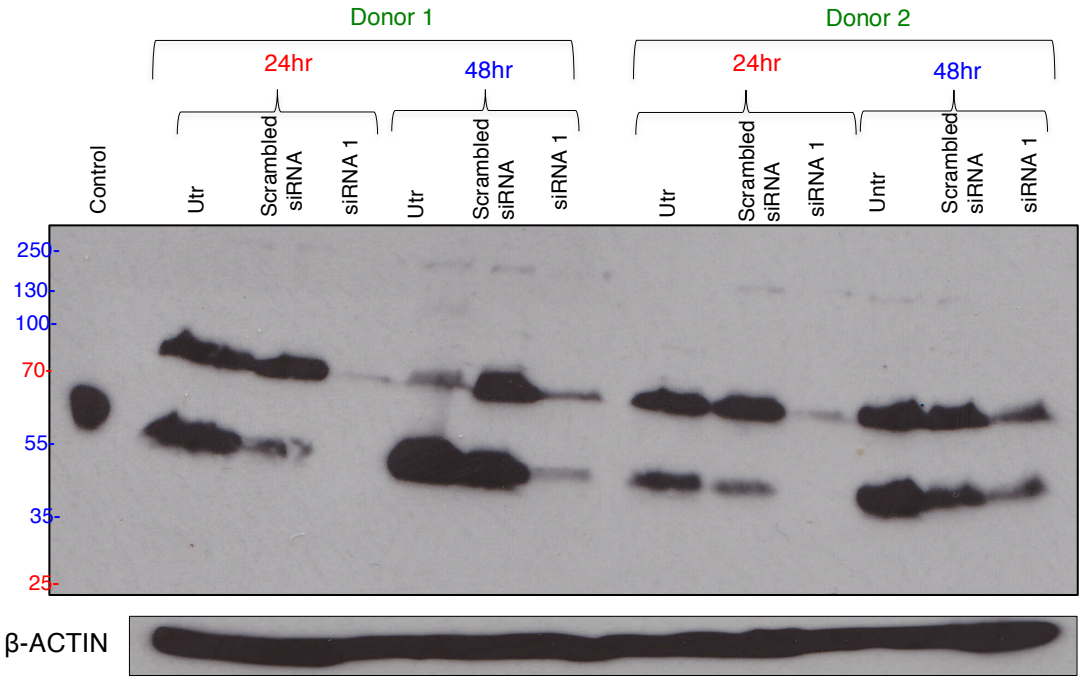


**Figure 7.5: Testing CREB3L2 knockdown in human differentiating B-cells (Day-3).** Day-3 B-cells were transfected with 600pmoles of siRNA#1 and analysed at 24hr or 48hrs. . Lysates were analysed by Western blot for CREB3L2 expression. CREB3L2 (1-375 a.a.) was overexpressed in Hela cells and used as control for the cleaved product of CREB3L2. Utr, Un-transfected human B-cells. β-ACTIN was used as loading control.

Although 80-90% of CREB3L2 knockdown was achieved at the protein level, the effect on the mRNA level of *CREB3L2* was modest, showing a 1.6-fold reduction at 24 hours and normal expression levels by 48 hours (data not shown). While the changes in gene expression amongst the 3 donors did not reach statistical significance after false discovery rate correction, there were some interesting trends in genes that showed differential expression after CREB3L2 knockdown (Figure-7.6 and -7.7). For example, it is notable that amongst the genes that increase expression when CREB3L2 is knocked down, several are associated with plasma cell development, including *PRDM1*, *XBP1*, *CXCR4*, *MZB1* and *JCHAIN* as well as genes that are associated with ER-stress responses such as *CERC1*, *SYVN1*, *RRBP1* and *SDF2L1(141, 142).* On the other hand, genes that were lower such as *PLAC8*, *BNIP3* and *PFKFB4* have been linked to autophagy (143, 144). Although the changes were not significant, the fact that some of the most highly differentially expressed genes were common to the S1P/S2P inhibition experiment, such as *ALDOC1*, *PFKFB4*, *BNIP3* and *CD83* (Figure-7.6), suggests that the changes might reach significance if the experiment was repeated.

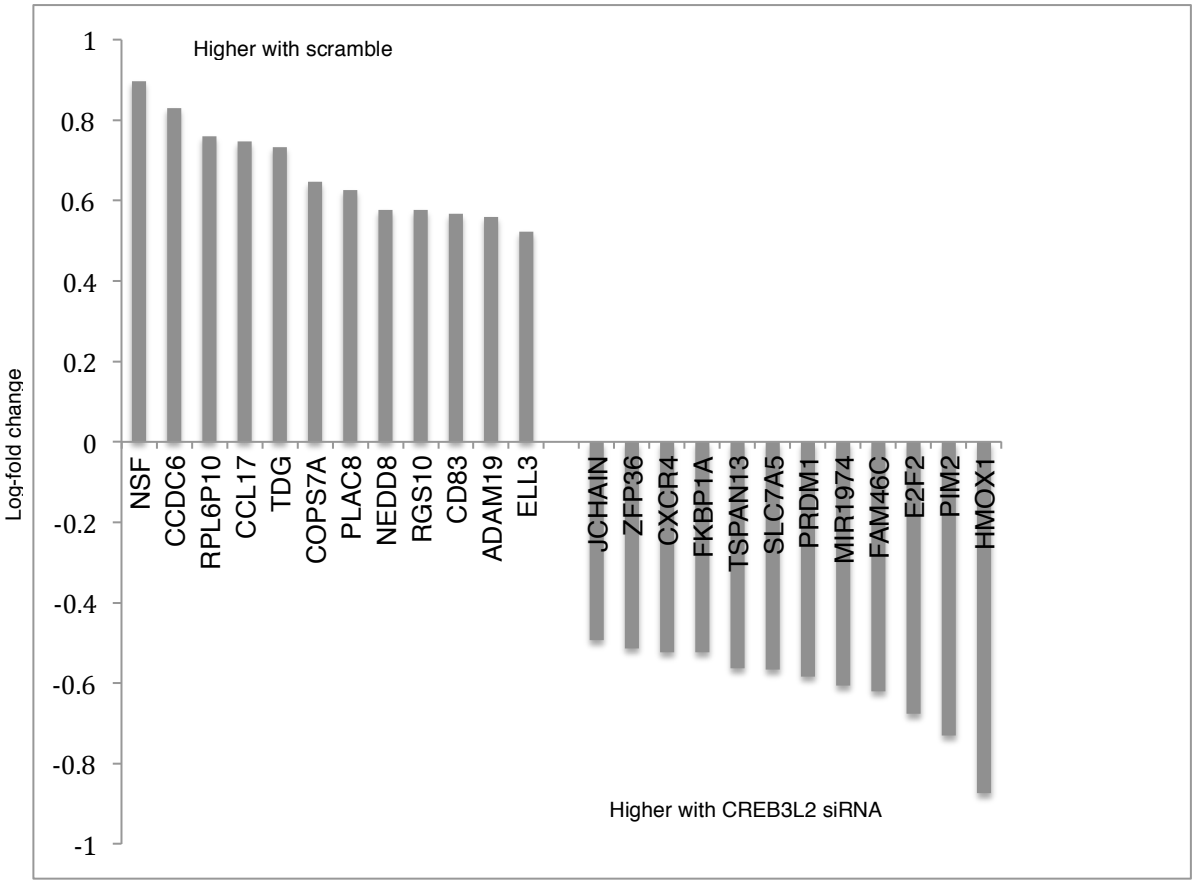


**Figure-7.6:** Gene expression analysis was performed on triplicate knockdown samples and example changes in genes at 24 hours are shown.

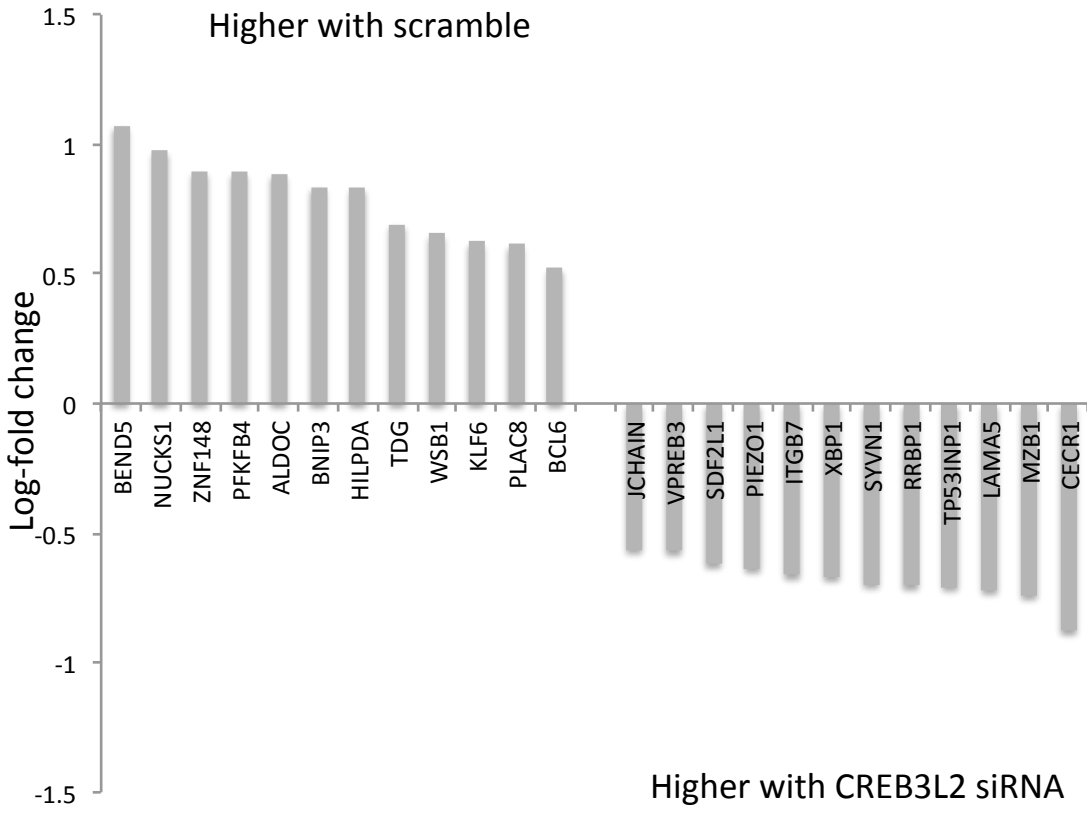


**Figure-7.7:** Gene expression analysis was performed on triplicate knockdown samples and example changes in genes at 48 hours are shown.

## 7.2 Assessment of direct CREB3L2 targets by Chromatin Immunoprecipitation

### 7.2.1 Chromatin Immunoprecepitation Assay (ChIP)

ChIP is used to identify the interaction between a protein (e.g. transcripition factor) and some genomic DNA (e.g target genes). In Chapter-3, two commercial antibodies against CREB3L2 were shown to work for immunoprecipitation and would likely also be effective reagents to use in ChIP. Therefore, initial experiments were performed in myeloma cell lines (U266 and H929) and human differentiated plasmablasts to identify CREB3L2 target genes.

ChIP was performed in U266 cells and analysed by real time-PCR (Figure-7.8). The loci evaluated were based on previously identified CREB3L2 target genes (35, 84, 85) and genes featuring potential CRE regulatory motifs. Of the seven loci evaluated, the results highlight *XBP1* and *ATF4* as possible CREB3L2 target genes in U266.

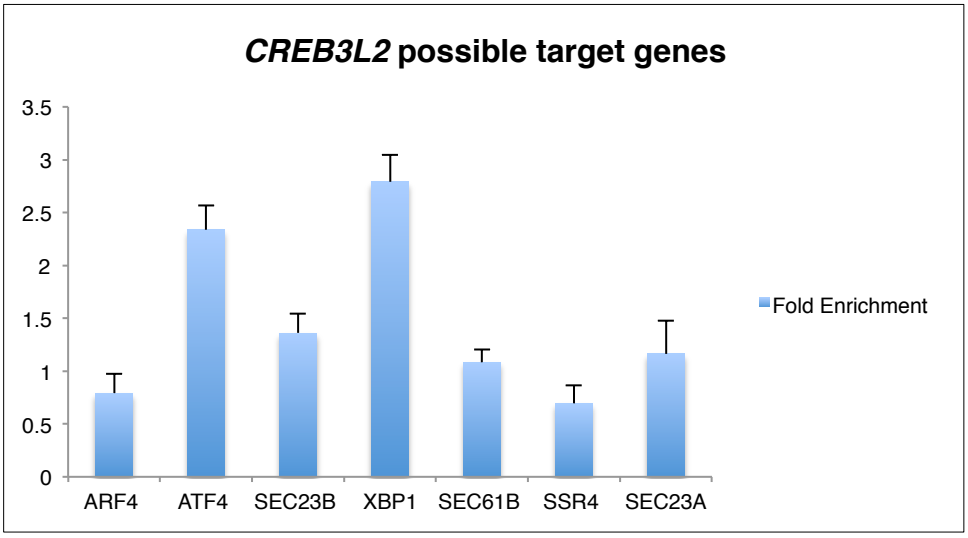


**Figure-7.8: Evaluation of CREB3L2 binding to predicted target genes in the myeloma cell line U266.** Duplicate ChIPs were performed using anti-CREB3L2 and chromatin prepared from U266 cells. The data are averages of the two ChIPs plotted as fold enrichment relative to a control ChIP with rabbit IgG.

As shown in Chapter-3, CREB3L2 is expressed and cleaved in myeloma cell lines (H929 and U266) upon treatment with one of the ER stressors (thapsigargin; TG) for 2 hr or 4 hrs. Therefore, U266 and H929 cells were treated with TG for 4 hrs and then the ChIP samples were prepared and analysed by real time-PCR (Figure-7.9). Additionally, the cells were pre-treated with 10μM PF-429242 for 24 hrs prior to ChIP-qPCR (Figure-7.9).

The results show an increase in the fold enrichment relative to isotype control upon 1μM TG treatment for the proposed targets *ATF4*, *SEC23B* and *XBP1* (Figure-7.9). Consistent with the result in Figure-7.6, there was no enrichment

of binding at the *ARF4* locus. In contrast, there was a sharp decrease in the fold enrichment upon 10μM PF-429242 treatment, providing further evidence that there is an interaction between CREB3L2 and the possible target genes.

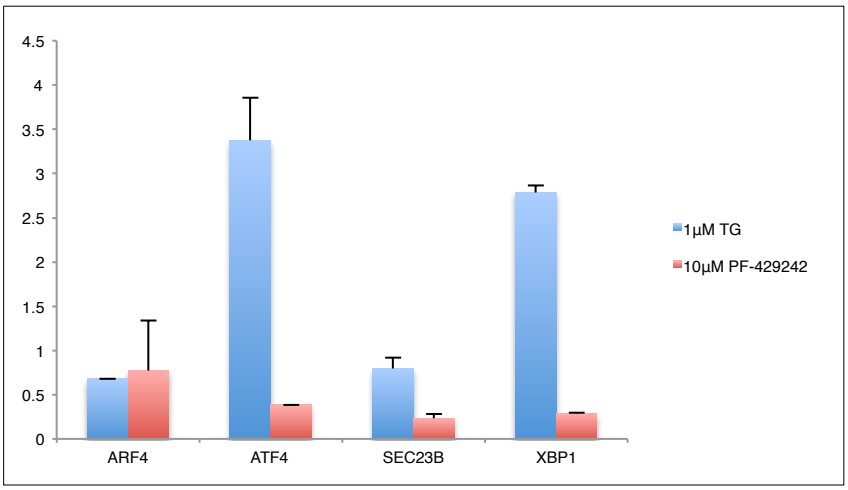


**Figure-7.9: Evaluation of CREB3L2 binding to target genes following 1μM thapsigargin (TG) or 10μM PF-429242 treatment in U266.** Duplicate ChIPs were performed using anti-CREB3L2 and chromatin prepared from U266 cells. The data are averages of the two ChIPs plotted as fold enrichment relative to a control ChIP with rabbit IgG.

In addition, H929 cells were treated with the ER stressor (TG), S1P inhibitor (10μM PF-429242) or S2P inhibitor (10μM Nelfinavir) and the fold enrichment of CREB3L2 binding to target genes was obtained (Figure-7.10). In the steady state, CREB3L2 binding was detected at both *ATF4* and *XBP1*. Upon treatment with ER stressor (TG), the level of CREB3L2 binding increased, with good enrichment at *ATF4* and *XBP1* and weak binding to *SEC32B*. Treatment with10μM PF-429242 or 10μM Nelfinavir reduced binding to levels equivalent or below that seen in steady state, giving further credibility to the ChIP results.

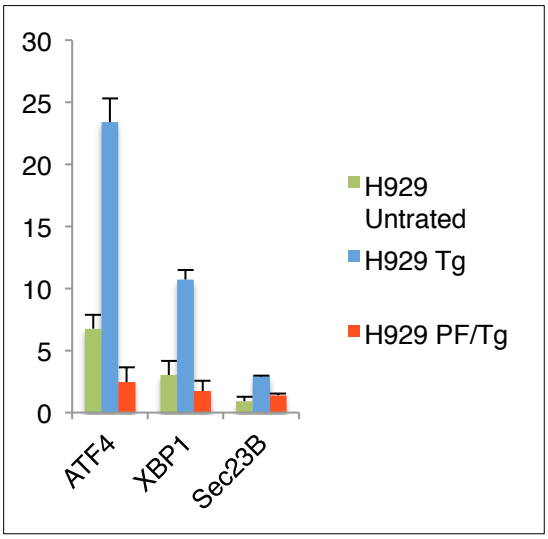


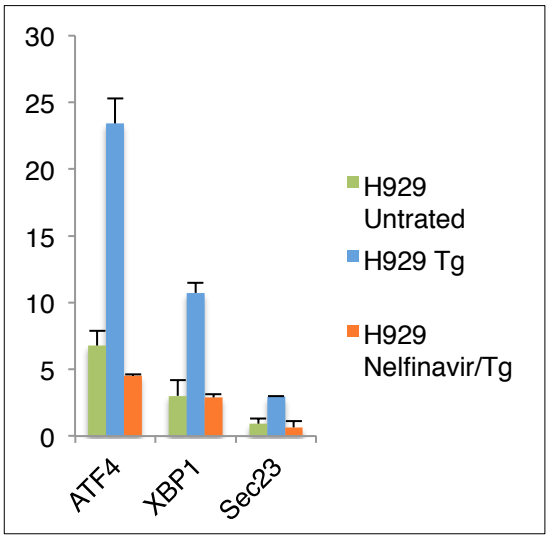


**Figure-7.10: Evaluation of CREB3L2 binding to target genes following 1μM thapsigargin (TG), 10μM PF-429242 or 10μM Nelfinavir treatment in H929.** Duplicate ChIPs were performed using anti-CREB3L2 and chromatin prepared from H929 cells. The data are averages of the two ChIPs plotted as fold enrichment relative to a control ChIP with rabbit IgG.

### 7.2.2 ChIP-seq

The experiments presented in the previous three figures suggest that the CREB3L2 antibody works for ChIP and has the potential to be used to identify novel targets of this transcription factor. Moreover, since the binding motif of CREB3L2 is predicted to be similar to that of other CREB or ATF family members and CREB3L2 is likely to work alongside other UPR-related transcription factors, it was of interest to determine the extent to which CREB3L2 binding is detected in proximity to these other factors. To this end, ChIP samples were prepared from Day-6 in vitro generated plasmablasts using antibodies against CREB3L2, ATF6 and XBP1. The resulting material was subject to next generation sequencing and analysed for detection of peaks associated with binding.

In total, 69,515 peaks were associated with CREB3L2, 30,260 with ATF6 and 492 with XBP1. The degree of overlap of these three transcription factors was then calculated. The number of overlapping peaks is shown in Figure-7.11. Although the total number of XBP1 peaks was relatively small, there was a substantial amount of overlap with the other two transcription factors. ATF6 peaks were observed in 25% of the XBP1-associated loci and CREB3L2 binding occurred in 18% of the same loci as XBP1. Additionally, all 3 factors were found to co-localise in 78 peak regions, which equates to 16% of XBP1 bound sites.

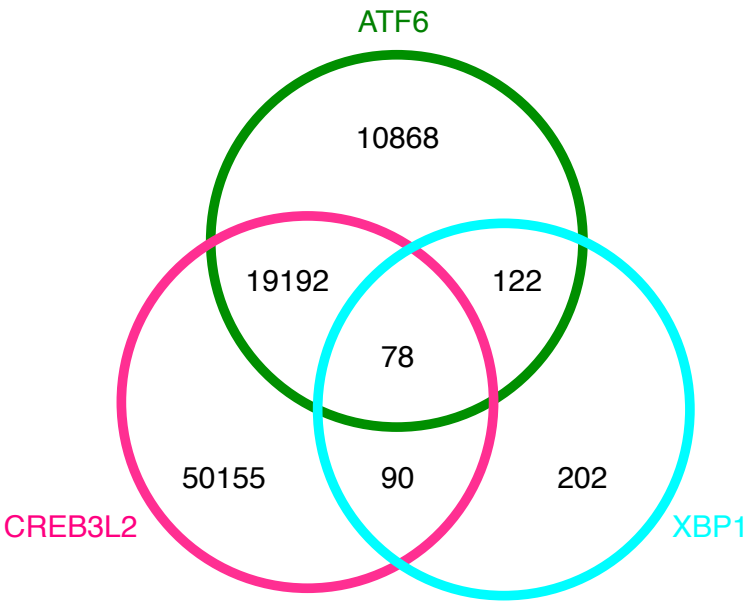


**Figure-7.11: Distribution of CREB3L2, ATF6 and XBP1 peaks in plasmablasts.** ChIP-seq for ATF6, CREB3L2 and XBP1 was performed using day 6 plasmablasts. The overlap of binding for the indicated transcription factor is shown on the Venn diagram.

To provide evidence that the observed peaks were meaningful in terms of the function of these TFs, binding patterns were evaluated in loci identified in the gene expression experiments from Chapter-6 and Chapter-7. Figure-7.12 shows the occupancy of loci that were differentially expressed after incubation of differentiating B-cells with the S1P or S2P inhibitors. Interestingly, the 4 selected genes show evidence of ATF6 and CREB3L2 binding, but no detectable XBP1.

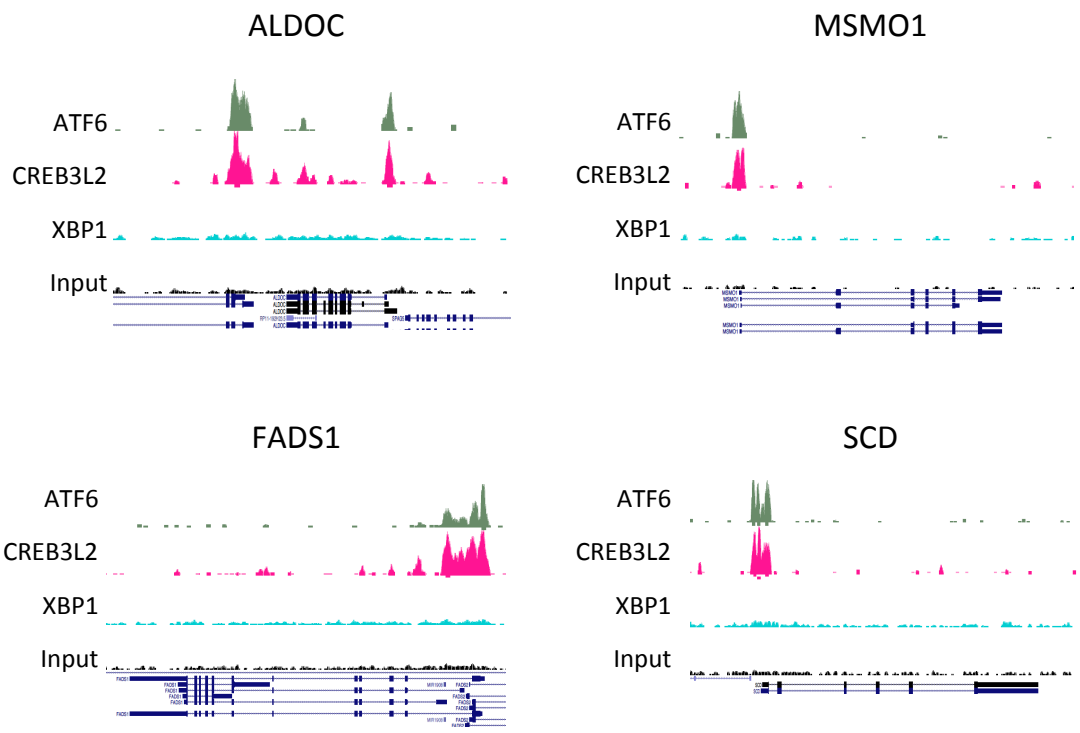


**Figure-7.12: Occupancy of ATF6, CREB3L2 and XBP1 in loci that were differentially expressed after S1P/S2P inhibition.** ChIP-seq was performed using day 6 plasmablasts with the transcription factor indicated on the left. Genomic input was used for normalisation. Example tracks for *ALDOC*, *MSMO1*, *FADS1* and *SCD* loci are displayed with the gene structure shown at the bottom.

Similarly, representative loci that showed changes upon siRNA-mediated knockdown of CREB3L2 had evidence of direct binding by this factor (Figure-7.13 and 7.14). While these are only a few examples, the genes that were down-regulated after siRNA treatment only have ATF6 and CREB3L2 binding whereas the genes that were more highly expressed are also bound by XBP1.

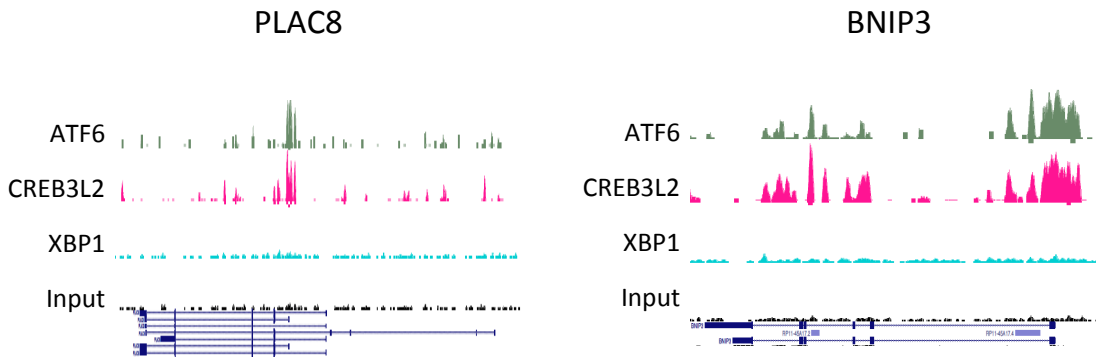


**Figure-7.13: Occupancy of ATF6, CREB3L2 and XBP1 in loci that were more highly expressed in scramble transfected cells.** ChIP-seq was performed using day 6 plasmablasts with the transcription factor indicated on the left. Genomic input was used for normalisation. Example tracks for *PLAC8* and *BNIP3* loci are displayed with the gene structure shown at the bottom.

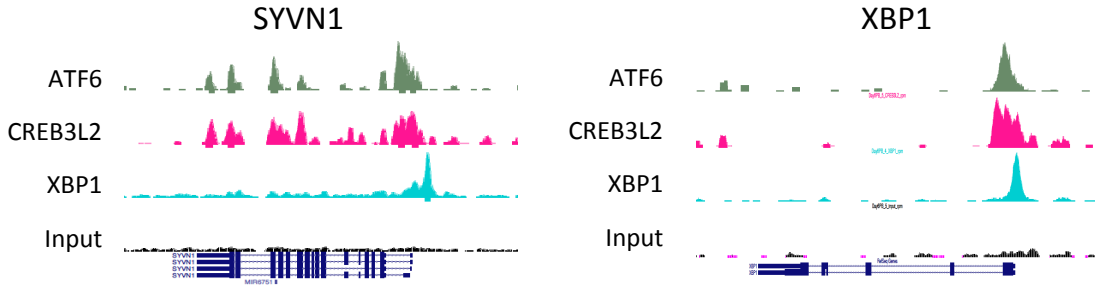


**Figure-7.14: Occupancy of ATF6, CREB3L2 and XBP1 in loci that were more highly expressed in CREB3L2-siRNA transfected cells.** ChIP-seq was performed using day 6 plasmablasts with the transcription factor indicated on the left. Genomic input was used for normalisation. Example tracks for *SYVN1* and *XBP1* loci are displayed with the gene structure shown at the bottom.

Finally, as an indication of whether CREB3L2 is likely to be regulating the UPR in ASCs, examples of UPR-associated genes were examined for the presence of binding. Genes classically associated with the UPR, including *ATF4*, *HSP90B1* and *HERPUD1* showed occupancy by the 3 factors. The 78 genes featuring this binding pattern are likely to make important contributions to the ability of ASCs to adapt to high-level immunoglobulin secretion. *UFL1* is a gene not previously associated with plasma cell differentiation, but has been highlighted by the results of the ChIP-seq experiment.

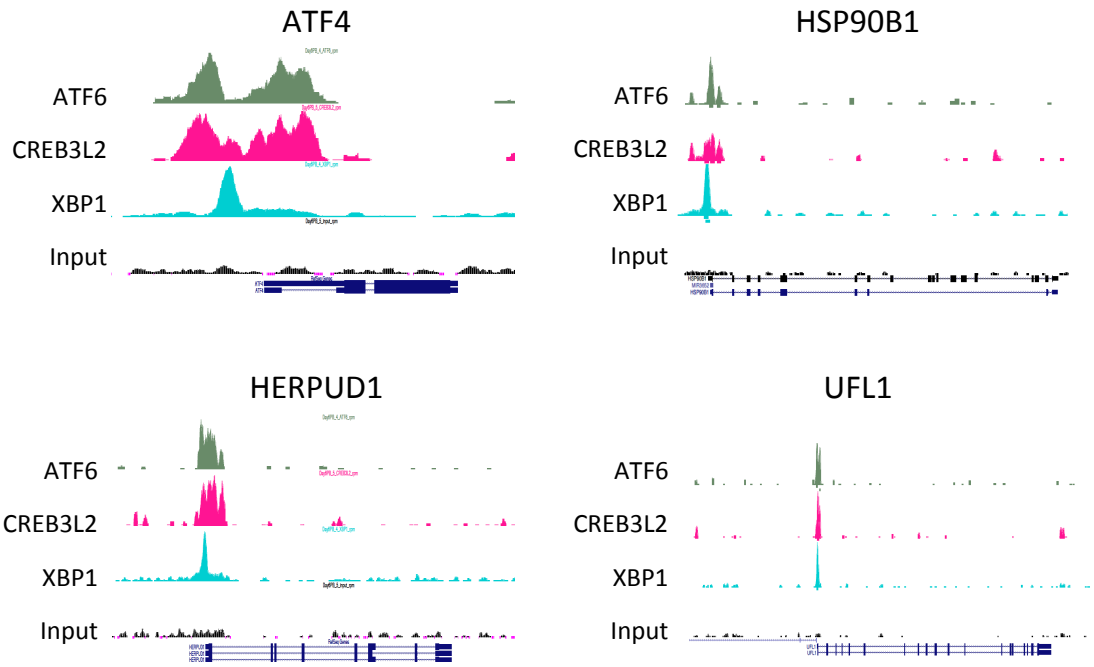


**Figure-7.15: Occupancy of ATF6, CREB3L2 and XBP1 in loci that are associated with the UPR.** ChIP-seq was performed using day 6 plasmablasts with the transcription factor indicated on the left. Genomic input was used for normalisation. Example tracks for *ATF4, HSP90B1, HERPUD1* and *UFL1* loci are displayed with the gene structure shown at the bottom.

## 7.3 Discussion

The previous chapters have established that active CREB3L2 is incrementally expressed in primary B-cells making the transition to become ASCs and is also observed in neoplastic cell lines representative of these stages. CREB3L2 is induced by ER-stress and active CREB3L2 is generated by proteolytic cleavage mediated by S1P/S2P. The experiments in the preceding chapters provided evidence that pathways downstream of S1P/S2P can profoundly influence the outcome of plasma cell differentiation. The goal of this chapter was to establish the contribution of CREB3L2 to this process.

Initially, attempts were made to knockdown CREB3L2 using siRNA to determine the effect of reduced CREB3L2 protein levels. CREB3L2 was effectively targeted in two different myeloma cell lines (U266 and H929), reaching a near complete loss of protein by 48 hours post transfection. Likewise, introduction of siRNA into Day-3 differentiating B-cells resulted in almost undetectable levels of CREB3L2 at a 48hr time point. However, the negative control siRNA also led to a reduction in the amount of CREB3L2, particularly at the 24hr time point. While the reason for this is not precisely known, siRNAs can be associated with off-target effects such as microRNA-like recognition of other targets, activation of TLRs or overload of the RNAi processing machinery (145). Since the knockdown appeared to be quite efficient in the primary cells, microarray analysis of the mRNA expression in these samples was carried out.

Although the protein levels of CREB3L2 were dramatically reduced, the change in *CREB3L2* message level was modest. This could be due to the siRNA exerting its effect at the level of translation, similar to a microRNA (146). Disappointingly, the change in gene expression when comparing *CREB3L2* siRNA treated samples to the control siRNA was also modest and did not reach statistical significance. This may be in part due to the fact that the control siRNA also had an impact on CREB3L2 levels. Additional

experiments would be required to establish a more specific knockdown, potentially using alternative siRNAs or an shRNA vector. Nonetheless, there were some genes that looked promising as targets of CREB3L2 regulation. For example BNIP3 has a documented role in autophagy(147, 148) and mitophagy in particular. BNIP3 has been shown to regulate the levels of mitochondria in response to increased demands on mitochondrial respiratory activity(149) as might also be experienced in ASC. A recent publication also identified a role for BNIP3 in the survival of long-lived “memory” NK cells (150) that are generated after an initial proliferative response to virus followed by a contraction phase, similar to what is observed during the plasmablast to plasma cell transition.

It was noticeable that a number of genes associated with plasma cell differentiation and ER-stress were in fact up-regulated upon CREB3L2 knockdown, contrary to what might have been predicted. Although the precise binding motif of CREB3L2 is yet to be established, the underlying DNA sequence is likely to be very similar to that recognised by other CREB or ATF family members. Upon knockdown of CREB3L2 these may be able to substitute to provide some degree of redundancy. This may also partly explain why a greater effect was seen with the S1P/S2P inhibitors. During knockdown of CREB3L2 these other factors may overcompensate and actually lead to increased levels of transcripts such as *PRDM1*, *XBP1* and *MZB1* in an attempt to restore normal production of ASCs.

In keeping with this hypothesis, a high degree of overlap was observed in the regions bound the UPR-related TFs CREB3L2, ATF6 and XBP1. A sampling of the bound regions found that transcripts altered in the gene expression studies were indeed occupied by the affected factors. The previous example of *BNIP3* is a case in point, with ATF6 and CREB3L2 binding to the promoter region and possibly intronic regulatory regions as well. At present, the ChIP-seq data has undergone only preliminary bioinformatics analysis; so additional conclusions will require more in-depth data mining. For example, it will be

possible to identify the types of sites bound by the TFs using *de novo* motif discovery. This will provide insight into whether the TFs are likely to bind in tandem or may in fact compete for the same site. The ChIP-seq tracks depicted above show a very close overlap of the ATF6 and CREB3L2 peaks. The current data cannot distinguish whether these bind simultaneously. Using additional methodology such as EMSA would help to address this question.

Another area of investigation would be to perform gene ontology analysis of the loci that are associated with particular combinations of the TFs. The results shown in Figure-7.14 and 7.15 are suggestive that co-occupancy of all three TFs is associated with regulation of UPR-responsive genes. The identification of loci bound by these TFs also provides scope for identifying new players in plasma cell differentiation. As shown in Figure-7.15 the gene *UFL1* has pronounced peaks for all three TFs at the promoter. UFL1 is a ligase for ubiquitin-fold modifier 1 (UFM1) which has recently been characterised as an ubiquitin-like protein. The process of conjugating UFM1 to target proteins has been termed ufmylation and has been linked to the ER-stress response, fatty acid metabolism and haematopoiesis(151-154). The range of processes associated with UFL1-regulation makes it an attractive potential downstream target of CREB3L2 to study in the future.

In conclusion, although some of the data requires further analyses and validation, overall the data presented in this chapter support the initial hypothesis that CREB3L2 directly regulates genes that are important to the UPR and are likely to be required for successful adaptation to the ER-stress encountered during PC differentiation.

## 8. Final Discussion

The current consensus in the literature is that B-cell differentiation is regulated by the serial action of several transcription factors such as PAX5, BCL6, IRF4, BLIMP1 and XBP1(12, 13, 18) (Figure-8.1). PAX5 is required for initial B-cell lineage instruction and subsequent maintenance of the B-cell program in mature B-cells. Expression of PAX5 prevents ASC development in part by repressing XBP1 function, which is essential for plasma cell differentiation. Once mature B-cells receive the appropriate signal these can form(5, 6) GC, the site of selection for B-cells that secrete high-affinity antibodies. BCL6 is the central transcriptional regulator of the GC as evidenced by the fact that BCL6 deletion prevents GC formation(12, 13, 22). In addition, it represses the exit of B-cells from the GC and exerts a repressive effect on *IRF4* and *BLIMP1*, two transcription factors that are crucial for plasma cell differentiation(23, 24). It has been proposed that BCR, CD40 and TLR signalling leads to activation of NFκB which in turn promotes IRF4-mediated repression of *BCL6*. BCR signalling also leads to BCL6 phosphorylation and degradation, thus removing BCL6 repression on *BLIMP1* and *IRF4(23).* Hence, after the correct signals are received, plasma cell differentiation proceeds and establishment of the full secretory phenotype is accomplished by expression of XBP1. However, data suggests that early ASC can still form in the absence of XBP1(5, 6) therefore posing the problem of how ASCs cope with their metabolic requirements prior to the expression of XBP1.

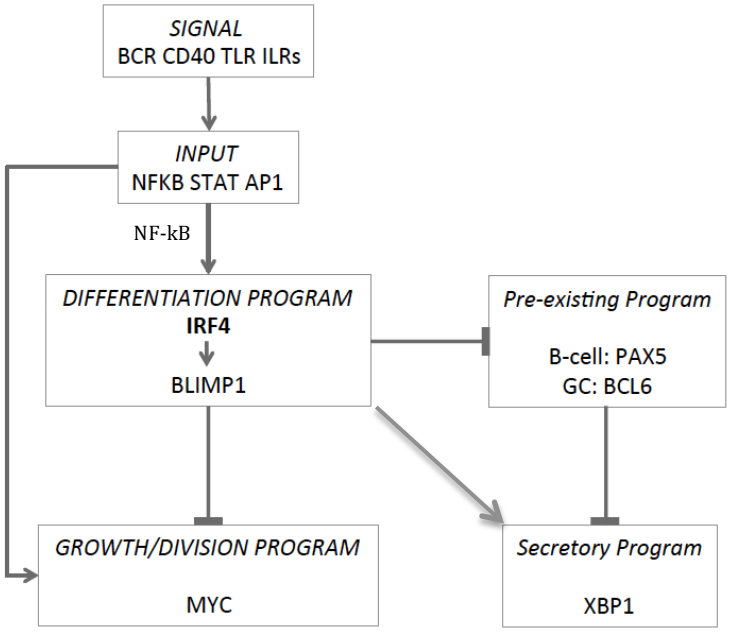


**Figure-8.1**: Schematic of the regulatory network controlling plasma cell differentiation. Figure from Reuben Tooze.

During the transition from B-cell to plasma cell, the cells undergo dramatic morphological and biochemical changes related to the increased burden of immunogolublin production. Immunoglobulins, and proteins in general, are synthesised and properly folded in the ER. There are many factors that can affect the integrity and homeostasis of the ER, such as the toxic accumulation of misfolded proteins, which can impact on cell survival. However, the cells have adapted a physiological signalling pathway called the UPR to counteract these effects(69).

The UPR is required during the transition from ABC to plasmablast and XBP1 is a key component of the conserved response to ER stress(50). However, there are additional arms of the UPR that may be acting prior to or in conjunction with XBP1. For example, following ER stress, regulated intramembrane proteolysis (RIP) via S1P/S2P cleavage can generate active TFs that control target genes in the nucleus and resolve ER stress. The sterol regulatory element binding proteins (SREBPs), ATF6 and their structural homologs (CREB3L2) are regulated by RIP during a UPR (155).

The gene expression profile data published by Cocco et al. showed that the expression of *CREB3L2* is increased as B-cells transition to ASCs, prompting the hypothesis that CREB3L2 may be a critical participant in the ASC-associated UPR(4). Moreover, the consistent expression of *CREB3L2* in ABC-DLBCL points to a role in the early stages of transition from activated B-cell to plasmablast. The high expression in ABC-DLBCL might also be linked to a particular role in disease pathogenesis with the prospect of targeted intervention.

In this project, the two transcripts of *CREB3L2* (isform-1 and isoform-2) were found to be expressed in cell lines derived from B-lineage tumours including the ABC-DLBCL lines OCI-Ly3 and OCI-Ly10 and myeloma lines H929 and U266. While the function of the short form remains speculative, it is possible that the additional form of CREB3L2 may function as a dominant-negative or plays a role in regulating CREB3L2 levels (75). To further characterise the expression of CREB3L2, the level of protein in the cell lines was examined using two ER-stressors (TG and DTT) to investigate the relationship between a UPR and CREB3L2 levels. The results revealed a direct relationship between CREB3L2 activation and UPR induction; upon ER-stress by TG or DTT, the FL and CF of CREB3L2 were induced and increased with time.

Having established the pattern in B-cell tumour lines related to the transition between activated B-cell and ASC, it was of interest to determine the pattern

during a normal differentiation. Thus, the protein expression of CREB3L2 was examined in human B-cells isolated from normal donors and differentiated in vitro. The results revealed that the two forms of CREB3L2 (FL and CF) were expressed increasingly from Day-3 B-cells to Day-13 ASCs and since the UPR is required during B-cell differentiation, it is likely that CREB3L2 is participating in this response (30).

Thus, based on the results obtained from B-cell lines and primary cells, CREB3L2 is expressed at the earliest stages of plasma cell differentiation and then increases, as the cells become ASCs. The generation of CREB3L2 cleaved form coincides with immunoglobulin production and would fit with a response to ER stress. This pattern is similar to CREB3L2 expression in differentiating chondrocytes (79). In this lineage, differentiation is accompanied by an increase in the production of cartilage matrix proteins, resulting in ER stress. In this setting, CREB3L2 is required for enhanced ER to Golgi trafficking and is essential for the generation of mature chondrocytes. The similar requirements of the two cell lineages during differentiation make it likely that CREB3L2 will behave in a similar fashion in both instances.

CREB3L2, ATF6 and SREBPs are regulated by RIP via S1P/S2P cleavage. Therefore, inhibiting S1P/S2P may prevent adaptation to stress and lead to cell death. Thus, the impact of S1P and S2P inhibitors on UPR signalling elements in myeloma and ABC-DLBL cell lines were initially examined using AEBSF (S1P inhibitor), PF-429242 (S1P inhibitor) and Nelfinavir (S2P inhibitor).

AEBSF was first tested as an inhibitor of S1P in ABC-DLBL cell lines OCI-Ly3 and OCI-Ly10. The results showed that AEBSF led to a loss of all forms of CREB3L2, which was unanticipated according to a previous publication (96). However, an additional study by Colgan et al. showed similar results to those obtained in this project, with an overall loss of SREBP-2 (113). Since AEBSF can inhibit a wide range of serine proteases, the utility of this drug for studying CREB3L2 was limited.

Therefore compounds that have higher selectivity, PF-429242 (S1P inhibitor) and Nelfinavir (S2P inhibitor), were examined. Treatment with PF-429242 led to the predicted loss of the cleaved form accompanied by an increase in the full-length protein. However, Nelfinavir treatment affected both forms of CREB3L2. Despite this unanticipated result, Nelfinavir has been used previously to assess the role of S2P-regulated TFs during the UPR (156), so it was included in experiments to provide additional evidence for a potential role of TFs made active by RIP. In addition to the observed effects on CREB3L2, both PF-429242 and Nelfinavir led to a loss of other UPR-related TFs. The reduction in ATF6 was expected, but the accompanying loss of XBP1 was surprising. The detection of ATF6 and CREB3L2 binding to the *XBP1* promoter (Figure-7.14) suggested the possibility of transcriptional regulation. However, in contrast to the CREB3L2 knockdown experiment, the levels of *XBP1* transcript were not affected by PF-429242 or Nelfinavir treatment (data not shown). Postranslational mechanisms regulating XBP1 protein stability have been described (157, 158) and may instead account for the observed difference.

Accompanying the change in TF protein expression, application of either PF-429242 or Nelfinavir had a profound effect on the biology of differentiating B-cells (Figure-8.2). Treatment of activated B-cells with the drugs led to a dramatic reduction in cell number that was mirrored by an increase in autophagy and reduced proliferation. These effects were first observed within 36 hours of incubation with the inhibitors and resulted in poor survival of ASCs.

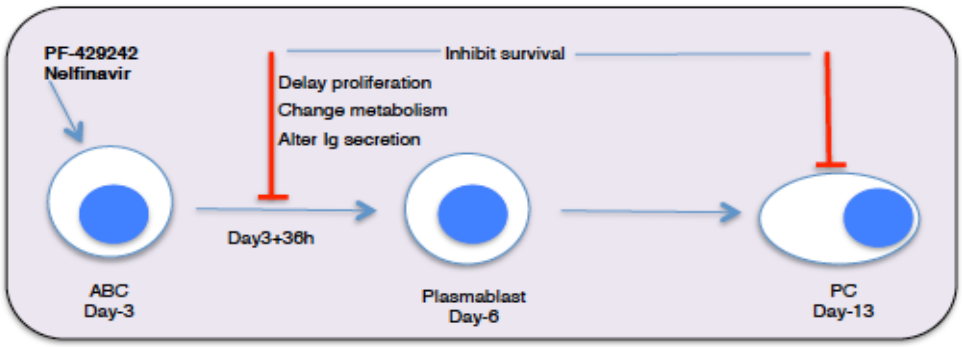


**Figure-8.2: The impact of PF-429242 and Nelfinavir on plasma cell differentiation.** Day-3 activated B-cells (ABCs) were assessed at timed intervals following treatment with S1P/S2P inhibitors. The inhibitors exhibited a range of effects, including a delay in proliferation after release from CD40L, changes in metabolic gene expression signatures, reduction in immunoglobulin secretion and increased autophagy associated with reduced

Interestingly, PF-429242 treatment led to the emergence of two phenotypically distinct populations ($CD38^{high}$ and $CD38^{low}$) and had a differential impact on the secretory capacity of surviving cells. The results revealed a failure to properly up-regulate CD38 compared to the control, indicative of an interference with ASC commitment and the potential impact of PF-429242 on naïve versus memory cells. In addition, the results showed a preferential effect of PF-429242 on IgG secreting cells compared to the control and IgM secreting cells suggestive of possible role of S1P-regulated events on CSR during B-cell differentiation.

To provide a deeper understanding of the changes linked to S1P/S2P regulated pathways, gene expression analysis was undertaken on ASCs that had been exposed to inhibitors for 72 hours. The gene expression profile suggested a major effect on cellular metabolism, impinging on biosynthetic pathways involving sterols, lipids and cholesterol. The regulation of such pathways would be in keeping with the proposed role for S1P/S2P-cleaved TFs being activated by the UPR to prepare the cell for increased protein production. For example, SREBP-1 and SREBP-2 are known to be involved in

lipid synthesis at the same time they are stimulated in response to ER stress(159). Moreover, reduction in UPR-associated PERK leads to a decrease in eIF2α phosphrylation, which in turn reduces the expression of C/EBP, a known regulator of the synthesis of lipids(69).

However, since the S1P/S2P inhibitors affect multiple TFs it is difficult to attribute changes to a single RIP-activated factor. Therefore, several experiments were conducted to determine the contribution of CREB3L2, such as loss-of-function using knockdown and ChIP-seq to examine CREB3L2 target genes. The knockdown experiments, while apparently achieving successful reduction in protein levels, did not generate statistically significant changes in gene expression. Despite the limitations, some genes looked promising as targets of CREB3L2 regulation such as *BNIP3* that is described in Chapter-7.

Contrary to what is predicted for the involvement of CREB3L2 in plasma cell development, the gene expression profile of CREB3L2 knockdown has shown several genes that are associated with plasma cell differentiation and ER-stress were up-regulated. One of the possible reasons is that upon knockdown CREB3L2, other structurally similar proteins may substitute for CREB3L2 due to the similarities in the DNA binding affinity between CREB3L2 and other CREB/ATF members. This may provide an additional explanation for the greater effect upon using S1P/S2P inhibitors. Furthermore, knockdown of CREB3L2 may lead to an increase in levels of some transcripts such as *PRDM1*, *XBP1* and *MZB1* in an attempt to restore normal production of ASCs.

In summary, the data obtained support the initial hypothesis predicting a role for CREB3L2 in plasma cell differentiation through the regulation of genes required for adaptation to ER stress. Moreover, the results suggest that CREB3L2 might be acting upstream of XBP1. The protein expression pattern showed that CREB3L2 is induced, cleaved and can be inhibited from Day-3 in the differentiation protocol whereas, XBP1 is expressed later, around Day-5.

Although preliminary, the ChIP-seq experiment points to a combined effort by CREB3L2, ATF6 and XBP1 in the regulation of UPR-responsive genes. Based on the timing of expression and the relatively restricted number of XBP1 targets identified, it may be that CREB3L2, possibly in conjunction with ATF6 or SREBPs, provides the first wave of metabolic reprogramming, followed by XBP1 reinforcement.

In conclusion, the results presented in this project suggest that CREB3L2 is involved in the early commitment to ASC fate prior to the requirement for XBP1 through synchronized processes such as cell division, CSR and metabolic reprogramming. These data highlight the importance of S1P/S2P in the B-cell to plasma cell transition and potentially alter the current view of the networks involved in this process (Figure-8.3).

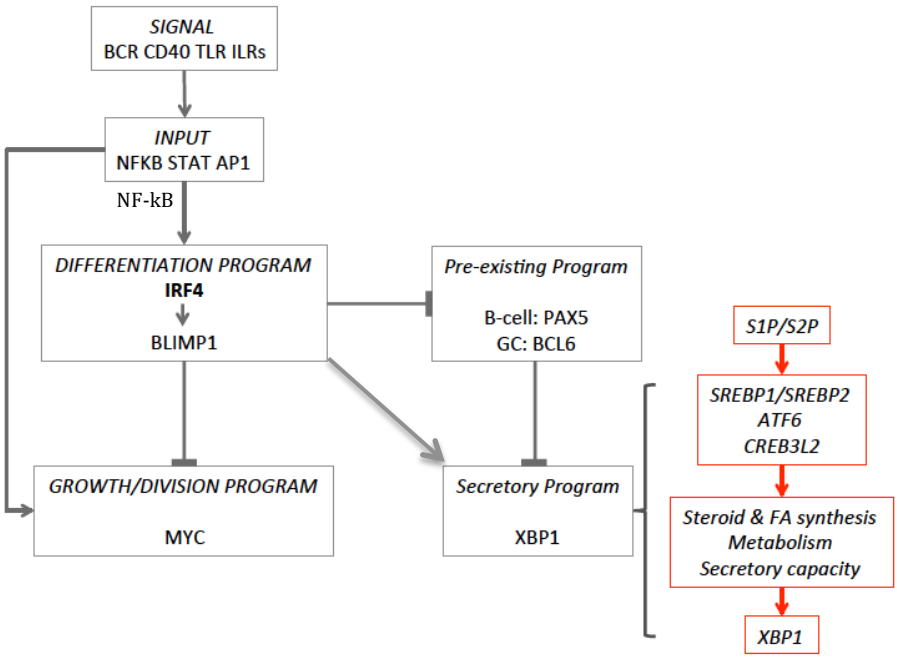


**Figure-8.3**: Schematic adding S1P/S2P function as essential for differentiation and development of secretory capacity at the ABC to plasmablast transition.

On a final note, it is worth revisiting the idea that CREB3L2 may be playing a unique role in ABC-DLBCL. In the OCI-Ly3 and OCI-Ly10 cell lines, CREB3L2 was expressed at constitutively high levels for both the full length as well as the cleaved form. Although the levels could be further augmented by ER stress, this suggests that in ABC-DLBCL another pathway may be promoting CREB3L2 expression. In glioma, CREB3L2 was identified as part of an essential pathway for proliferation and survival involving MCL1 (81). In this setting, the serine/threonine kinase PAK1 activates RAS-MAPK signalling leading to an increase in CREB3L2. CREB3L2 then transcriptionally activates *ATF5*, another transcription factor, which regulates the expression of MCL1, a BCL2 family regulator of apoptosis. This same pathway is also operational in chondrocytes (82). In B-lymphocytes PAK1 can be activated downstream of BCR signalling(160). One of the defining features of ABC-DLBCL is constitutive BCR signalling, often through the mutation of *CD79A* and/or *CD79B(161).* This may lead to PAK1 activation and subsequently high levels of *CREB3L2*. Interestingly, the CREB3L2 ChIP-seq revealed the presence of 3 peaks of binding on the *ATF5* locus, with no detectable ATF6 or XBP1 (Figure-8.4 and data not shown). It is plausible that the CREB3L2-ATF5-MCL1 axis is also functional in ABC-DLBCL and perhaps normal plasma cells as well, which require MCL1 for survival in the bone marrow(83). Since ATF6 and XBP1 are not usually expressed in ABC-DLBCL it would be of interest to further characterise the targets that are only bound by CREB3L2 and compare these between normal differentiating B-cells and ABC-DLBCL. Given the results obtained with S1P/S2P inhibitors in primary cell cultures, it would also be a priority in the future to evaluate the impact of these drugs on ABC-DLBCL.

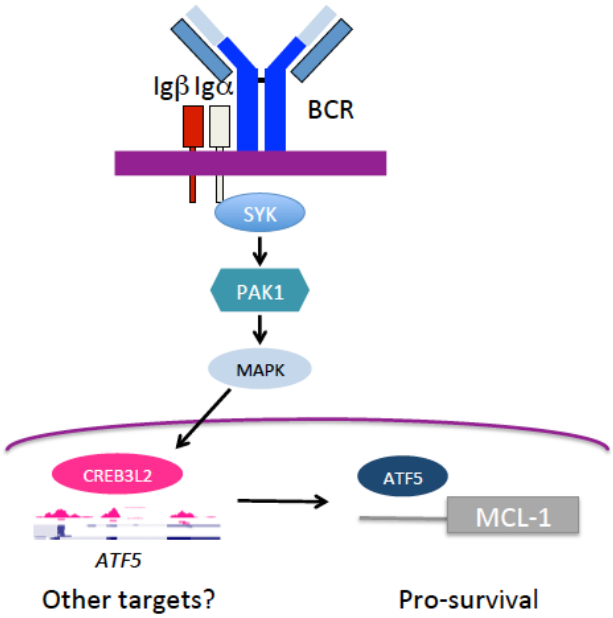


**Figure-8.4**: **Model for CREB3L2 participation in the maintenance of ABC-DLBCL.** Constitutive BCR signalling triggers the activation of PAK1 and MAPK, which increase the expression of CREB3L2. CREB3L2 activates the *ATF5* locus leading to up-regulation of the anti-apoptotic protein MCL1. Other targets of CREB3L2 may similarly contribute to lymphomagenesis.

## References

1. Glick D, Barth S, Macleod K. Autophagy: cellular and molecular mechaisms. Journal Pathol. 2010;221(1):3-12.
2. Chan CP, Kok KH, Jin DY. CREB3 subfamily transcription factors are not created equal: Recent insights from global analyses and animal models. Cell & bioscience. 2011;1(1):6. PubMed PMID: 21711675. Pubmed Central PMCID: 3116243.
3. Benjamini E CR, Sunshine G,. Immunology. Fourth Edition ed. Canada: Wiley-liss; 2000. 121-9, 35-43 p.
4. Cocco M, Stephenson S, Care MA, Newton D, Barnes NA, Davison A, et al. In vitro generation of long-lived human plasma cells. Journal of immunology. 2012 Dec 15;189(12):5773-85. PubMed PMID: 23162129.
5. Todd DJ, McHeyzer-Williams LJ, Kowal C, Lee AH, Volpe BT, Diamond B, et al. XBP1 governs late events in plasma cell differentiation and is not required for antigen-specific memory B cell development. The Journal of experimental medicine. 2009 Sep 28;206(10):2151-9. PubMed PMID: 19752183. Pubmed Central PMCID: 2757870.
6. Taubenheim N, Tarlinton DM, Crawford S, Corcoran LM, Hodgkin PD, Nutt SL. High rate of antibody secretion is not integral to plasma cell differentiation as revealed by XBP-1 deficiency. Journal of immunology. 2012 Oct 1;189(7):3328-38. PubMed PMID: 22925926.
7. Chan TD, Brink R. Affinity-based selection and the germinal center response. Immunological reviews. 2012 May;247(1):11-23. PubMed PMID: 22500828.
8. Shi W, Liao Y, Willis S, Taubenheim N, Inouye M, Tarlinton D, et al. Transcriptional profiling of mouse B cell terminal differentiation defines a signature for antibody-secreting plasma cells. Nature immunology. 2015;16:663-73.
9. Liu YJ, Zhang J, Lane PJ, Chan EY, MacLennan IC. Sites of specific B cell activation in primary and secondary responses to T cell-dependent and T cell-independent antigens. European journal of immunology. 1991 Dec;21(12):2951-62. PubMed PMID: 1748148.
10. Parker DC. T cell-dependent B cell activation. Annual review of immunology. 1993;11:331-60. PubMed PMID: 8476565.
11. Herlands RA, Christensen SR, Sweet RA, Hershberg U, Shlomchik MJ. T cell-independent and toll-like receptor-dependent antigen-driven activation of autoreactive B cells. Immunity. 2008 Aug 15;29(2):249-60. PubMed PMID: 18691914.
12. Nutt SL, Taubenheim N, Hasbold J, Corcoran LM, Hodgkin PD. The genetic network controlling plasma cell differentiation. Seminars in immunology. 2011 Oct;23(5):341-9. PubMed PMID: 21924923.
13. Shapiro-Shelef M, Calame K. Regulation of plasma-cell development. Nature reviews Immunology. 2005 Mar;5(3):230-42. PubMed PMID: 15738953.
14. Klein U, Dalla-Favera R. Germinal centres: role in B-cell physiology and malignancy. Nature reviews Immunology. 2008 Jan;8(1):22-33. PubMed PMID: 18097447.

15. Goodnow CC, Vinuesa CG, Randall KL, Mackay F, Brink R. Control systems and decision making for antibody production. Nature immunology. 2010 Aug;11(8):681-8. PubMed PMID: 20644574.
16. Calame KL, Lin KI, Tunyaplin C. Regulatory mechanisms that determine the development and function of plasma cells. Annual review of immunology. 2003;21:205-30. PubMed PMID: 12524387.
17. shukla V, Lu R. IRF4 and IRF8: Governing the virtues of B lymphocytes. Front Biol (Beijing). 2014;9(4):269-82.
18. Fairfax KA, Kallies A, Nutt SL, Tarlinton DM. Plasma cell development: from B-cell subsets to long-term survival niches. Seminars in immunology. 2008 Feb;20(1):49-58. PubMed PMID: 18222702.
19. Calame KL. Plasma cells: finding new light at the end of B cell development. Nature immunology. 2001 Dec;2(12):1103-8. PubMed PMID: 11725300.
20. Schebesta M, Heavey B, Busslinger M. Transcriptional control of B-cell development. Current opinion in immunology. 2002 Apr;14(2):216-23. PubMed PMID: 11869895.
21. Horcher M, Souabni A, Busslinger M. Pax5/BSAP maintains the identity of B cells in late B lymphopoiesis. Immunity. 2001 Jun;14(6):779-90. PubMed PMID: 11420047.
22. Fukuda T, Yoshida T, Okada S, Hatano M, Miki T, Ishibashi K, et al. Disruption of the Bcl6 gene results in an impaired germinal center formation. The Journal of experimental medicine. 1997 Aug 4;186(3):439-48. PubMed PMID: 9236196. Pubmed Central PMCID: 2199007.
23. Shapiro-Shelef M, Lin KI, McHeyzer-Williams LJ, Liao J, McHeyzer-Williams MG, Calame K. Blimp-1 is required for the formation of immunoglobulin secreting plasma cells and pre-plasma memory B cells. Immunity. 2003 Oct;19(4):607-20. PubMed PMID: 14563324.
24. Crotty S, Johnston RJ, Schoenberger SP. Effectors and memories: Bcl-6 and Blimp-1 in T and B lymphocyte differentiation. Nature immunology. 2010 Feb;11(2):114-20. PubMed PMID: 20084069. Pubmed Central PMCID: 2864556.
25. Kallies A, Hasbold J, Fairfax K, Pridans C, Emslie D, McKenzie BS, et al. Initiation of plasma-cell differentiation is independent of the transcription factor Blimp-1. Immunity. 2007 May;26(5):555-66. PubMed PMID: 17509907.
26. Shaffer AL, Emre NC, Romesser PB, Staudt LM. IRF4: Immunity. Malignancy! Therapy? Clinical cancer research : an official journal of the American Association for Cancer Research. 2009 May 1;15(9):2954-61. PubMed PMID: 19383829. Pubmed Central PMCID: 2790720.
27. Ochiai K, Maienschein-Cline M, Simonetti G, Chen J, Rosenthal R, Brink R, et al. Transcriptional Regulation of Germinal Center B and Plasma Cell Fates by Dynamical Control of IRF4. Immunity. 2013 May 23;38(5):918-29. PubMed PMID: 23684984. Pubmed Central PMCID: 3690549.
28. Klein U, Casola S, Cattoretti G, Shen Q, Lia M, Mo T, et al. Transcription factor IRF4 controls plasma cell differentiation and class-switch recombination. Nature immunology. 2006 Jul;7(7):773-82. PubMed PMID: 16767092.
29. Iwakoshi NN, Lee AH, Glimcher LH. The X-box binding protein-1 transcription factor is required for plasma cell differentiation and the unfolded protein response. Immunological reviews. 2003 Aug;194:29-38. PubMed PMID: 12846805.

30. Gass JN, Gunn KE, Sriburi R, Brewer JW. Stressed-out B cells? Plasma-cell differentiation and the unfolded protein response. Trends in immunology. 2004 Jan;25(1):17-24. PubMed PMID: 14698280.
31. Reimold AM, Iwakoshi NN, Manis J, Vallabhajosyula P, Szomolanyi-Tsuda E, Gravallese EM, et al. Plasma cell differentiation requires the transcription factor XBP-1. Nature. 2001 Jul 19;412(6844):300-7. PubMed PMID: 11460154.
32. Todd DJ, Lee AH, Glimcher LH. The endoplasmic reticulum stress response in immunity and autoimmunity. Nature reviews Immunology. 2008 Sep;8(9):663-74. PubMed PMID: 18670423.
33. Malhotra JD, Kaufman RJ. The endoplasmic reticulum and the unfolded protein response. Seminars in cell & developmental biology. 2007 Dec;18(6):716-31. PubMed PMID: 18023214. Pubmed Central PMCID: 2706143.
34. Hebert DN, Molinari M. In and out of the ER: protein folding, quality control, degradation, and related human diseases. Physiological reviews. 2007 Oct;87(4):1377-408. PubMed PMID: 17928587.
35. Asada R KS, Kondo S, Saito A, Imaizumi K,. The signaling from endoplasmic reticulum-resident bZIP transcription factors involved in diverse cellular physiology. Journal of Biochemistry. 2011.
36. Masciarelli S, Sitia R. Building and operating an antibody factory: redox control during B to plasma cell terminal differentiation. Biochimica et biophysica acta. 2008 Apr;1783(4):578-88. PubMed PMID: 18241675.
37. Harding HP, Calfon M, Urano F, Novoa I, Ron D. Transcriptional and translational control in the Mammalian unfolded protein response. Annual review of cell and developmental biology. 2002;18:575-99. PubMed PMID: 12142265.
38. Cao SS KR. Unfolded protein response. Current Biology [Internet]. 2012; 22(R622).
39. Hu CC, Dougan SK, McGehee AM, Love JC, Ploegh HL. XBP-1 regulates signal transduction, transcription factors and bone marrow colonization in B cells. The EMBO journal. 2009 Jun 3;28(11):1624-36. PubMed PMID: 19407814. Pubmed Central PMCID: 2684024.
40. Credle J, Finer-Moore J, Papa F, Stroud R, Walter P. On the mechanism of sensing unfolded protein in the endoplasmic reticulum. Proceedings of the National Academy of Sciences of the United States of America. 2005;102(52):18773-83.
41. Gardner B, Walter P. Unfolded proteins are Ire1-activating ligands that directly induce the unfolded protein response. Science. 2011;333(6051):1891-4.
42. Zhou J, Liu C, Back S, Clark R, Peisach D, Xu Z, et al. The crystal structure of human IRE1 luminal domain reveals a conserved dimerization interface required for activation of the unfolded protein response. Proceedings of the National Academy of Sciences of the United States of America. 2006;103(39):14343-8.
43. Liu C, Schroder M, Kaufman RJ. Ligand-independent dimerization activates the stress response kinases IRE1 and PERK in the lumen of the endoplasmic reticulum. Journal Biol Chem. 2000;275(32):24881-5.
44. Wiest D, Burkhardt J, Hester S, Hortsch M, Meyer D, Argon Y. Membrane biogensis during B cell differentiation: most endoplasmic reticulum proteins are expressed coordinately. Journal cell biol. 1990;110(5):1501-11.

45. Harding HP, Novoa I, Bertolotti A, Zeng H, Zhang Y, Urano F. Translational regulation in the cellular response to biosythetic load on the endoplasmic reticulum. Cold spring harb perspect biol. 2001;66:499-508.
46. Ma Y, Hendershot LM. The unfolded tale of the unfolded protein response. Cell. 2001;107(7):827-30.
47. Morris J, Dorner A, Edwards C, Hendershot L, Kaufman RJ. Immunoglobulin binding protein (BiP) function is required to protect cells from endoplasmic reticulum stress but is not required for the secretion of selective proteins. Journal Biol Chem. 1997;272(7):4327-34.
48. Calfon M, Zeng H, Urano F, Till J, Hubbard S, Harding HP, et al. IRE1 couples endoplasmic reticulum load to secretory capacity by processing the XBP-1 mRNA. Nature. 2002;415(6867):92-6.
49. Lewis M, Mazzarella R, Green M. Structure and assembly of the endoplasmic reticulum. The synthesis of three major endoplasmic reticulum proteins during lipopolysaccharide-induced differentiation of murine lymphocytes. Journal Biol Chem. 1985;260(5):3050-7.
50. Gass JN, Gifford NM, Brewer JW. Activation of an unfolded protein response during differentiation of antibody-secreting B cells. The Journal of biological chemistry. 2002 Dec 13;277(50):49047-54. PubMed PMID: 12374812.
51. Gass JN, Jiang HY, Wek RC, Brewer JW. The unfolded protein response of B-lymphocytes: PERK-independent development of antibody-secreting cells. Molecular immunology. 2008 Feb;45(4):1035-43. PubMed PMID: 17822768. Pubmed Central PMCID: 2677759.
52. Aragon I, Barrington R, Jackowski S, Mori K, Brewer JW. The apecialized unfolded protein response of B lymphocytes: ATF6alpha-independent development of antibody-secreting B cells. Molcular Immunol. 2012;51(3-4):347-55.
53. Brewer JW, Jackowski S. UPR-mediated membrane biogenesis in B cells. Biochem Res. 2012.
54. Jassens S, Pulendran B, Lambrecht B. Emerging functions of the unfolded protein response in immunity. Nature Immunol. 2014;15(10):910-9.
55. Reimold AM, Ponath PD, Li YS, Hardy RR, David CS, Strominger JL, et al. Transcription factor B cell lineage-specific activator protein regulates the gene for human X-box binding protein 1. The Journal of experimental medicine. 1996 Feb 1;183(2):393-401. PubMed PMID: 8627152. Pubmed Central PMCID: 2192461.
56. Tirosh B, Iwakoshi NN, Glimcher LH, Ploegh HL. XBP-1 specifically promotes IgM synthesis and secretion, but is dispensable for degradation of glycoproteins in primary B cells. The Journal of experimental medicine. 2005 Aug 15;202(4):505-16. PubMed PMID: 16103408. Pubmed Central PMCID: 2212843.
57. Iwakoshi NN, Lee AH, Vallabhajosyula P, Otipoby KL, Rajewsky K, Glimcher LH. Plasma cell differentiation and the unfolded protein response intersect at the transcription factor XBP-1. Nature immunology. 2003 Apr;4(4):321-9. PubMed PMID: 12612580.
58. Shaffer AL, Shapiro-Shelef M, Iwakoshi NN, Lee AH, Qian SB, Zhao H, et al. XBP1, downstream of Blimp-1, expands the secretory apparatus and other organelles, and increases protein synthesis in plasma cell differentiation. Immunity. 2004 Jul;21(1):81-93. PubMed PMID: 15345222.

59. Liu J, Srivastava R, Che P, Howell S. An endoplasmic reticulum stress response in arabidopsis is mediated by proteolytic processing nuclear relocation of a memrane-associated transcription factor, bZIP28. American society of plant biologist. 2007;19(12):4111-9.
60. Murakami T, Kondo S, Ogata M, Kanemoto S, Saito A, Wanaka A, et al. Cleavage of the membrane-bound transcription factor OASIS in response to endoplasmic reticulum stress. Journal of neurochemistry. 2006 Feb;96(4):1090-100. PubMed PMID: 16417584.
61. Lee K, Tirasophon W, Shen X, Michalak M, Prywes R, Okada T, et al. IRE1-mediated unconventional mRNA splicing and S2P-mediated ATF6 cleavage merge to regulate XBP1 in signaling the unfolded protein response. Genes & development. 2002 Feb 15;16(4):452-66. PubMed PMID: 11850408. Pubmed Central PMCID: 155339.
62. Yoshida H, Matsui T, Yamamoto A, Okada T, Mori K. XBP1 mRNA is induced by ATF6 and spliced by IRE1 in response to ER stress to produce a highly active transcription factor. Cell. 2001 Dec 28;107(7):881-91. PubMed PMID: 11779464.
63. Shen J CX, Hendershot L, Prywes R,. ER stress regulation of ATF6 localization by dissociation of BiP/GRP78 binding and unmasking of Golgi localization signals. Cell Press. 2002;3(1):99-111.
64. Espenshade PJ. SREBPs: sterol-regulated transcription factors. Journal of cell science. 2006 Mar 15;119(Pt 6):973-6. PubMed PMID: 16525117.
65. Eberle D, Hegarty B, Bossard P, Ferre P, Foufelle F. SREBP transcription factors: master regulators of lipid homeostasis. Biochimie. 2004 Nov;86(11):839-48. PubMed PMID: 15589694.
66. Sato R. SREBPs: protein interaction and SREBPs. The FEBS journal. 2009 Feb;276(3):622-7. PubMed PMID: 19143831.
67. Kondo S, Saito A, Hino S, Murakami T, Ogata M, Kanemoto S, et al. BBF2H7, a novel transmembrane bZIP transcription factor, is a new type of endoplasmic reticulum stress transducer. Molecular and cellular biology. 2007 Mar;27(5):1716-29. PubMed PMID: 17178827. Pubmed Central PMCID: 1820470.
68. Kondo S, Saito A, Asada R, Kanemoto S, Imaizumi K. Physiological unfolded protein response regulated by OASIS family members, transmembrane bZIP transcription factors. IUBMB life. 2011 Apr;63(4):233-9. PubMed PMID: 21438114.
69. Bravo R, Parra V, Rodriguez A, Torrealba N, Paredes F, Wang Z, et al. Endoplasmic reticulum and the unfolded protein response: dynamics and metabolic integration. Int Rev Cell Mol Biol. 2013;301:215-9.
70. Rose B, Tamvakopoulos GS, Dulay K, Pollock R, Skinner J, Briggs T, et al. The clinical significance of the FUS-CREB3L2 translocation in low-grade fibromyxoid sarcoma. Journal of orthopaedic surgery and research. 2011;6:15. PubMed PMID: 21406083. Pubmed Central PMCID: 3063187.
71. Panagopoulos I, Moller E, Dahlen A, Isaksson M, Mandahl N, Vlamis-Gardikas A, et al. Characterization of the native CREB3L2 transcription factor and the FUS/CREB3L2 chimera. Genes, chromosomes & cancer. 2007 Feb;46(2):181-91. PubMed PMID: 17117415.
72. Panagopoulos I, Mertens F. Characterization of the human CREB3L2 gene promoter. Oncology reports. 2009 Mar;21(3):615-24. PubMed PMID: 19212619.

73. Matsuyama A, Hisaoka M, Shimajiri S, Hayashi T, Imamura T, Ishida T, et al. Molecular detection of FUS-CREB3L2 fusion transcripts in low-grade fibromyxoid sarcoma using formalin-fixed, paraffin-embedded tissue specimens. The American journal of surgical pathology. 2006 Sep;30(9):1077-84. PubMed PMID: 16931951.
74. Mertens F, Fletcher CD, Antonescu CR, Coindre JM, Colecchia M, Domanski HA, et al. Clinicopathologic and molecular genetic characterization of low-grade fibromyxoid sarcoma, and cloning of a novel FUS/CREB3L1 fusion gene. Laboratory investigation; a journal of technical methods and pathology. 2005 Mar;85(3):408-15. PubMed PMID: 15640831.
75. Panagopoulos I, Monsef N, Collin A, Mertens F. Characterization of an alternative transcript of the human CREB3L2 gene. Oncology reports. 2010 Nov;24(5):1133-9. PubMed PMID: 20878102.
76. Jourdan M, Caraux A, De Vos J, Fiol G, Larroque M, Cognot C, et al. An in vitro model of differentiation of memory B cells into plasmablasts and plasma cells including detailed phenotypic and molecular characterization. Blood. 2009 Dec 10;114(25):5173-81. PubMed PMID: 19846886. Pubmed Central PMCID: 2834398.
77. Gutierrez NC, Ocio EM, de Las Rivas J, Maiso P, Delgado M, Ferminan E, et al. Gene expression profiling of B lymphocytes and plasma cells from Waldenstrom's macroglobulinemia: comparison with expression patterns of the same cell counterparts from chronic lymphocytic leukemia, multiple myeloma and normal individuals. Leukemia. 2007 Mar;21(3):541-9. PubMed PMID: 17252022.
78. Hino K, Saito A, kido M, Kanemoto S, asada R, Takai T, et al. Master regulator for chondrogensis , Sox9, regulates transcriptional activation of the endoplasmic reticulum stress transducer BBF2H7/CREB3L2 in chondrocytes. Journal Biol Chem. 2014;289(20):13810-20.
79. Saito A, Hino S, Murakami T, Kanemoto S, Kondo S, Saitoh M, et al. Regulation of endoplasmic reticulum stress response by a BBF2H7-mediated Sec23a pathway is essential for chondrogenesis. Nature cell biology. 2009 Oct;11(10):1197-204. PubMed PMID: 19767744.
80. Ishikura-Kinoshita S, Saeki H, Tsuji-Naito K. BBF2H7-mediated Sec23A pathway is required for endoplasmic reticulum-to-Golgi trafficking in dermal fibroblasts to promote collagen synthesis. The Journal of investigative dermatology. 2012 Aug;132(8):2010-8. PubMed PMID: 22495181.
81. Sheng Z, Li L, Zhu LJ, Smith TW, Demers A, Ross AH, et al. A genome-wide RNA interference screen reveals an essential CREB3L2-ATF5-MCL1 survival pathway in malignant glioma with therapeutic implications. Nature medicine. 2010 Jun;16(6):671-7. PubMed PMID: 20495567. Pubmed Central PMCID: 2882506.
82. Izumi S, Saito A, Kanemoto S, Kawasaki N, Asada R, Iwamoto H, et al. The endoplasmic reticulum stress transducer BBF2H7 suppresses apoptosis by activating the ATF5-MCL1 pathway in growth plate cartilage. The Journal of biological chemistry. 2012 Oct 19;287(43):36190-200. PubMed PMID: 22936798. Pubmed Central PMCID: 3476286.
83. Peperzak V VI, Walker J, Glaser SP, Lepage M, Coquery SM, Erickson LD, Fairfax K, Mackay F, Strasser A, Nutt SL, Tarlinton DM,. Mcl-1 is essential for the survival of plasma cells. Nature immunology. 2013;14:290-7.

84. Yamamoto K, Yoshida H, Kokame K, Kaufman RJ, Mori K. Differential contributions of ATF6 and XBP1 to the activation of endoplasmic reticulum stress-responsive cis-acting elements ERSE, UPRE and ERSE-II. J Biochem. 2004 Sep;136(3):343-50. PubMed PMID: 15598891.
85. Acosta-Alvear D, Zhou Y, Blais A, Tsikitis M, Lents NH, Arias C, et al. XBP1 controls diverse cell type- and condition-specific transcriptional regulatory networks. Molecular cell. 2007 Jul 6;27(1):53-66. PubMed PMID: 17612490.
86. Care MA, Cocco M, Laye J, Barnes NA, Huang Y, Wang M, et al. SPIB and BATF provide alternate determinants of IRF4 occupancy in diffuse large B-cell lymphoma linked to disease heterogeneity. Nucleic Acids Res. 2014;42(12):7591-610.
87. Care M, Barrans S, Worrillow L, Jack A, Westhead D, Tooze R. A microarray platform-independent classification tool for cell of origin class allows comparative analysis of gene expression in diffuse large B-cell lymphoma. PLoS One. 2013;8(2).
88. biotech Ap. GST Gene Fusion System 1997.
89. Kondo S, Hino S, Saito A, Kanemoto S, Kawasaki N, Asada R, et al. Activation of OASIS family, ER stress transducers, is dependent on its stabilization. Cell death differentiation. 2012;19(12):1939-49.
90. Saito A, Kanemoto S, Zhang Y, Asada R, Hino K, Imaizumi K. Chondrocyte proliferation regulated by secrted luminal domain of ER stress transducer BBF2H7/CREB3L2. Molecular cell. 2014;3(1):127-39.
91. Martello M, Remondini D, Borsi E, Santacroce M, Procacci M, Pezzi A, et al. Opposite activation of the Hedgehog pathway in CD138+ plasma cells and CD138-CD19+ Bcells identifies two subgroups of patients with multiple myeloma and different prognosis. Leukemia. 2016.
92. Dierk C, Grbic J, Zirlik K, Beigi R, Englund N, Guo G, et al. Essential role of stromally induced hedgehog signaling in B-cell malignancies. Nature medicine. 2007;13(8):944-51.
93. Sacedon R, Diez B, Nunez V, Hernandez C, Gutierrez NC, Cejalvo T, et al. Sonic hedgehog is produced by follicular dendritic cells and protects germinal center B cells from apoptosis. Journal of Immunol. 2005;174(3):1456-61.
94. Singh R, Kim J, Davuluri Y, Drakos E, Cho-vega J, Amin H, et al. Hedgehog signaling pathway is activated in diffuse large B-cell lymphoma and contributes to tumor cell survival and proliferation. Leukemia. 2010;24(5):1025-36.
95. Iwamoto H, Matsuhisa K, Saito A, Kanemoto S, Asada R, Hino K, et al. Promotion of cancer cell proliferation by cleaved and secreted luminal domains of ER stress transducer BBF2H7. PLoS One. 2015.
96. Okada T, Haze K, Nadanaka S, Yoshida H, Seidah N, Hirano Y, et al. A serine protease inhibitor prevents endoplasmic reticulum stress-induced cleavage but not transport of the membrane-bound transcription factor ATF6. Journal of Biochemistry. 2003;278(33):31024-32.
97. Hawkins J, Robbins M, Warren L, Xia D, Petras S, Valentine J, et al. Pharmacologic inhibition of site 1 protease inhibits sterol regulatory element-binding protein processing and reduces lipogenic enzyme gene expression and lipid synthesis in cultured cells and experimental animals. Journal pharmacol Exp Ther. 2008;326(3):801-8.

98. Guan M, Fousek K, Jiang C, Guo S, Synold T, Xi B, et al. Nelfinavir induces liposacrcoma apoptosis through inhibition of regulated intramembrane proteolysis of SREBP-1 and ATF6. Clinical cancer Res. 2011;17(7):1796-806.
99. Hay B, Abrams B, Zumbrunn A, Valentine J, Warren L, Petras S, et al. Aminopyrrolidineamide inhibitors of site-1 protease. Bloorg Med Chem Lett. 2007;17(16):4411-4.
100. Oslowski C, Urano F. Measuring ER stress and the unfolded protein response using mammalian tissue culture system. Methods Enzymol. 2011;490:71-92.
101. Gardner B, Pincus D, Gotthardt K, Gallagher C, Walter P. Endoplasmic reticulum stress sensing in the unfolded protein response. Cold spring harb perspect biol. 2013;5(3).
102. Smith M, Pleogh H, Weissman J. Road to ruin: targeting proteins for degradation in the endoplasmic reticulum. Science. 2011;334(6059):1086-90.
103. Chhabra S, Jain S, Wallace C, Hong F, Liu B. High expression of endoplasmic reticulum chaperone grp94 is a novel molecular hallmark of malignant plasma cells in multiple myeloma. Journal Hematol Oncol. 2015;8(77).
104. Wang S, Kaufman RJ. The impact of the unfolded protein response on human disease. Journal cell biol. 2012;197(7):857-67.
105. Guan M, Su L, Yuan Y, Li H, Chow W. Nelfinavir and Nelfinavir analogs block site-2 protease cleavage to inhibit castration-resistant prostate cancer. scientific reports. 2015.
106. Pai V, Nahata M. Nelfinavir mesylate: a protease inhibitor. Ann Pharmacother. 1999;33(3):325-39.
107. Penhard X, Goujard C, Legard M, Taburet A, Diquet B, Mentre F, et al. Population pharmacokinetic anaylsis for nelfinavir and its metabolite M8 in virologically controlled HIV-infected patients on HAART. Br Journal Clinical Pharmacol. 2005;60(4):390-403.
108. Bruning A, Gingeimaier A, Friese K, Mylonas I. New prospects for nelfinavir in non-HIV-related disease. Curr Mol pharmacol. 2010;3(2):91-7.
109. DeBose-Boyd R, Brown M, Li W, Nohturfft A, Goldstein J, Espenshade PJ. Transport-dependent proteolysis of SREBP: relocation of site-1 protease from Golgi to ER obviates the need for SREBP transport to Golgi. Cell. 1999;99(7):703-12.
110. Wang X, Sato R, Brown M, Hua X, Goldstein J. SREBP-1, a membrane-bound transcription factor released by sterol-regulated proteolysis. Cell. 1994;77(1):53-62.
111. Yokoyama C, Wang X, Briggs M, Asdmon A, Wu J, Hua X, et al. SREBP-1, a basic-helix-loop-helix-leucine zipper protein that controls transcription of the low density lipoprotein receptor gene. cell. 1993;75(1):187-97.
112. Ye J, Rawson R, Komuro R, Chen X, Dave U, Prywes R, et al. ER stress induces cleavage of membrane-bound ATF6 by the same proteases that process SREBPs. Molecular Cell Biology. 2000;6(6):1355-64.
113. Colgan S, Tang D, Werstuck G, Austin R. Endoplasmic reticulum stress causes the activation of sterol regulatory element binding protein-2. The international journal of biochemistry & cell biology. 2007;39:1843-51.
114. LIarena M, Bailey D, Curtis H, O'Hare P. Different mechanisms of recognition and ER retention by transmembrane transcription factor CREB-H and ATF6. Traffic. 2010;11(1):48-69.

115. Guo B, Li Z. Endoplasmic reticulum stress in hepatic steatosis and inflammatory bowl disease. Front Genet. 2014;242.
116. Mimura N, Fulciniti M, Gorgun G, Tai Y, Cirsea D, Santo L, et al. Blockade of XBP1 splicing by inhibition of IRE1alpha is a promising theraputic option in multiple myeloma. Blood. 2012;119(24):5772-81.
117. Turner M, Hawkins E, Hodgkin PD. Quantitative regulation of B cell division destiny by signal strength. Journal Immunol. 2008;181:374-82.
118. Nutt SL, Hodgkin PD, Tarlinton D, Corcoran LM. The generation of antibody-secreting plasma cells. Nature Reviews Immunology. 2015;15:160-71.
119. Ogata M, Hino S, Saito A, Morikawa K, Kondo S, Kanemoto S, et al. Autophagy is activated for cell survival after endoplasmic reticulum stress. Molecular Cell Biology. 2006;26(24):9220-31.
120. Hoyer-Hansen M, Jaattela M. Connecting endoplasmic reticulum stress to autophagy by unfolded protein response and calcium. Cell death and differentiation. 2007;14(9):1576-82.
121. Avery D, Ellyard J, Mackay F, Corcoran LM, Hodgkin PD, Tangye S. Increased expression of CD27 on activated human memory B cells correlates with their commitment to the plasma cell lineage. Journal of immunology. 2005;174:4034-42.
122. Jourdan M, Caraux A, Caron G, Robert N, Fiol G, Reme T, et al. Characterization of a transitional preplasmblast population in the human B cell to plasma cell differentiation. Journal of Immunol. 2011;187(8):3931-41.
123. Benhamron S, Pattanayak S, Berger M, Tirosh B. mTOR activation promotes plasma cell differentiation and bypass XBP-1 for immunoglobulin secretion. Molecular Cell Biology. 2015;35(1):153-66.
124. Chevrier S, Emslie D, Shi W, Kratina T, Wellard C, Karnowski A, et al. The BTB-ZF transcription factor Zbtb20 is deriven by Irf4 to promote plasma cell differentiation and longivity. Journal Exp Medicine. 2014;211(5):827-40.
125. Sciammas R, Shaffer AL, Schatz J, Zhao H, Staudt LM, Singh H. Graded expression of interferon regulatory factor-4 coordinates isotype switching with plasma cell differentiation. Immunity. 2006;25(2):225-36.
126. Duffy K, Wellard C, Markham J, Zhou J, Holmberg R, Hawkins E, et al. Activation-induced B cell fates are selected by intracellular stochastic competition. Science. 2012;335(6066):338-41.
127. Hasbold J, Corcoran LM, Tarlinton D, Tangye S, Hodgkin PD. Evidence from the generation of immunoglobulin G-secreting cells that stochastic mechanisms regulate lymphocyte differentiation. Nature immunology. 2004;5(1):55-63.
128. Oram J, Lawn R. ABCA1. The gatekeeper for eliminating excess tissue cholestrol. Journal lipid Res. 2001;42(8):1173-9.
129. Graham A. Mitochondrial regulation of macrophage cholestrol homeostasis. Free Radic Biological Medicine. 2015;89:982-92.
130. Dong X, Tang S. Insulin-induced gene: a new regulator in lipid metabolism. Peptides. 2010;31(11):2145-50.
131. Lam W, Becker A, Kennerly K, Finck B, Pearce E, Bhattacharya D. Mitochondrial pyruvate import promotes long-term survival of antibody-secreting plasma cells. Immunity. 2016;45:60-73.

132. Tellier J, Shi W, Minnich M, Liao Y, Crawford S, Smyth G, et al. Blimp-1 controls plasma cell function through the regulation of immunoglobulin secretion and the unfolded protein response. Nature Immnol. 2016;7(3):323-30.
133. Raman V, Akondy R, Rath S, Bal V, George A. Ligation of CD27 on B cells in vivo during primary immunization enhancesbcommitment to memory B cell responses. Journal Immunol. 2003;171(11):5876-81.
134. Randall T, Heath A, Santos-Argumedo L, Howard M, Weissman I, Lund F. Arrest of B lymphocyte terminal differentiation by CD40 signaling: Mechanism for lack of antibody-secreting cells in germinal centers. Immunity. 1998;8(6):733-42.
135. Upadhyay M, Priya G, Ramesh P, Madhavi M, Rath S, Bal V, et al. CD40 signaling drives B lymphocytes into an intermidate memory-like state, poised between naive and plasma cells. Journal cell physiol. 2014;229(10):1387-96.
136. Basu S, Kaw S, D'souza L, Vaidya T, Bal V, Rath S, et al. Constitutive CD40 signaling calibrates differentiation outcomes in responsing B cells via multiple molecular pathways. Journal Immunol. 2016.
137. Mizushima N. Autophagy: process and function. Genes & development. 2007;21(22):2861-73.
138. Pengo N, Scolari M, Oliva L, Milan E, Mainoldi F, Raimondi A, et al. Plasma cells require autophagy for sustainable immunoglobulin production. Nature Immunol. 2013;14(3):298-305.
139. Fox D, Duronio R. Endoreplication and polyploidy: insights into development and disease. Development. 2013;140:3-12.
140. Grigaravicius P, Kaminska E, Hubner C, Mckinnon P, Deimling A, Frappart P. Rint1 inactivation triggers genomic instability, ER stress and autophagy inhibition in the brain. Cell death and differentition. 2015;23:454-68.
141. Minnich M, Tagoh H, Bonelt P, Axelsson E, Fischer M, Cebolla B, et al. Multifunctional role of the transcription factor Blimp-1 in coordinating plasma cell differentiation. Nature Immunol. 2016;17(3):331-43.
142. Soustek M, Puigserver P. Interrupting synoviolin play at the ER: a plausible action to elevate mitochondrial energetics and silence obesity. The EMBO journal. 2015;34(8):981-3.
143. Chiu H, Yeh Y, Wang Y, Huang W, Ho S, Lin P, et al. Combination of the novel histone deacetylase inhibitor YCW1 and radiation induces autophagic cell death through the downregulation of BNIP3 in triple negative breast cancer cells in vitro and in an orthotopic mouse model. Molecular cancer. 2016;15(1).
144. Kinsey C, Balakrishnan V, O'Dell M, Huang J, Newman L, Whitney-Miller C, et al. Plac8 links oncogenic mutations to regulation of autophagy and is critical to pancreatic cancer progression. Cell Rep. 2014;7(4):1143-55.
145. Jackson A, Linsley P. Recognizing and avoiding siRNA off-target effects for target identification and theraputic application. Nature reviews Drug discovery. 2010;9(1):57-67.
146. Doench J, Petersen C, Sharp P. siRNAs can function as miRNAs. Genes & development. 2003;17(4):438-42.
147. Hamacher-Brady A, Brady N, Logue S, Sayen M, Jinno M, Kirshenbaum L, et al. Response to myocardial ischemia/reperfusion injury involves Bnip3 and autophagy. Cell death and differentition. 2007;14(1):146-57.
148. Hanna R, Quinsay M, Orogo A, Giang K, Rikka S, Gustafsson A. Microtubule-associated protein 1 light chain 3 (LC3) interacts with Bnip3

protein to selectively remove endoplasmic reticulum and mitochondria via autophagy. Journal Biol Chem. 2012;287(23):19094-104.
149. Glick D, Zhang W, Beaton M, Marsboom G, Gruber M, Simon C, et al. BNip3 regulates mitochondrial function and lipid metabolism in the liver. MCB journals. 2012;32(13):2570-84.
150. O'Sullivan T, Johnson L, Kang H, Sun J. BNIP3 and BNIP3L-mediated mitophagy promotes the generation of natural killer cell memory. Immunity. 2015;43(2):331-42.
151. Gannavaram S, Connelly P, Daniels M, Duncan R, Salotra P, Nakhasi H. Deletion of mitochondrial associated ubiquitin fold modifier protein Ufm1 in Leishmania donovani results in loss of beta-oxidation of fatty acids and blocks cell division in the amastigote stage. Molecular Microbiol. 2012;86(1):187-98.
152. Tatsumi K, Yamamoto-Mukai H, Shimizu R, Waguri S, Sou Y, Sakamoto A, et al. The Ufm1-activating enzyme Uba5 indispensable for erythroid differentiation in mice. Nat commun. 2011;8(2).
153. Zhang M, Zhu X, Zhang Y, Cai Y, Chen J, Sivaprakasam S, et al. RCAD/Ufl1, a Ufm1 E3 ligase, is essential for hematopoietic stem cell function and murine hematopoiesis. Cell death and differentiation. 2015;22:1922-34.
154. Zhang Y, Zhang M, Wu J, Lei G, Li H. Transcriptional regulation of the Ufm1 conjugation system in response to disturbance of the endoplasmic reticulum homeostasis and inhibition of vesicle trafficking. PLoS One. 2012.
155. Lal M, Caplan M. Regulated intramembrane proteolysis: signaling pathways and biological functions. Physiology (Bethesda). 2011;266(1):34-44.
156. Guan M, Fousek K, Chow W. Nelfinavir inhibits regulated intramembrane proteolysis of sterol regulatory element binding protein-1 and activating transcription factor 6 in castration-resistant prostante cancer. The FEBS journal. 2012;279(13):2399-411.
157. Chae U, Park S, Kim B, Suo W, Min J, Lee J, et al. Crtical role of XBP1 in cancer signaling is regulated by PIN1. Biochemistry journal. 2016.
158. Uemura A, Taniguchi M, Matsuo Y, Oku M, Wakabayashi S, Yoshida H. UBC9 regulates the stability of XBP1, a key transcription factor controlling the ER stress response. Cell Struct Funct. 2013;38(1):67-79.
159. Colgan S, Al-Hashimi A, Austin R. Endoplasmic reticulum stress and lipid dysregulation. Expert review in molecular medicine. 2011;13.
160. Tybulewicz V, Henderson R. Rho family GTPases and their regulators in lymphocytes. Nature reviews Immunology. 2009;9(9):630-44.
161. Basso K, Dalla-Favera R. Germinal centres and B cell lymphomagenesis. Nature reviews Immunology. 2015;15(3):172-84.

# Appendix

Appendix-1: The map structure of pIRES-2EGFP vector.

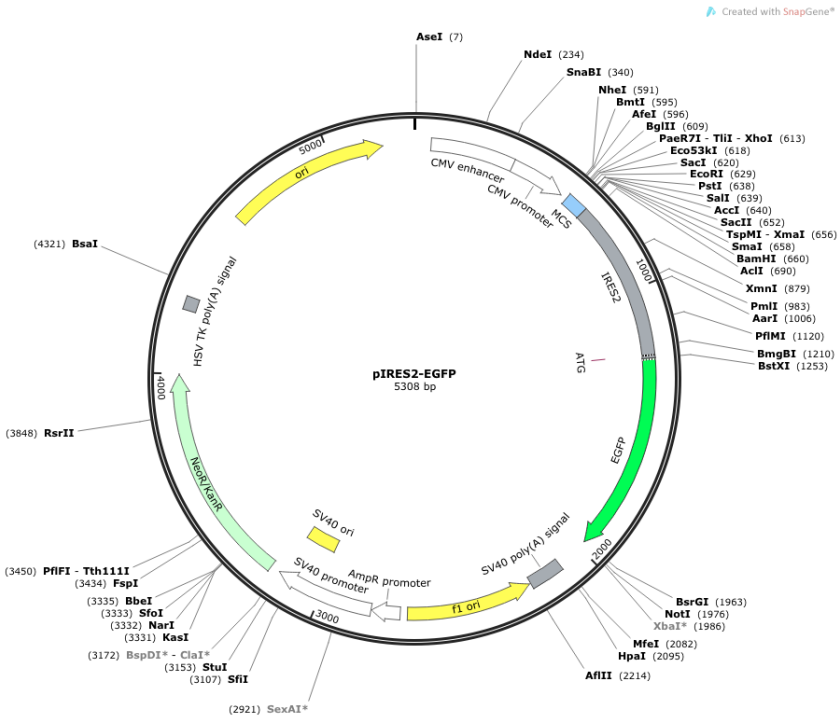


Appendix-2: The map structure of pGEX6P-1 vector.

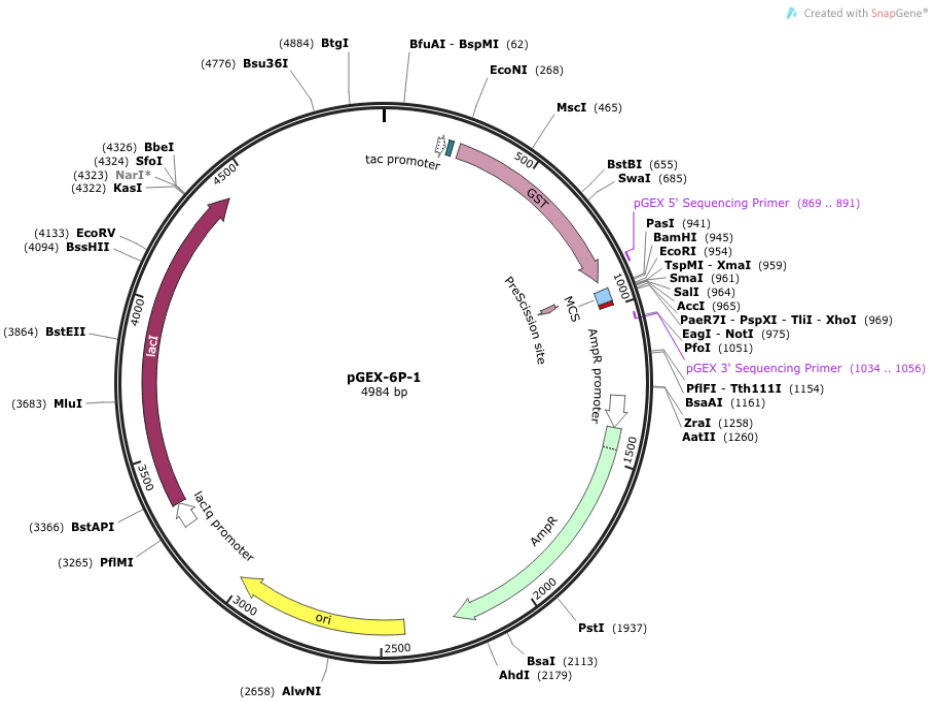

Appendix-3: The cloned part of CREB3L2 in pIRES-2EGFP and pGEX6P-1 vectors.

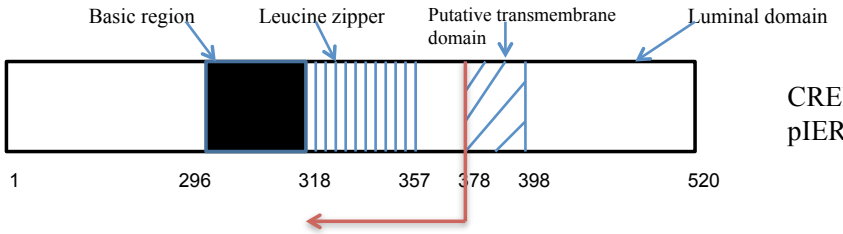


CREB3L2
pIERS2EGFP

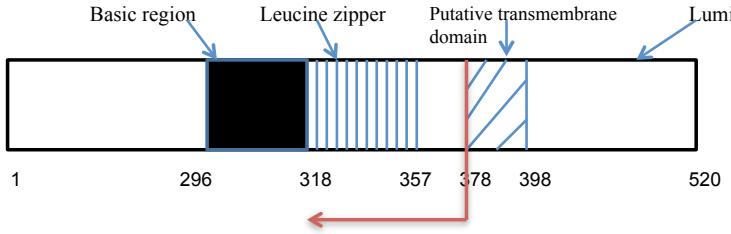


CREB3L2
pGEX6P-1